Universitat Politècnica de Catalunya

Doctoral Program:

Automatic Control, Robotics and Computer Vision

Universidad de los Andes

Doctoral Program:

Engineering

Doctoral Thesis

Modeling and Control in Open-Channel Irrigation Systems

Gregory Conde

Advisors:

Carlos Ocampo Martínez, PhD

Nicanor Quijano, PhD

July 2021

To God,
to my country,
to my beloved wife,
to my adorable daughter,
to my parents,
to my sisters,
to my nephews.

Acknowledgements

This is the opportunity to express my sincerest gratitude to those who have been part of this interesting journey.

First, to my advisor, Prof. Nicanor Quijano from Universidad de los Andes. Thank you for giving me the opportunity and support. I recognize your continuous effort and patience during all this time, and your expertise was invaluable along the construction of this doctoral dissertation. Also, to my advisor, Prof. Carlos Ocampo-Martinez from Universitat Politécnica de Catalunya. Thank you for your encouragement and wise advises. Your ideas, questions, and comments, brought this work to a higher level. I thank the opportunity to having work with this great team, and I congratulate both of you for providing new horizons and opportunities to many engineers as me.

Second, I thank the projects and institutions that supporting me: i) the Doctoral Support Program of the Universidad Central, Bogotá, Colombia; ii) the VII Convocatoría Interna de Investigación of the Universidad Central; iii) the Universidad de los Andes, Bogotá, Colombia; iv) Proyectos de Investigación Conjunta Universidad de Ibagué, Universidad de los Andes (2019-2021); v) the Universitat Politécnica de Catalunya, Barcelona, España; vi) the Institut de robòtica i informàtica industrial; and the CSIC Project MuYSCA (Ref. COOPA20246).

Third, I thank my colleagues from the Universidad de los Andes, Dr. Francisco Combita, Jorge Lopez, Juan Pablo Martínez, Luis Burbano and the other researchers of the GIAP, for the opinions and discussions that helped on the improvement of this thesis. Moreover, I tahnk my officemates in the Universitat Politécnica de Catalunya, Dr. Jenny Diaz, Dr. Unni Raveendran, Dr. Pau Segovia, and Dr. Wicak Ananduta, for their kindness and interesting discussions.

Finally, thanks to my wife Nini Herrera for your unending support, patience, and love along all this time. Thanks a lot to my daughter Sofia Conde for waiting during the time I borrowed. Thanks to my father Odilio Conde for being the best example, and thanks to my mother Maria Dolores Méndez for having awoken my curiosity.

Gregory Conde
Bogotá, 2021

Abstract

Water is the most important element of food production, and the easiest and most cost-efficient way to transport it is through open-channel irrigation systems (OCIS). These types of systems have a high agricultural and ecological impact. However, most of the OCIS lack automation at mitigating the economic and environmental costs that the waste of water in OCIS is causing. Additionally, most automated systems lack control and estimation strategies that increase the system efficiency. This thesis is devoted to exploring existing research around modeling, control, and estimation strategies in OCIS, in order to identify improvement opportunities and propose new modeling, estimation, and control strategies that increase their efficiency.

First, this dissertation reviews and discusses the existent modeling, estimation, and control strategies that have been reported in the OCIS field. Throughout the review process, it has been identified that due to the complexity of the fundamental models that describe the OCIS dynamics, multiple control-oriented modeling strategies have been reported. These modeling strategies have been classified and discussed, finding the need for control-oriented models that include the following:

- potential energy balances along the channels;
- the nonlinear hydraulic dynamics of the OCIS;
- useful to describe the dynamic behavior of interacting OCIS.

In addition, the need for estimation strategies designed from accurate models that include potential energy balances and nonlinear descriptions of the OCIS dynamics is identified. Also, it is established that the most common control objective in OCIS is to maintain a constant depth at the upstream or downstream end of the channels, and this control objective induces constant losses due to leaks and seepage. From the identified gaps, two control-oriented modeling strategies have been proposed, which include information about potential energy balances along the channels, nonlinear hydraulic dynamics to describe the OCIS, and are useful to describe the dynamic behavior of interacting OCIS. The modeling strategies have been validated, obtaining that by using approximated mass and potential energy balances (M&PEB) an accurate description of the OCIS dynamics can be reached.

Therefore, the proposed control-oriented modeling strategy designed from approximated M&PEB is used in the development of deterministic and stochastic strategies for detection isolation and magnitude estimation of unknown flows such as leaks and seepage.

The estimation strategies have been designed from the enhancement of a moving horizon estimation (MHE) approach with the inclusion of detection and isolation mechanisms.

In the control area, the development and implementation of conventional control strategies for OCIS are explored, and a nonlinear control strategy for interacting channels is proposed. Finally, the proposed control-oriented modeling strategy designed from approximated M&PEB is used in the design of an efficient optimization-based control approach for OCIS. This is a nonlinear model predictive control strategy that takes advantage of the control-oriented modeling strategy accuracy, and available information of the users' demands in the development of an optimization problem with a finite horizon, which is solved at each time instant with the objective to minimize losses caused by leaks and seepage while the users demands and operational and hydraulic restrictions of the OCIS are satisfied.

Resumen

El agua es el elemento más importante de la producción de alimentos y la forma más fácil y rentable de transportarla es a través de sistemas de riego de canal abierto (SRCA). Este tipo de sistemas tienen un alto impacto agrícola y ecológico. Sin embargo, la mayoría de los SRCA carecen de sistemas de automatización que mitiguen los costos económicos y ambientales acarreados por el desperdicio de agua. Adicionalmente, la mayoría de los SRCA automatizados carecen de estrategias de control y estimación que aumenten la eficiencia del sistema. Esta tesis está dedicada a explorar investigaciones existentes en torno a estrategias de modelado, control y estimación en SRCA, con el fin de identificar oportunidades de mejora y proponer nuevas estrategias de modelado, estimación y control que aumenten la eficiencia de estos. Primero, esta disertación revisa y discute las estrategias de modelado, estimación y control que se han reportado en el campo de los SRCA. A lo largo del proceso de revisión, se ha identificado que debido a la complejidad de los modelos fundamentales que describen las dinámicas de los SRCA, aparecen reportadas múltiples estrategias de modelado orientadas al control. Estas estrategias de modelado han sido clasificadas y discutidas, encontrando la necesidad de modelos orientados al control que incluyan lo siguiente:

- balances de energía potencial a lo largo de los canales;
- las no linealidades de las características hidráulicas que describen la dinámica de los SRCA;
- que puedan ser útiles para describir el comportamiento dinámico de SRCA que interactúan.

Además, se identifica la necesidad de estrategias de estimación diseñadas a partir de modelos precisos, que incluyan balances de energía potencial y descripciones no lineales de las dinámicas de los SRCA. También se identifica que el objetivo de control más común en los SRCA es mantener una profundidad constante en el extremo aguas arriba o aguas abajo de los canales, y este objetivo de control induce pérdidas constantes debido a fugas y filtraciones. A partir de las brechas identificadas, se han propuesto dos estrategias de modelado orientadas al control, las cuales incluyen información sobre los balances de energía potencial a lo largo de los canales, incluyen las no linealidades de las características hidráulicas que describen las dinámicas de los SRCA, y son útiles para describir el comportamiento dinámico de SRCA que interactúan. Las estrategias de modelado han sido validadas, obteniendo que mediante el uso de balances aproximados de masa y energía potencial (BM&EP) se puede llegar a una descripción precisa de las dinámicas de los

SRCA. Por lo tanto, la estrategia de modelado orientada al control propuesta a partir de BM&EP se utiliza en el desarrollo de estrategias determinísticas y estocásticas para la detección, el aislamiento, y la estimación de las magnitudes de flujos desconocidos, tales como fugas y filtraciones, que puedan afectar los SRCA. Las estrategias de estimación se han desarrollado modificando, mediante la inclusión de mecanismos de detección y aislamiento, una estrategia de estimación de horizonte móvil (EHM).

En el área de control, se explora el desarrollo e implementación de estrategias de control convencionales para SRCA y se propone una estrategia de control no lineal para canales interactivos. Finalmente, la estrategia de modelado orientada al control propuesta a partir de BM&EP se utiliza en el desarrollo de un enfoque de control eficiente para SRCA. La estrategia propuesta, es una estrategia de control predictivo no lineal basado en modelo, la cual aprovecha la precisión de la estrategia de modelado e información sobre las demandas de los usuarios en el desarrollo de un problema de optimización con horizonte finito, el cual se resuelve en cada instante de tiempo con el objetivo de minimizar las pérdidas ocasionadas por fugas y filtraciones al mismo tiempo que se satisfacen las demandas de los usuarios y las restricciones operativas e hidráulicas propias de los SRCA.

Contents

List of Figures

List of Tables

Notation

Symbol	Description
$\mathbb{Z}$	Set of integers
$\mathbb{R}$	Set of real numbers
$\mathbb{R}^n$	Space of n-dimensional (column) vector with real entries
$\mathbb{R}^{n\times m}$	Space of n by m matrices with real entries
$\|.\|$	2-norm of a vector
x_{m_i}	Depth at the m position of the i^{th} channel
$x(k)$	k indicates a discrete instant of time
$x(k+j \mid k)$	Prediction of x at time instant k for the time instant $k+j$
$\hat{x}$	The super script indicates that $\hat{x}$ is an estimated parameter
$\hat{\bar{x}}$	Estimated expected parameter
$\mathbb{E}(x)$	Expected value of the variable
$\bar{x}$	The super script indicates that $\bar{x}$ is an equilibrium point
δx	δ indicates small variation close and operation region
$\Delta x(k)$	Used to indicate variation respect an instant time (i.e., $\Delta x(k) = \Delta x(k) - \Delta x(k-1)$)
$x_{m_i}^{max}$	Maximum variable value at the m position of the i^{th} channel
$x_{m_i}^{min}$	Minimum variable value at the m position of the i^{th} channel

Acronyms

Acronym	Description
OCIS	Open-Channel Irrigation Systems
SVE	Saint-Venant Equations
DIMEUF	Detection, Isolation, and Magnitude Estimation of Unknown Flows
NLMPC	Nonlinear Model Predictive Control
CPED	Constant Potential Energy Difference
M&PEB	Mass and Potential Energy Balances
ID	Integrator Delay
LQR	Linear Quadratic Regulator
LQG	Linear Quadratic Gaussian Regulator
MPC	Model Predictive Control
IDZ	Integrator Delay Zero
OE	Output-Error
ARX	Autoregressive Exogenous
ARMAX	Autoregressive Moving Average with Exogenous Inputs
MAE	Maximum Absolute Error
IAE	Integral of the Absolute Error
StE	Steady-State Error
ISE	Integral Square Error
IAW	Absolute Gate Movement
IAQ	Integrated Absolute Discharge Change
ZI	Position Sensor
ZC	Position Control
LI	Level Indicator
FC	Flow Control
FB	Feedback
FF	Feedforward
PID	Proportional-Integral-Derivative
BC	Boundary Control
LPV	Linear Parameter-Varying
AVIS	Head Loss Automatic Gates
AVIO	High Head Loss Automatic Gates
SWMM	Storm Water Management Model
HEC-RAS	Hydrologic Engineering Center River Analysis System

SOBEK	Software Package for River, Urban or Rural Management
HC	Hydraulic Characteristics
OC	Operational Conditions
MHE	Moving Horizon Estimation
ODEs	Ordinary Differential Equations

Chapter 1

Introduction

1.1 Motivation

Through irrigation, it is possible to compensate the amount of water that crops need in dry seasons and to extend the productive land away from natural water sources. The easiest and most economical way to transport water in agriculture is through open-channels. Usually, water is taken from rivers and transported by using intricate networks of channels to each user. These networks are known as open-channel irrigation systems (OCIS). Nearly 70% of the water consumed in the world is used for irrigation (OECD, 2018), and most of the water is transported through open-channels. Moreover, the world population grows continuously. In 1980, the world population was around 4.4 billion. Now, there are about 8 billion people and in 2060 the population will likely increase to 10.2 billion (United Nations Department of Economic and Social Affairs Population Division, 2021). Consequently, in 40 years food production must increase by 30%.

On the other hand, the irrigation process has a high environmental impact since the water taken from a river reduces its flow, affecting life in the river and the surrounding ecosystem. Therefore, as it is highlighted by Lamnabhi-Lagarrigue et al. (2017), it is necessary to develop new approaches to increase food production by increasing the efficiency of the OCIS, where "efficiency is seen as the ratio of the volume of water delivered to the users and the volume of water extracted from the source" (Mareels et al., 2005).

This doctoral dissertation is focused on the exploration and proposition of alternatives that let the inclusion of control theory to increase the efficiency of the OCIS. More specifically, in OCIS, the fields of modeling, estimation, and control have been explored identifying punctual research gaps, which have been addressed.

In modeling, a rigorous analytical description of the OCIS can be reached by using the Saint-Venant Equations (SVE). However, due to the complexity of these equations, their direct use for estimation and control system design is impractical. Therefore, in the literature there are reports of multiple control-oriented modeling strategies, which are obtained by simplification of the SVE or by observation and empirical knowledge of the OCIS. However, in this thesis it has been observed that in OCIS, the control-oriented models that have been reported in the literature present limitations in the modeling of interacting channels, and do not include information about potential energy along them.

Similarly, the development of modeling and estimation strategies, useful for determining the magnitude and location of unknown flows such as seepage and leaks, appears as a valuable tool to increase the efficiency of the OCIS. However, it has been identified that in OCIS, most of the strategies reported on detection, isolation, and magnitude estimation of unknown flows (DIMEUF) have been developed from linear models that do not include information about energy balances along the channels, where these balances are fundamental to distinguish changes of levels due to conduction effects, from changes of levels due to unknown flows. Finally, in control, most of the OCIS are human-operated and present losses for overflows and inopportune control action effects.

These problems can be overcome by the inclusion of automatic controllers, which are usually designed to maintain a constant level at either the upstream or downstream end of the channels, ensuring water availability for the users. In the literature, multiple control strategies developed to maintain constant upstream or downstream channel levels have been reported. However, in OCIS the main source of losses are leaks and seepage, which are functions of the channels' levels. In that form, constant upstream or downstream levels guarantee constant leaks or seepage, reducing the OCIS efficiency.

In this order of ideas, in this doctoral dissertation, modeling, estimation, and control strategies aimed to cover the exposed research gaps are proposed. In modeling, two approximated modeling strategies useful for interacting OCIS, which include information about potential energy along the channels have been proposed. The first modeling strategy uses mass balances and assumes a constant potential energy difference along the channels, and the second one uses approximated mass and potential energy balances to improve the description of the potential energy difference along the channels. Finding that by using the approximated mass and energy balances, an accurate description of the OCIS dynamics can be reached.

In estimation, the modeling approach developed from simplified mass and energy balances is used in the development of deterministic and stochastic DIMEUF strategies, which can be used to detect, isolate, and estimate the magnitude of leaks and seepage at the upstream or downstream parts of the channels.

In control, the dissertation starts with an illustrative example that contextualizes a description of the most popular control-oriented modeling strategy reported in the literature, which is used in the development of the most common control techniques and configurations that have been reported in the OCIS control field. Moreover, in order to deal with the control problem of interacting channels, from the proposed control-oriented model that assumes a constant potential energy difference along the channels, a nonlinear model-based control strategy for interacting OCIS that ensures the stability of the closed-loop controlled scheme despite nonlinearities, internal delays, and channel interactions is proposed. Finally, with the objective of minimizing losses due to leaks and seepage, it is proposed a nonlinear model predictive control (NLMPC) strategy designed from simplified mass and energy balances, which uses previous request information of the users, with the objective of supplying an appropriate amount of water to the users minimizing losses due to seepage and leaks. In the development, sufficient controllability and reachability conditions that guarantee the stability of the closed-loop controlled scheme have been presented.

1.2 Research Questions

This dissertation is devoted to the development of modeling, estimation and control strategies that contributes to efficiency maximization in OCIS. The main goal of this thesis is motivated by the following key research questions:

(Q1) *What is the current context of modeling, estimation, and control in OCIS, and what are the main research gaps in this context that contribute to the OCIS efficiency increase?*

(Q2) *What are the decision features to select or design a suitable control-oriented modeling strategy for OCIS?*

(Q3) *How to design implementable approaches for recursive DIMEUF such as leaks and seepage in OCIS?*

(Q4) *How can the optimization-based control techniques contribute to improving the OCIS efficiency?*

Each of these research questions has been addressed through this thesis, and all of them contribute to the development of modeling, estimation, and control strategies aimed at efficiency maximization in the OCIS. Question (Q1) is devoted to understand and explain the process and to the identification of research gaps in modeling, estimation, and control that contribute to the OCIS efficiency increase. On the other hand, answers to questions (Q2)-(Q4) are the main contributions of this doctoral thesis.

1.3 Thesis Outline

This dissertation is divided into six chapters, and the main ideas and connections among chapters are presented in Figure 1.1. The contents of Chapters 2-6 are described next.

Chapter 2: Literature Review

This chapter provides a detailed review of modeling, DIMEUF, and control of OCIS towards providing useful information in the establishment of the state of the art, the acceptability of the existent techniques, and the challenges that remain open for future research. In this regard, the review is developed around a proposed classification for modeling, estimation, and control approaches. Moreover, a discussion with the aim of establishing suitable modeling, estimation, and control approaches and the research gaps that need to be addressed are also established. This chapter answers the research question (Q1), and is mostly based on the following publication:

- G. Conde, N. Quijano, and C. Ocampo-Martinez, "Modeling and control in open-channel irrigation systems: A review", Annual Reviews in Control, vol. 51, pp. 153–171, 2021.

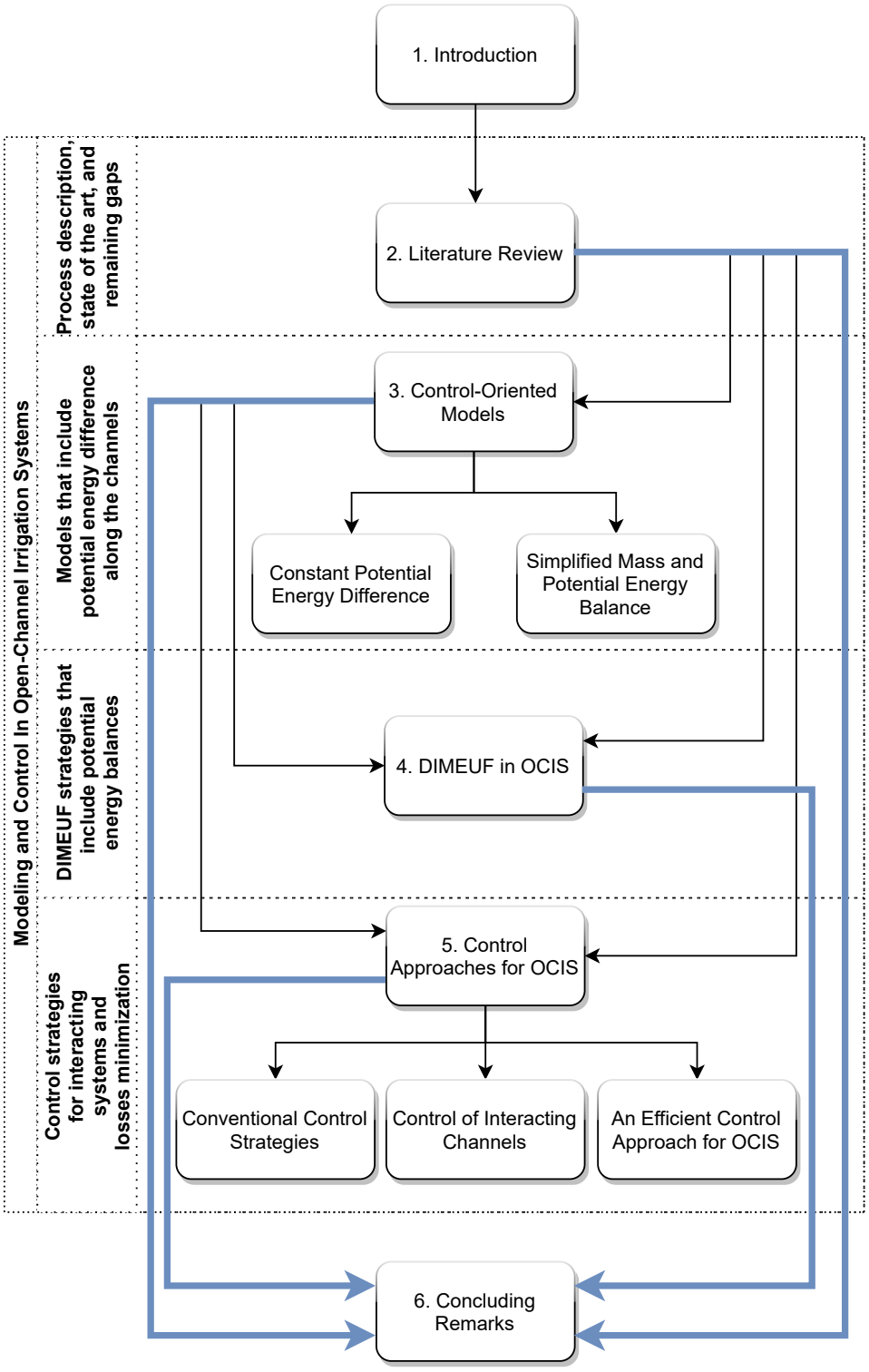

Fig. 1.1. Outline of the thesis. Blue arrows indicate the construction of the concluding remarks, and black arrows indicate read-before relations.

Chapter 3: Control-Oriented Modeling Approaches for OCIS

This chapter presents the analyses of three control-oriented modeling approaches useful to describe the nonlinear dynamic behavior of interacting OCIS. The first one is a previously reported modeling approach that does not include information about potential energy along the channels. The second one is a proposed approach that assumes a constant potential energy difference (CPED) along the channels. The latter is another proposed approach developed from approximated mass and potential energy balances (M&PEB) along the channels. This chapter answers the research question (Q2), and is based on the following publications:

- G. Conde, N. Quijano, and C. Ocampo-Martinez, "Modeling and control of interacting irrigation channels," in Proceedings of the 4th IEEE Colombian Conference on Automatic Control (CCAC), 2019, pp. 1–6.
- G. Conde, N. Quijano, and C. Ocampo-Martinez, "Control-oriented modeling approach for open-channel irrigation systems", in Proceedings of the IFAC 21s World Congress, 2020, pp. 16630–16635.

Chapter 4: DIMEUF in OCIS

This chapter explores the development of deterministic and stochastic strategies for DIMEUF in OCIS. The DIMEUF strategies are designed from the proposed control-oriented modeling approach that has been developed from approximated mass and potential energy balances, obtaining two estimation strategies that take into account the effects of flow conduction. This chapter answers the research question (Q3), and is based on the following publications:

- G. Conde, N. Quijano, and C. Ocampo-Martinez, "An Unknown Input Moving Horizon Estimator for Open-Channel Irrigation Systems," in Proceedings of the European Control Conference (to appear), 2021.
- G. Conde, N. Quijano, and C. Ocampo-Martinez, "Detection, isolation, and magnitude estimation of unknown flows in open-channel irrigation systems," IEEE Access, vol. 9, pp. 115348–115369, 2021.

Chapter 5: Control Approaches for OCIS

This chapter covers the findings in developed research on control for OCIS. The chapter starts with an illustrative example that shows a contextualized description of the most popular control-oriented modeling strategy, and the most common control techniques and configurations that have been reported in the OCIS control field. Moreover, from the control-oriented model that assumes a constant potential energy difference along the channels, a nonlinear model-based control strategy for interacting OCIS that ensures the stability of the closed-loop controlled scheme despite nonlinearities, internal delays, and channel interactions is proposed. Finally, an efficient control strategy for OCIS is

proposed. The strategy is developed with the objective of supplying an appropriate amount of water to the users minimizing losses due to seepage and leaks. In the design process, sufficient controllability and reachability conditions that guarantee the controlled system stability are presented. This chapter answers the research question (Q4), and is based on the following publications:

- G. Conde, N. Quijano, and C. Ocampo-Martinez, "Modeling and control in open-channel irrigation systems: A review", Annual Reviews in Control, vol. 51, pp. 153–171, 2021.
- G. Conde, N. Quijano, and C. Ocampo-Martinez, "Modeling and control of interacting irrigation channels," in Proceedings of the 4th IEEE Colombian Conference on Automatic Control (CCAC), 2019, pp. 1–6.
- G. Conde, C. Ocampo-Martinez, and N. Quijano, "An efficient control approach for open-channel irrigation systems," Water Resources Research (submitted), 2021.

Chapter 6: Concluding Remarks

This chapter provides some concluding remarks regarding the results obtained and presented in Chapters 2-5. The key research questions, introduced in Section 1.2, are evaluated. Furthermore, this chapter also suggests some open questions for future research.

Chapter 2

Literature Review

In most countries, the operation of the OCIS is in charge of user associations, which maintain the system under suitable conditions, manage the economic resources, and calculate, assign, and supply the appropriate amount of water to the users. The water assignment process can be performed in multiple modes, such as:

Rotational mode: In this mode, the central administration develops the supply policies and allocates the amount of water and time duration of the flow delivered to each user.

On-request mode: In this mode, the user must request in advance the amount of hydraulic resource that will be used.

On-demand mode: In this mode, the user is free to take water from the system when it is needed.

According to the assignment process and the hydraulic features of the system, the central administration must calculate the water levels and flows throughout the OCIS, which are regulated by gates and weirs. The positions of the gates and weirs are calculated with the aim of assigning a specific amount of water to each user. Most of the OCIS operate in rotational and in on-request modes in absence of automatic control systems. Therefore, each regulation structure is manually adjusted by operators, who must carry out this task throughout many kilometers of channels and hundreds of regulation structures. In the normal operation of the OCIS, it is common to find disturbances such as flow variations at the source, channel obstructions, leaks, overflows, and demand changes. These types of disturbances lead to water spillages that affect the OCIS efficiency (Litrico and Fromion, 2006a).

In order to promote the implementation of automatic control in OCIS, in the last three decades, multiple works that review the advances in modeling and control of OCIS have been reported. For instance, Malaterre (1995) presents an exhaustive characterization of regulation methods for OCIS, showing the need to unify definitions and concepts in a field where there is a convergence of civil, hydraulic, and control engineers. Schuurmans (1997) shows basic principles for understanding the control problem in OCIS, explaining the finite-difference model and proposing the integrator delay (ID) model to

adjust the real dynamic behavior of OCIS in a simple way. Moreover, in the control area, Schuurmans (1997) presents the implementation of traditional controllers such as the linear quadratic regulator (LQR) and the linear quadratic Gaussian regulator (LQG). Malaterre et al. (1998) review and classify the implemented controllers according to the variables (controlled, measured, control-action), the logic of control (type and direction), and design technique. Furthermore, Malaterre and Baume (1998) explore several modeling techniques and control strategies. Mareels et al. (2005) and Cantoni et al. (2007) discuss some aspects such as infrastructure automation, control objectives, and system identification. Weyer (2008) shows alternatives in centralized and decentralized control. Moreover, Malaterre (2008) reviews the main concepts and strategies in the control of OCIS. Over the last decade, the task committee on recent advances in canal automation provides a practical guide on OCIS automation (Wahlin and Zimbelman, 2014). This guide covers topics about supervisory control and data acquisition, as well as fundamentals in the design and implementation of control strategies. Finally, Ding et al. (2018) provide a review focused on applications of model predictive control in agriculture, where it can be highlighted that, in agriculture, OCIS is the area that shows more MPC applications.

As can be seen, the OCIS control problem is an issue of interest, which has been continuously studied and reported in several works. Equally important, the selection of an accurate control-oriented model of the system is a key stage that must be addressed before selecting, designing, and implementing a control strategy. Additionally, the development of strategies for detection, isolation, and magnitude estimation of unknown flows (DIMEUF) such as seepage and leaks appears as a valuable tool to increase the efficiency of the OCIS. However, it has been identified that in the reported reviews, the topics of control-oriented modeling and DIMEUF have not been broadly addressed. Therefore, in the OCIS field, there is a need to:

- Review recent modeling, DIMEUF, and control techniques that have been reported.
- Establish the suitability of existent techniques.
- Report challenges that remain open for future research.

In this way, the motivation of this chapter is to provide a detailed review of modeling, DIMEUF, and control of OCIS towards providing useful information in the establishment of the state of the art, the suitability of the existent techniques, and the challenges that remain open for future research.

2.1 Process Description

In the current framework, an open-channel is a structure used to transport water. Typically, open-channels present a trapezoidal shape, but there are channels with cylindrical, parabolic, rectangular, and irregular shapes. In the literature, there is not a unified notation for the inputs, outputs, and state variables of OCIS. In Figure 2.1, the proposed representation for OCIS is shown. In this case, the channel p_i is fed by the flow q_i that

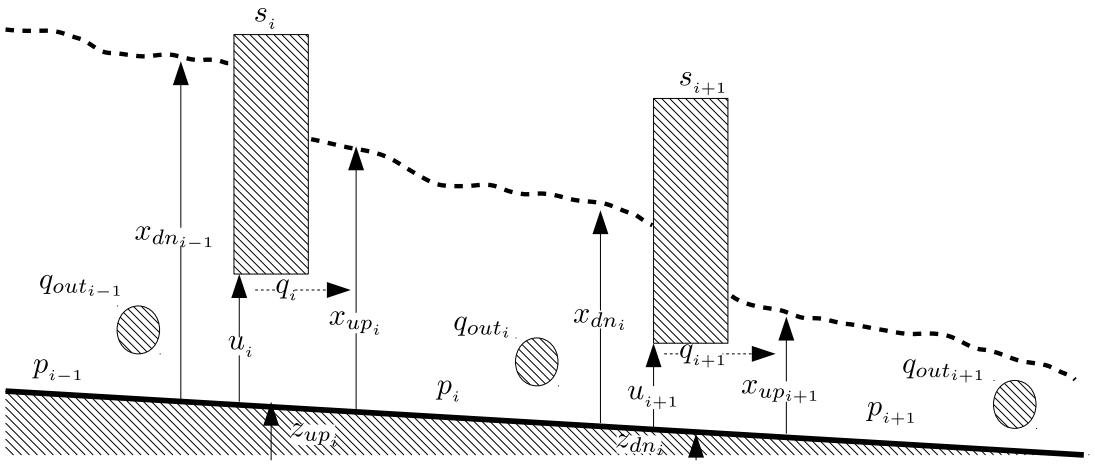

Fig. 2.1. Proposed representation for OCIS.

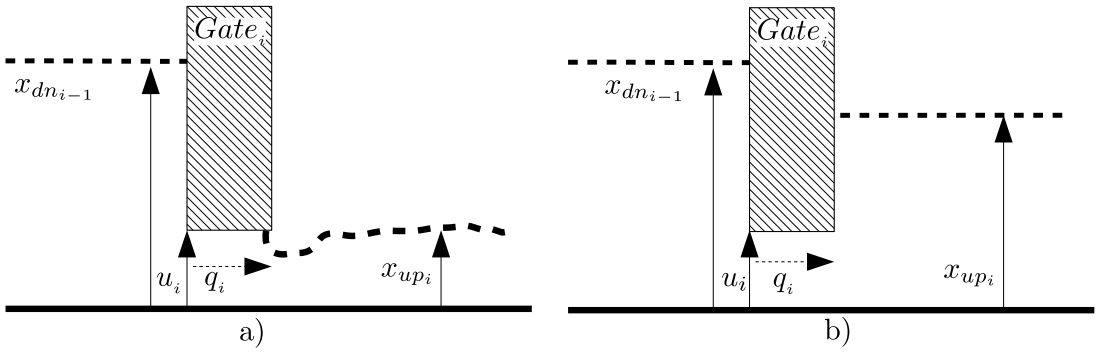

Fig. 2.2. Flow relation for: a) Gate in free flow. b) Gate in submerged flow.

comes from the upstream channel p_{i-1}. Besides, m_i is a position inside p_i, from the upstream end of the channel, and x_{m_i} represents the depth at the m_i position. For control purposes, the most important output variables are the upstream and downstream depths of a channel, denoted by x_{up_i} and x_{dn_i}, respectively. From the channel p_i there could be multiple outflows to other channels or users. In Figure 2.1, the outflows are simplified into an outlet flow q_{out_i}, and the flow that feeds the downstream channel q_{i+1}. The most notorious feature is that, in steady-state, the volume in a channel increases when the inflow increases, and decreases when the outflow increases. The flow q_i has an hydraulic relationship with the regulation structures, and these structures can be divided into gates (Figure 2.2) and weirs (Figure 2.3), which can be in free flow or submerged flow (Litrico and Fromion, 2009). In Table 2.1, the most common mathematical relationships for the discharge through each type of regulation structure are given, where u_i (m) is the position of the regulation structure, w_i (m) the width of the regulation structure, g the gravity constant, c_i (with appropriate dimensions) the discharge coefficient. For gates in free flow, the parameter ι has been included as a modeling-tuning parameter in reason of some modeling and simulation algorithms use $\iota = 0$ (e.g., Wahlin and Zimbelman 2014), and other strategies use $\iota = 0.5$ (e.g., Lewis 2017).

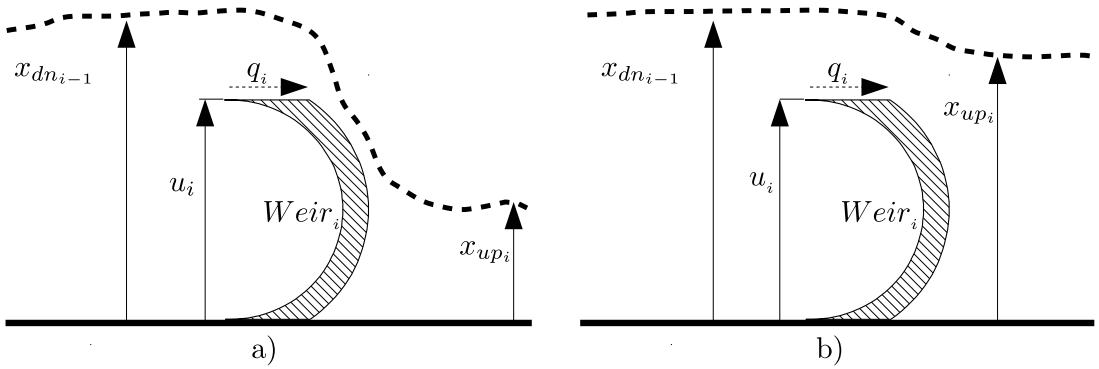

Fig. 2.3. Flow relation for: a) Weir in free flow. b) Weir in submerged flow.

Table 2.1. Flow relation for different categories of regulation structures

	Free flow	Submerged flow
Gate	$q_i = c_i w_i u_i \sqrt{2g}\sqrt{x_{dn_{i-1}} - \iota u_i}$	$q_i = c_i w_i u_i \sqrt{2g}\sqrt{x_{dn_{i-1}} - x_{up_i}}$
Weir	$q_i = c_i w_i \sqrt{2g}(x_{dn_{i-1}} - u_i)^{3/2}$	$q_i = c_i w_i \sqrt{2g}(x_{dn_{i-1}} - x_{up_i})^{3/2}$

2.2 Modeling

A control-oriented model is a mathematical representation of a system that is used for the description, explanation, and prediction of its behavior, which helps to understand its dynamics and design control systems with the aim of reaching a desirable performance. Obtaining control-oriented models for OCIS is an aspect that has a high number of alternatives, and there is not a final rule for choosing a modeling methodology. In 1871, Adhemar Jean Claude Barre de Saint-Venant proposed appropriate simplifications to adjust the Navier-Stokes equations to channels and derived the Saint-Venant equations (Darrigol, 2006), which describe the dynamics of infinitesimal flow in one direction. Since then, the Saint-Venant equations (SVE) have been the most used mathematical tool for modeling open-channels and rivers. The SVE are two non-linear partial differential equations given by

$$w_{m_i}\frac{\partial x_{m_i}}{\partial t} = -\frac{\partial q_{m_i}}{\partial m} - s_{m_i}, \tag{2.1a}$$

$$\frac{\partial q_{m_i}}{\partial t} = -2\beta\frac{q_{m_i}}{a_{m_i}}\frac{\partial q_{m_i}}{\partial x} + \beta w_{m_i}\frac{{q_{m_i}}^2}{{a_{m_i}}^2}\frac{\partial x_{m_i}}{\partial x} - \frac{|q_{m_i}|\, q_{m_i} g n^2}{a_{m_i}{r_{x_i}}^{4/3}} + g\left(z_{s_i} - \frac{\partial x_{m_i}}{\partial x}\right)a_{m_i}, \tag{2.1b}$$

where (2.1a) is related to mass conservation, and (2.1b) is related to momentum conservation. Moreover, w_{m_i} is the channel width, s_{m_i} is a variable associated with leaks, β is a momentum correction coefficient, a_{m_i} is the wetted surface, r_{m_i} is the hydraulic radius, z_{s_i} is the channel's slope, and n is the Manning's resistance coefficient. The variables x_{m_i} and q_{m_i} are related to depth and flow, respectively (Chaudhry, 2008; Schuurmans, 1997). The direct use of the SVE for control systems design is impractical (Rabbani et al., 2010), and this affirmation can be corroborated analyzing the works reported by

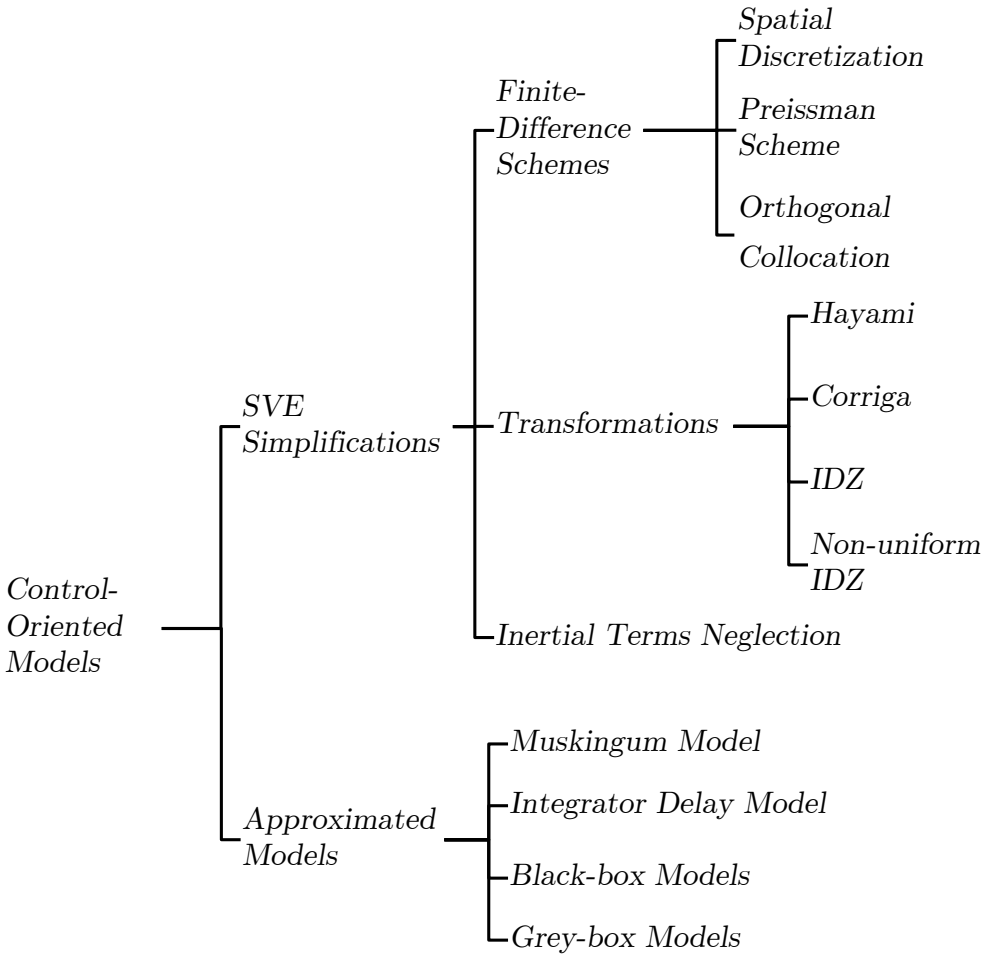

Fig. 2.4. Classification of control-oriented models for OCIS.

Liu et al. (1995) and Dos Santos and Prieur (2008), where the development of control strategies using the non-linear partial SVE shows unsystematic procedures. Therefore, in the literature, there are multiple types of control-oriented models that describe the dynamics of irrigation channels and, as shown in Figure 2.4, these models can be classified into two fields: i) models that come from analytical simplifications of the SVE; and, ii) models that come from approximations, observations, and assumptions of the dynamic behavior of the OCIS.

2.2.1 Models Obtained from Simplifications of the SVE

These models could be divided into three subgroups. In the first group, for the linearized and non-linearized SVE, explicit and implicit finite-difference schemes are proposed. Balogun et al. (1988) present an explicit spatial discretization of the SVE where each channel is divided into sections, and for each section one differential equation for depth and another differential equation for flow are obtained. The weakness of this kind of discretized models is that their stability depends on the discretization step size. Therefore, in order

to obtain a stable control-oriented model, the obtained model has a high order. this modeling strategy is used in several reported works (e.g., Reddy 1990b; Garcia et al. 1992; Mohan Reddy et al. 1992; Mohan Reddy 1995; Reddy 1996; Mohan Reddy and Jacquot 1999; Durdu 2004, 2006; Lemos et al. 2009; Durdu 2010; Feng and Wang 2011; Shang et al. 2011; Xu et al. 2012; Breckpot et al. 2013; Soler et al. 2013a; Cen et al. 2017; Bonet et al. 2017; Lacasta et al. 2018). On the other hand, Malaterre (1998) uses an implicit Preissmman finite-difference scheme, with the advantage that the stability of the model does not depend on the discretization step size, and Liu et al. (1998) propose the use of this scheme in the development of a control strategy based on an inverse solution of the nonlinear SVE. The use of control-oriented models based on the Preissmman scheme has been reported in multiple studies (e.g., Pages et al. 1998; Malaterre and Khammash 2003; Figueiredo et al. 2013). Dulhoste et al. (2004) propose the use of an orthogonal collocation method to obtain a finite-dimensional model. The advantage of this numerical method relies on its less-computational effort with respect to other numerical methods in the solution of partial differential equations. However, when the main purpose is to obtain a control-oriented model, the orthogonal collocation method is not the best option, since the mathematical synthesis of the method is harder than the spatial discretization and the Preissmman scheme. Finally, the Lattice Boltzmann method, which has been proposed to solve partial differential equations such as the SVE, has been also used in the development of control-oriented models for OCIS. The Lattice Boltzmann method has shown that is efficient and accurate (Pham et al., 2010; Le-Duy-Lay et al., 2017). Moreover, Van Thang et al. (2017) establish that the control-oriented models obtained by using this method are suitable to describe networks of OCIS that are coupled with diverse kinds of hydraulic regulation structures.

In the second subgroup, the continuous spatial structure is preserved. However, linearizations, transformations, and partial solutions of the linearized SVE are proposed. Hayami (1951) propose the linearization of the SVE with the intention of analyzing the flow in rivers. Later, Corriga et al. (1980) propose the Laplace transformation of the linearized SVE with the aim of obtaining analytical solutions that describe the behavior of the level and flow along the channels. Then, the analytical solutions are evaluated in the boundary conditions obtaining delayed transfer functions that describe the relationship between channel inflow and outflow. The modeling strategy proposed by Corriga et al. (1980) has been adopted by Reddy (1990a) and Qiao and Yang (2010), who perform a more detailed explanation of the linearization of the SVE. One disadvantage of this strategy is that the model parameters are based on mean values of variables in steady-state conditions (Schuurmans, 1997). Litrico and Fromion (2004a) show that the linearized Laplace transform of the SVE are spatial linear ordinary differential equations that are solved obtaining a transfer function matrix with x_{up} and x_{dn} as outputs, and q_i and q_{i+1} as inputs. This model is called the *integrator delay zero* (IDZ), which has been contrasted with the frequency domain response and time response of linearized SVE numerically solved with a Preissmmann scheme showing a similar behavior (Litrico and Fromion, 2004b). Additionally, Litrico and Fromion (2004c) propose a systematic procedure to use the IDZ to obtain control-oriented models of OCIS. This modeling strategy shows more accurate behavior than other techniques in resonant systems (Clemmens et al., 2017),

and recently, has been used for modeling, control, and estimation purposes (e.g., Horváth et al. 2014b; Puig et al. 2015; Dalmas et al. 2017; Segovia et al. 2017, 2018c,b). Similar to the work developed by Litrico and Fromion (2004a), Ouarit et al. (2003) establish a transfer function matrix, where the flow is also an output of the system, and the inputs are related to the regulation structures position. The advantage of this model is that there are not assumptions of uniform regime along the channel, consequently, this model has been called as an *IDZ model in non-uniform regime* (Dalmas et al., 2017).

Finally, another reported way to simplify the SVE is to neglect their inertial terms. This strategy has been reported by Papageorgiou (1983) and Montero et al. (2013). In the modeling strategy reported by Papageorgiou (1983), a first-order delay differential equation that describes a relation between the downstream depth and upstream depth of a channel is obtained. This strategy is reported again by Papageorgiou and Messmer (1985). On the other hand, in the strategy reported by Montero et al. (2013), a more complex partial differential equation that needs to be solved using numerical methods is obtained. It must be highlighted that the simplified modeling strategy proposed by Papageorgiou (1983) could be useful for obtaining control-oriented models that include the nonlinear behavior of gates and weirs in submerged and free flows.

Given these models, it is identified that most of the simplified modeling strategies require operational information of the system. For instance, key parameters of the simplified models proposed by Hayami (1951), Corriga et al. (1980), and Litrico and Fromion (2004a), need information about mean flow velocity, which can change in the presence of strong disturbances like obstructions or even with level and/or flow changes. Moreover, in the cases of finite-difference schemes, models with high order are obtained. These aspects can be considered as drawbacks in control systems designs. Therefore, in order to avoid these issues, some researchers have contributed to the development of new approximated modeling strategies with practical assumptions.

2.2.2 Approximated Models

The approximated models such as the Muskingum model, ID, the grey-box models, and the black-box models, are models that have been developed from practical assumptions, using basic physical principles, observations, and empirical knowledge. Even though the approximated models do not have rigorous physical fundament, the reported works have shown that the approximated modeling strategies are an important alternative to obtain control-oriented models for OCIS. Therefore, a more detailed description of these strategies is given next.

The Muskingum model, proposed by McCarthy (1939) from observations of the Muskingum river data, is one of the most widely used models for flow routing analysis. The Muskingum model has a mass balance per channel and an storage-discharge equation, which are used to obtain a transfer function that relates the inflow with the outflow of a channel. This information is not useful when the objective is to control either the upstream or downstream channel depth. However, it is possible to assume a two-part channel division, where the first part is described by the Muskingum model, and the sec-

ond part is a reservoir described by the continuity equation, obtaining a transfer function that relates the inflow and the downstream level (Horváth et al., 2014b).

In his doctoral thesis, Schuurmans (1997) proposes the ID model, which is inspired by the modeling strategy proposed by Corriga and includes the phenomenon known as *backwater profile*. The characteristic of this phenomenon is that, at the downstream end of the channel, there is an accumulation of water. In this model, the channel is assumed to be divided into two parts: the first part corresponds to a uniform flow, and the other (considered as the backwater), where the system is analyzed as a reservoir. In that form, the depth along the uniform part is a function of the flow, and the backwater part is modeled as a mass balance with an inflow delay. The main advantage of this strategy is the simplicity of the model. Therefore, in the literature, the ID model is one of the most reported modeling strategy for OCIS, which has been used for control design in multiple studies (e.g. Wahlin 2004; Litrico and Fromion 2004c,a; Koenig et al. 2005; van Overloop et al. 2005; Litrico and Fromion 2006b; Litrico et al. 2007; van Overloop et al. 2008a; Litrico and Fromion 2009; van Overloop et al. 2010a; Horváth et al. 2014b; Bolea et al. 2014c; van Overloop et al. 2014; Horváth et al. 2015b,a; Zheng et al. 2019).

The use of measured data is another important option to obtain control-oriented models for OCIS. This strategy called identification can be used to obtain models without physical knowledge of the system (black-box models), or models that present a structure based on the physical knowledge of the system (grey-box models) (Horváth et al., 2014b).

The black-box or experimental models can only be obtained with measurements from a real system, and the result does not describe the physical phenomena, (it only describes the relationship between the measurement input and output data (Roffel and Betlem, 2007)). For example, Begovich et al. (2007) use a matrix of second-order discrete transfer functions in the identification of four open-channels, where the validation results show a high correlation between the real system and the obtained model in a variation depth zone of 0.04m. The parametric identification method can be either batch or recursive. In the batch identification method, by an experimental procedure, a set of input and output data is acquired from the system and, with the use of an optimization algorithm, the parameters of the model are obtained. On the other hand, in the recursive method, the parameters of the system are obtained during the control process, and the obtained model could be used in tuning the controller in real-time. One important advantage of the recursive optimization is that this method is useful to deal with time-variant parameter systems (Rivas Perez et al., 2007) and nonlinearities (Diamantis et al., 2011). The structure selection is another important aspect in the identification process, which can be outup-error (OE), autoregressive exogenous (ARX), autoregressive moving average with exogenous inputs (ARMAX), and Box–Jenkins, among others (Roffel and Betlem, 2007). The most common structure used in systems identification is the ARMAX structure, since it includes dynamics of the disturbances (Rivas Perez et al., 2007). However, Sepulveda (2007) presents a detailed methodology to obtain identification models using ARX structures in real channels. Another important technique used to obtain control-oriented models for OCIS is the step response identification, in which from a step stimulus at the input, a transfer function that describes a similar behavior is adjusted. In OCIS, the transfer function is usually a second-order delayed function (e.g., Feliu-Batlle et al. 2007,

2009a; Blesa et al. 2010; Feliu-Batlle et al. 2011; Bolea et al. 2014a) or a first-order delayed function (e.g., Romera et al. 2013; Bolea et al. 2014b). On the other hand, OCIS that are deep, short, smooth, and have low flows are expected to be dominated by resonance behavior. In these cases, the order of the resultant transfer function is higher because there are resonant characteristics that, in short channels, are more dominant (van Overloop et al., 2014). Therefore, van Overloop et al. (2014) propose the *integrator resonance model* composed of one integrator and one underdamped second-order transfer function. This model has the particularity of not having a time delay. The model is validated with a laboratory channel, which is controlled with predictive controllers designed from *ID model*, *ID model plus a first-order filter*, and the *integrator resonance model*. The system controlled with predictive controllers designed from *integrator resonance model* shows the best performance.

The use of data-driven modeling tools is also presented in the development of models that describe the dynamics of OCIS. Tavares et al. (2013) propose a comparison between models based on neural networks, fuzzy systems, and linear systems. The result shows that describing the behavior of OCIS, the neural networks are slightly better than the linear and fuzzy systems. Herrera et al. (2013) use pattern search methods in online identification of the time-varying delay of OCIS. This strategy, called *multi-model scheme*, uses a set of models with diverse and updated time delays, where a pattern search algorithm estimates the amount of the corresponding time delay. On the other hand, in the field of grey-box models, Weyer (2001) proposes a control-oriented model based on a simplified mass balance, assuming that the water volume in the channel is proportional to the water level and there is a time delay in the channel inflow. Therefore, the model proposed has a differential equation by channel that describes a mass balance, where the nonlinear flow relation of the regulation structures is incorporated. This modeling strategy has been used for control design, and leak detection in multiple works (e.g., Weyer 2002; Zhang and Weyer 2005; Li et al. 2005; Ooi and Weyer 2005; Mareels et al. 2005; Choy and Weyer 2006; Weyer 2006; Cantoni et al. 2007; Ooi and Weyer 2008b; Weyer and Bastin 2008; Weyer 2008; Ooi and Weyer 2008a, 2011; Bedjaoui and Weyer 2011). In OCIS, the reported grey-box models are nonlinear models, and these models are more accurate than the linear models representing the dynamics of OCIS (Weyer, 2001). Additionally, these models could be used to test the behavior of linear controllers in presence of nonlinearities associated with the regulation structures. However, in most of the cases, the grey-box models have been only used for systems with weir structures in free flow. In these cases, the flow is only a function of the regulation structure upstream depth. Eurén and Weyer (2005) use grey-box models in a system with both undershoot and overshoot regulation structures. However, this work is developed in a single channel, without opportunities to analyze the configuration of the model when there are channel interactions.

2.3 Control of OCIS

In OCIS, the principal objective is to deliver the appropriate amount of water to each user. In a well-operated system, the intake water must be equal to the water used or, in other words, the wastage of water should be reduced to a minimum (Weyer, 2008).

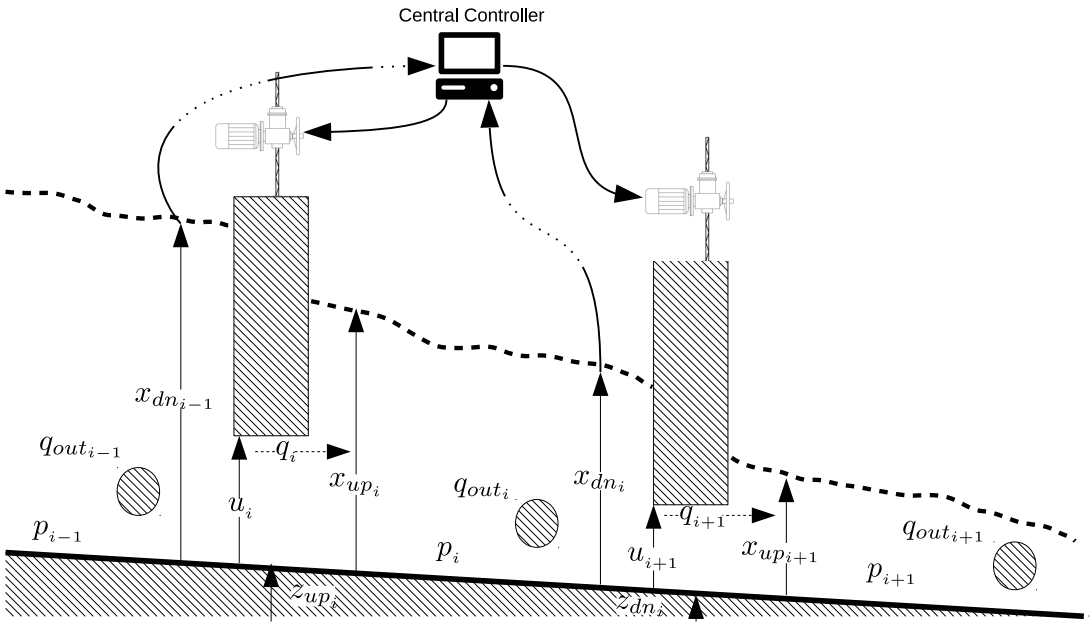

Fig. 2.5. Example of two channels controlled with a centralized control architecture.

Ideally, this is an easy task when there are no dynamics in the system. However, OCIS are complex systems with long delays, high channel interactions, intermittent demands, disturbances, and multiple inputs and outputs. Consequently, the control of OCIS can be analyzed using multiple approaches, which are complex to classify (Malaterre et al., 1998). However, these approaches, which have been classified in control architectures, control objectives, control-action variables, control configurations, and control strategies are presented next.

2.3.1 Control Architectures

The most common control architecture in OCIS is the centralized control architecture. As shown in Figure 2.5, in the centralized control architecture (e.g., Begovich et al. 2007; Nasir et al. 2018; Aydin et al. 2017; Horváth et al. 2015b,a), a central controller uses the vector of system measurements to compute the vector of control signals (Malaterre, 1995). On the other hand, as shown in Figure 2.6, in a decentralized architecture (e.g., Gomez et al. 2002; van Overloop et al. 2005; Segovia et al. 2017; Weyer 2008), only local upstream or downstream information of a channel is used to compute the control strategy. Finally, in a distributed architecture (Figure 2.7), the control system computation uses local and adjacent information establishing cooperation among local controllers (Le-Duy-Lay et al., 2017).

In centralized architectures, it is possible to reach a better performance than in both decentralized and distributed architectures. However, a decentralized or distributed control system offers the opportunity of keeping the system controlled (with a possible performance degradation) even if part of the information is lost. In addition, non-centralized architectures allow partial implementations in channels according to budget and relevance.

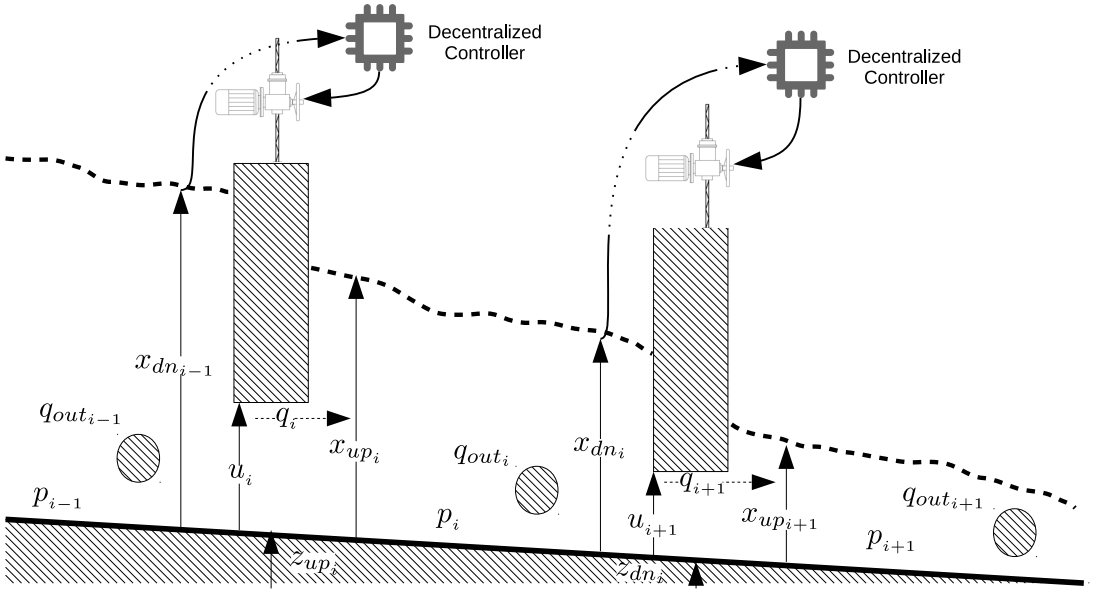

Fig. 2.6. Example of two channels controlled with a decentralized control architecture.

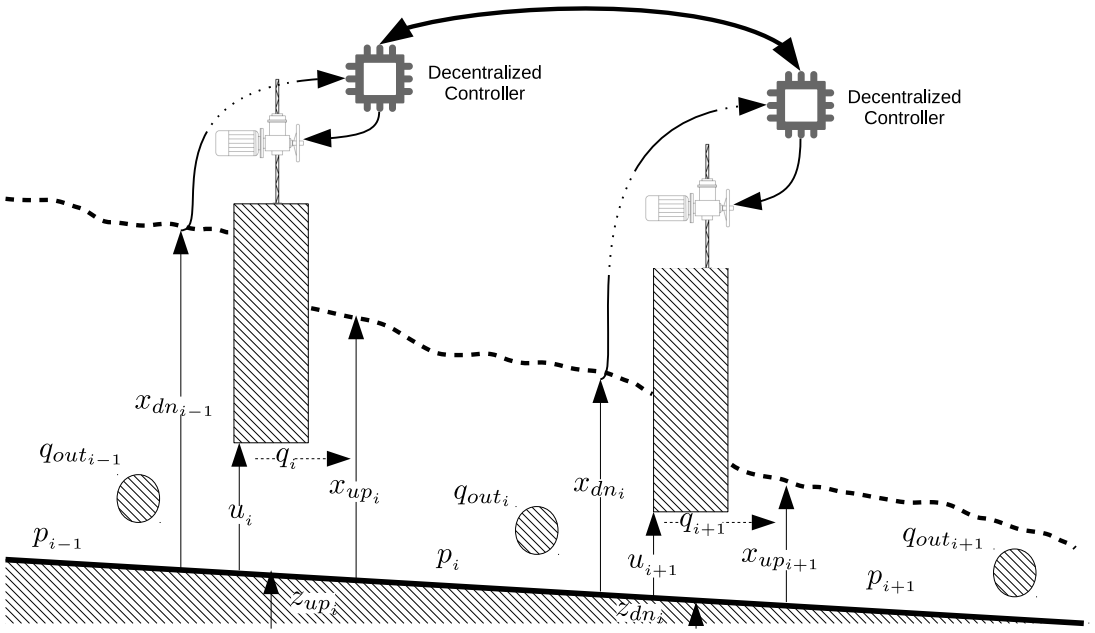

Fig. 2.7. Example of two channels controlled with a distributed control architecture.

Although OCIS are strongly coupled systems, in some cases for decentralized schemes, each channel is taken as an independent system and the control design only deals with the problem of controlling a particular channel. This kind of approach can lead to unacceptable performance or even instability of the whole system (Schuurmans, 1997). On the other hand, some authors propose to join the advantage of the centralized and decentralized architectures into a hierarchical control architecture. As shown in Figure 2.8,

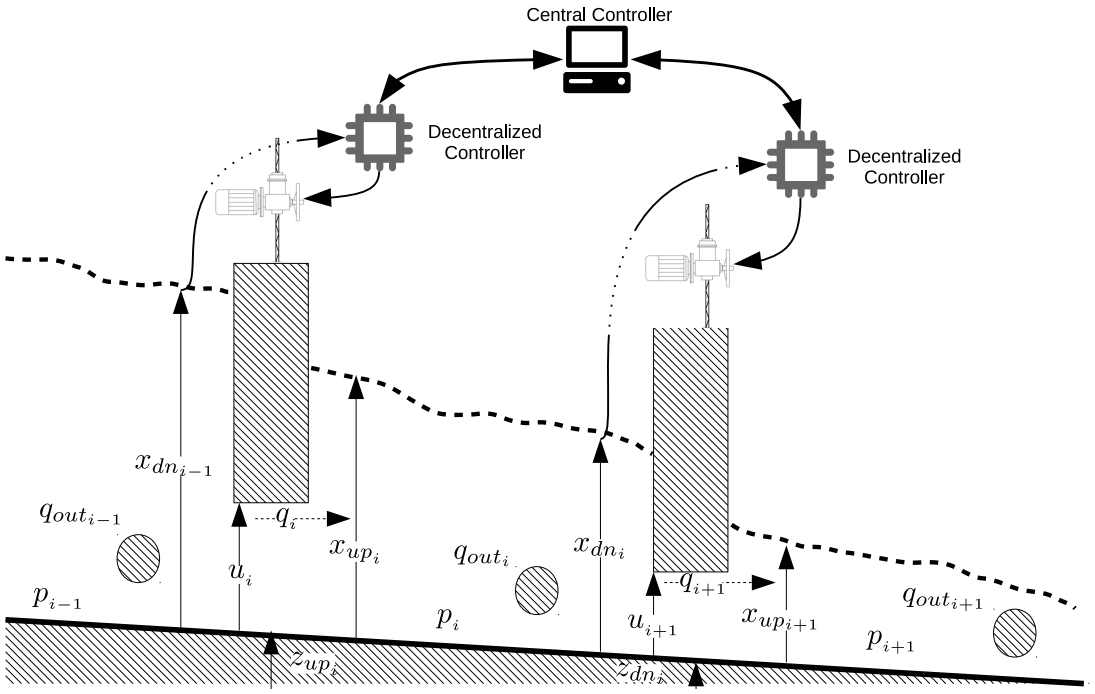

Fig. 2.8. Example of two channels controlled with a hierarchical control architecture.

in the hierarchical control architecture, the performance of a system under decentralized schemes is enhanced with coordination of a centralized controller. In this architecture, the decentralized controllers keep the system controlled even if the communication is lost, and in order to enhance the overall performance and even to prevent risks, the centralized system modifies the targets of the decentralized systems (e.g. Zafra-Cabeza et al. 2011; Fele et al. 2014; Sadowska et al. 2015a; Farhadi and Khodabandehlou 2016). For the sake of simplicity, and the need of a centralized controller, in this review, the hierarchical control architecture is treated as a case of centralized control architecture.

2.3.2 Control Objectives

Usually, in OCIS, a constant depth is set at each channel, and with the position adjustment of the outlet structure, the discharges are regulated to each user (Cantoni et al., 2007). In decentralized and distributed control architectures, the use of the terms *upstream control* and *downstream control* is common. As shown in Figure 2.9 in the upstream control, a fixed level upstream of the cross regulation structure is maintained (e.g., Malaterre 2008; Rijo and Arranja 2010; Clemmens et al. 2017; Figueiredo et al. 2013), while in the downstream control, as shown in Figure 2.10, the level is maintained downstream of the cross regulation structure (e.g., Malaterre 2008). Additionally, the upstream and downstream controllers can be placed close, intermediate, or far away from the regulation structure. In the literature, there are no reports about the use of intermediate downstream and upstream control, since this implies measuring the depth in an intermediate part of the channel and the hardware adequacy far from the cross structures is impractical.

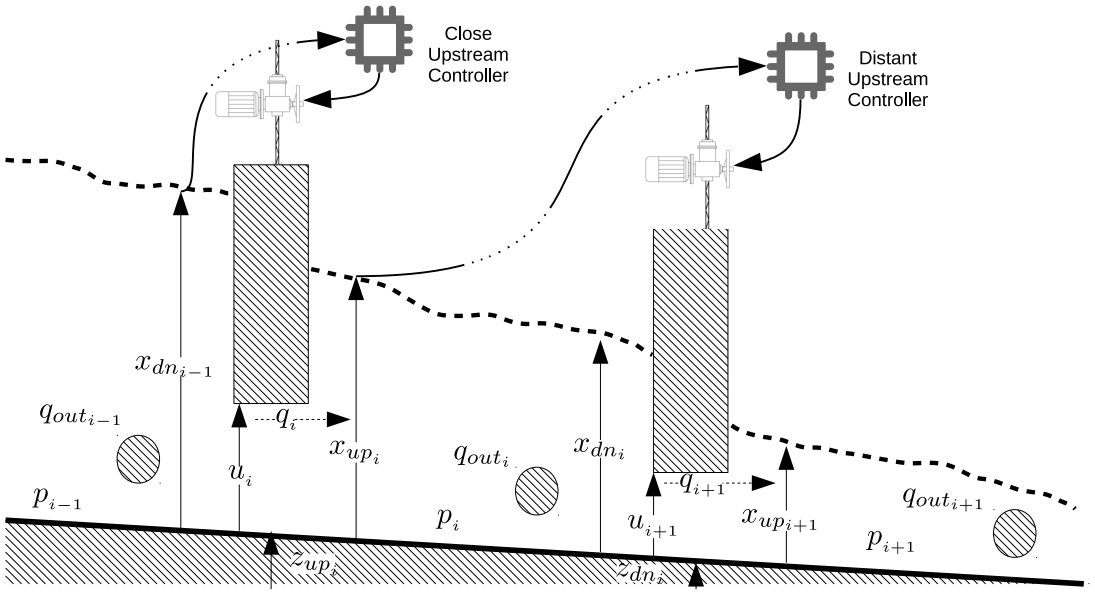

Fig. 2.9. Examples of close and distant upstream control objectives.

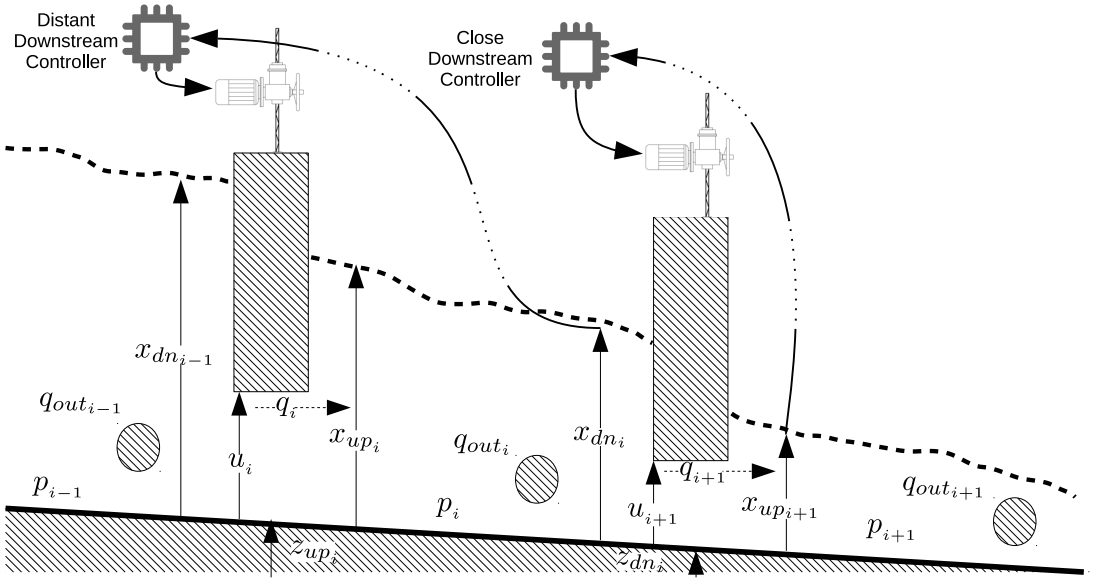

Fig. 2.10. Examples of close and distant downstream control objectives.

Distant upstream control is another infrequent alternative. For instance, Lemos and Sampaio (2015) establish that this configuration does not guarantee a water level along the channel. Additionally, Rato et al. (2007) compare the effectiveness of an adaptive controller implemented in an open-channel, first controlling the upstream level close to the regulation structure, and second testing the same strategy controlling the upstream level distant from the regulation structure. In the first configuration, the results of the adaptive strategy present an appropriate behavior, but in the second configuration, the adaptive strategy shows oscillations and undesirable performance. Regulate the upstream level

close to the regulation structure is the most common control method in OCIS (Clemmens et al., 2017). This method requires a flow control at the intake of the system, where the intake flow is calculated in order to satisfy the users' demands. Therefore, excess in the intake flow will result in spills. In contrast, deficiencies in the intake flow, losses, or unforeseen demands will result in deficient flow at the system downstream.

In downstream control, each regulator delivers the amount of flow to maintain the level downstream of the cross structure. Therefore, this is known as a completely automatic method of controlling water levels (e.g., Wahlin and Zimbelman 2014). In the close downstream control case, the objective is to maintain a constant level at the upstream end of the channel, and in the distant case, the level is maintained at the downstream end of the channel. One advantage of controlling the level at the upstream end of the channel is that there is always a storage volume to supply rapidly unforeseen demands (Malaterre, 2008). From a control perspective, there are no reports about the advantages or drawbacks of the distant downstream controllers. However, it is necessary to mention that Malaterre (1995) points out that when the depth at the downstream end of a channel is controlled, there are not inconveniences with the slope of the channel, reducing construction costs.

Moreover, the controller can be multivariable and the controlled variables could be: i) the upstream depth (e.g., Rijo and Arranja 2010; Breckpot et al. 2013); ii) the downstream depth (e.g., Nasir et al. 2018; Aydin et al. 2017; Le-Duy-Lay et al. 2017; Horváth et al. 2015b,a); iii) the channel inflow or outflow (e.g., Puig et al. 2015; Litrico and Georges 1999); iv) the outlet flow; or v) a combination of depths and flows (e.g., Balogun et al. 1988; Breckpot et al. 2013).

Finally, the accomplishment of the control objectives can be measured by using key performance indicators. In the reported literature, the most used indicators are proposed by Clemmens et al. (1998), which are oriented to examine the amount of error in the water levels, and the excessive position variations that the regulation structures present. As it is shown by Clemmens et al. (1998), the desirable situation is to maintain a fixed level along the channel and, with the position adjustment of the regulation structure, deliver the appropriate amount of water to the users. Moreover, because excessive gates and flows changes produce mechanical wear and water levels oscillations, to reduce excessive gates and flows changes is desired. The key performance indicators can be used as a measure of performance for controlled systems (e.g., Xu et al. 2012; Munir et al. 2012; Soler et al. 2013a; Bonet et al. 2017; Ke et al. 2018; Zheng et al. 2019), and as a design criteria in optimal controllers (e.g., Feliu-Batlle et al. 2011; Ke et al. 2018). A relation of the principal key performance indicators is presented in Table 2.2, where:

- The maximum absolute error (MAE) is the maximum normalized error between the desired and measured level.
- The integral of the absolute error (IAE) accounts for the cumulative level error along a time period (T).
- The steady-state error (StE) is the maximum absolute level error during a time period when the steady state has been reached.

Table 2.2. Key performance indicators for error in water levels and changes in flows and gates, where the level error at the downstream end of the channel is considered and $\mathbf{x_{dn_i}} = [x_{dn_i}(0)\ x_{dn_i}(1)\ ...\ x_{dn_i}(N_f-1)]^\top \in \mathbb{R}^{N_f}$ is the vector of the level measurements, $x_{\mathrm{ref_i}}$ is considered as a desired level, $\mathbf{x}_{\mathrm{ref_i}} = [x_{\mathrm{ref_i}}(0)\ x_{\mathrm{ref_i}}(1)\ ...\ x_{\mathrm{ref_i}}(N-1)]^\top \in \mathbb{R}^{N_f}$ is considered as a desired level vector, and $\bar{\mathbf{x}}_{\mathbf{dn_i}}$ is the mean of $\mathbf{x_{dn_i}}$.

Variable of interest	**Key Performance Indicator**
Error in water levels	$MAE = max\left(\frac{\left\lvert \mathbf{x_{dn_i}} - \mathbf{x}_{\mathrm{ref_i}} \right\rvert}{x_{\mathrm{ref_i}}}\right)$ $IAE = \frac{\frac{1}{N_f}\sum_{k=0}^{N_f-1}\left\lvert x_{dn_i}(k) - x_{\mathrm{ref_i}} \right\rvert}{x_{\mathrm{ref_i}}}$ $StE = max\left(\frac{\left\lvert \bar{\mathbf{x}}_{\mathbf{dn_i}} - \mathbf{x}_{\mathrm{ref_i}} \right\rvert}{x_{\mathrm{ref_i}}}\right)$
Gates and flow change	$IAQ = \sum_{k=0}^{N_f}\left(\lvert q_i(k) - q_i(k-1)\rvert\right) - \lvert q_i(0) - q_i(N_f)\rvert$ $IAW = \sum_{k=0}^{N_f}\left(\lvert u_i(k) - u_i(k-1)\rvert\right) - \lvert u_i(0) - u_i(N_f)\rvert$

- The integral square error (ISE) also accounts for the cumulative level error and weights large deviations.
- The absolute gate movement (IAW) relates to positions changes of the regulation structures.
- The integrated absolute discharge change (IAQ) accounts for flow variations.

2.3.3 Control-Action Variables

Certain dynamics could be associated with the movement of the regulation structures and the necessary instrumentation. In controlled systems, most of these dynamics are modified with master-slave control configurations, which are shown in Figure 2.11, where the most usual configurations are presented. In the first case, a position control is shown, where ZI is a position sensor and ZC is a position control that regulates the voltage for the servo-motor (Sepulveda, 2007). In the second case, a more elaborated control scheme is shown, where LI corresponds to the level indicators and FC is a flow control (Schuurmans, 1997). The inclusion of master-slave flow control is useful to divide the control problem into sub-problems, where the dynamical and non-linear relations that there are between flow, regulation structure position, regulation structure mechanism, and water levels can be overcome. Therefore, assuming that the controlled structure has zero steady-state error, high damping factor and short time constant, the model of an open-channel irrigation system could be reduced to a linear model with time delays, where the system input is a flow instead of a regulation structure position.

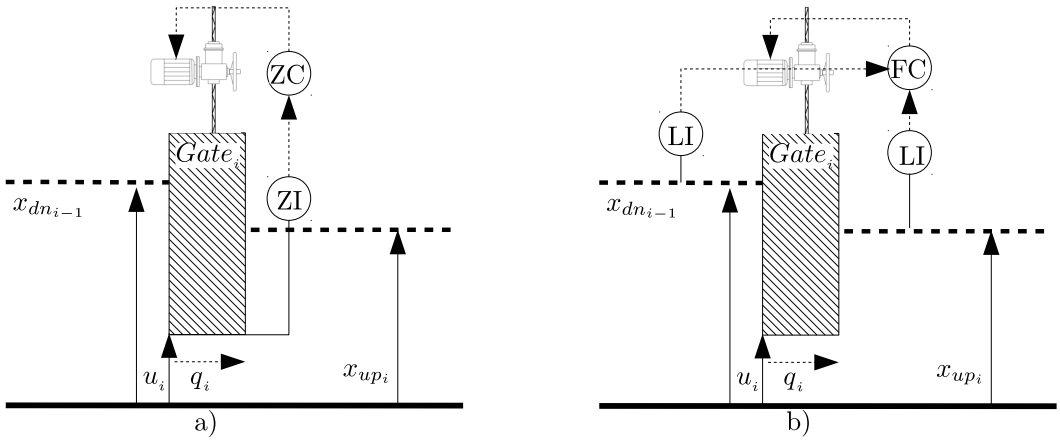

Fig. 2.11. Master-slave configuration examples: a) Aperture gate control. b) Flow control.

2.3.4 Control Configurations

In OCIS control, choosing between feedback (FB) and feedforward (FF) control configurations or a combination of both ($FB + FF$) also is possible. In FB configuration, the channel inflow or outflow generally changes in order to decrease the error between the controlled variable and a desired level or flow. In FF configuration, the channel inflow or outflow changes according to previous information about demands. Each configuration has its advantages and drawbacks. With FB configuration (e.g., Breckpot et al. 2013; Rijo and Arranja 2010; Durdu 2010; Weyer 2008; Litrico and Fromion 2006a; Durdu 2006), the rejection of disturbances and uncertainties such as source-level variations, leaks, unexpected demands, meteorological fluctuations, and changes in parameters of the system can be reached. However, improper design of the controller could lead to oscillations or even instability. On the other hand, in FF configuration, OCIS have fewer fluctuations and faster response. However, with this configuration, the rejection of disturbances and uncertainties is unavailable (van Overloop et al., 2008b). Some research works take advantage of both configurations ($FB + FF$), obtaining faster responses and the possibility to reject disturbances and uncertainties (e.g., Gomez et al. 2002; van Overloop et al. 2014; Sadowska et al. 2015a; Puig et al. 2015; Horváth et al. 2015a,b; Le-Duy-Lay et al. 2017; Aydin et al. 2017; Nasir et al. 2018).

2.3.5 Control Strategies

Finally, the control of OCIS could be seen as a problem of multiple inputs or multiple outputs, with or without disturbances, represented by linear or non-linear models. In this sense, multiple control strategies have been tested and reported in the literature. Next, a brief introduction to the most common strategies is presented and some examples are identified.

PID Control

Proportional-integral-derivative (PID) control is the most commonly used control algorithm in the industry, as well as in OCIS (Litrico et al., 2007). Several studies that use PID controllers to maintain a fixed level in the OCIS have been reported. For example, Burt et al. (1998) establish methods and strategies for tuning upstream PI controllers; Litrico and Georges (1999) compare the performance of a PID controller with a pole placement controller with Smith Predictor; Litrico et al. (2003) investigate the convenience between using a PI controller to maintain a fixed upstream level or a fixed downstream level; van Overloop et al. (2005) modify a PI controller with a first-order filter with the aim to reduce resonant oscillations that are induced from neighbor channels; Lozano et al. (2010) evaluate the performance between a downstream PI controller and a distant downstream PI controller; Figueiredo et al. (2013) test a PI downstream controller in a system with fourth channels; Bolea et al. (2014c), in a real system, assess the behavior of a PI controller designed from a Muskingum model and other from an ID; recently, Arauz et al. (2020); Ke et al. (2020) present two PI tuning methods, that have been designed using the ID modeling approach. It is important to realize that the control strategy proposed by Arauz et al. (2020) has been tested in specialized software (SOBEK), showing that optimally tuned PI controllers are successful for level regulation of OCIS. Other studies simply use the PID controllers to compare the performance of more sophisticated control strategies (e.g., Malaterre and Khammash 2003; Zheng et al. 2019). On the other hand, the design and structure of the PID controllers have been modified with the aim of overcoming uncertainties that are associated with the OCIS. These modifications can be split into two categories: one category is conformed by PID controllers designed in frequency domain considering the robustness of the controlled system (e.g., Litrico and Fromion 2006b; Feliu-Batlle et al. 2007, 2009a, 2011). Another one is conformed by the use of adaptive parameters that must adapt to the controlled system (e.g., Litrico et al. 2007; Bolea et al. 2014a).

LQR and LQG

One of the most popular strategies in the control of OCIS is based on the use of optimal controllers, where the objective is to find a control law that minimizes a quadratic cost function formulated from the representation of the system in state-space. This strategy is known as linear quadratic regulator (LQR), whose advantage is that the control law is a gain vector that weighs the states of the system, being this vector obtained by a systematic solution of the Riccati equation (Kirk, 2004). It has been shown that, in systems modeled by explicit and implicit finite-difference schemes, the use of LQR is popular because this strategy is practical for controlling systems with a large number of states (e.g., Balogun et al. 1988; Reddy 1990b; Mohan Reddy et al. 1992; Schuurmans 1997; Mohan Reddy and Jacquot 1999; Durdu 2006, 2004). In the same direction, the linear quadratic Gaussian (LQG) control, which corresponds to an LQR control with a Kalman filter as an estimator for the non-measurable states, becomes a popular alternative when the systems are modeled using explicit and implicit finite-difference schemes (e.g., Mohan Reddy 1995; Reddy 1996; Schuurmans 1997; Mohan Reddy and Jacquot

1999; Durdu 2006, 2010). Similarly, the LQR control strategy could be used in either decentralized or distributed control schemes. For example, Ke et al. (2018) analyze the behavior of optimally tuned single-input and single-output (SISO) PI controllers designed from control-oriented models obtained with the ID approach. One drawback is that LQR are linear controllers designed to have a desired behavior in a region close to an operation point.

Model Predictive Control (MPC)

Essentially, MPC is a control strategy that has aroused the interest of researchers in control of OCIS (e.g., Begovich et al. 2007; Sepulveda 2007; van Overloop et al. 2008b; Lemos et al. 2009; Negenborn et al. 2009; van Overloop et al. 2010a,a; Cembrano et al. 2011; Xu et al. 2012; Breckpot et al. 2013; Figueiredo et al. 2013; van Overloop et al. 2014; Horváth et al. 2014b; Sadowska et al. 2015a; Puig et al. 2015; Horváth et al. 2015a,b; Cen et al. 2017; Segovia et al. 2017; Le-Duy-Lay et al. 2017; Aydin et al. 2017; Nasir et al. 2018; Zheng et al. 2019). This is due to the benefits that MPC offers in terms of optimality and prediction. Additionally, this kind of controller can be designed from any control-oriented model previously presented and can be used in centralized, distributed, and decentralized architectures. This control strategy is composed of four elements: i) a prediction model; ii) a set of constraints; iii) a cost function; and iv) an optimization algorithm. The mathematical model of the system must be synthesized in discrete-time, and can be expressed in state-space or transfer function representations. The prediction model is developed from a discrete-time model of the system and the current value of the state variables. The maximum and minimum values that limit the operation range of the controlled system are incorporated into the constraints set for the system inputs and state variables, and the cost function synthesizes the performance criteria with a linear or non-linear combination of the prediction model and the set of constraints. Finally, the optimization algorithm searches for the optimal control sequence over a prediction time horizon that minimizes the cost function (Maciejowski, 2002). One drawback of the MPC is that the behavior of this strategy has a high dependency on the system model, and when there are disturbances not included in the model, the controller could show undesirable behaviors (Lemos et al., 2009; Horváth et al., 2015b). This problem can be overcome with the inclusion of adaptive strategies (Lemos et al., 2009), and the use of incremental states and incremental actions (Horváth et al., 2015b; Aydin et al., 2017).

Other Control Strategies

PID, LQR, and MPC are the most reported strategies in control of OCIS. However, control systems is a dynamic field, where multiple control strategies are continuously emerging, and some of these strategies have been tested in control of OCIS. For instance, when OCIS are seen as a multi-input multi-output problem or single-input single-output problem with uncertainties, the H_∞ control strategy is a convenient option since it produces a solution that can explicitly include robust performance in the design procedure, taking into account explicitly information or assumptions on the uncertainties. In this strategy, the objective is to find a proper control law that stabilizes the closed-loop system and

minimizes the H_∞ norm of an augmented linear model that takes into account the uncertainties associated with disturbances and operational point changes (Litrico and Fromion, 2003, 2006a; Cantoni et al., 2007).

To the best of the author knowledge, there are only two reported strategies where the SVE have been used directly as a control-design model: the first one, reported by Liu et al. (1995), is based on an explicit solution procedure of the SVE, which has been tested in a simulated OCIS with six channels showing high sensitivity to variations in physical dimensions of the channels and low sensitivity to variations in coefficients of the regulation structures; and the second one, reported by Dos Santos and Prieur (2008), where a nonlinear control technique, which uses directly the SVE and is called a boundary control (BC), is established. The control strategy is tested in a simulated system and in a small prototype, concluding that the controlled system presents suitable results, even though the proposed control technique is unsystematic.

Machine learning is a field that has been growing constantly and has been broadly applied in the solution of complex problems. In the control of OCIS, Hernández and Merkley (2010a); Shahverdi and Monem (2015); Shahverdi et al. (2016, 2020) use software agents that interact with models of the OCIS in order to maximize a reward function that is related to the regulation structures adjustment and the levels of the system. This technique, known as reinforcement learning, has been implemented using specialized simulation software where the OCIS are numerically solved, then, the strategy finds the optimal operational solution for each regulation structure, and this solution is applied to the irrigation system (Hernández and Merkley, 2010a). The main advantage is that this control strategy does not need an explicit model of the system, for this is considered a model-free strategy (Shahverdi et al., 2016). The OCIS controlled using reinforcement learning have shown satisfactory performance. However, to the best of the author knowledge, no previous reports exist on the use of machine learning in the control of real OCIS.

Another interesting control technique that has been reported is the linear parameter-varying (LPV) control, where the OCIS are modeled as parametrized linear systems with parameters that change with the operation point. Bolea et al. (2014b) propose the description of the OCIS as an LPV system, and subsequently, establish a PID with a Smith predictor LPV controller in order to deal with the nonlinearities and variable delays that describe the OCIS (Bolea et al., 2014a). The LPV controller is implemented in a real system with successful results. Similarly, adaptive control strategies, where there is a need to recursively identify the parameters, have been explored (e.g. Diamantis et al. 2011; Herrera et al. 2013).

Finally, the small head loss automatic gates (French acronym: AVIS) and the high head loss automatic gates (French acronym: AVIO), which are hydro-mechanical downstream controllers (Wahlin and Zimbelman, 2014), can be included as another kind of control strategy for OCIS. The drawback of these regulation structures is that they are more complex to develop than conventional gates or weir structures. These regulation structures are developed in France and have been manufactured in other countries, often unsuccessfully (Wahlin and Zimbelman, 2014).

2.4 DIMEUF

In OCIS, another important field is conformed with works reported around the field of fault diagnosis and DIMEUF (Koenig et al., 2005; Bedjaoui et al., 2006; Besançon et al., 2008; Weyer and Bastin, 2008; Bedjaoui et al., 2008, 2009; Blesa et al., 2010; Bedjaoui and Weyer, 2011; Pocher et al., 2012; Amin et al., 2013a; Akhenak et al., 2013; Duviella et al., 2013; Horváth et al., 2014a; Segovia et al., 2018a). These works highlight the importance in the selection of an appropriate modeling approach, which is fundamental in the development of strategies for detection and estimation of unknown variables. For example, as emphasized by Blesa et al. (2010), DIMEUF strategies designed from linear models (Koenig et al., 2005; Bedjaoui et al., 2006; Besançon et al., 2008; Bedjaoui et al., 2008; Amin et al., 2013a,b; Akhenak et al., 2013; Duviella et al., 2013; Horváth et al., 2014a; Segovia et al., 2018a) are only valid close to an operation region. Hence, in order to increase this region, some works have explored the development of DIMEUF strategies using non-linear models such as numerical solutions of the Saint-Venant Equations (SVE) and approximated models. In reported works that have designed DIMEUF strategies using approximated models (Weyer and Bastin, 2008; Blesa et al., 2010; Bedjaoui and Weyer, 2011; Pocher et al., 2012), it is found that the approximated models do not contemplate energy balances along the channels, and this could lead to inaccurate DIMEUF. For example, Bedjaoui et al. (2008) test strategies for magnitude estimation of unknown flows in a real system, reporting drift in the results, concluding that this drift is due to the growth of weeds, which affects the flow conduction. Moreover, the OCIS are usually affected by sedimentation that also changes the resistance and conduction offered along the channels. Meanwhile, in reported works that design DIMEUF strategies from numerical solutions of the SVE, the complexity of the algorithm is one of the key aspects. Therefore the obtained algorithms can be divided as:

- Algorithms that only detect or isolate (e.g., Bedjaoui et al. 2009).
- Algorithms where the estimation process must be performed off-line (e.g., Bedjaoui and Weyer 2011).

Therefore, in order to increase the DIMEUF accuracy, the development of online DIMEUF approaches designed directly from the SVE is a highly complex and unpractical strategy, and new solutions need to be addressed.

2.5 Discussion

As previously stated, modeling and control of OCIS are complex problems with several choices and constraints that should be taken into account. In OCIS, the most common and appropriate approaches could be developed around the following questions:

- What are the decision features to select a suitable control-oriented modeling strategy for OCIS?

- Which are the requirements for a suitable DIMEUF strategy applied to OCIS?
- Which control approaches might be suitable to increase the efficiency of the OCIS?
- In the field of modeling, DIMEUF, and control of OCIS, which are the research gaps and challenges that must be addressed?

Next, some ideas that address these questions are discussed.

2.5.1 Selecting a Suitable Control-Oriented Modeling Strategy

Most of the control-oriented modeling strategies have been tested in the designing of controllers for real systems, showing useful results. For example, Sepulveda (2007), Lemos et al. (2009), Rabbani et al. (2009a), Figueiredo et al. (2013), van Overloop et al. (2014), and Horváth et al. (2014b) have shown in real systems the results of the implementation of controllers designed from simplified modeling strategies. On the other hand, Rivas Perez et al. (2007), Litrico et al. (2007) Sepulveda (2007), Begovich et al. (2007), Feliu-Batlle et al. (2007), van Overloop et al. (2008a), Feliu-Batlle et al. (2009a), Feliu-Batlle et al. (2009b), van Overloop et al. (2010c), Feliu-Batlle et al. (2011), Tavares et al. (2013), Bolea et al. (2014a), van Overloop et al. (2014), Horváth et al. (2014b), Sadowska et al. (2015a), and Cescon and Weyer (2017) have shown in real systems the results of the implementation of controllers designed from approximated models. However, the availability of a real system to test the behavior of designed control approaches is often unusual. For this reason, in the reviewed literature, only 25% of the works have reported the implementation and analysis of control techniques in real systems. In other cases, the control tests are developed over the control-design model, showing the obtained results as validated data, even though in OCIS, usually, the control-design models are linear models that do not describe most of the hydraulic behavior of real OCIS. In order to perform more rigorous control tests, one alternative could be to test the designed controllers in systems modeled with the SVE. However, the comprehension, codification and stability analyses of implicit or explicit numerical algorithms that solve the SVE of OCIS could be seen as complex tasks.

A second alternative could be the use of specialized hydraulic software such as:

1. The storm water management model (SWMM) software, developed by the Environmental Protection Agency of the United States (Lewis, 2017), which is of free distribution and use but with limited control systems alternatives.

2. The river analysis system developed for the hydrologic engineering center of the U.S. Army Corps of Engineers (HEC-RAS) is a specialized hydraulic software useful for modeling rivers and open-channels. The HEC-RAS also is of free distribution and use, and let the coupling with other softwares such as Matlab (e.g. Leon and Goodell 2016) and Python (e.g. Dysarz 2018).

3. The software for simulation and integration of control for canals (SIC), which has shown to be suitable for testing control strategies in OCIS (van Overloop et al.,

Table 2.3. Comparison between reported approaches for detection, isolation, and magnitude estimation of unknown flows in OCIS.

Work	***Estimation Model***	***Flow Description***	Estimation Strategy	***Detection***	***Isolation***	***Estimation***	***Conduction***	***Online***	***Nonlinear Modeling***
(Koenig et al., 2005)	ID	Linear flow relation	Bank of unknown-input observers	✓	✓			✓	
(Bedjaoui et al., 2006)	ID	Linear flow relation	Bank of unknown-input observers			✓		✓	
(Besançon et al., 2008)	Linearized SVE	Linear flow relation	High gain observer	✓	✓			✓	
(Weyer and Bastin, 2008)	Grey-box	Nonlinear flow relation	Discrepancies between model and real system	✓				✓	✓
(Bedjaoui et al., 2008)	Linearized SVE	Linear flow relation	i) Detection of measurement deviations ii) Kalman filter	✓	✓		✓	✓	
(Bedjaoui et al., 2009)	Numerical solutions of the SVE	Linear flow relation	i) Discrepancies between model and real system ii) Bank of linear observers	✓	✓		✓	✓	✓
(Blesa et al., 2010)	Linear parameter variance	Nonlinear flow relation	Discrepancies between model and real system	✓	✓			✓	✓
(Bedjaoui and Weyer, 2011)	i) Grey-box ii) Numerical solutions of the SVE	Nonlinear flow relation	i) Discrepancies between model and real system ii) Extended Kalman filter iii) Heuristic strategy	✓	✓	✓	✓		✓

2014), and offers a wide number of control alternatives (in this case, this software needs a license to be used).

4. The integrated software package for river, urban or rural management (SOBEK) developed by the institute for applied research Deltares, which solves the SVE of hydraulic systems and lets the online coupling with Matlab, opening the control alternatives to the multiple control strategies that in Matlab can be developed (this software also needs a license to be used).

A final alternative is the use of approximated control-oriented models capable of describing most of the hydraulic behavior of real OCIS, without the intrinsic accuracy of the SVE. One example is the *grey-box model* proposed by Weyer (2008), which includes a mass balance and the non-linear hydraulic description of the regulation structures. However, most of these models are focused on obtaining control-oriented models for OCIS with weir regulation structures in free flow, where there is no interaction between adjacent channels. This aspect is highly relevant, because gates in submerged flow, where the inflow and outflow are a function of the upstream and downstream depth of the structure, are the most common discharge structures in OCIS (U. S. Department of the Interior, 2001). Therefore, the development of new approximated modeling strategies that describe the behavior of OCIS with different types of regulation structures is a challenge that needs to be further addressed.

2.5.2 Selecting a Suitable DIMEUF Approach

In contrast to modeling and control, the field of DIMEUF in OCIS reports few works. A proposed classification of the reported research around DIMEUF is presented in Table 2.3, where the most relevant characteristics of the proposed approaches are identified. In this table, it is observed that few works directly use the SVE in the design of estimation strategies. Most of the estimation strategies prefer the use of simplifications and approximations of the OCIS dynamics, such as the ID model, grey-box models, and LPV models. Note that the recent estimation strategies are developed by using nonlinear hydraulic descriptions of the flows. Moreover, it is observed the lack of an estimation strategy useful to:

- Detect the existence of an unknown flows.
- Establish the localization of the detected unknown flows.
- Estimate the magnitude of the unknown flows.

Similarly, it is highlighted that the online operation of the DIMEUF strategies appears as a requisite. Additionally, despite the complexity, in order to improve the behavior of the DIMEUF strategies, the recently reported works have opted for the use of nonlinear models. In this table, it is also highlighted that the DIMEUF strategies designed from approximated models do not consider conduction conditions of the OCIS, which can induce drift in the estimation results.

Therefore, in OCIS, the DIMEUF, appears as an open field, where the upcoming works must be aimed at the design of strategies useful to detect, isolate, and accurately estimate the unknown flows. In order to obtain accurate unknown flow estimations, the nonlinearities that characterize the OCIS behavior must be included in the estimation strategies. Furthermore, in the design of DIMEUF strategies, the inclusion of the OCIS conduction conditions is an important challenge in order to either reduce or eliminate the drift on the estimation results that habitual phenomena, such as sedimentation or weeds growth, can induce.

2.5.3 Selecting a Suitable Control Approach

Along of the review, multiple control approaches have been outlined. Therefore, it is developed a classification of the available and most common OCIS control approaches that have been reported in the literature. First, in Figure 2.12 a proposed classification of the available control approaches for OCIS is shown. In this classification, the sets of OCIS control alternatives are highlighted. For example, a control approach could be developed using the following choices:

- as a control architecture, a centralized control architecture;
- as a control objective, maintains a constant depth at the downstream end of the channels;

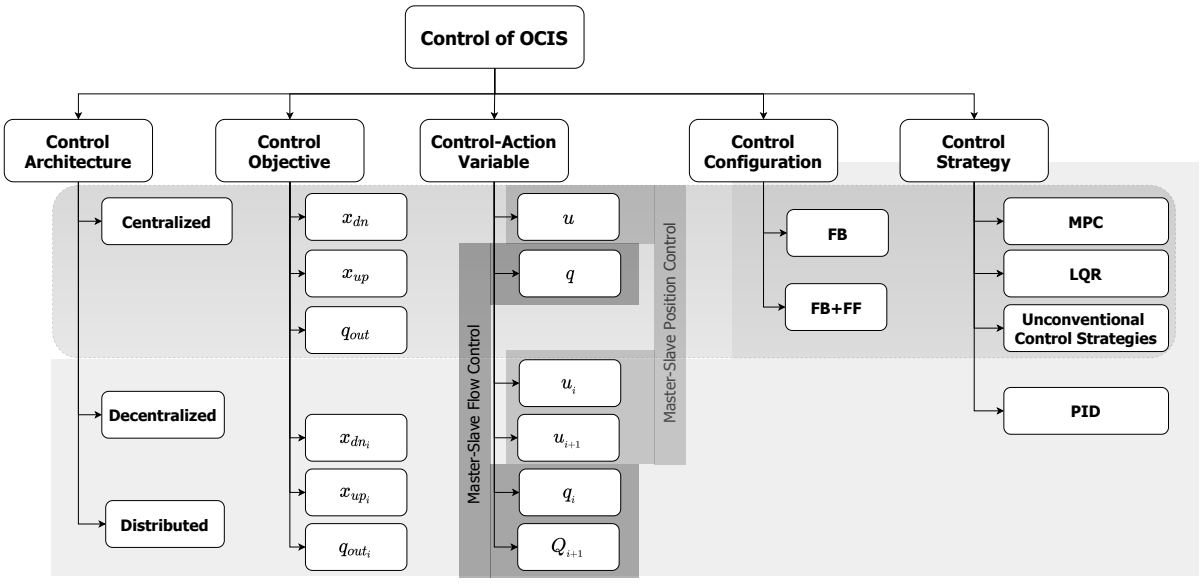

Fig. 2.12. Proposed classification of control approaches for OCIS.

- as a control-action variable, the regulation structures position, which demands the inclusion of master-slave position controllers;
- as a control configuration, a FB configuration;
- as a control strategy, an MPC controller.

On the other hand, from Figure 2.12, it is also highlighted that a conventional PID control strategy is not available as centralized control architecture, and that MPC, LQR, and the other reported control strategies can be used in centralized, decentralized, and distributed control architectures. Additionally, in this classification (Figure 2.12), the use of a pure FF configuration has been discarded because this control configuration is no more than an open-loop operation of the system, and do not offer alternatives to reject disturbance or model uncertainties. Moreover, in Figure 2.12, it is highlighted the kind of master-slave control implementation that needs to be developed for each control-action variable. The proposed classification (Figure 2.12) is an interesting starting point in the identification of possible control approaches for OCIS. However, if this classification is complemented with the classification for possible control-oriented modeling alternatives, presented in Figure 2.4, A high number of combinations can be obtained.

In Table 2.4, it is presented a categorization of the available modeling and control approaches reported in the literature during the last years, where the main OCIS control choices are identified. In this table, the main aspects such as the control objective, the control-action variable, and the control-oriented model are included.

From Table 2.4, one of the most important aspects that can be highlighted is that, in OCIS, the most common control objective is to maintain a constant amount of water in each channel. Usually, this objective is reached using, as the controlled variable, the upstream depth or the downstream depth at the end of the channels. On the other hand, some few works explore the problem of controlling the flow that leaves the channels. One

Table 2.4. Reported works in control of OCIS, which have been classified according to the control-objective reported, the control-action variable used, and the control-oriented model selected.

Controlled Variable	*Control-Action Variable*	*Control-Oriented Model*	*Source*
x_{dn} x_{dn_i}	u_i u_{i+1} $[u_i\, u_{i+1} \cdots]^T$	Finite Differences	Lemos et al. 2009, Feng and Wang 2011, Shang et al. 2011, Soler et al. 2013a, Breckpot et al. 2013, Soler et al. 2013b, Bonet et al. 2017, Cen et al. 2017
		ID	Ke et al. 2018
		black-box Model	Litrico et al. 2007, Begovich et al. 2007, Feliu-Batlle et al. 2007, Feliu-Batlle et al. 2009a, Feliu-Batlle et al. 2009b, Lozano et al. 2010, Feliu-Batlle et al. 2011, Munir et al. 2012
		Grey-Box Model	Cantoni et al. 2007, Domingues et al. 2011, Herrera et al. 2013, Bolea et al. 2014b, Sadowska et al. 2015a, (Horváth et al., 2015a)
	q_i q_{i+1} $[q_i\, q_{i+1} \cdots]^T$	Finite Differences	Xu et al. 2012, Figueiredo et al. 2013, Wagenpfeil et al. 2013, Zeng et al. 2020
		SVE Transformations (IDZ, Hayami model)	Goudiaby et al. 2013, van Overloop et al. 2014, Horváth et al. 2014b, Janon et al. 2016, Segovia et al. 2017, Segovia et al. 2019
		Muskingum	Bolea et al. 2014c, Horváth et al. 2014b
		ID	Negenborn et al. 2009, van Overloop et al. 2010a, Bolea et al. 2014c, van Overloop et al. 2014, Horváth et al. 2014b, Nasir et al. 2018, Zheng et al. 2019, Hashemy Shahdany et al. 2019, Arauz et al. 2020, Ke et al. 2020
		Grey-Box Model	van Overloop et al. 2014, Horváth et al. 2015a, Horváth et al. 2015b, Aydin et al. 2017, Le-Duy-Lay et al. 2017, Tian et al. 2019
x_{up} x_{up_i}	u_i u_{i+1} $[u_i\, u_{i+1} \cdots]^T$	SVE	Dos Santos and Prieur 2008
		Finite Differences	Durdu 2010, Feng and Wang 2011, Breckpot et al. 2013, Cen et al. 2017, Lacasta et al. 2018
		Black-Box Model	Hernández and Merkley 2010b, Hernández and Merkley 2010a
	q_i q_{i+1} $[q_i\, q_{i+1} \cdots]^T$	SVE Transformations (IDZ, Hayami model)	Segovia et al. 2017, Clemmens et al. 2017
		Black-Box Model	Tavares et al. 2013
		Grey-Box Model	Tian et al. 2019
q_{i+1}	q_i	SVE Transformations (IDZ, Hayami model)	Rabbani et al. 2009a, Rabbani et al. 2010, Puig et al. 2015
		Black-Box Model	Diamantis et al. 2011,
		Grey-Box Model	Bolea et al. 2014a

reason for this trend might be that if the controlled variable is the channel level, the OCIS can be described with a linear model, which is valid in a small region around the operation point of the system. Therefore, the controller can be designed in order to maintain the level of the channel into this region. On the other hand, if the controller only regulates the outflow, the channel level could be even at a point that does not guarantee the flow generation, or at a point that can generate overflows. However, most of the reported works that regulate outflows do not incorporate the feedback of the channel level.

Additionally, Table 2.4 also points out that the level regulation at the downstream end of a channel is more common than level regulation at the upstream end. This fact is well-accepted since controlling the level at the downstream end of the channel is easiest to prevent overflows due to water accumulation at the downstream end of the channel. Moreover, in Table 2.4 it is shown that, in order to maintain a constant level at the downstream end of the channel, using as a control-action variable the position of the regulation structure, most authors prefer as control-oriented model the use of finite differences, black-box models, and grey-box models. On the other hand, in the case of maintaining the constant level at the downstream end of the channel, using as a control-action variable the channel inflow, the ID model is the preferred control-oriented modeling strategy. As can be seen, the information in this table can be useful in the development and implementation of

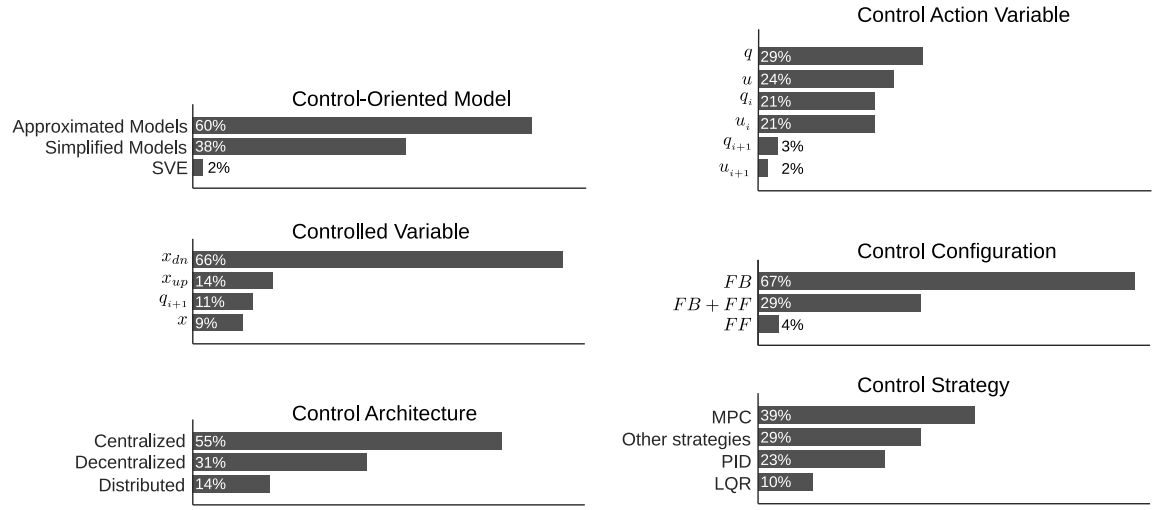

Fig. 2.13. Quantification of the modeling and control options reported in the literature.

control strategies for OCIS, since, this table can be used to identify the most common OCIS control approaches and the sources where these approaches are reported.

In order to discuss about the reported control strategies, in Table 2.5, a chronological compilation of the reported control strategies for OCIS is presented. From this table, it can be highlighted that in OCIS, the most reported control strategies are PID and MPC. On the other hand, Malaterre (1995) shows that between 1980-1995, the LQR control strategy has been one of the most reported strategies for control of OCIS. However, it is shown that between 2007-2019, the interest in the research around using LQR for control of OCIS has been low. Similarly, Table 2.5 shows that there is a low interest in the exploration of other control strategies applied to OCIS. Another aspect to be highlighted is that the study around PID strategies for OCIS has been decreasing, and contrarily, the interest around MPC strategies has been growing. This increasing interest can be associated with the versatility that in the field of OCIS the MPC strategies offer, i.e., in Figure 2.12 it is shown that the MPC strategy can be designed for the multiple control approaches presented in OCIS, let the inclusion of the schedule of the demands (e.g., Zheng et al. 2019), and offers the alternative of include multiple objectives into the control problem (e.g., Segovia et al. 2019).

Moreover, in order to quantify the collected information, in Figure 2.13, bar charts that show the relation of modeling and control options that have been reported in the literature are presented. From this figure, it can be inferred that:

- Due to the simplicity of the approximated models, most of the researchers (60%) use these kind of modeling strategies.
- Close to the 90% of the reported works are focused on maintaining a constant depth in the OCIS, and usually (66%) this objective is reached by a control system that regulates the level at the downstream end of the channels.
- In the literature, it is reported so far a similar interest around studying centralized and non-centralized control architectures, and despite that the OCIS are strongly

Table 2.5. Chronological compilation of reported control strategies for OCIS.

	PID	**MPC**	**LQR**	**Other Control Strategies**
2007	Litrico et al. 2007, Feliu-Batlle et al. 2007	Begovich et al. 2007		Cantoni et al. 2007
2008		van Overloop et al. 2008b		Dos Santos and Prieur 2008
2009	Lemos et al. 2009, Feliu-Batlle et al. 2009a, Feliu-Batlle et al. 2009b	Lemos et al. 2009, Negenborn et al. 2009		
2010	Lozano et al. 2010, Rijo and Arranja 2010	van Overloop et al. 2010a	van Overloop et al. 2010a, Durdu 2010	Hernández and Merkley 2010a, Hernández and Merkley 2010b, Blesa et al. 2010
2011	Domingues et al. 2011 , Feliu-Batlle et al. 2011, Feng and Wang 2011, Shang et al. 2011		Feng and Wang 2011	Diamantis et al. 2011
2012	Munir et al. 2012	Xu et al. 2012		Munir et al. 2012
2013	Herrera et al. 2013	Soler et al. 2013a, Breckpot et al. 2013, Soler et al. 2013b, Figueiredo et al. 2013, Wagenpfeil et al. 2013		Goudiaby et al. 2013
2014	Bolea et al. 2014c	van Overloop et al. 2014, Horváth et al. 2014b		Bolea et al. 2014a
2015	Sadowska et al. 2015a	Puig et al. 2015, Horváth et al. 2015a, Horváth et al. 2015b	Sadowska et al. 2015a	
2016				
2017	Clemmens et al. 2017	Segovia et al. 2017, Bonet et al. 2017, Aydin et al. 2017, Cen et al. 2017, Le-Duy-Lay et al. 2017		
2018		Nasir et al. 2018	Ke et al. 2018	Lacasta et al. 2018
2019	Zheng et al. 2019	Zheng et al. 2019	Zheng et al. 2019, Tian et al. 2019, Segovia et al. 2019	Liao et al. 2019
2020	Ke et al. 2020			Shahverdi et al. 2020, Zeng et al. 2020
2021	Conde et al. 2021b	Conde et al. 2021b	Conde et al. 2021b, Nasir et al. 2021	

coupled systems and the distributed architectures lead to partial implementation of controllers overcoming the problems that decentralized architectures presents, distributed control architectures appear as the less popular architecture in OCIS control research.

- There is a slight preference in the use of the flow than the use of the structure position as control-action variable.
- Only 30% of the reported works take the advantage of using $FB + FF$ configurations, which can be used to mitigate the delays and strong perturbations due to programmed outlet flows (Malaterre, 2008).
- In OCIS, the MPC strategy emerges as the most studied control strategy.

Finally, it has been mentioned that the OCIS are usually manually controlled by operators, which can not take immediate action in order to mitigate the effects of disturbances. Therefore, even the implementation of the most simple and traditional control approaches can lead to increasing the OCIS efficiency. However, the research in control of OCIS must be conducted towards new control approaches that increase the efficiency of these systems, which means control approaches that increase the relation between used and taken water. However, in this review, it is highlighted that most of the reported research is focused on the control objective of maintaining fixed levels or volumes into the channels, and there are not reports that incorporate sources of losses like overflows, leaks, and evaporation into the control problem. Specifically, losses due to leaks halve the efficiency of the OCIS (Swamee et al., 2002). This problem has been analyzed from the structural construction of the channels (Swamee et al., 2002), but the specific challenge of design control algorithms for transporting water, minimizing losses due to leaks is a problem that has not been properly addressed so far.

2.5.4 Remaining Gaps

At this point, it has been identified that the development of suitable control-oriented modeling strategies and new control approaches that increase the efficiency of the OCIS is an open problem that must be addressed. However, this is not the unique research gap that in modeling and control of OCIS remains uncover. Therefore, some future directions from previous literature reviews in control of OCIS, and other identified gaps are listed next.

- In controlled systems, the flow through the regulation gate structures can change abruptly when the gate aperture changes close to the water surface, causing undamped oscillations in the channels levels. This problem is accentuated in channels that are short, flat, and deep (van Overloop et al., 2014). This problem was first identified by Schuurmans (1997). Then, Litrico and Fromion (2004b) analyzed the problem in the frequency domain, and van Overloop et al. (2014) developed and evaluated modeling and control strategies for channels sensible to oscillatory effects. However, more works and validation of multiple control and estimation strategies for oscillatory OCIS are needed.
- Since the dynamics of the OCIS are non-linear, the exploration of non-linear controllers in OCIS is recommended (Schuurmans, 1997). However, there are few reports around non-linear control techniques for OCIS.
- In order to increase the efficiency in the use of water for agricultural systems, the integration of control of OCIS with crop behavior is an important challenge that must be addressed (Lamnabhi-Lagarrigue et al., 2017). This challenge has been explored by Hassani et al. (2019), with the development of an economic-operational framework used in a most economically efficient allocation of water, showing that this kind of development would improve the management of agricultural systems, improving economic, social, and environmental indicators under drought scenarios. However, the development of models and control strategies that explicitly account for static and dynamic interactions between water conveyance and crop behavior is

a complex task that remains pending. In this direction, the exploration of cropping systems models such as WOFOST (de Wit et al., 2019), and LINTUL3 (Shibu et al., 2010) is recommended.

- The problems of detection and identification of failures, and DIMEUF has been studied in few works (e.g., Weyer and Bastin 2008, Bedjaoui and Weyer 2011, Amin et al. 2013a, Amin et al. 2013b, Segovia et al. 2018b). Additionally, robbery is one of the most important problems in OCIS. This problem is well analyzed in (Canute, 1971). However, the development of unknown input estimation strategies able to distinguish between the dynamical effect of a robbery episode or a leak is a topic that has not been fully solved.
- The moving horizon estimation (MHE) is a strategy that in recent years has received high attention. This estimation strategy can be formulated from a comprehensive description of the system, where the unknown parameters can be associated with uncertainties instead of residuals (Franze and Famularo, 2018). However, to the best of the author knowledge, the MHE strategy has not been reported for DIMEUF in OCIS.
- In OCIS, some operation conditions promote the sedimentation and growth of algae and bryophytes (Wahlin and Zimbelman, 2014), obstructing the channels. Therefore, in these systems, the maintenance operations must be frequent. However, to the best of the author knowledge, only the work developed by Fovet et al. (2013) has been reported around the use of control strategies to mitigate the algae grown in OCIS.
- In most cases the OCIS are manually controlled. This fact is basically associated to cost efficiency and security reasons. In this operation mode, the operator only uses local information from the point where the actuated gate is located. Therefore, the behavior of the controlled system is generally far from an optimal operation condition (van Overloop et al., 2015). This problem has been addressed by Maestre et al. (2014); Sadowska et al. (2015b); van Overloop et al. (2015) with the inclusion of human agents in the sensing and actuation of model predictive controllers. This is an interesting idea that has shown desired results in simulated systems. However, there are few works around this problem and, to the best of the author knowledge, there are no reports of the implementation of this control strategy in real systems.
- The development of control algorithms that include uncertainty effects appears as an interesting field that could increase the performance of the OCIS. The OCIS are continuously exposed to uncertain demands and meteorological effects. When the OCIS work on-demand mode, the outlet flows are seen as unknown disturbances that should be compensated by using a control strategy. However, Reddy (1996); Mohan Reddy and Jacquot (1999); Nasir et al. (2018) claim that with the use of historical outlet flows data and/or climatic conditions, it may be possible to describe these disturbances as uniform random variables, where the predicted average is equal to the outlet flow and there is a significant disturbance component with statistical information, which can be included in the control strategy. This is a promising control strategy. However, there are no descriptions about the algorithms that use these climatic predictions, and/or historical outlet flows data, in the prediction of

the users' demands. On the other hand, due to recent advances in meteorological effects prediction, the control of systems under meteorological effects is a challenging problem that is receiving more attention (Maestre et al., 2012). For example, Raso et al. (2013); Maestre et al. (2012); Raso et al. (2014); Ficchì et al. (2016) report the use of ensemble forecasting in the design of tree-based model predictive controllers for drainage water systems and reservoirs. In this control approach, the forecast uncertainty is used to set up a multistage stochastic problem, with the objective of finding multiple optimal strategies according to multiple forecast possibilities, showing that this control approach enhances the adaptivity to forecast uncertainty, improving the operational performance.

- In OCIS, both water quantity and quality criteria must be addressed. For example, salinity is a common problem in irrigated coastal areas (e.g., Aydın et al. 2019). However, the development of control systems that integrate water quantity and quality is scarce. This problem is broadly addressed by Xu (2013), where two simplified modeling strategies that relate quality and quantity are proposed, and the implementation of MPC controllers is evaluated, showing that both, quality and quantity can be controlled. However, real implementations and more studies around real-time quality measurement and consideration of uncertainties remain pending.
- Most of the rivers, lakes, and wetlands are supported by groundwater. Almost all the consumed freshwater is either groundwater or has been groundwater (Darnault, 2008). Therefore, this is a resource that must be protected, and its contamination and overexploitation must be avoided. However, as it is reported by Zhang et al. (2018), due to agricultural activities, nitrogen pollution of groundwater is growing. On the one hand, the OCIS are a direct recharge source for phreatic water. Therefore, the incorporation of measurement and control strategies that avoid groundwater contamination is an important task that must be addressed. On the other hand, as it is shown by Hashemy Shahdany et al. (2018), in many irrigation districts, groundwater is overexploited due to poor operational performance of the irrigation systems, and the groundwater consumption can be drastically reduced with the incorporation of suitable control strategies. Therefore, the development and implementation of control strategies that reduce groundwater consumption must be promoted.
- The SVE offers a fundamental and generalized description of the OCIS. However, due to the SVE complexity, its direct use for control systems design has been avoided. However, the OCIS are slow systems, and the current technology, as well as current model-based control algorithms (e.g., non-linear model predictive control), appears as an implementable strategy that could offer new objectives such as loss minimization.

2.6 Summary

This chapter has presented a detailed literature review regarding modeling, magnitude estimation of unknown flows, and control in OCIS. The review has been developed around

a proposed classifications for modeling, estimation, and control approaches. Moreover, a discussion with the aim of establishing suitable modeling, estimation, and control approaches and the research gaps that need to be addressed also has been established.

From the discussion, it is concluded that most of the simplified and approximated models reported are an oversimplification of the OCIS dynamics, which are not useful to test the behavior of the controllers under realistic conditions, and the grey-box models are an attractive option for control systems design and testing. However, most of the grey-box models reported are only useful for systems with weir structures in free-flow. This oversimplification also affects the development and performance of the unknown flows estimation strategies, where no consideration of conduction conditions can induce drift in the estimation results. Additionally, in the discussion, a classification of the control approaches for OCIS is given, and the most common control approaches are presented, highlighting that the most common control objective is to maintain a constant depth at the end of the channels. MPC is the control strategy that is getting the highest and growing attention, and towards increasing the efficiency of the OCIS, the new control approaches must be focused on increasing the efficiency of the systems reducing losses due to leaks, evaporation, and overflows.

The identified modeling, estimation, and control problems are the guiding thread in the development of this thesis. In Chapter 3 two approximated modeling strategies that consider information about conduction conditions of the channels and can be used in the dynamic description of systems with undershoot gates in submerged flow are proposed. Moreover, in Chapter 4 the proposed strategy that has shown the most accurate description of the OCIS is used in the development of a strategy for detection, isolation, and magnitude estimation of unknown flows that considers potential and energy balances along the channels. Furthermore, in Chapter 5 the design and implementation of conventional control strategies is explored, the development of a non-linear control strategy for open-channels with undershoot gates in submerged flows is proposed, and a non-linear model predictive control strategy designed to reduce losses due to leaks and seepage is also proposed.

Chapter 3

Control-Oriented Modeling Approaches for OCIS

In OCIS, the incorporation of automatic control strategies is considered as one of the most reliable way to reduce losses (Zheng et al., 2019). In order to reach the most favorable behavior of the controlled system, the existence of accurate models for simulation and control design is essential. As it has been shown in Chapter 2, the direct use of the SVE for control systems design is impractical. For this reason, in the literature there are reported the use of simplified and approximated control-oriented modeling approaches. However, it has been identified the need of new control-oriented modeling approaches that can be used to:

- Analyse most of the dynamic behavior of the real system, even with adverse conditions, disturbances, noise, parameter variations, etc.
- Obtain models used for control systems design and analyses of performance indices at an operation region.
- Test the designed controllers in presence of external disturbances and realistic scenarios.
- Describe the nonlinear dynamic behavior of open channels that are interconnected with gates in submerged-flow, where the flow depends on the upstream and downstream depths of the regulation structure.
- Include information about potential energy balances along the channels.

Therefore, in this chapter, the analyses of three control-oriented modeling approaches that could accomplish with the proposed requirements are performed. First, it is analyzed a simplified modeling approach proposed by Litrico and Fromion (2004a), which is obtained by linearization and Laplace transformation of the SVE. However, in this analysis, the nonlinear hydraulic relationships of the regulation structures are conserved. Second, it is proposed a modeling approach that assumes a constant potential energy difference (CPED), which describes the dynamical behavior of the system by using a mass balance

and the hydraulic mathematical descriptions of the regulation structures, assuming that after a time delay and adjusted by a constant, the dynamic behavior at the downstream end of the channel is similar to the dynamic behavior at the upstream end. Third, it is proposed a modeling approach that includes the nonlinear hydraulic relationships of the regulation structures, and mass and potential energy balances (M&PEB) that describe the dynamical behavior of the OCIS. These approaches are evaluated by using the test case proposed by Clemmens et al. (1998) that is implemented in EPA-SWMM (reference model).

3.1 Modeling Approaches

3.1.1 Integrator Delay Zero (IDZ) Modeling Approach

The IDZ modeling approach has been proposed by Litrico and Fromion (2004a) showing that for an open channel, the linearized Laplace transform of the SVE are spatial linear ordinary differential equations that are solved obtaining a transfer function matrix with x_{up} and x_{dn} as outputs, and q_i and q_{i+1} as inputs, where the parameters of the matrix can be obtained from the physical parameters of the system. For low frequencies, this modeling approach describes an open channel with two differential equations given by

$$\begin{aligned} a_{up_i}\dot{x}_{up_i}(t) =& q_i(t) - q_{i+1}(t-\tau_i) - q_{out_i}(t-\tau_i) \\ a_{dn_i}\dot{x}_{dn_i}(t) =& q_i(t-\tau_i) - q_{i+1}(t) - q_{out_i}(t). \end{aligned}$$

In this approach, the system can be analyzed as two storage units. In the first storage unit, with area a_{up_i}, the channel inflow enters at a time t, and the channel outflow leaves the storage unit after a time delay τ_i. In the second storage unit, with area a_{dn_i}, the channel inflow enters at a time $t-\tau_i$, and the channel outflow leaves the storage unit at a time t. In the original form of the IDZ the hydraulic relations of the regulation structures are linearized in order to obtain a model for control design. In this work, the nonlinear relations of the flows are conserved in order to obtain a nonlinear description of the OCIS and validate the IDZ as a control-oriented modeling strategy.

3.1.2 Constant Potential Energy Difference (CPED)

This modeling approach has been proposed by using a mass balance per channel. In this model, it is assumed that the upper part of the channel i has a depth x_{up_i} and the lower part of the channel has a depth $l_{h_i}x_{up_i}(t-\tau_i)$. That means that after a time delay, the level at the lower part of the channel is similar to the level at the upper part but attenuated by a constant l_{h_i} associated with a difference of potential along the channel. The mass balance is described as follows:

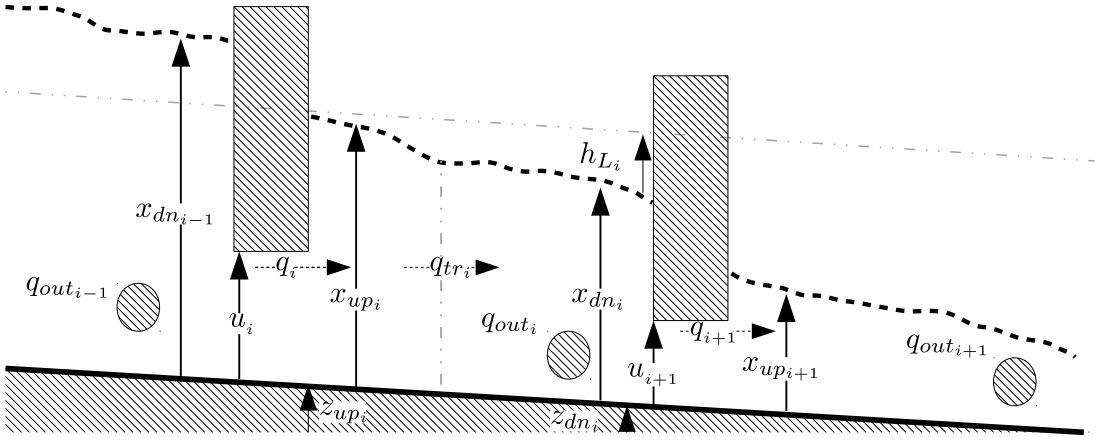

Fig. 3.1. Graphical description for the proposed energy and mass balances.

$$
\begin{aligned}
a_i \dot{x}_{up_i}(t) = & \overbrace{w_i u_i(t) \sqrt{2g} c_i \sqrt{l_{h_{i-1}} x_{up_{i-1}}(t-\tau_{i-1}) - x_{up_i}(t)}}^{q_i(t)} \\
& - \overbrace{w_{i+1} u_{i+1}(t) \sqrt{2g} c_{i+1} \sqrt{l_{h_i} x_{up_i}(t-\tau_i) - x_{up_{i+1}}(t)}}^{q_{i+1}(t)} \\
& - \overbrace{w_{out_i} u_{out_i}(t) \sqrt{2g} c_{out_i} \sqrt{l_{h_i} x_{up_i}(t-\tau_i) - 0.5 u_{out_i}(t)}}^{q_{out_i}(t)} .
\end{aligned}
$$

It is important to mention that parameters such as area (a_i), discharge structure width, and the discharge coefficient can be obtained by structural channel information. Other parameters such as the time delay and the potential energy difference could be obtained from experimental data.

3.1.3 Simplified Mass and Potential Energy Balance (M&PEB)

In this modeling approach, the inclusion of potential energy balances in the description of the dynamical behavior of the OCIS is proposed. In this approximation, the modeling approach assumes mass balances for two storage units per channel and a transition flow between each storage unit. The transition flow is obtained from a simplification of the concept of energy conservation along each channel. Figure 3.1 shows a representation of the modeling approach, where the mass balance is given by

$$
\begin{aligned}
a_{up_i} \dot{x}_{up_i}(t) &= q_i(t) - q_{tr_i}(t) \\
a_{dn_i} \dot{x}_{dn_i}(t) &= q_{tr_i}(t) - q_{out_i}(t) - q_{i+1}(t),
\end{aligned}
\tag{3.1}
$$

with the flows $q_i(t)$, $q_{i+1}(t)$, and $q_{out_i}(t)$ obtained from the flows associated with each discharge structure. The flow transition ($q_{tr_i}(t)$) is obtained from an energy balance given by

$$z_{up_i} + x_{up_i} + \frac{{v_{up_i}}^2}{2g} = z_{dn_i} + x_{dn_i} + \frac{{v_{dn_i}}^2}{2g} + h_{l_i}, \tag{3.2}$$

where the difference between z_{up_i} and z_{dn_i} is the potential energy related to the channel inclination, v_{up_i} and v_{dn_i} are the upstream and downstream mean flow velocity, $\frac{{v_{up_i}}^2}{2g}$ and $\frac{{v_{dn_i}}^2}{2g}$ are the kinetic energy at the upper and lower part of the channel. Besides, h_{l_i} is known as the head loss due to friction, which can be described by the Darcy-Weisbach equation (U. S. Department of the Interior, 2001) by

$$h_{l_i} = f_i \frac{l_i {v_i}^2}{d_{h_i} 2g},$$

where f_i is the friction factor, l_i is the channel length and d_{h_i} is the hydraulic diameter. In this model, an equal mean flow velocity along the channel is assumed, therefore the mean flow velocity could be approximated by $v_{up_i} = v_{dn_i} = \frac{q_{tr_i}}{w_i x_{up_i}}$. On the other hand, f_i is a function of the Reynolds number, which is a relation between the viscous and inertial forces in a fluid (Chaudhry, 2008). Therefore, the strongest assumption is to describe the parameters $f_i, l_i, d_{h_i}, g, w_i$ with a unique transition constant k_{tr_i} that could be obtained from experimental tests. Then, assuming that $h_{l_i} \approx \frac{q_{tr_i}^2}{{k_{tr_i}}^2 x_{up_i}^2}$, and performing the energy balance (3.2), the flow transition is given by

$$q_{tr_i} = k_{tr_i} x_{up_i} \sqrt{x_{up_i} - x_{dn_i} + z_{up_i} - z_{dn_i}}. \tag{3.3}$$

The transition constant k_{tr_i} can be obtained analysing the system in steady state, where $q_i = q_{tr_i}$. On the other hand, the values of a_{up_i} and a_{dn_i} can be obtained using data fitting techniques as shown by Ljung (2010).

3.2 Test Case and Experiment Settings

In order to obtain a reference model and analyze the behavior of the modeling approaches, the test case proposed by Clemmens et al. (1998) is implemented in EPA-SWMM. This test case is based on the Corning canal in California and has been proposed by the ASCE Task Committee on Canal Automation Algorithms as a standardized test case on canals with well-studied and realistic properties, where the variations in the pool lengths of the channels presents a challenge in modeling and control. The test case is composed by eight channels with cross regulation structures of the type undershoot gates in submerged flow, and outlet regulation structures of the same type. The simulation diagram of the system is shown in Figure 3.2, where the hydraulic dimensions and operational conditions are given in Table 3.1.

On the other hand, in order to validate the behavior of the presented modeling approaches in a broad operation region, a variation routine for cross and outlet regulation structures is proposed, where from the operational conditions of the system, at a time of 100 hours, the first cross regulation structure (u_1) is closed in a 30%, and each 100 hours each regulation structure is changed in a 50%. From the test, it is observed that

Table 3.1. Hydraulic Characteristics (HC) and Operational Conditions (OC) of the test case.

p_1	HC	l_1	7000 (m)
		w_1	7 (m)
		z_{up_1}	4,4 (m)
		z_{dn_1}	3,29 (m)
		w_{c_1}	7 (m)
		w_{out_1}	1 (m)
	OC	x_{up_1}	2,38 (m)
		x_{dn_1}	2,84 (m)
		u_1	0,35 (m)
		u_{out_1}	0,22 (m)

p_2	HC	l_2	3000 (m)
		w_2	7 (m)
		z_{up_2}	3,29 (m)
		z_{dn_2}	2,83 (m)
		w_{c_2}	7 (m)
		w_{out_2}	1 (m)
	OC	x_{up_2}	2,65 (m)
		x_{dn_2}	2,93 (m)
		u_2	1,18 (m)
		u_{out_2}	0,22 (m)

p_3	HC	l_3	3000 (m)
		w_3	7 (m)
		z_{up_3}	2,83 (m)
		z_{dn_3}	2,36 (m)
		w_{c_3}	7 (m)
		w_{out_3}	1 (m)
	OC	x_{up_3}	2,7 (m)
		x_{dn_3}	3,02 (m)
		u_3	0,95 (m)
		u_{out_3}	0,21 (m)

p_4	HC	l_4	4000 (m)
		w_4	6 (m)
		z_{up_4}	2,36 (m)
		z_{dn_4}	1,73 (m)
		w_{c_4}	6 (m)
		w_{out_4}	1 (m)
	OC	x_{up_4}	2,7 (m)
		x_{dn_4}	3,12 (m)
		u_4	0,85 (m)
		u_{out_4}	0,21 (m)

p_5	HC	l_5	4000 (m)
		w_5	6 (m)
		z_{up_5}	1,73 (m)
		z_{dn_5}	1,1 (m)
		w_{c_5}	6 (m)
		w_{out_5}	1 (m)
	OC	x_{up_5}	2,83 (m)
		x_{dn_5}	3,31 (m)
		u_5	0,78 (m)
		u_{out_5}	0,2 (m)

p_6	HC	l_6	3000 (m)
		w_6	5 (m)
		z_{up_6}	1,1 (m)
		z_{dn_6}	0,63 (m)
		w_{c_6}	5 (m)
		w_{out_6}	1 (m)
	OC	x_{up_6}	2,78 (m)
		x_{dn_6}	3,11 (m)
		u_6	0,59 (m)
		u_{out_6}	0,2 (m)

p_7	HC	l_7	2000 (m)
		w_7	5 (m)
		z_{up_7}	0,63 (m)
		z_{dn_7}	0,31 (m)
		w_{c_7}	5 (m)
		w_{out_7}	1 (m)
	OC	x_{up_7}	2,66 (m)
		x_{dn_7}	2,89 (m)
		u_7	0,53 (m)
		u_{out_7}	0,21 (m)

p_8	HC	l_8	2000 (m)
		w_8	5 (m)
		z_{up_8}	0,31 (m)
		z_{dn_8}	0 (m)
		w_{c_8}	5 (m)
		w_{out_8}	1 (m)
	OC	x_{up_8}	5 (m)
		x_{dn_8}	2,42 (m)
		u_8	2,67 (m)
		u_{out_8}	0,42 (m)
		w_{out_9}	0,22 (m)
		u_9	0,13 (m)

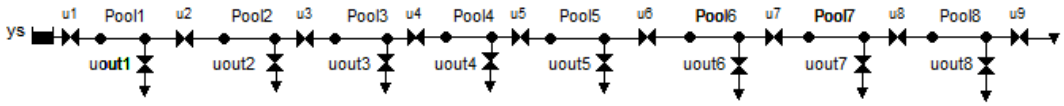

Fig. 3.2. Simulation diagram of the implemented simulation in SWMM.

the average constant time of the channels is 50×10^3s. Therefore, the reference system is sampled with a sampled time (τ_s) of 1×10^3s. The obtained data are used to adjust the parameters of the modeling approaches CPED and M&PEB. In the CPED approach, the areas (a_i) are assumed to be the physical area of each channel. To obtain the l_{h_i} constant, the system is analyzed at the steady-state operation, where $x_{dn_i} = l_{h_i} x_{up_i}$. For each channel, x_{dn_i} and x_{up_i} are obtained from Table 3.1. The delays τ_i are obtained from the dynamic behavior of the reference system. In the M&PEB approach, the transition constants (k_{tr_i}) are obtained analysing the system steady-state operation (3.1), where $q_i = q_{tr_i}$. The flows q_i are obtained using the respective flow relations, and the flows q_{tr_i} are obtained using 3.3. The values of the areas a_{up_i} and a_{dn_i} are obtained by data fitting, where it is used the system described by

$$a_{up_i} \frac{x_{up_i}(k+1) - x_{up_i}(k)}{\tau_s} = q_i(k) - q_{tr_i}(k)$$
$$a_{dn_i} \frac{x_{dn_i}(k+1) - x_{dn_i}(k)}{\tau_s} = q_{tr_i}(k) - q_{out_i}(k) - q_{i+1}(k).$$

Therefore, it is proposed to solve the optimization problem given by

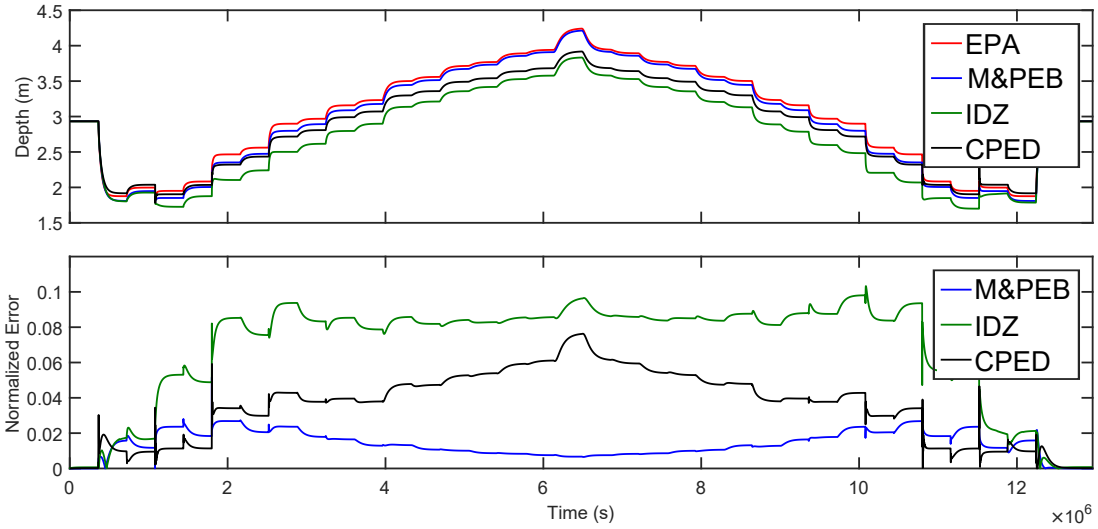

Fig. 3.3. Behavior comparison of the simulated systems at the downstream level of the fourth channel.

$$\begin{aligned} &\min_{\theta_{a_i}} \quad \|\phi_{x_i}\theta_{a_i} - y_{q_i}\|^2 \\ &\text{s.t.} \\ &a_{up_i} + a_{dn_i} = a_i, \end{aligned} \tag{3.4}$$

where, for an experiment with n data,

$$\phi_{x_i} = \begin{bmatrix} \frac{x_{up_i}(k+1) - x_{up_i}(k)}{\tau_s} & \frac{x_{dn_i}(k+1) - x_{dn_i}(k)}{\tau_s} \\ \frac{x_{up_i}(k+2) - x_{up_i}(k+1)}{\tau_s} & \frac{x_{dn_i}(k+2) - x_{dn_i}(k+1)}{\tau_s} \\ \vdots & \vdots \\ \frac{x_{up_i}(k+n) - x_{up_i}(k+n-1)}{\tau_s} & \frac{x_{dn_i}(k+n) - x_{dn_i}(k+n-1)}{\tau_s}, \end{bmatrix}$$

$$y_{q_i} = \begin{bmatrix} q_i(k) - q_{out_i}(k) - q_{i+1}(k) \\ q_i(k+1) - q_{out_i}(k+1) - q_{i+1}(k+1) \\ \vdots \\ q_i(k+n-1) - q_{out_i}(k+n-1) - q_{i+1}(k+n-1) \end{bmatrix},$$

and $\theta_{a_i} = [a_{up_i} \quad a_{dn_i}]^\top$. Here, the constraint $a_{up_i} + a_{dn_i} = a_i$ is included to ensure that the overall area of the approximated model be equal to the physical system area. In that form, this modeling strategy guarantees that the overall mass balance of the approximated model is identical to the overall mass balance of the real system.

On the other hand, the parameters a_{up_i}, a_{dn_i}, τ_{up_i}, and τ_{dn_i} of the IDZ model are obtained using the equations for uniform flow proposed by Litrico and Fromion (2004c).

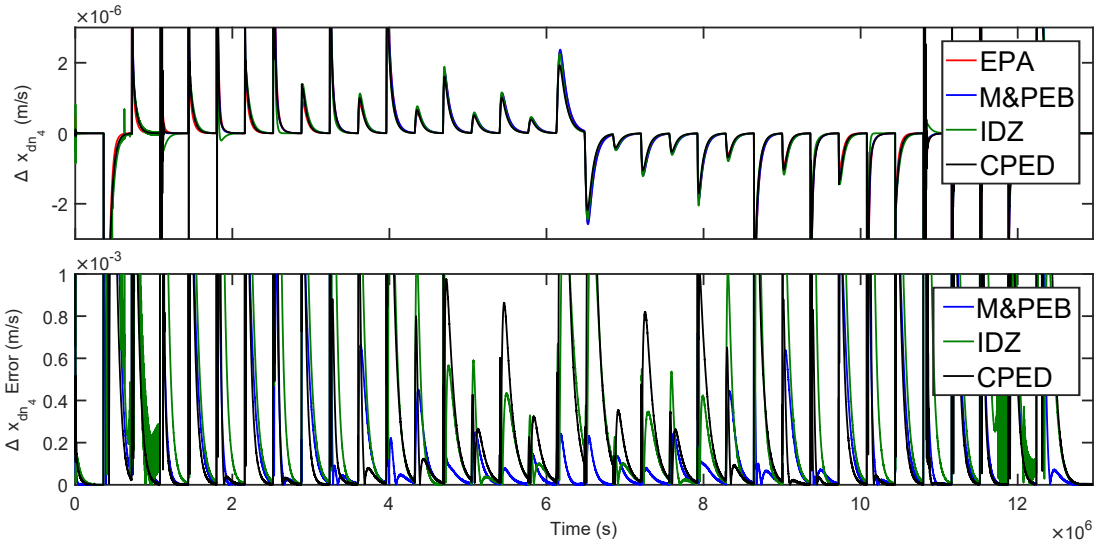

Fig. 3.4. Comparison between $\dot{x}_{dn_4}$ of the reference model and the modeling approaches.

3.3 Results and Discussion

Due to the difficulty of showing analysis data of the 16 depths of the systems, the detailed comparisons of the dynamic behavior of the simulated systems are performed at an intermediate part of the system. i.e., at the downstream level of the fourth channel. Therefore, a comparison of the behavior of the simulated systems is shown in Figure 3.3. Additionally, in this figure, a comparison of the normalized error between the reference model and each modeling approach is shown. From these comparisons, it is possible to establish that the evaluated modeling approaches offer an accurate description of the reference model, with normalized errors lower than a 10% of the overall variation of the system. Also, it is highlighted that the M&PEB modeling approach describes a more accurate behavior than the CPED approach and than the IDZ approach. In the CPED approach and in the IDZ approach the error is increased at higher depths. However, it is observed that instead of this error, the behavior of the modeling approaches has a high dynamical relation with the reference model. Therefore, in order to only compare the dynamical behavior of the modeling approaches, in Figure 3.4 a comparison between $\dot{x}_{dn_4}$ of the reference model and the modeling approaches is presented, where the derivative is approximated using a difference relation. Additionally, in Figure 3.4, the normalized absolute error between $\dot{x}_{dn_4}$ of the reference model and the modeling approaches is presented. From these comparisons, it is observed a high dynamic relation between the reference model and the modeling approaches. Furthermore, it is observed that the M&PEB modeling approach presents a more accurate behavior than the other two approaches. On the other hand, at some times, the IDZ presents a contrary direction of the dynamics; in other words, the IDZ shows a water level increase when the reference model is showing a water level decreases.

In Figure 3.5, the normalized mean absolute errors between the reference model and the modeling approaches for all x_{up}, x_{dn}, and the approximations of $\dot{x}_{up}$, and $\dot{x}_{dn}$ are presented. From the comparison of the level errors, it is observed that, for the eight

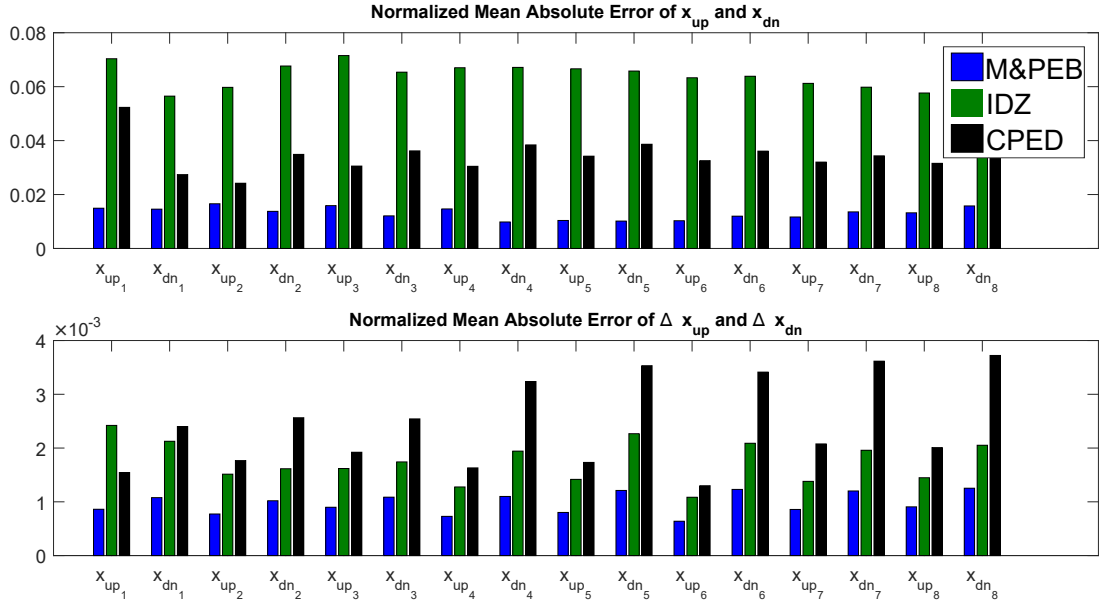

Fig. 3.5. Normalized mean absolute errors between the reference model and the modeling approaches for the eight pools.

channels, the M&PEB approach describes with almost three times lowest error than the other models, the behavior of the reference model. On the other hand, for the eight channels, the three approaches show extremely low error describing the dynamic behavior of the reference model, and the M&PEB approach presents the high dynamic relation.

The results of the comparisons show that with the use of the simplified and approximated modeling approaches the dynamical behavior of the OCIS can be described. It is evident that describing the nonlinear behavior of the OCIS, the M&PEB approach presents better performance than the other approaches. That is because the IDZ and the first modeling approach lost the nonlinear relationship that exists between the difference of potential and the flow along a channel. Finally, the CPED modeling approach could be presented as the simplest one, because it describes the dynamics of an open channel using only one differential equation. However, the first approach, and the IDZ approach include delays that increase the complexity of the simulation and control design strategies.

3.4 Summary

In this chapter, two approximated control-oriented modeling approaches for OCIS have been proposed. The first approach has been designed assuming of a constant potential energy difference along the channels, while the second one has been designed by the development of approximated mass and potential energy balances for each channel. The effectiveness of the proposed strategies have been validated against a specialized software that solves the SVE of hydraulic systems, and against the integrator delay zero, which is a well-known simplified modeling strategy reported in the literature. The results show that the dynamic behavior of OCIS with undershoot gates in submerged flow can be described

by using approximated and simplified modeling strategies. Moreover, the validation results show that, by the development of approximated mass and energy balances for each channel, a more accurate description of the OCIS dynamics can be reached. Therefore, in Chapter 4 the proposed modeling strategy that uses simplified mass and energy balances for each channel is used in the design of strategies for detection, isolation, and magnitude estimation of unknown flows.

Chapter 4

DIMEUF in OCIS

The design of modeling and estimation strategies, useful for determining the magnitude and location of unknown flows such as seepage and leaks, appears as a valuable tool to increase the efficiency of the OCIS. However, as it has been identified, in OCIS, most of the strategies reported on DIMEUF have been designed from linear models that do not include information about energy balances along the channels, where these balances are fundamental to differentiate changes of levels due to conduction effects, from changes of levels due to unknown flows. In this chapter, the development of DIMEUF strategies designed from the proposed OCIS modeling approach that includes M&PEB is addressed. The designed strategies are based on an MHE approach, which is known for its inherent capability of handling complex nonlinear systems and let the inclusion of additional physical information of the system by the use of constraints (Zou et al., 2020). Along the development of the estimation strategies, it has been identified that:

- In order to obtain accurate estimations of the unknown flow's magnitude, the MHE strategy must be enhanced with the addition of detection and isolation mechanisms.
- In the OCIS high inflow or outflow variations produce small level variations of the system, and the unknown flows can easily be masked into small variations of level measurements (i.e, measurement noise). Therefore, in the design of strategies for DIMEUF rigorous noise analysis must be performed.

More specifically, in this chapter a new approach for DIMEUF in OCIS is presented, which takes into account the effects of flow conduction and is designed by enhancing an MHE approach with the inclusion of detection and isolation mechanisms. Then, from the proposed estimation approach, a stochastic DIMEUF strategy that contemplates the effects of measurement noise is also proposed.

4.1 Problem Statement

In OCIS, leaks can be given by accidental losses of water through orifices. A common example of a leak is illustrated by Weyer and Bastin (2008), describing a gate letting water through, even when it is fully closed. Another example can be given when water

percolates through channel fissures. In these cases, such losses can be modeled as functions of the level, where these unknown flows are localized, i.e., $\kappa_{m_i}(t)g(x_{m_i}(t))$, where x_{m_i} is the level at the m_i^{th} position and κ_{m_i} is a parameter related to the size of the orifice or fissures aperture (Harr, 1991). In the following, the hydraulic description of an unknown flow at the upstream part of the channel i is expressed as

$$s_{up_i}(t) = \kappa_{up_i}(t)\sqrt{x_{up_i}(t)}, \quad \kappa_{up_i}(t) \geq 0, \tag{4.1}$$

where $\kappa_{up_i}(t)$ is a parameter that could suddenly change and is associated with the upstream orifice aperture. The hydraulic description of a leak at the downstream part of the channel is expressed as

$$s_{dn_i}(t) = \kappa_{dn_i}(t)\sqrt{x_{dn_i}(t)}, \quad \kappa_{dn_i}(t) \geq 0, \tag{4.2}$$

where $\kappa_{dn_i}(t)$ is the parameter associated with the downstream orifice aperture.

Simulation Model

Once the unknown flows have been defined, by using the proposed simplified modeling strategy that performs mass and energy balances for each channel, the system can be described by

$$a_{up_i}\dot{x}_{up_i}(t) = q_i(t) - q_{tr_i}(t) - s_{up_i}(t) \tag{4.3a}$$
$$a_{dn_i}\dot{x}_{dn_i}(t) = q_{tr_i}(t) - q_{out_i}(t) - q_{i+1}(t) - s_{dn_i}(t) \tag{4.3b}$$
$$y_{up_i}(t) = x_{up_i}(t) \tag{4.3c}$$
$$y_{dn_i}(t) = x_{dn_i}(t), \tag{4.3d}$$

where $y_{up_i}(t) \geq 0$ and $y_{dn_i}(t) \geq 0$ are the measured upstream and downstream levels, respectively. Flows $q_i(t) \geq 0$, $q_{i+1}(t) \geq 0$, and $q_{out_i}(t) \geq 0$ can be obtained by measuring the levels associated with the respective regulation structure.

Estimation Model

At this point, the OCIS can be modeled using two non-linear differential equations that describe mass and energy balances for each channel. Now, with the objective to develop a strategy for DIMEUF, by using an Euler discretization method, the modeling approach (4.3) is used in the development of a discrete-time estimation model as follows:

$$\begin{aligned}
\hat{x}_{up_i}(k+1) &= \hat{x}_{up_i}(k) + \frac{\tau_s}{a_{up_i}}(q_i(k) - \hat{q}_{tr_i}(k) - \hat{s}_{up_i}(k)), \\
\hat{x}_{dn_i}(k+1) &= \hat{x}_{dn_i}(k) + \frac{\tau_s}{a_{dn_i}}(\hat{q}_{tr_i}(k) - q_{out_i}(k) - q_{i+1}(k) - \hat{s}_{dn_i}(k)),
\end{aligned} \tag{4.4}$$

where τ_s (s) is the sampling time; $\hat{x}_{up_i}(k) \geq 0$, $\hat{x}_{dn_i}(k) \geq 0$, $\hat{q}_{tr_i}(k) \geq 0$, $\hat{s}_{up_i}(k) \geq 0$, and $\hat{s}_{dn_i}(k) \geq 0$, are considered unknown variables to be estimated. These variables

correspond to the upstream level, the downstream level, the flow transition, and the upstream and downstream leaks, respectively. In contrast, the flows $q_i(k) \geq 0$, $q_{out_i}(k) \geq 0$, and $q_{i+1}(k) \geq 0$ are considered known variables that can be obtained from measurements of the real system. A compact description of the discrete-time estimation model (4.4) is given by

$$\begin{aligned} \hat{x}_i(k+1) &= G_i \hat{x}_i(k) + H_i \hat{\psi}_i(k) + H_{f_i} \xi_i(k), \\ \hat{y}_i(k) &= \hat{x}_i(k), \end{aligned} \tag{4.5}$$

where the variables correspond to:

The vector of unknown states

$$\hat{x}_i(k) = [\hat{x}_{up_i}(k)\ \hat{x}_{dn_i}(k)]^\top$$

The vector of unknown flows to be estimated

$$\hat{\psi}_i(k) = [\hat{q}_{tr_i}(k)\ \hat{s}_{up_i}(k)\ \hat{s}_{dn_i}(k)]^\top$$

The vector of known flows

$$\xi_i(k) = [q_i(k)\ q_{out_i}(k)\ q_{i+1}(k)]^\top$$

The vector of unknown outputs to be estimated

$$\hat{y}_i(k) = [\hat{y}_{up_i}(k)\ \hat{y}_{dn_i}(k)]^\top$$

The state matrix

$$G_i = \begin{bmatrix} 1 & 0 \\ 0 & 1 \end{bmatrix}$$

The unknown flows matrix

$$H_i = \begin{bmatrix} \frac{\tau_s}{a_{up_i}} & -\frac{\tau_s}{a_{up_i}} & 0 \\ -\frac{\tau_s}{a_{dn_i}} & 0 & -\frac{\tau_s}{a_{dn_i}} \end{bmatrix}$$

The known flows matrix

$$H_{f_i} = \begin{bmatrix} \frac{\tau_s}{a_{up_i}} & 0 & 0 \\ 0 & -\frac{\tau_s}{a_{dn_i}} & -\frac{\tau_s}{a_{dn_i}} \end{bmatrix}$$

Note that, according to the hydraulic descriptions of the unknown flows given in (3.3), (4.1), and (4.2), the vector of unknown flows $\hat{\psi}_i(k)$ can be described as a linear combination of known or measured variables and unknown parameters as

$$\hat{\psi}_i(k) = \Omega_i(k) \hat{\theta}_i(k),$$

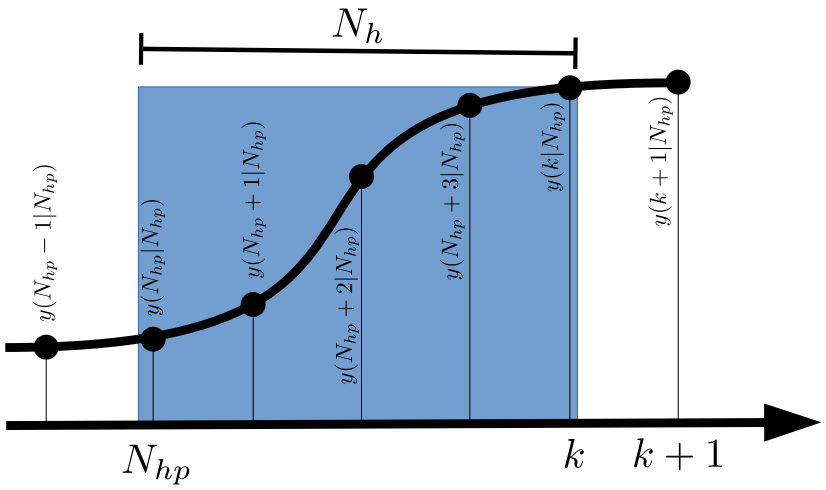

Fig. 4.1. Graphical description of data over an estimation window.

where $\Omega_i(k) \in \mathbb{R}^{3\times 3}$ is a matrix of hydraulic relations that can be obtained from measurements of the real system by

$$\Omega_i(k) = \begin{bmatrix} \gamma_i(k) & 0 & 0 \\ 0 & \sqrt{y_{up_i}(k)} & 0 \\ 0 & 0 & \sqrt{y_{dn_i}(k)} \end{bmatrix},$$
$$\gamma_i(k) = y_{up_i}(k)\sqrt{y_{up_i}(k) - y_{dn_i}(k) + z_{up_i} - z_{dn_i}},$$

and $\hat{\theta}_i(k) \in \mathbb{R}^3$ is a vector of time-varying unknown parameters to be estimated, described as

$$\hat{\theta}_i(k) = [\hat{k}_{tr_i}(k)\ \hat{k}_{up_i}(k)\ \hat{k}_{dn_i}(k)]^\top.$$

These unknown parameters are associated to real and non-negative physical variables such as areas and conduction coefficients (i.e., $\hat{k}_{tr_i}(k)$, $\hat{k}_{up_i}(k)$, $\hat{k}_{dn_i}(k) \geq 0$). This is important information that must be included into the estimation strategies.

In order to estimate the vector of unknown parameters $\hat{\theta}_i(k)$, the MHE strategy is considered. This is an optimization-based estimation strategy that consists in minimizing a cost function defined over a receding time window of inputs and outputs data with fixed length (Alessandri et al., 2008). This technique is known for its inherent capability of handling complex nonlinear systems with constraints (Zou et al., 2020), showing that it could be a suitable strategy to deal with the estimation problem in OCIS. However, following, it is shown that the direct use of the MHE strategy leads to inaccurate estimations of the unknown parameters. As it is shown in Figure 4.1, in the MHE strategy an estimation window with length N_h that starts in $N_{hp} = k - N_h + 1$ and ends in k is established. Note that the notation $\hat{y}_i(k \mid N_{hp})$ indicates that the data $\hat{y}_i(k)$ depends on the conditions at time N_{hp}. Over this window, the estimation of the model (4.4) is given by

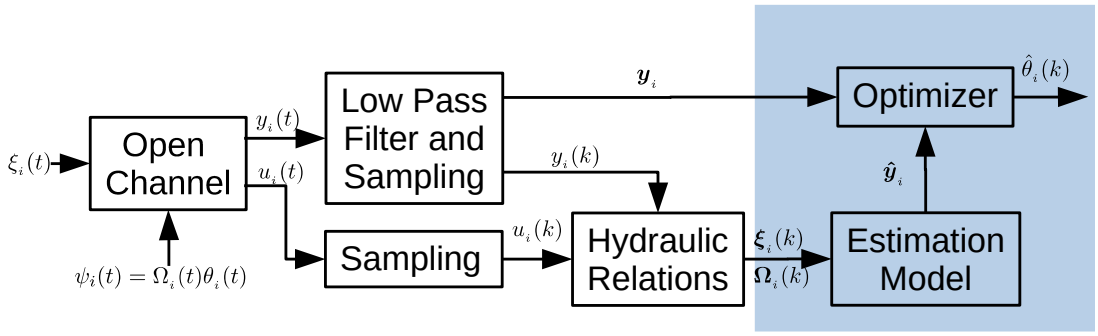

Fig. 4.2. Estimation mechanism.

$$\hat{\boldsymbol{y}}_i = \boldsymbol{\Phi}_i \hat{x}_i(N_{hp} \mid N_{hp}) + \boldsymbol{B}_i \boldsymbol{\Omega}_i(k) \hat{\boldsymbol{\theta}}_i(k) + \boldsymbol{B}_{f_i} \boldsymbol{\xi}_i(k), \tag{4.6}$$

where

$$\begin{aligned}
\hat{\boldsymbol{y}}_i &= [\hat{y}_i(N_{hp}+1 \mid N_{hp})^\top \quad \hat{y}_i(N_{hp}+2 \mid N_{hp})^\top \quad \cdots \quad \hat{y}_i(k+1 \mid N_{hp})^\top]^\top, \\
\boldsymbol{\Phi}_i &= [(G_i)^\top \quad (G_i^2)^\top \quad \cdots \quad (G_i^{N_h})^\top]^\top, \\
\boldsymbol{B}_i &= \begin{bmatrix} H_i & \mathbf{0} & \cdots \\ G_i H_i & H_i & \cdots \\ \vdots & \vdots & \vdots \\ \boldsymbol{G}_i^{N_h-1} H_i & \boldsymbol{G}_i^{N_h-2} H_i & \cdots \end{bmatrix}, \\
\boldsymbol{\Omega}_i(k) &= \text{diag}(\Omega_i(N_{hp} \mid N_{hp}) \quad \Omega_i(N_{hp}+1 \mid N_{hp}) \quad \cdots \quad \Omega_i(k \mid N_{hp})), \\
\hat{\boldsymbol{\theta}}_i(k) &= [\hat{\theta}_i(N_{hp} \mid N_{hp})^\top \quad (\hat{\theta}_i(N_{hp}+1 \mid N_{hp}))^\top \quad \cdots (\hat{\theta}_i(k \mid N_{hp}))^\top]^\top \\
\boldsymbol{B}_{f_i} &= \begin{bmatrix} H_{f_i} & \mathbf{0} & \cdots \\ G_i H_{f_i} & H_{f_i} & \cdots \\ \vdots & \vdots & \vdots \\ G_i^{N_h-1} H_{f_i} & G_i^{N_h-2} H_{f_i} & \cdots \end{bmatrix}, \\
\boldsymbol{\xi}_i(k) &= [\xi_i(N_{hp} \mid N_{hp})^\top \quad (\xi_i(N_{hp}+1 \mid N_{hp}))^\top \quad \cdots (\xi_i(k \mid N_{hp}))^\top]^\top,
\end{aligned}$$

with $\hat{\boldsymbol{y}}_i \in \mathbb{R}^{2N_h}$, $\boldsymbol{\Phi}_i \in \mathbb{R}^{2N_h \times 2}$, $\boldsymbol{B}_i \in \mathbb{R}^{2N_h \times 3N_h}$, $\boldsymbol{\Omega}_i(k) \in \mathbb{R}^{3N_h \times 3N_h}$, $\hat{\boldsymbol{\theta}}_i(k) \in \mathbb{R}^{3N_h}$, $\boldsymbol{B}_{f_i} \in \mathbb{R}^{2N_h \times 3N_h}$, $\boldsymbol{\xi}_i(k) \in \mathbb{R}^{3N_h}$, and $\mathbf{0}$ a null matrix with appropriate dimensions.

In order to find the estimated parameters $\hat{\boldsymbol{\theta}}_i(k)$ that minimizes the deviation between estimated and measured levels, first, the development of a conventional MHE strategy is formulated. A block diagram of the MHE strategy is shown in Fig. 4.2, where additionally to the estimation model and the optimization stage, it is taken into account that the known flow measurements $\xi(k)$ and the known hydraulic relations $\Omega_i(k)$ are obtained from levels measurements and positions of the regulation structures (Table 2.1). Also, it is assumed that the level measurements are performed using ultrasound sensors, and these measurements should be sampled and filtered. Therefore, a low-pass filter stage and a sampling stage are included. As a result, as long as the noise is sufficiently attenuated (in the estimation mechanism), the proposed objective function to be minimized can be given by

$$\boldsymbol{V}_i = \|\boldsymbol{y}_i - \hat{\boldsymbol{y}}_i\|^2_{\mathcal{R}_{1_i}} + \|\hat{\boldsymbol{\theta}}_i(k-1) - \hat{\boldsymbol{\theta}}_i(k)\|^2_{\mathcal{R}_{2_i}}, \tag{4.7}$$

where $\boldsymbol{y}_i$ is a vector of the measured levels given by

$$\boldsymbol{y}_i = [y_i(N_{hp}+1 \mid N_{hp})^\top \quad y_i(N_{hp}+2 \mid N_{hp})^\top \cdots \quad y_i(k+1 \mid N_{hp})]^\top,$$

with $\boldsymbol{y}_i \in \mathbb{R}^{2N_h}$. In (4.7), the term $\|\hat{\boldsymbol{\theta}}_i(k-1) - \hat{\boldsymbol{\theta}}_i(k)\|^2_{\mathcal{R}_{2_i}}$ is included as a forgetting factor that takes into account the influence of past estimations (Baillieul and Samad, 2015), where $\hat{\boldsymbol{\theta}}_i(k-1)$ is the sequence of unknown parameters estimated in a previous iteration. Moreover, $\mathcal{R}_{1_i} \in \mathbb{R}^{2N_h \times 2N_h}$ and $\mathcal{R}_{2_i} \in \mathbb{R}^{3N_h \times 3N_h}$ are diagonal and positive definite weighting matrices that penalize the estimation error and the forgetting factor, respectively. The constraints inclusion is used to add information to the estimation problem (Rawlings et al., 2017), then, as the unknown parameters must be positive, the minimization problem is proposed as

$$\begin{aligned} &\min_{\hat{\boldsymbol{\theta}}_i(k)} \quad \boldsymbol{V}_i \\ &\text{s.t.} \\ &\hat{\boldsymbol{\theta}}_i(k) \geq 0. \end{aligned} \tag{4.8}$$

Note that the reachability of suitable sequences of the unknown parameters ($\hat{\boldsymbol{\theta}}_i(k)$) depends on the convexity of the objective function (4.7). In Lemma 1, it is shown that the use of a conventional MHE strategy does not guarantee an optimal estimation of $\hat{\boldsymbol{\theta}}_i(k)$.

Lemma 1. *From the objective function (4.7), only sub-optimal estimations of $\hat{\boldsymbol{\theta}}_i(k)$ can be reached.*

Proof. A necessary condition for any local minimum to be a global minimum is the convexity of the objective function (4.7). This condition can be reached if the Hessian with respect to $\hat{\boldsymbol{\theta}}_i(k)$ is positive definite, i.e.,

$$\nabla^2_{\hat{\boldsymbol{\theta}}_i(k)} \boldsymbol{V}_i = \boldsymbol{\Omega}_i(k)^\top \boldsymbol{B}_i^\top \mathcal{R}_{1_i} \boldsymbol{B}_i \boldsymbol{\Omega}_i(k) + \mathcal{R}_{2_i} \succ \boldsymbol{0}. \tag{4.9}$$

Since $\mathcal{R}_{1_i}$ and $\mathcal{R}_{2_i}$ are positive defined, the condition established in (4.9) is achieved if $\boldsymbol{\Omega}_i(k)^\top \boldsymbol{B}_i^\top \boldsymbol{B}_i \boldsymbol{\Omega}_i(k) \succ \boldsymbol{0}$.

A sufficient condition for $\boldsymbol{\Omega}_i(k)^\top \boldsymbol{B}_i^\top \boldsymbol{B}_i \boldsymbol{\Omega}_i(k) \succ \boldsymbol{0}$ is that the rank of $\boldsymbol{B}_i \boldsymbol{\Omega}_i(k)$ should be equal to $3N_h$. But, given the dimensions of $\boldsymbol{B}_i$ and $\boldsymbol{\Omega}_i(k)$, the maximum rank of $\boldsymbol{B}_i \boldsymbol{\Omega}_i(k)$ is $2N_h$. Therefore, the condition (4.9) and an optimal estimation of $\hat{\boldsymbol{\theta}}_i(k)$ cannot be reached.

However, by definition, $\boldsymbol{\Omega}_i(k)^\top \boldsymbol{B}_i^\top \boldsymbol{B}_i \boldsymbol{\Omega}_i(k)$ is positive semi-definite (Bhatia, 2015), then, the term

$$\boldsymbol{\Omega}_i(k)^\top \boldsymbol{B}_i^\top \mathcal{R}_{1_i} \boldsymbol{B}_i \boldsymbol{\Omega}_i(k)$$

is positive semi-definite.

Therefore, the Hessian $\nabla^2_{\hat{\boldsymbol{\theta}}_i(k)} \boldsymbol{V}_i$ is positive semi-definite and only sub-optimal estimations of $\hat{\boldsymbol{\theta}}_i(k)$ can be guaranteed. □

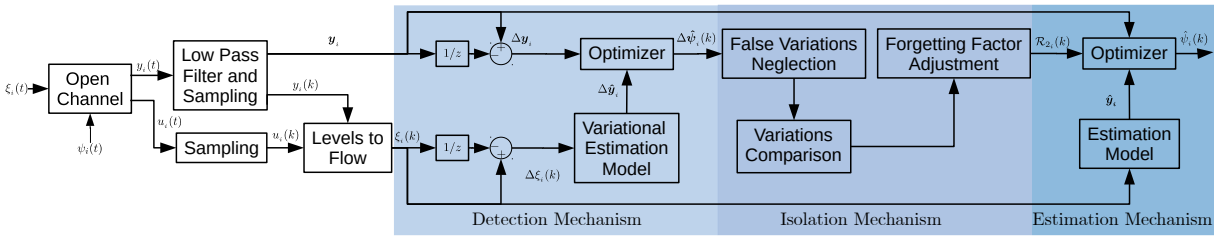

Fig. 4.3. Proposed detection, isolation, and estimation mechanisms.

A contextualized explanation of the problem can be synthesized in that the minimization of the error between the upstream and downstream levels can be reached with inaccurate combinations of the estimated unknown flows. Therefore, if only an unknown flows estimation algorithm is used, inaccurate estimations of the unknown parameters can be reached.

According to the approximate model order (4.3), the maximum rank of $\boldsymbol{B}_i$ is $2N_h$. Therefore, if only two unknown inputs are considered, the convexity of the objective function can be guaranteed. For the two inputs case, H_i is in $\mathbb{R}^{2\times 2}$, and the rank of $\boldsymbol{B}_i$ is still $2N_h$. This solution can be reached by estimation of the total amount of the upstream unknown flows $(-q_{tr_i}(t) - s_{up_i}(t))$ and the total amount of the downstream unknown flows $(q_{tr_i}(t) - s_{dn_i}(t))$. Then, by direct addition of the upstream and downstream unknown flows, the total amount of unknown flows that affect an open-channel can be estimated. This problem is solved in (Conde et al., 2021a) by using an MHE strategy. Other strategies such as unbiased minimum-variance state estimation (Darouach and Zasadzinski, 1997), and state estimators with quadratic boundedness (Alessandri et al., 2006) could be explored to solve this issue. However, by using the two unknown-inputs consideration, the upstream and downstream origins of the unknown flows cannot be established. Therefore, as a proposed solution, following, an enhanced strategy that includes detection and isolation mechanisms is proposed.

4.2 Proposed Approach

In order to overcome the non-convex estimation problem, in Figure 4.3 an enhanced strategy for DIMEUF is proposed, where: i) the detection mechanism uses information about variations of the known flows $(\Delta\xi_i(k))$ and variations of the measured levels $(\Delta y_i(k+1))$ to estimate variations of the unknown flows $(\Delta\hat{\psi}_i(k))$; ii) in the isolation mechanism, the information about the estimated variations of the unknown flows are used to establish the origin of the unknown flow, which can be an either upstream or downstream unknown flow; and iii) in the estimation algorithm, the forgetting factor of the unlikely unknown flow is penalized in order to estimate the flow transition and the corresponding unknown flow that minimizes the objective function (4.7).

Next, deterministic and stochastic analyses of the proposed strategies are performed. The deterministic analysis is developed assuming that the noise can be sufficiently attenuated by the filtering stage. On the other hand, the stochastic analysis is developed

including information about remaining measurement noise that can affect the detection, isolation, and estimation processes.

4.2.1 Deterministic Approach

Note that under the assumption that the measurement noise can be sufficiently attenuated, the difference between the estimation mechanisms (Figures 4.2 and 4.3) is that in the proposed strategy for DIMEUF the weighting matrix that penalizes the forgetting factor ($\mathcal{R}_{2_i}(k)$) is time varying. This weighting matrix is adjusted by the isolation mechanism, which receives information from the detection mechanism as it is described next.

Detection Mechanism

The proposed detection mechanism is developed using a similar MHE strategy than the developed for the estimation mechanism, with the difference that in the detection strategy, the objective is to estimate the variations of the unknown flows. Therefore, from the proposed estimation model (4.5), a variational estimation model is derived as

$$\begin{aligned} \Delta\hat{x}_i(k+1) &= G_i\Delta\hat{x}_i(k) + H_i\Delta\hat{\psi}_i(k) + H_{f_i}\Delta\xi_i(k) \\ \Delta\hat{y}_i(k) &= \Delta\hat{x}_i(k), \end{aligned} \tag{4.10}$$

where, $\Delta\hat{x}_i(k+1) = \hat{x}_i(k+1) - \hat{x}_i(k)$; $\Delta\hat{\psi}_i(k) = \hat{\psi}_i(k) - \hat{\psi}_i(k-1)$; and $\Delta\xi_i(k) = \xi_i(k) - \xi_i(k-1)$. Note that the variational estimation model maintains the same state and input matrices than the estimation model (4.5). Therefore, over an estimation window, the variational estimation model is given by

$$\Delta\hat{\boldsymbol{y}}_i = \boldsymbol{\Phi}_i\Delta\hat{x}_i(N_{hp} \mid N_{hp}) + \boldsymbol{B}_i\Delta\hat{\boldsymbol{\psi}}_i(k) + \boldsymbol{B}_{f_i}\Delta\boldsymbol{\xi}_i(k),$$

where

$$\begin{aligned} \Delta\hat{\boldsymbol{y}}_i &= [\Delta\hat{y}_i(N_{hp}+1 \mid N_{hp})^\top \quad \Delta\hat{y}_i(N_{hp}+2 \mid N_{hp})^\top \quad \cdots \quad \Delta\hat{y}_i(k+1 \mid N_{hp})^\top]^\top, \\ \Delta\hat{\boldsymbol{\psi}}_i(k) &= [\Delta\hat{\psi}_i(N_{hp} \mid N_{hp})^\top \quad \Delta\hat{\psi}_i(N_{hp}+1 \mid N_{hp})^\top \quad \cdots \quad \Delta\hat{\psi}_i(k \mid N_{hp})^\top]^\top. \\ \Delta\boldsymbol{\xi}_i(k) &= [\Delta\xi_i(N_{hp} \mid N_{hp})^\top \quad \Delta\xi_i(N_{hp}+1 \mid N_{hp})^\top \quad \cdots \quad \Delta\xi_i(k \mid N_{hp})^\top]^\top, \end{aligned}$$

with $\Delta\hat{\boldsymbol{y}}_i \in \mathbb{R}^{2N_h}$, $\Delta\hat{\boldsymbol{\psi}}_i(k) \in \mathbb{R}^{3N_h}$, $\Delta\boldsymbol{\xi}_i(k) \in \mathbb{R}^{3N_h}$.

In the detection strategy, the objective is to find the vector of variations of the unknown flows ($\Delta\hat{\boldsymbol{\psi}}_i(k)$) that minimizes the quadratic error between the variations of the measured levels ($\Delta\boldsymbol{y}_i$) and the variations of the estimated levels ($\Delta\hat{\boldsymbol{y}}_i$). Therefore, it is proposed to minimize the cost function given by

$$\boldsymbol{J}_i = \|\Delta\boldsymbol{y}_i - \Delta\hat{\boldsymbol{y}}_i\|^2_{\mathcal{D}_{1_i}} + \|\Delta\hat{\boldsymbol{\psi}}_i(k-1) - \Delta\hat{\boldsymbol{\psi}}_i(k)\|^2_{\mathcal{D}_{2_i}}, \tag{4.11}$$

where the vector of variations of the measured levels is given by

$$\Delta\boldsymbol{y}_i = [\Delta y_i(N_{hp}+1 \mid N_{hp})^\top \quad \Delta y_i(N_{hp}+2 \mid N_{hp})^\top \quad \cdots \Delta y_i(k+1 \mid N_{hp})^\top]^\top.$$

Besides, $\|\Delta\hat{\boldsymbol{\psi}}_{i}(k-1)-\Delta\hat{\boldsymbol{\psi}}_{i}\|(k)^{2}{}_{\mathcal{D}_{2_i}}$ is included as a forgetting factor, and $\Delta\hat{\boldsymbol{\psi}}_{i}(k-1)$ is the vector of variations of unknown flows estimated in a previous iteration. Moreover, $\mathcal{D}_{1_i}\in\mathbb{R}^{2N_h\times 2N_h}$ and $\mathcal{D}_{2_i}\in\mathbb{R}^{3N_h\times 3N_h}$ are diagonal and positive definite weighting matrices that penalize the variational estimation error and the forgetting factor, respectively.

Isolation Mechanism

As it is shown in Figure 4.3, the proposed isolation mechanism uses unknown flows estimated variations ($\Delta\hat{\boldsymbol{\psi}}_{i}(k)$) to establish the possible origin of the unknown flow and penalizes the corresponding forgetting factor of the unlikely unknown flow. This is developed under the following assumption.

Assumption 1 (No simultaneous variations of leaks)**.** *In an open-channel, upstream and downstream variations of unknown flows do not coincide at the same time.*

Based on Assumption 1, the isolation mechanism can be described as a signal comparison mechanism, where: i) a threshold value (Λ_{Δ_i}) is established in order to discriminate between noise and real variations of unknown flows; ii) the magnitudes of the estimated upstream and downstream variations of unknown flows are compared in order to establish the feasible origin of the variation; and iii) in the objective cost function of the estimation mechanism (4.7), the diagonal weighting matrix that penalizes the forgetting factor ($\mathcal{R}_{2_i}$) is adjusted as
$\mathcal{R}_{2_i}=\text{diag}(\mathcal{R}_{ktr_i}\ \ \mathcal{R}_{kup_i}\ \ \mathcal{R}_{kdn_i}\ \ \mathcal{R}_{ktr_i}\ \ \mathcal{R}_{kup_i}\ldots\ \mathcal{R}_{kdn_i})$, and the isolation mechanism modifies $\mathcal{R}_{ktr_i}$, $\mathcal{R}_{kup_i}$, and $\mathcal{R}_{kdn_i}$ as follows:

- if an upstream unknown flow variation is most likely, then $\mathcal{R}_{ktr_i}=\alpha_i$, $\mathcal{R}_{kup_i}=\alpha_i$, $\mathcal{R}_{kdn_i}=\beta_i$;
- if a downstream unknown flow variation is most likely, then $\mathcal{R}_{ktr_i}=\alpha_i$, $\mathcal{R}_{kup_i}=\beta_i$, $\mathcal{R}_{kdn_i}=\alpha_i$;

where, if $\beta_i >> \alpha_i$, the change of the unlikely unknown parameter is avoided, and the minimization of the objective function of the estimation mechanism (4.7) is performed by $k_{tr_i}(k)$ and the unknown parameter of the origin of the variation $k_{up_i}(k)$ or $k_{dn_i}(k)$.

Estimation Mechanism

Finally, the information of the isolation mechanism is included in the cost function of the estimation mechanism as follows:

$$\boldsymbol{V}_{i}=\|\boldsymbol{y}_{i}-\hat{\boldsymbol{y}}_{i}\|^{2}_{\mathcal{R}_{1_i}}+\|\hat{\boldsymbol{\theta}}_{i}(k-1)-\hat{\boldsymbol{\theta}}_{i}(k)\|^{2}_{\mathcal{R}_{2_i}(k)}. \tag{4.12}$$

The cost function is minimized in order to obtain the magnitudes of the estimated parameters $\hat{k}_{tr_i}(k)$ $\hat{k}_{up_i}(k)$, and $\hat{k}_{dn_i}(k)$. Note that the magnitude of leaks and seepage can be obtained by linear combinations of the estimated parameters and functions of the upstream and downstream measured levels (4.1).

4.2.2 Stochastic Approach

Even though the deterministic approach contemplates noise reduction with the inclusion of a low-pass filter, the remaining measurement noise can affect the detection, isolation, and estimation processes. Therefore, in this section, mechanisms that maximize the likelihood detection and likelihood estimation of the unknown flows are designed. The stochastic approach maintains the same detection, isolation, and estimation sequence of the deterministic approach (see Fig. 4.3). However, for the sake of simplicity, the stochastic estimation mechanism is discussed first, and then the stochastic detection and isolation mechanisms are addressed.

Stochastic Estimation Mechanism

In the stochastic estimation mechanism, the remaining measurement noise after filtering is considered. Moreover, as the known inputs q_i, q_{out_i}, and q_{i+1} are obtained from measurements of the levels (see Table 2.1), the remaining measurement noise can also affect the model dynamics. Consequently, an estimation model that includes remaining measurement noise information can be stated by

$$\begin{aligned} \hat{x}_i(k+1) &= G_i\hat{x}_i(k) + H_i\hat{\psi}_i(k) + H_{f_i}\xi_i(k) + \omega_i(k), \\ \hat{y}_i(k) &= \hat{x}_i(k) + \nu_i(k), \end{aligned} \tag{4.13}$$

where $\omega_i(k) = [\omega_{up_i}(k) \;\; \omega_{dn_i}(k)]^\top$ is the process estimation noise, $\omega_{up_i}(k)$, and $\omega_{dn_i}(k)$ are normally distributed noise, with zero mean and standard deviation $\sigma_{\omega up_i}$ and $\sigma_{\omega dn_i}$, respectively. Similarly, $\nu_i(k) = [\nu_{up_i}(k) \; \nu_{dn_i}(k)]^\top$ is the remaining measurement noise, with zero mean and standard deviation $\sigma_{\nu up_i}$ and $\sigma_{\nu dn_i}$, respectively.

In order to consider the remaining measurement noise, and the expected values of the levels, the estimation is performed under the following assumption.

Assumption 2 (Expected estimated levels)**.** *Over an estimation window, the expected values of $\boldsymbol{y}_i$ can be estimated from*

$$\hat{\bar{\boldsymbol{y}}}_i = \boldsymbol{\Phi}_i\hat{x}_i(N_{hp} \mid N_{hp}) + \boldsymbol{B}_i\boldsymbol{\Omega}_i(k)\boldsymbol{T}_i\hat{\bar{\theta}}_i(k) \; + \boldsymbol{B}_{f_i}\boldsymbol{\xi}_i(k) + \boldsymbol{W}_i(k) + \boldsymbol{N}_i, \tag{4.14}$$

where $\hat{\bar{\boldsymbol{y}}}_i \in \mathbb{R}^{2N_h}$ is the vector of estimated expected values of the output,

$$\hat{\bar{\theta}}_i(k) = [\hat{\bar{k}}_{tr_i}(k) \; \hat{\bar{k}}_{up_i}(k) \; \hat{\bar{k}}_{dn_i}(k)]^\top \in \mathbb{R}^3$$

are the expected values of the unknown parameters, and $\boldsymbol{T}_i \in \mathbb{R}^{3N_h \times 3}$ is a block of identity matrices such that $\boldsymbol{T}_i\hat{\bar{\theta}}_i(k) \in \mathbb{R}^{3N_h}$. Finally, $\boldsymbol{W}_i(k) \in \mathbb{R}^{2N_h}$ and $\boldsymbol{N}_i \in \mathbb{R}^{2N_h}$ are the corresponding process and measurement noise vectors, respectively.

It is emphasized that additionally to the noise inclusion, the deterministic and stochastic cases (Equations (4.6) and (4.14)), differ in the configuration of the unknown parameters. Note that in (4.6), $\hat{\boldsymbol{\theta}}_i(k) \in \mathbb{R}^{3N_h}$ is the estimated unknown parameters for each instant of the estimation window. In contrast, in (4.14), it is considered that the unknown

parameters ($\hat{\bar{\theta}}_i(k) \in \mathbb{R}^3$) are the same over the entire estimation window. In that form, in the stochastic estimation mechanism, the objective is to find the unknown parameters ($\hat{\bar{\theta}}_i(k)$) that makes the vector of measured levels $\boldsymbol{y}_i$ most likely. For that a likelihood function must be established, where over an estimation window, the process covariance can be obtained from the estimation error $e_i = y_i(k+1) - \hat{\bar{y}}_i(k+1)$, and the covariance is the expected value given by

$$P_i(k+1) = \mathbb{E}\left(e_i(k+1)e_i(k+1)^\top\right). \tag{4.15}$$

Consequently, if a discrete model of the system is given by

$$\begin{aligned} x_i(k+1) &= G_i x_i(k) + H_i \psi_i(k) + H_{f_i}\xi_i(k), \\ y_i(k) &= x_i(k), \end{aligned} \tag{4.16}$$

and if the unknown flows ($\psi_i(k)$) are considered to be zero or identical to the unknown estimated flows ($\hat{\psi}_i(k)$), by subtraction, from (4.13) and (4.16), the estimated error can be written as

$$e_i(k+1) = G_i e_i(k) + \omega_i(k) + \nu_i(k+1).$$

Therefore, from (4.15), the process covariance is given by

$$P_i(k+1) = G_i P_i(k) G_i^\top + R + S, \tag{4.17}$$

where

$$R = \begin{bmatrix} \sigma^2_{\omega up_i} & 0 \\ 0 & \sigma^2_{\omega dn_i} \end{bmatrix}, \quad S = \begin{bmatrix} \sigma^2_{\nu up_i} & 0 \\ 0 & \sigma^2_{\nu dn_i} \end{bmatrix}.$$

Finally, the process covariance (4.17) is given by

$$\boldsymbol{\Sigma}_i(k) = \text{diag}[(P_i(N_{hp} \mid N_{hp}),\ P_i(N_{hp}+1 \mid N_{hp}), \cdots\ P_i(k \mid N_{hp}))]. \tag{4.18}$$

The process covariance contains information about the deviation that the expected values present over an estimation window. Next, the process covariance is included in the development of the likelihood function used to find the expected values of $\hat{\bar{\theta}}_i(k)$. Then given the process covariance (4.18) and the estimation process (4.14), a probability density function (likelihood function) can be formulated as

$$f(\boldsymbol{y}_i \mid \hat{\bar{\boldsymbol{\theta}}}_i(k)) = \frac{1}{(2\pi)^{N_h}\left|\boldsymbol{\Sigma}_i(k)\right|^{1/2}} e^{-\frac{1}{2}\boldsymbol{\Upsilon}}, \tag{4.19}$$

where

$$\boldsymbol{\Upsilon} = (\boldsymbol{y}_i - \hat{\bar{\boldsymbol{y}}}_i)\boldsymbol{\Sigma}_i(k)^{-1}(\boldsymbol{y}_i - \hat{\bar{\boldsymbol{y}}}_i).$$

Now, the goal is to find the estimated values $\hat{\bar{\theta}}_i(k)$ that makes the measured vector ($\boldsymbol{y}_i$) most likely. Therefore, the probability density function (4.19) must be maximized

with respect to $\hat{\bar{\theta}}_i(k)$. However, as it is shown by Verhaegen and Verdult (2007), for the sake of simplicity, the logarithm of (4.19) can be maximized leading to the following minimization problem

$$\underset{\hat{\bar{\theta}}_i(k)}{\text{minimize}} \quad \boldsymbol{\Upsilon}. \tag{4.20}$$

Similarly to the deterministic case, in the objective function, in order to retain influence of past estimations, also the forgetting factor ($\|\hat{\bar{\theta}}_i(k-1) - \hat{\bar{\theta}}_i(k)\|^2_{\mathcal{R}_{s_i}}$) can be included, leading to the cost function

$$\boldsymbol{V}_{s_i} = \|\boldsymbol{y}_i - \hat{\boldsymbol{y}}_i\|^2_{\boldsymbol{\Sigma}_i(k)^{-1}} + \|\hat{\bar{\theta}}_i(k-1) - \bar{\theta}_i(k)\|^2_{\mathcal{R}_{s_i(k)}}, \tag{4.21}$$

where $\mathcal{R}_{s_i}(k) \in \mathbb{R}^{3\times 3}$ is used to penalize the forgetting factor. Moreover, if constraints on the unknown parameters are included, the minimization problem of the estimation mechanism is formulated as

$$\begin{aligned} &\min_{\hat{\bar{\theta}}_i(k)} \quad \boldsymbol{V}_{s_i} \\ &\text{s.t.} \\ &\hat{\bar{\theta}}_i(k) \geq 0. \end{aligned} \tag{4.22}$$

Note that by following a similar analysis as in Lemma 1, the convexity of the stochastic objective function (4.21) can be reached if the rank of $\boldsymbol{B}_i\boldsymbol{\Omega}_i(k)\boldsymbol{T}_i$ is $3N_h$, but given the dimensions of $\boldsymbol{B}_i$, $\boldsymbol{\Omega}_i(k)$, and $\boldsymbol{T}_i$, the maximum rank $\boldsymbol{B}_i\boldsymbol{\Omega}_i(k)\boldsymbol{T}_i$ is $2N_h$. Therefore, in order to obtain accurate estimations of the unknown flows, in the stochastic approach, stochastic detection and isolation mechanisms must be included.

Stochastic Detection and Isolation Mechanisms

In the stochastic case, by following a similar procedure as employed in the derivation of the variational estimation model of the deterministic case, from (4.13), the variational estimation model is given by

$$\begin{aligned} \Delta\hat{x}_i(k+1) &= G_i\Delta\hat{x}_i(k) + H_i\Delta\hat{\psi}_i(k) + H_{f_i}\Delta\xi_i(k) + \omega_{\Delta i}(k) \\ \Delta\hat{y}_i(k) &= \Delta\hat{x}_i(k) + \nu_{\Delta i}(k), \end{aligned} \tag{4.23}$$

where $\omega_{\Delta i}(k) = [\omega_{\Delta up_i}(k)\ \omega_{\Delta dn_i}(k)]^\top$ is related to the remaining process noise, $\omega_{\Delta up_i}(k)$ and $\omega_{\Delta dn_i}(k)$ are normally distributed noise with zero mean. Similarly, $\nu_{\Delta i}(k) = [\nu_{\Delta up_i}(k)\,\nu_{\Delta dn_i}(k)]^\top$ is related to the remaining measurement noise, where $\nu_{\Delta up_i}(k)$ and $\nu_{\Delta dn_i}(k)$ are normally distributed noises with zero mean. Similarly to the stochastic estimation mechanism, in order to consider the expected values of the level variations over an estimation window, the variational model (4.23) is presented under the following assumption.

Assumption 3 (Expected estimated variations)**.** *Over the estimation window, the expected values of $\Delta\boldsymbol{y}_i$ can be estimated from*

$$\Delta\hat{\tilde{\boldsymbol{y}}}_i = \boldsymbol{\Phi}_i \Delta\hat{x}_i(N_{hp} \mid N_{hp}) + \boldsymbol{B}_i \boldsymbol{T}_i \Delta\hat{\bar{\psi}}_i(k) + \boldsymbol{B}_{f_i} \Delta\boldsymbol{\xi}_i(k) + \boldsymbol{w}_{\Delta_i}(k) + \boldsymbol{n}_{\Delta_i},$$

where $\Delta\hat{\tilde{\boldsymbol{y}}}_i \in \mathbb{R}^{2N_h}$ *is the vector of estimated expected values of the output variations, and*

$$\Delta\hat{\bar{\psi}}_i(k) = [\Delta\hat{\bar{q}}_{tr_i}(k)\ \Delta\hat{\bar{s}}_{up_i}(k)\ \Delta\hat{\bar{s}}_{dn_i}(k)]^\top$$

is the vector of expected values of the unknown flows variations. Finally, $\boldsymbol{w}_{\Delta_i}(k) \in \mathbb{R}^{2N_h}$ *and* $\boldsymbol{n}_{\Delta_i} \in \mathbb{R}^{2N_h}$ *are the corresponding noise vectors.*

In the same way as in (4.17), the process covariance can be modeled as

$$P_{\Delta_i}(k+1) = G_i P_{\Delta_i}(k) G_i^\top + R_\Delta + S_\Delta,$$

Note that the measurement and process noises at different time instants are not correlated (i.e., there is no correlation between $\omega_i(k)$ and $\omega_i(k-1)$, and $\nu_i(k)$ and $\nu_i(k-1)$). Therefore, the noise standard deviations of $\omega_{\Delta up_i}(k)$, $\omega_{\Delta dn_i}(k)$, $\nu_{\Delta up_i}(k)$, and $\nu_{\Delta dn_i}(k)$ are given by $2\sigma_{\omega up_i}$, $2\sigma_{\omega dn_i}$, $2\sigma_{\nu up_i}$, and $2\sigma_{\nu dn_i}$, respectively. Hence,

$$R_\Delta = \begin{bmatrix} 2\sigma^2_{\omega up_i} & 0 \\ 0 & 2\sigma^2_{\omega dn_i} \end{bmatrix}, \quad S = \begin{bmatrix} 2\sigma^2_{\nu up_i} & 0 \\ 0 & 2\sigma^2_{\nu dn_i} \end{bmatrix}.$$

As a result, the process covariance ($\boldsymbol{\Sigma}_{\Delta_i}(k) \in \mathbb{R}^{3N_h \times 3N_h}$) can be calculated yielding to a diagonal matrix of the form

$$\boldsymbol{\Sigma}_{\Delta_i}(k) = \mathrm{diag}(P_{\Delta_i}(N_{hp} \mid N_{hp}), P_{\Delta_i}(N_{hp}+1 \mid N_{hp}), \cdots \quad P_{\Delta_i}(k \mid N_{hp})). \tag{4.24}$$

Consequently, following the same procedure to obtain (4.21), the estimation of the unknown flow variation, can be reached by minimizing the following objective function

$$\boldsymbol{J}_{\boldsymbol{s_i}} = \|\boldsymbol{\Delta y}_i - \boldsymbol{\Delta\hat{\tilde{y}}}_i\|^2_{\boldsymbol{\Sigma}_{\Delta_i}(k)^{-1}} + \|\Delta\hat{\bar{\psi}}_i(k-1) - \Delta\hat{\bar{\psi}}_i(k)\|^2_{\mathcal{D}_{s_i}}, \tag{4.25}$$

where $\mathcal{D}_{s_i} \in \mathbb{R}^{3\times3}$ penalize the forgetting factor.

Likewise as in the deterministic case, in the stochastic case, the isolation mechanism uses the estimation of the expected unknown flow variations to establish the origin of the unknown flow and to penalize the corresponding forgetting factor of the estimation mechanism.

4.3 Simulation Test

The proposed deterministic and stochastic strategies are tested using the benchmark based on the Corning canal in California, which has been presented by Clemmens et al. (1998) and the ASCE Task Committee on Canal Automation Algorithms as a standardized testbed on canals with well-studied and realistic properties.

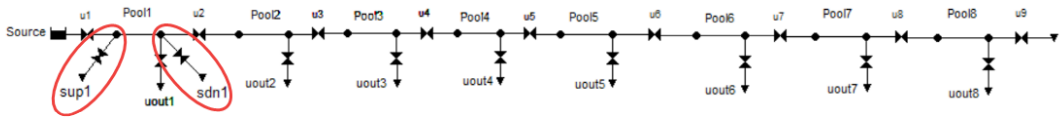

Fig. 4.4. Case study simulation in EPA-SWMM.

The testbed has been implemented SWMM as it is presented in Figure 4.4. Even though the testbed is composed by eight channels, since the estimation strategies present the same structure for any channel, the simulation is limited to only one channel (the first channel of the testbed in Figure 4.4). This is a rectangular channel with the following dimensions: length of 7000m, width of 7m, upstream elevation of 4.4m, and downstream elevation of 3.29m. As it is highlighted in Figure 4.4, in the first channel, in order to emulate the unknown flows to be detected and estimated, two orifices with variable areas from 0 to 0.04m^2 have been included. A more detailed description of the design and implementation process follows.

4.3.1 Sampling Time

Although most of the OCIS are large-scale systems with very slow dynamics, it has been observed that the time response of the system variation can be almost ten times faster than the system dynamics. Therefore, in order to capture the dynamics of the system variation, the sampling time has been selected by analysis of the time response level variation. In this analysis, the classical control rule of choosing a sampling time ten times smaller than the rise time (Litrico and Fromion, 2009) is used, yielding to a sampling time of $\tau_s = 100$s.

4.3.2 Model Areas

The values of the model areas (a_{up_i}, and a_{dn_i}) have been obtained by data fitting, where, if absence of unknown flows and reduced noise measurements is assumed, the unknown flow transition can be neglected by the addition of the two mass balances that describe the system (4.3), which, using an Euler method, can be discretized yielding to

$$\frac{a_{up_i}}{\tau_s}(\hat{x}_{up_i}(k+1) - \hat{x}_{up_i}(k)) + \frac{a_{dn_i}}{\tau_s}(\hat{x}_{dn_i}(k+1) - \hat{x}_{dn_i}(k)) = q_i(k) - q_{out_i}(k) - q_{i+1}(k). \tag{4.26}$$

In this case, $a_{up_1} = 21864$m^2, and $a_{dn_1} = 27136$m^2. It must be highlighted that in order to maintain a similar mass balance than in the real system, the data fitting problem has been forced to $a_{up_i} + a_{dn_i} = a_i$, where a_i is the channel area of the real system.

4.3.3 Noise and Low-Pass Filter

As it is shown by Wahlin and Zimbelman (2014), there is a close relationship between the measurement noise standard deviation and the sensor quality. In this case study, it is

considered that in OCIS, levels are measured with ultrasound sensors, and according to the quality of the commercial sensors, the measurement noise standard deviation could be between 1×10^{-3}m and 2.5×10^{-3}m. Therefore, the deterministic and stochastic algorithms have been tested with measurements obtained from the testbed implemented in the SWMM, and the measurements have been contaminated with noise of these standard deviations.

Moreover, it must be contemplated that in comparison with the system sampling time (τ_s), the sensor's sampling time should be small. This data availability is exploited with the integration of low-pass filters to reduce the measurement standard deviation. For this reason, a third-order low-pass filter is included with a cutoff frequency of 0.02Hz. This frequency is chosen by using the Nyquist-Shannon sampling theorem, and the selected sampling time of 100s. With the inclusion of the low-pass filter, the standard deviation of the remaining measurement noise is almost ten times lower than the original.

4.3.4 Weighting Matrices

Detection Weighting Matrices of the Deterministic Mechanism

In the deterministic mechanism, for the sake of simplicity, the detection weighting matrices of (4.11) can be described as $\mathcal{D}_{1_i} = d_{1_i}\boldsymbol{I_{2N_h}}$, and $\mathcal{D}_{2_i} = d_{2_i}\boldsymbol{I_{3N_h}}$, where d_{1_i}, and d_{2_i} are positive weighting constants and $\boldsymbol{I_{2N_h}}$, and $\boldsymbol{I_{3N_h}}$ are identity matrices with dimensions $2N_h \times 2N_h$ and $3N_h \times 3N_h$, respectively. In the deterministic case, the relation between the weighting parameters (d_{1_i}, and d_{2_i}) has been used as a tuning parameter. In the tuning procedure:

- the weighting parameter that penalizes the forgetting factor has been chosen as $d_{2_i} = 1$;
- Monte Carlo tests have been developed, where a key performance indicator (KPI) has been established in order to find the value of d_{1_i} that minimizes the detection error of the unknown flows.

The KPI (4.27) has been established in order to mitigate the noise detection and give strong penalization of large detection errors by

$$KPI = \sum_{k=1}^{k_f} \frac{(\Delta s_{up_i}(k) - \Delta \hat{s}_{up_i}(k))^4}{k_f - 1} + \frac{(\Delta s_{dn_i}(k) - \Delta \hat{s}_{dn_i}(k))^4}{k_f - 1}, \tag{4.27}$$

where k_f is the length of data used in the tests. The tests show that small values of d_{1_i} attenuate the estimation noise, but also increase inaccurate detections. On the other hand, large values of d_{1_i} increase the detection accuracy but also increase the noise detection. The results of the Monte Carlo tests are shown in Figure 4.5, where it is observed that d_{1_i} values close to 2×10^5 offer the lowest detection errors.

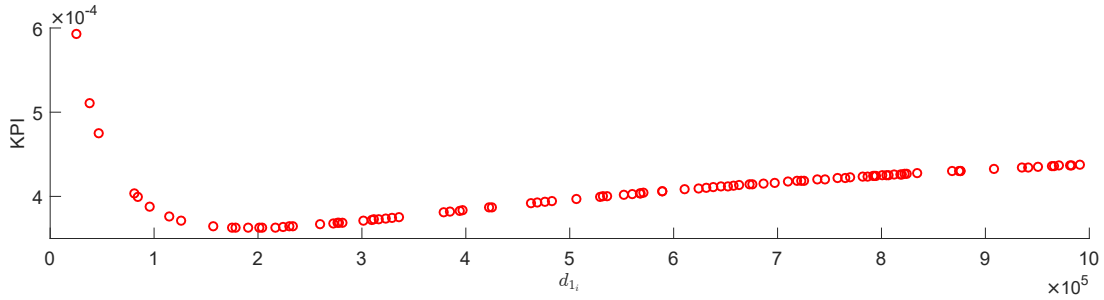

Fig. 4.5. Monte Carlo tests to establish the d_{1_i} values that offer the lowest detection errors.

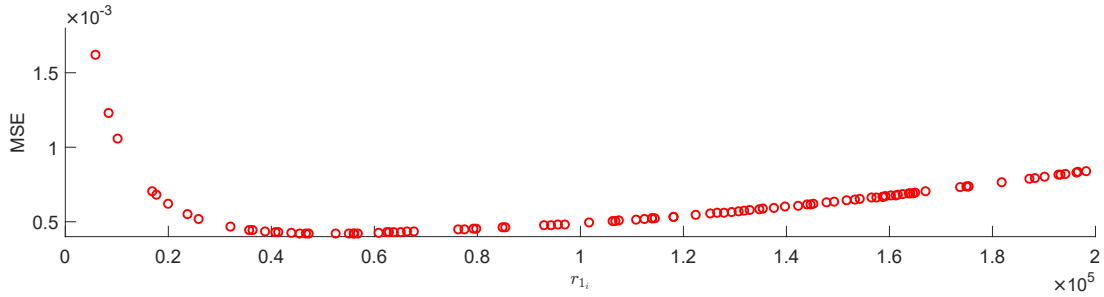

Fig. 4.6. Monte Carlo tests to establish the r_{1_i} values that offer the lowest estimation errors.

Estimation Weighting Matrices of the Deterministic Mechanism

Note that in the estimation cost function of the deterministic mechanism (4.7), the weighting matrix that penalizes the forgetting factor $\mathcal{R}_{2_i}$ is modified by the isolation mechanism. In this mechanism, the parameters α_i and β_i have been selected as $\alpha_i = 1$ and $\beta_i = 1 \times 10^6$, where the arbitrary value of β_i is higher enough to avoid the change of the unlikely flow. On the other hand, the weighting matrix $\mathcal{R}_{1_i}$ has been simplified as $\mathcal{R}_{1_i} = r_{1_i} \boldsymbol{I}_{\boldsymbol{2N_h}}$, where r_{1_i} is a tuning constant. In order to find accurate r_{1_i} values, Monte Carlo tests have been performed. In these tests, the r_{1_i} values are evaluated in order to minimize the mean square error (4.28) between the estimated and measured unknown flows by

$$MSE = \sum_{k=1}^{k_f} \frac{(s_{up_i}(k) - \hat{s}_{up_i}(k))^2}{k_f - 1} + \frac{(s_{dn_i}(k) - \hat{s}_{dn_i}(k))^2}{k_f - 1}. \tag{4.28}$$

As it is shown in Figure 4.6, it has been found that small values of r_{1_i} reduce the noise estimation with an inaccurate estimation of the unknown flows, and large values of r_{1_i} increase the estimation accuracy but also the noise estimation, finding that with r_{1_i} values close to 0.5×10^5, accurate and readable estimations of the unknown flows can be reached.

Weighting Matrices of the Stochastic Mechanism

Note that in the stochastic mechanism, the penalization matrices $\boldsymbol{\Sigma}_i(k)^{-1}$ and $\boldsymbol{\Sigma}_{\Delta_i}(k)^{-1}$ ((4.21) and (4.25), respectively), are obtained from the process covariances (4.18) and

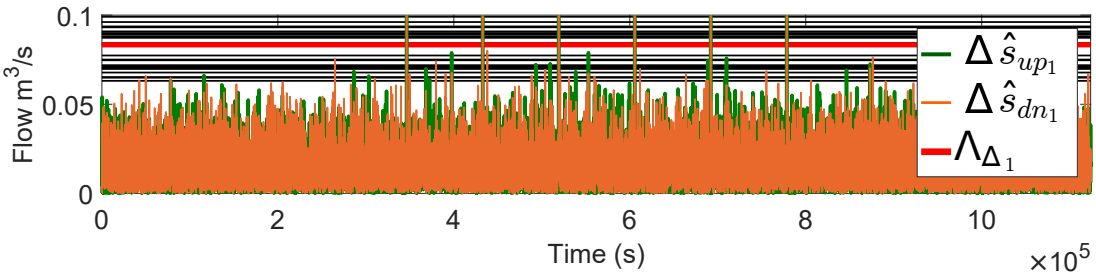

Fig. 4.7. Monte Carlo tests where the red line correspond to a threshold value of 4.5 times the maximum standard deviation of the estimated upstream and downstream unknown flow variations.

(4.24), where the information about the noise standard deviations ($\sigma_{\nu up_i}$, $\sigma_{\nu dn_i}$, $\sigma_{\omega up_i}$ and $\sigma_{\omega dn_i}$) is required. All the standard deviations have been obtained from system measurements at steady state. $\sigma_{\nu up_i}$, and $\sigma_{\nu dn_i}$ have been estimated directly from the standard deviation of the measured noise. The standard deviations associated to the flows measurements ($\sigma_{\omega up_i}$ and $\sigma_{\omega dn_i}$) have been estimated using the respective hydraulic relation presented in Table 2.1, and discretized multiplying by $\frac{\tau_s}{a_{up_i}}$ or $\frac{\tau_s}{a_{dn_i}}$ as appropriate. On the other hand, the forgetting penalization matrices ($\mathcal{D}_{s_i}$ and $\mathcal{R}_{s_i}(k)$) have been set as $\mathcal{D}_{s_i} = \boldsymbol{I_3}$, and $\mathcal{R}_{s_i}(k)$ is modified by the isolation mechanism with $\alpha_i = 1$ and $\beta_i = 1 \times 10^6$.

4.3.5 Isolation Mechanism Threshold

For the deterministic and stochastic cases, the threshold value has been adjusted from tests of the detection mechanisms at steady state, where the standard deviations of the estimated upstream and downstream unknown flow variations have been used to adjust the threshold value.

As it is shown in Figure 4.7, by the development of Monte Carlo tests, it has been found that a threshold value equal to 4.5 times the maximum standard deviation of the estimated upstream and downstream unknown flow variations avoids false detections and allows unknown flows detections.

4.3.6 Implementation

Finally, the deterministic and stochastic approaches are implemented by using Algorithms 1, and 2 respectively. In these algorithms, the f_l variable has been included to prevent false triggering of the stochastic and deterministic detection mechanisms.

4.4 Simulation Results and Discussion

In the simulation results, the deterministic and stochastic approaches are contrasted using filtered measurement noise, where a noise attenuation close to 20dB is obtained. Therefore, in order to test the approaches in the highest and lowest measurement noise scenarios, first, the approaches are contrasted with a filtered measurement noise with a

Algorithm 1 Deterministic estimation algorithm

Define, build, and obtain N_h, $\boldsymbol{\Phi}_i$, $\boldsymbol{B}_i$, $\boldsymbol{B}_{f_i}$, $\mathcal{D}_{1_i}$, $\mathcal{D}_{2_i}$, Λ_{Δ_i}, β_i, α_i, and $\mathcal{R}_{1_i}$.
while estimation is on **do**
  Acquire and evaluate $y_{up_i}(k)$, $y_{dn_i}(k)$, $u_i(k)$, $\xi_i(k)$, $\Delta y_{up_i}(k)$, $\Delta y_{dn_i}(k)$, $\Delta\xi_i(k)$
  if $k > N_h + 1$ **then**
    Obtain $\boldsymbol{y}_i$, $\boldsymbol{\xi}_i(k)$, $\Delta\boldsymbol{y}_i$, $\Delta\boldsymbol{\xi}_i(k)$
    Obtain $\boldsymbol{\Delta\hat{\psi}}$ by minimizing $\boldsymbol{J}_i$
    if $|\Delta\hat{s}_{up_i}(k)| < 0.1\Lambda_{\Delta_i}$ and $|\Delta\hat{s}_{dn_i}(k)| < 0.1\Lambda_{\Delta_i}$ **then**
      $f_l = 0$
    end if
    if $f_l = 0$ and $|\Delta\hat{s}_{up_i}(k)| > \Lambda_{\Delta_i}$ and $|\Delta\hat{s}_{up_i}(k)| > |\Delta\hat{s}_{dn_i}(k)|$ **then**
      $\mathcal{R}_{ktr_i} = \alpha_i$, $\mathcal{R}_{kup_i} = \alpha_i$, $\mathcal{R}_{kdn_i} = \beta_i$
    else if $f_l = 0$ and $|\Delta\hat{s}_{dn_i}(k)| > \Lambda_{\Delta_i}$ and $|\Delta\hat{s}_{dn_i}(k)| > |\Delta\hat{s}_{up_i}(k)|$ **then**
      $\mathcal{R}_{ktr_i} = \alpha_i$, $\mathcal{R}_{kup_i} = \beta_i$, $\mathcal{R}_{kdn_i} = \alpha_i$
    end if
    Build $\mathcal{R}_{2_i}$
    Obtain $\hat{\boldsymbol{\theta}}_i(k)$ by minimizing $\boldsymbol{V}_i$
    Obtain the unknown flow $\hat{\psi}_i(k) = \Omega_i(k)\hat{\theta}_i(k)$
  end if
end while

standard deviation of 1×10^{-4}m; and second, the approaches are contrasted with a filtered measurement noise with a standard deviation of 2.7×10^{-4}m.

4.4.1 Evaluation for the Smallest Noise Case

Figure 4.8 shows the performance comparison of the deterministic and stochastic detection mechanisms, where it is observed that when an unknown flow variation occurs, both approaches present estimated upstream and downstream unknown flows variations. Also, as expected, the stochastic mechanism presents the lowest noise amplitude. Additionally, in both cases, it is observed small false detections that account for the upstream and downstream levels interactions. Figure 4.9 shows the operation mode of the deterministic and stochastic isolation mechanisms, where the threshold Λ_{Δ_1} is established at six times the maximum experimental standard deviations between $\Delta\hat{s}_{up_1}$ and $\Delta\hat{s}_{dn_1}$. Therefore, only detections that overcome the threshold value are used to establish the origin of the unknown flow and change the corresponding forgetting factor. In Figure 4.9, the deterministic and stochastic strategies present similar behavior. However, the relations between the maximum detected variation and the threshold of the deterministic and stochastic approaches are close to 3.8 and 6.6, respectively. That means that the stochastic detection mechanism offers a better relationship between the estimated signal and the estimated noise. Therefore, with the stochastic mechanism, it is most likely to detect unknown flows from noisy measurements. In Figure 4.10, the behaviors of the deterministic and stochastic estimation mechanisms are shown, where the deterministic mechanism presents more

Algorithm 2 Stochastic estimation algorithm

Define, build, and obtain N_h, $\boldsymbol{\Phi}_i$, $\boldsymbol{B}_i$, $\boldsymbol{B}_{f_i}$, $\boldsymbol{\Sigma}_{\Delta_i}(k)$, $\mathcal{D}_{s_i}$, Λ_{Δ_i}, β_i, α_i, $\mathcal{R}_{s_i(k)}$, $\omega_i(k)$, $\nu_i(k)$, and $\boldsymbol{T}_i$.
while estimation is on **do**
  Acquire and evaluate $y_{up_i}(k)$, $y_{dn_i}(k)$, $u_i(k)$, $\xi_i(k)$, $\Delta y_{up_i}(k)$, $\Delta y_{dn_i}(k)$, $\Delta\xi_i(k)$
  if $k > N_h + 1$ **then**
    Obtain $\boldsymbol{y}_i$, $\boldsymbol{\xi}_i(k)$, $\Delta\boldsymbol{y}_i$, $\Delta\boldsymbol{\xi}_i(k)$
    Obtain $\Delta\hat{\bar{\psi}}_i(k)$ by minimizing $\boldsymbol{J}_{\boldsymbol{s_i}}$
    if $|\Delta\hat{\bar{s}}_{up_i}(k)| < 0.1\Lambda_{\Delta_i}$ and $|\Delta\hat{\bar{s}}_{dn_i}(k)| < 0.1\Lambda_{\Delta_i}$ **then**
      $f_l = 0$
    end if
    if $f_l = 0$ and $|\Delta\hat{\bar{s}}_{up_i}(k)| > \Lambda_{\Delta_i}$ and $|\Delta\hat{\bar{s}}_{up_i}(k)| > |\Delta\hat{\bar{s}}_{dn_i}(k)|$ **then**
      $\mathcal{R}_{ktr_i} = \alpha_i$, $\mathcal{R}_{kup_i} = \alpha_i$, $\mathcal{R}_{kdn_i} = \beta_i$
    else if $f_l = 0$ and $|\Delta\hat{\bar{s}}_{dn_i}(k)| > \Lambda_{\Delta_i}$ and $|\Delta\hat{\bar{s}}_{dn_i}(k)| > |\Delta\hat{\bar{s}}_{up_i}(k)|$ **then**
      $\mathcal{R}_{ktr_i} = \alpha_i$, $\mathcal{R}_{kup_i} = \beta_i$, $\mathcal{R}_{kdn_i} = \alpha_i$
    end if
    Build $\mathcal{R}_{s_i}$
    Obtain $\hat{\bar{\theta}}_i(k)$ by minimizing $\boldsymbol{V}_{s_i}$
    Obtain the unknown flow $\hat{\psi}_i(k) = \Omega_i(k)\hat{\bar{\theta}}_i(k)$
  end if
end while

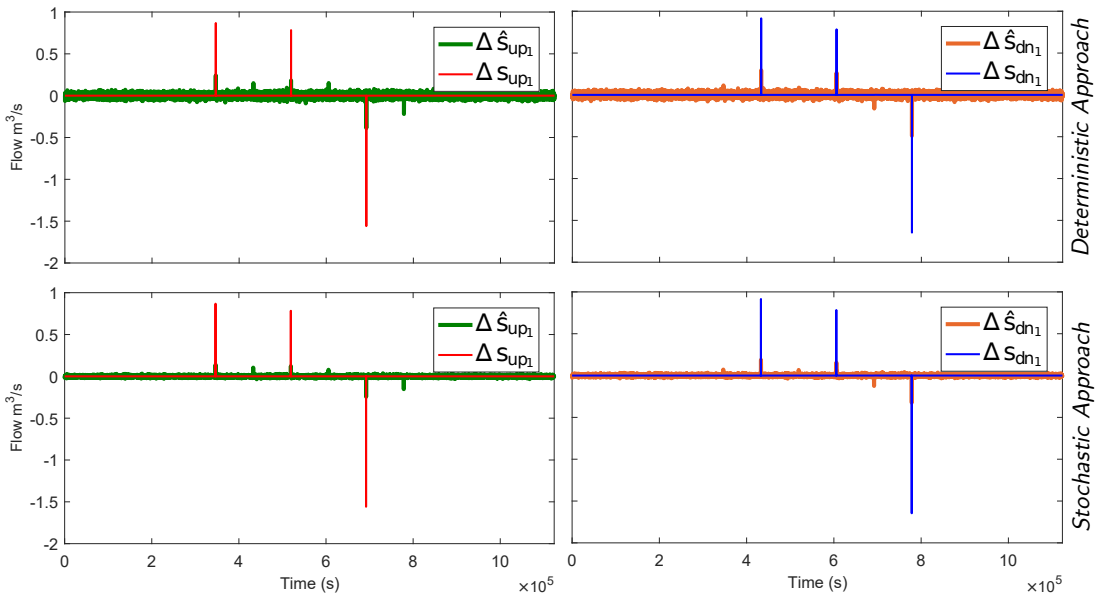

Fig. 4.8. Performance comparison of the deterministic and stochastic detection mechanisms.

accurate estimations than the stochastic mechanism. It occurs since the deterministic estimation mechanism finds the optimal unknown parameters ($\hat{k}_{tr_1}$, $\hat{k}_{up_1}$, and $\hat{k}_{dn_1}$) for

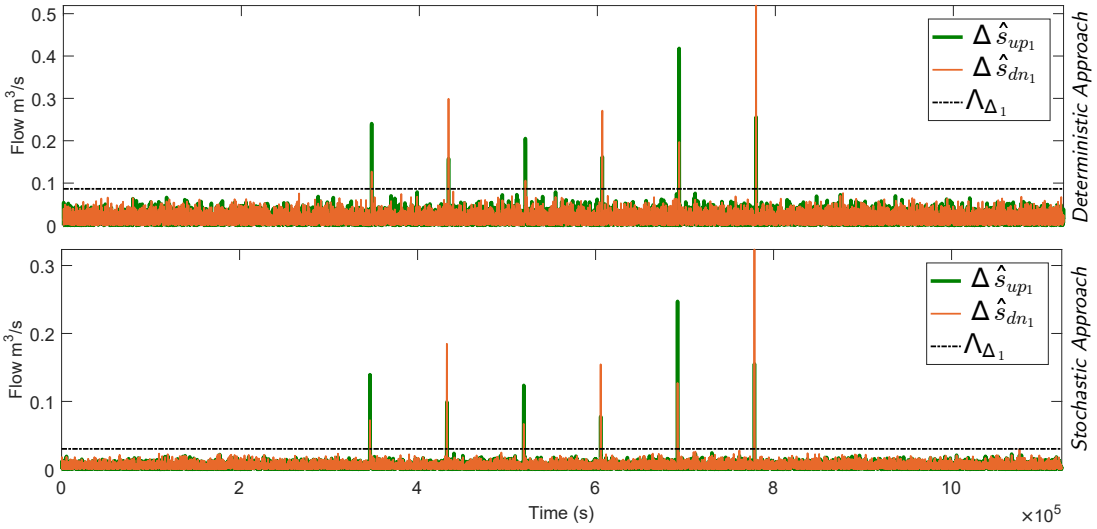

Fig. 4.9. Comparison of the deterministic and stochastic isolation mechanisms, only detections that overcome Λ_{Δ_1} are compared to establish the origin of the unknown flow.

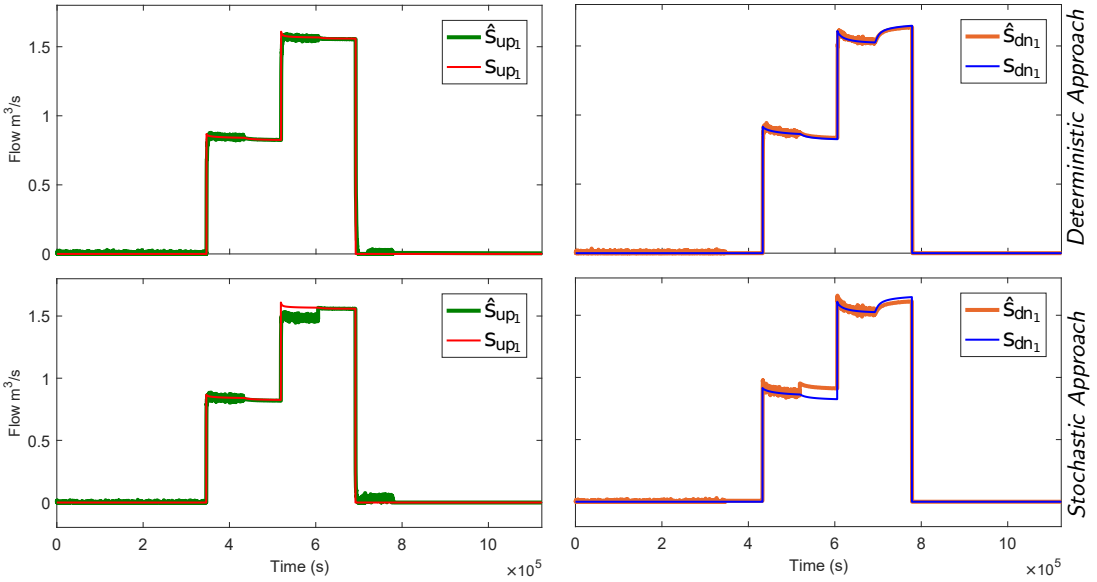

Fig. 4.10. Performance comparison of the deterministic and stochastic unknown flows estimators.

each time instant. On the other hand, in the stochastic approach, over the estimation window, it is found the expected value of the unknown parameters, showing difficulties for rapid changes response. However, it is observed that the estimations of the stochastic approach are suitable enough to be used for DIMEUF.

The total amount of the estimated unknown flows and the estimated flow transition are shown in Figure 4.11, where both, the deterministic and stochastic strategies present an ideal estimation of the total unknown flows. That means that despite the discrepancies that the upstream and downstream unknown flows may show, the estimation satisfy the

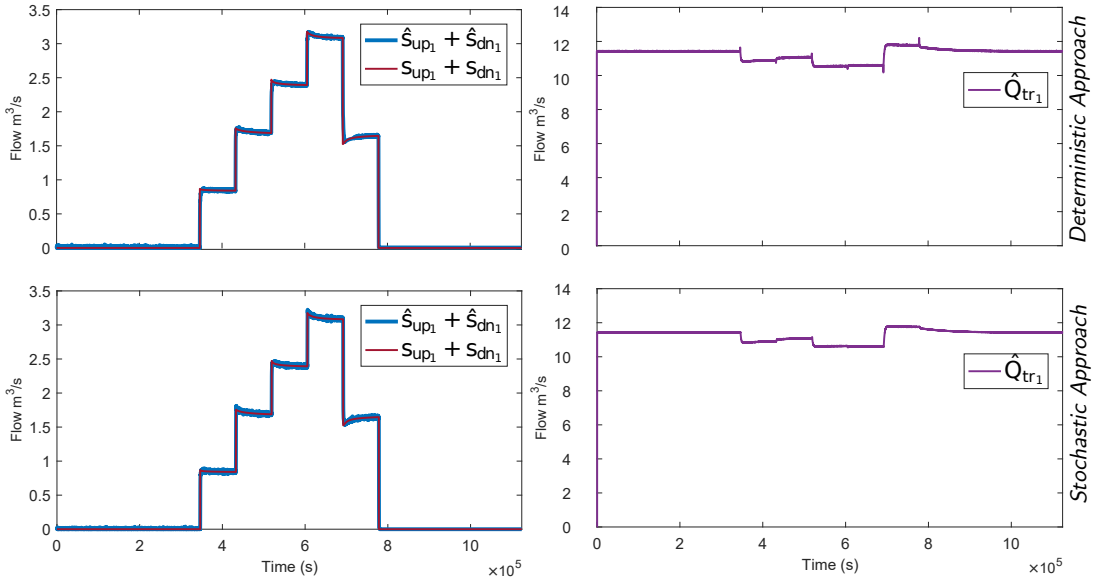

Fig. 4.11. Total amount of the estimated unknown flows and the estimated flow transition.

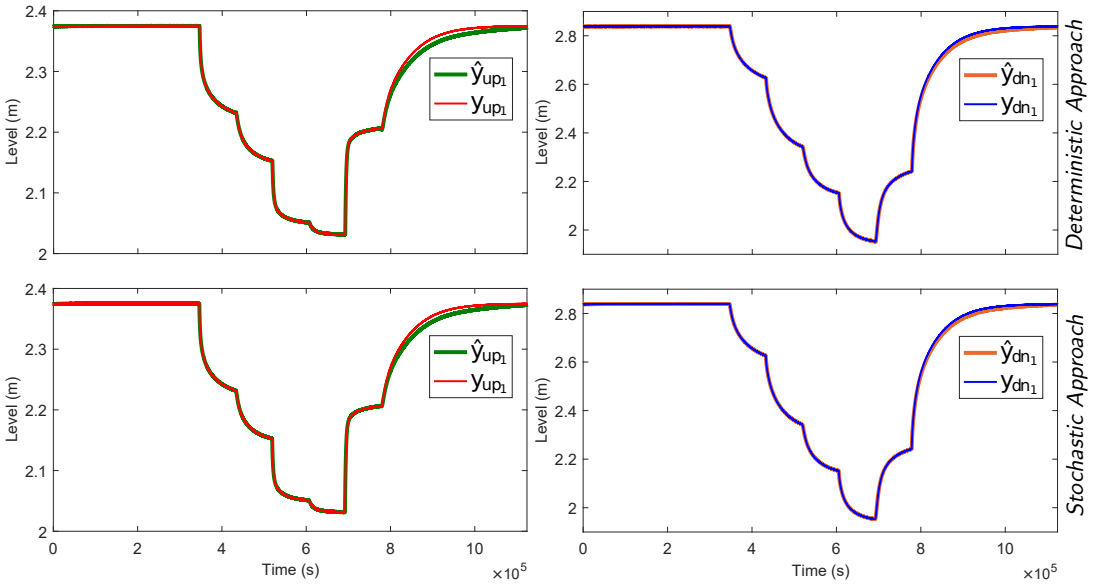

Fig. 4.12. Levels estimation comparison.

overall channel mass balance, and levels and flows discrepancies are compensated with the flow transition. Note that, in order to compensate rapid changes, the flow transition of the deterministic approach presents rapid variations.

The level's estimation of the deterministic and stochastic approaches are similar and accurate (Figure 4.12). This result corroborates the suitability of the selected modeling strategy because, despite the downstream level of the reference model changes almost a meter, the simplified selected strategy describes accurately the behavior of the system. Moreover, it is highlighted that in the measured and estimated level, the presence of

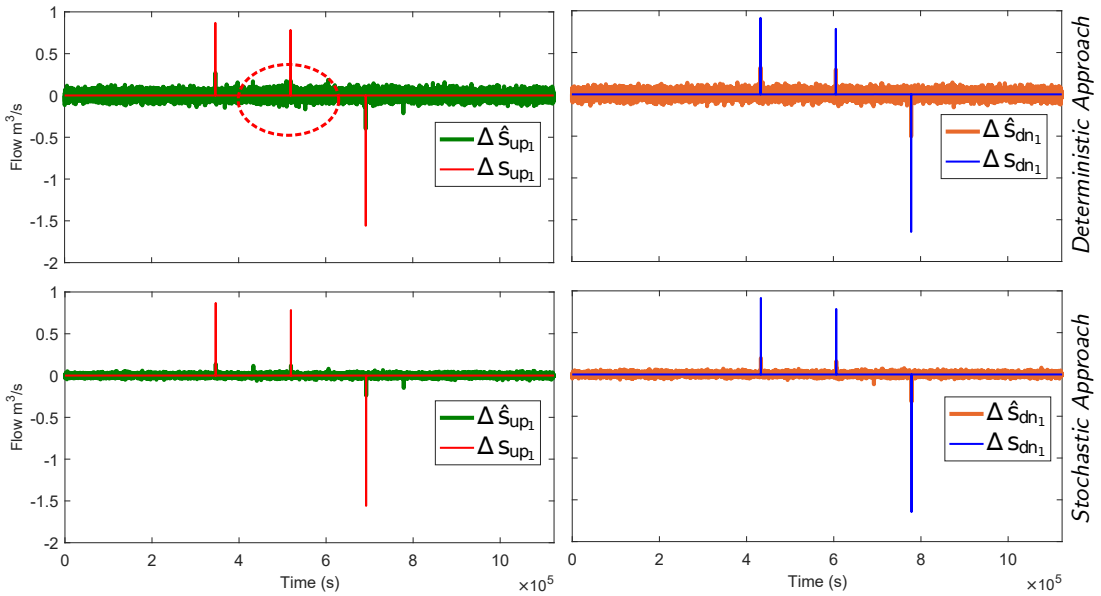

Fig. 4.13. Evaluation in presence of highly-noised measurements, where it is highlighted that the deterministic detection mechanism presents unreadable unknown flow detections.

remaining noise is almost imperceptible. This shows one of the hardest problems in the estimation of unknown flows in OCIS, where due to the usual large areas that the OCIS present, even large flow variations can be imperceptible from level measurements, or can be masked between measurement and process noises. For that, next, the behavior of the stochastic and deterministic approaches are tested in presence of highly-noised measurements.

4.4.2 Evaluation for the Highest Noise Case

Figure 4.13 shows the advantage of the stochastic strategy in the detection of unknown flows. In the deterministic strategy, it is observed that there are unreadable unknown flow detections, which are masked for the noise estimation. Similarly, in Figure 4.14 it is shown that the deterministic isolation mechanism is not capable of distinguish between the estimated noise and all the estimated unknown flow variations. On the other hand, the stochastic isolation mechanism is capable to accomplish with suitable detections for all variations.

Figure 4.15, shows how the isolation problems of the deterministic mechanism induce wrong penalizations and inaccurate estimations of the unknown flows. Conversely, in the stochastic mechanism, the highest noise induce negative effects to the estimation algorithm. However, in the stochastic mechanism, the estimated unknown flows are accurate enough to be used for DIMEUF.

In the deterministic case, the isolation mechanism problems also affect the total estimation flow (Figure 4.16), and the estimation of the upstream and downstream levels (Figure 4.17). In contrast, the stochastic mechanism only presents small discrepancies in

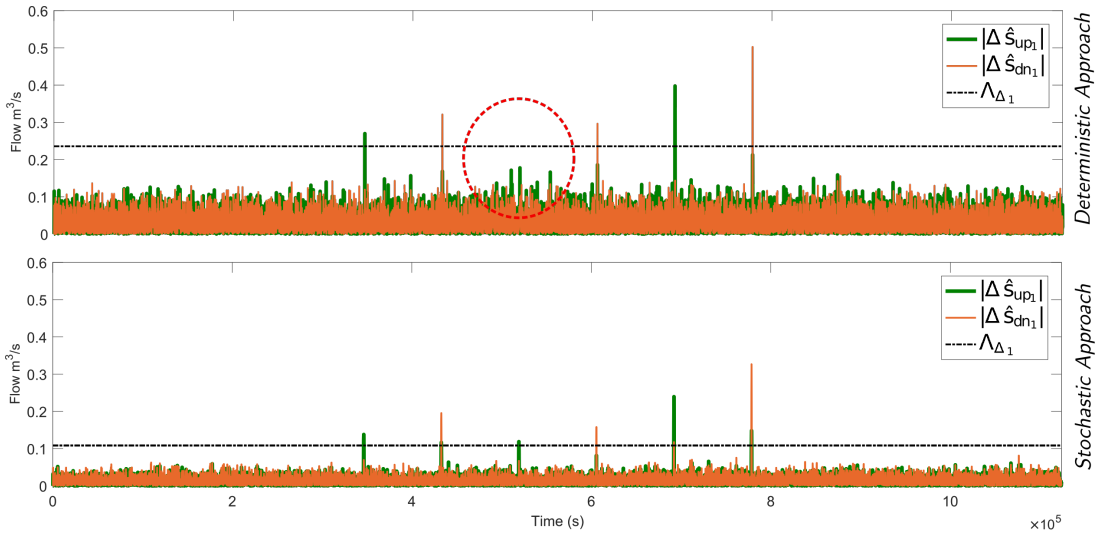

Fig. 4.14. Evaluation in presence of highly-noised measurements, where it is shown that the deterministic isolation mechanism is not capable of distinguish between the estimated noise and all the estimated unknown flow variations.

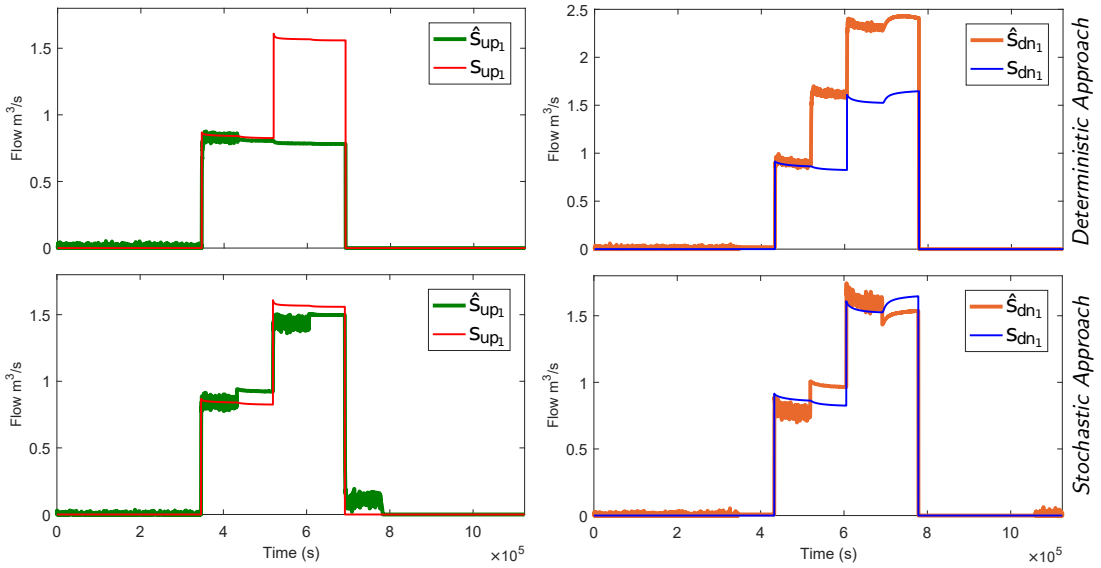

Fig. 4.15. Evaluation in presence of highly-noised measurements, where the isolation problems of the deterministic mechanism induce wrong penalizations and inaccurate estimations of the unknown flows.

the estimation of the upstream and downstream unknown flows (Figure 4.15), highlighting the proper performance of the stochastic strategy in presence of noisy measurements.

4.4.3 Unknown Flows Estimation Errors Comparison

In order to summarize the performance comparison among the deterministic and stochastic approaches under the smallest and highest noise scenarios, Fig. 4.18 shows the box

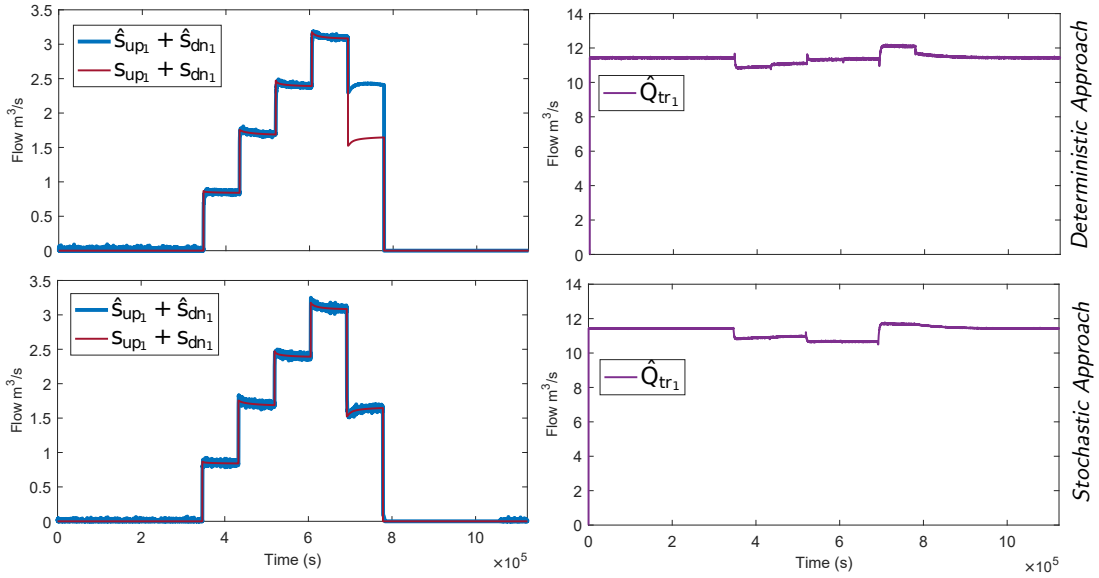

Fig. 4.16. Evaluation in presence of highly-noised measurements, where it is highlighted that the isolation mechanism problems of the deterministic case also affect the total flow estimated.

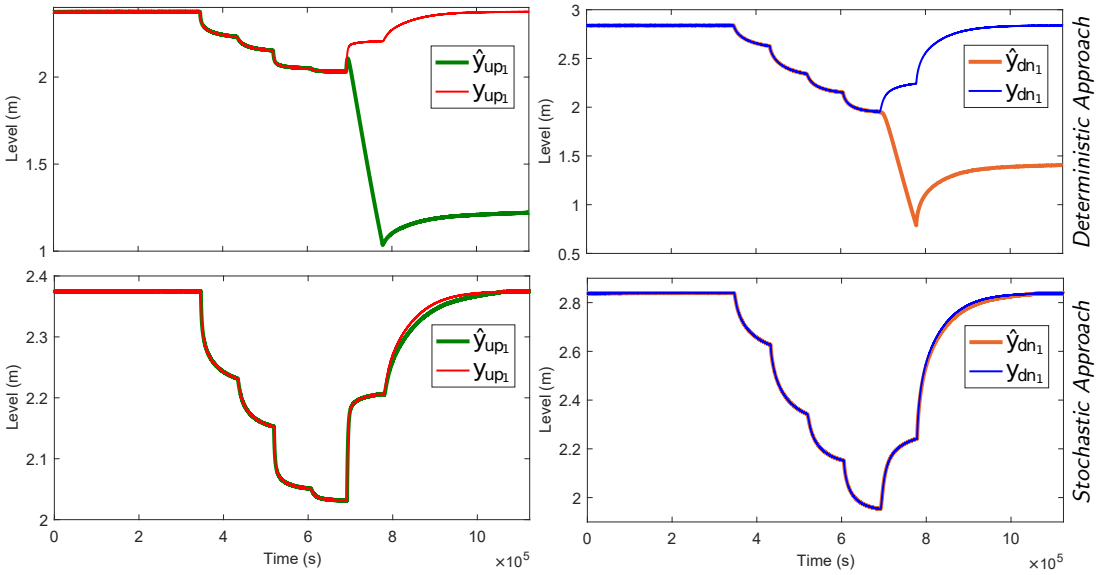

Fig. 4.17. Evaluation in presence of highly-noised measurements, where it is shown how the isolation mechanism problems of the deterministic case also affect the estimation of the upstream and downstream levels.

plots corresponding to distribution data of the upstream plus downstream unknown flows estimation error, where the red lines are the average error value, and the blue lines are first and third quartiles (25^{th} percentile and 75^{th} percentile), showing that even tough the distribution is not normal, in the four cases the error is distributed close to zero. The black lines represent the upstream and downstream limits that contain about 93%

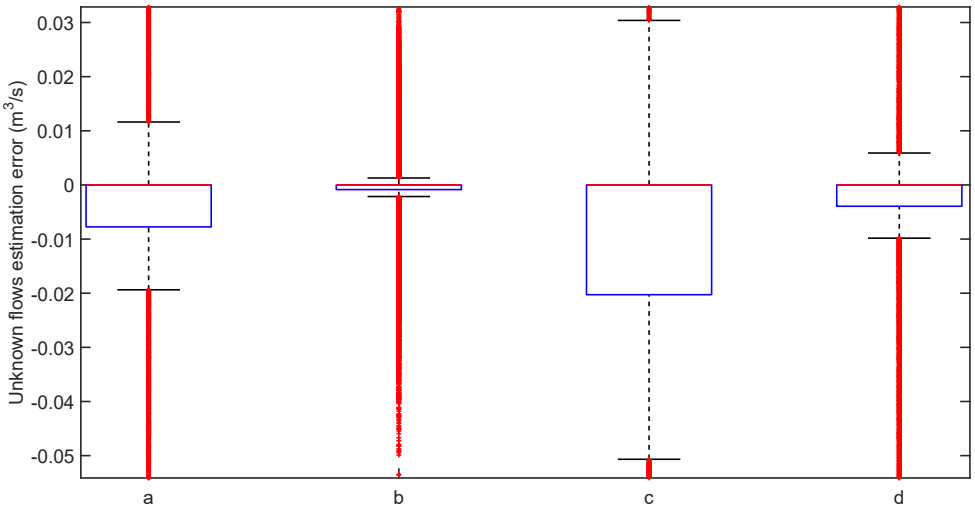

Fig. 4.18. Comparison of the upstream plus downstream unknown flows estimation error, where: a. corresponds to the evaluation for the smallest noise case of the deterministic approach; b. corresponds to the evaluation for the smallest noise case of the stochastic approach; c. corresponds to the evaluation for the highest noise case of the deterministic approach; and d. corresponds to the evaluation for the highest noise case of the stochastic approach.

of the data, the red marks correspond to the outliers (0.7% of the data). This comparison reveals the advantage of using the stochastic approach (b, d). In the smallest and highest noise scenarios, the data dispersion of the stochastic approach is smaller than the data dispersion presented for the deterministic approach. It must be highlighted that, according to the data distribution, in both scenarios, by using the stochastic approach the estimation precision is increased almost ten times. This finding justifies the use of the stochastic over the deterministic approach.

4.4.4 Hydraulic Conditions

Despite the developed test has been performed over a realistic system, and the estimation strategies have been contrasted against data obtained from a modeling tool that numerically solves the SVE of the hydraulic systems (obtaining successful results), one question arises over the operative hydraulic conditions of the proposed DIMEUF strategies. Note that the selected simplified modeling strategy is the fundamental element of the DIMEUF approaches. Therefore, the operative hydraulic conditions of the estimation strategies can be addressed from hydraulic analyses of the different flows that conform the simplified modeling strategy.

Concerning the known channel inflows and outflows, by using the respective flow relations, such as the presented in Table 2.1, the modeling strategy can be easily adapted to multiple types of hydraulic structures. On the other hand, the flow transition in (3.3) presents a hydraulic condition that must be analyzed. The flow transition only is real if the head loss due to friction (h_{L_i}) is strictly positive. In that way, the proposed estimation

approaches are only useful in OCIS with a considerable potential decay. In order to illustrate this claim, the testings of the estimation strategies using a canal inspired on lateral canal WM of the Maricopa Stanfield Irrigation and Drainage District in central Arizona, reported by Clemmens et al. (1998) is also proposed. This canal is chosen because it presents hydraulic characteristics that are highly different from the characteristics of the Corning canal. The WM canal is a 100m length canal, with upstream elevation of 3.6m, downstream elevation of 3.3m, and width of 1.5m. Moreover, due to the short length of the WM canal, their potential decay can be easily changed by modification of the channel roughness.

In this order of ideas, in Fig. 4.19, the performance of a stochastic DIMEUF strategy over the WM channel is shown. In this case, the WM channel has been simulated in EPA-SWMM using a Manning roughness coefficient of 0.004 $s/m^{1/3}$, and the DIMEUF strategy has been designed following the same procedure that had been exposed to the Corning canal. Moreover, in Fig. 4.19, the behavior of the head loss due to friction is shown. Note that despite the head loss due to friction is small, this is always positive and the DIMEUF strategy reaches an accurate estimation of the unknown flows. On the other hand, in Fig. 4.19, the head loss due to friction behavior of the WM channel with a Manning roughness coefficient of 0.001 $s/m^{1/3}$, is shown, where it is observed that the head loss due to friction is close to zero, and there are sections that show negative values of the head loss due to friction. This negative values, which could be attained to the equal mean flow velocity assumption of the approximated model, make impossible the implementation of the developed DIMEUF strategies. This result, which could be interpreted as a limitation of the simplified modeling strategy and therefore of the DIMEUF strategies, can be overcome if, for control and estimation purposes, the channels that have a small head loss due to friction are modeled as a unique storage unit, with area equal to the channel area and known inflows modeled by using the hydraulic relation given in Table 2.1. In this case, there is a limitation on identifying the either upstream or downstream unknown flow origin, and there is no need to use detection and isolation mechanisms. Another option, which is out of this work scope, could be to eliminate the modeling assumption of an equal mean flow velocity along the channel. This solution implies to use of the SVE in order to establish differential equations that describe the momentum conservation. This information could be used to identify the instant differences between the momentum conservation of the real and modeled systems. Therefore, the development of DIMEUF strategies designed from the SVE have the potential of improving the reached results in this work. However, due to the complexity of the SVE, and the probable model order increases, this development is not evident.

4.5 Summary

In this chapter, the proposed control-oriented modeling strategy developed from approximated mass and potential energy balances has been used in the design of two strategies for DIMEUF. Therefore, the estimation strategies take into account the effects of flow conduction. These strategies have been designed exploiting the advantages that the MHE approach shows in dealing with constrained non-linear systems. The proposed strategies

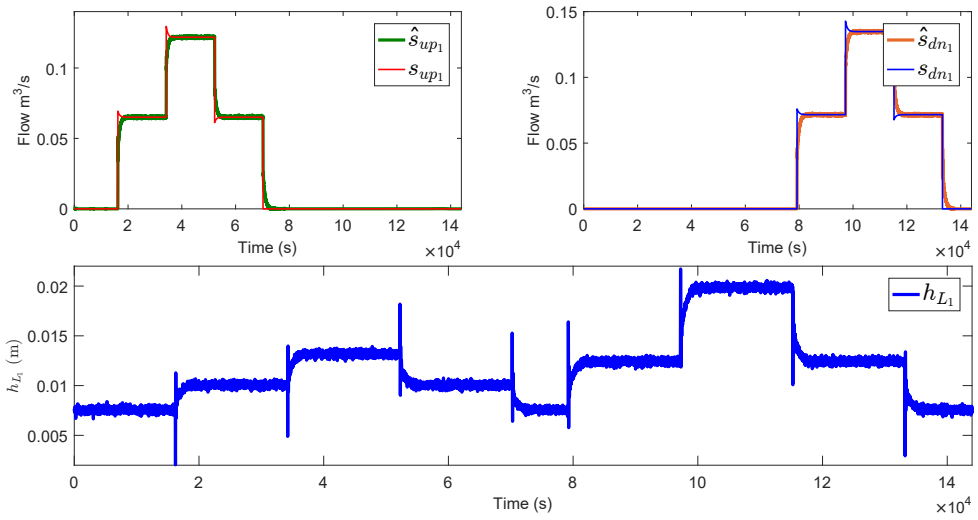

Fig. 4.19. Head loss due to friction for channel with high roughness coefficient.

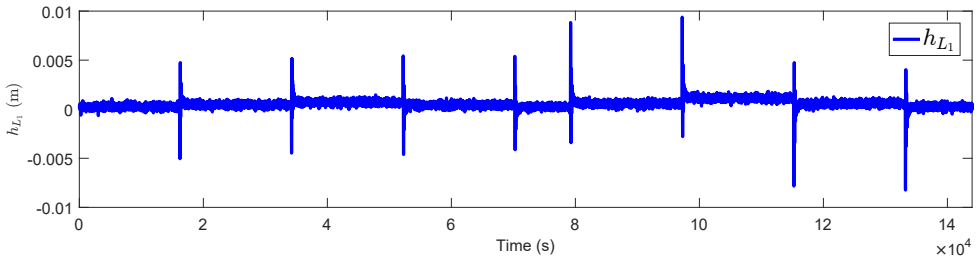

Fig. 4.20. Head loss due to friction for channel with low roughness coefficient.

also take advantage of the forgetting factor, which has been used to overcome the problem of sub-optimal unknown flow estimations observed with the direct use of an MHE. The strategies have been designed from deterministic and stochastic points of view, and have been tested by using two well-known benchmarks with different characteristics. The test shows that by including information about noise and expected level values the estimation performance increase, and that the proposed estimation strategies offer an accurate estimation of unknown flows in channels with considerable decay of potential. However, it is highlighted that channels with small decay of potential can be modeled as reservoirs, with the corresponding adaptation of the estimation strategies. Note that the accurate estimations of the unknown flows can be used to take opportune actions in the affected channels, but also can be used to improve accuracy and considered information in control-oriented models (i.e., parameters associated with leaks and seepage). In this order of ideas, knowing that parameters associated with unknown flows such as leaks and seepage can be estimated, in Chapter 5 multiple control strategies are presented, where one of these strategies is developed to minimize losses associated with leaks and seepage.

Chapter 5

Control Approaches for OCIS

In OCIS, flows and levels are controlled with hydraulic regulation structures, and each regulation structure position is calculated by an administrator of the irrigation district, who is the person that assigns the appropriate amount of water to the users. Commonly, each regulation structure is manually adjusted by operators, whom perform these tasks throughout kilometers of channels, adjusting hundreds of hydraulic structures. In the normal operation of the OCIS disturbances are common (e.g., flow variation at the source, channel obstructions, leaks, and even water robbery), and with this kind of manual system operation, there are no possibilities of an opportune intervention. These disturbances might cause overflows, incorrect water supply to the users, and a high environmental impact. Automatic control strategies might be one technological option in order to deal with these issues. This chapter presents the developed research on control alternatives for OCIS.

First, in Section 5.1, an illustrative example is proposed with the objective to show a contextualized description of the most popular modeling strategy (integrator delay), and the most common control techniques that have been reported in the OCIS control field (PID, LQR, and MPC)(Conde et al., 2021b). Moreover, in the illustrative example, centralized and distributed architectures are described under feedback and feedback+feedforward configurations. Some examples dealing with control-action variable and control objectives are shown. On the other hand, as it has been shown in Chapter 3, the integrator delay and other control-oriented models reported, do not include information about channel interactions. Therefore, in order to design control strategies for interacting OCIS, in Section 5.2, from the proposed control-oriented model that assumes a constant potential energy difference along the channels, a nonlinear model-based control strategy for interacting OCIS that ensures the system stability despite nonlinearities, internal delays, and channel interactions is proposed.

Finally, in Section 5.3, in order to contribute to the waste of water reduction, an efficient control approach for OCIS capable to reduce the waste of water by up to 50%, is presented. The proposed approach is a non-linear model predictive control strategy that operates under request mode and has been designed from a simplified modeling strategy. In the design of the non-linear model predictive control strategy, sufficient controllability and reachability conditions that guarantee the controlled system stability

have been presented. Moreover, the proposed control strategy has been tested using a well-known testbed proposed in the literature, and the results show that by using this strategy an appropriate amount of water to the users can be supplied and the waste of water can be reduced.

5.1 Conventional Control Strategies: An Illustrative Example

The objective of this section is to show an illustrative example that includes descriptions of the most popular modeling strategy (ID), and the most common control techniques that have been reported in the OCIS field (PID, LQR, and MPC). Moreover, in this example, there are descriptions of centralized and distributed architectures, feedback and feedback+feedforward configurations, as well as descriptions about control-action variable and control objective. In this direction, an OCIS with three channels is proposed, where the control objective is to maintain a constant depth at the downstream end of the channels, overcoming disturbances and outlet flows. The three channels are modeled using the ID control-oriented modeling strategy, and at the end of each channel, a permanent outflow is assumed to be regulated with an undershoot gate. Therefore, the outlet flow of the channel i is given by $k_{out_i}\sqrt{x_{dn_i}}$, where k_{out_i} is a constant. The model of the proposed system is given by

$$\begin{aligned} a_1\dot{x}_{dn1} &= -k_{out1}\sqrt{x_{dn1}} + q_1(t-\tau_1) - q_2 - q_{out1} \\ a_2\dot{x}_{dn2} &= -k_{out2}\sqrt{x_{dn2}} + q_2(t-\tau_2) - q_3 - q_{out2} \\ a_3\dot{x}_{dn3} &= -k_{out3}\sqrt{x_{dn3}} + q_3(t-\tau_3) - q_{out3}, \end{aligned} \tag{5.1}$$

where $a_1 = 1000\text{m}^2$, $a_2 = 2000\text{m}^2$, $a_3 = 1000\text{m}^2$, $\tau_1 = 200\text{s}$, $\tau_2 = 300\text{s}$, $\tau_3 = 200\text{s}$. The k_{out_i} parameters are given by $k_{out1} = \sqrt{2}$, $k_{out2} = \sqrt{1.5}$, and $k_{out3} = 1$. In the case study, the three most common control strategies are tested (PID, MPC, and LQR). Consequently, in order to obtain a design model, the proposed system is linearized at an equilibrium point given by

$$0 = -k_{out_i}\sqrt{\bar{x}_{dn_i}} + \bar{q}_i(t-\tau_i) - \bar{q}_i - \bar{q}_{out_i}, \tag{5.2}$$

where $\bar{x}_{dn1} = 2\text{m}$, $\bar{x}_{dn2} = 1.5\text{m}$, $\bar{x}_{dn3} = 1\text{m}$, $\bar{q}_1 = \bar{q}_1(t-\tau_1) = 4.5\text{m}^3/\text{s}$, $\bar{q}_2 = \bar{q}_2(t-\tau_2) = 2.5\text{m}^3/\text{s}$, $\bar{q}_3 = \bar{q}_3(t-\tau_3) = 1\text{m}^3/\text{s}$, $\bar{q}_{out_i} = 0\text{m}^3/\text{s}$. Hence, the following linearized model is obtained:

$$\begin{aligned} a_1\delta\dot{x}_{dn1} &= -\frac{1}{2}\delta x_{dn1} + \delta q_1(t-\tau_1) - \delta q_2 - \delta q_{out1} \\ a_2\delta\dot{x}_{dn2} &= -\frac{1}{2}\delta x_{dn2} + \delta q_2(t-\tau_2) - \delta q_3 - \delta q_{out2} \\ a_3\delta\dot{x}_{dn3} &= -\frac{1}{2}\delta x_{dn3} + \delta q_3(t-\tau_3) - \delta q_{out3}, \end{aligned} \tag{5.3}$$

where $\delta x_{dn_i}(t)$, $\delta q_i(t)$, and $\delta q_{out_i}(t)$ are levels and flow variations around the equilibrium point. The linearized system describes a highest bandwidth given by $\omega_b = 1/2000$ rad/s.

Therefore, following the recommendations presented by Litrico and Fromion (2009), the linear system is discretized with 100s sampling time (τ_s), obtaining the following linear discrete-time system:

$$\begin{aligned}
\delta x_{dn_1}(k+1) &= a_{11}\delta x_{dn_1}(k) + a_{12}\delta q_1(k-2) + b_{12}\delta q_2(k) + b_{d_{11}}\delta q_{out_1}(k) \\
\delta x_{dn_2}(k+1) &= a_{44}\delta x_{dn_2}(k) + a_{45}\delta q_2(k-3) + b_{43}\delta q_3(k) + b_{d_{42}}\delta q_{out_2}(k) \\
\delta x_{dn_3}(k+1) &= a_{88}\delta x_{dn_3}(k) + a_{89}\delta q_3(k-2) + b_{d_{83}}\delta q_{out_3}(k),
\end{aligned} \tag{5.4}$$

where $\delta x_{dn_i}(k)$, $\delta q_i(k)$, and $\delta q_{out_i}(k)$ are the levels and flow variations at time instant k. Moreover, $a_{11} = \left(1 - \frac{\tau_s}{2a_1}\right)$; $a_{12} = \frac{\tau_s}{a_1}$;$b_{12} = -\frac{\tau_s}{a_1}$; $b_{d_{11}} = -\frac{\tau_s}{a_1}$; $a_{44} = \left(1 - \frac{\tau_s}{2a_2}\right)$; $a_{45} = \frac{\tau_s}{a_2}$;$b_{43} = -\frac{\tau_s}{a_2}$; $b_{d_{42}} = -\frac{\tau_s}{a_2}$; $a_{88} = \left(1 - \frac{\tau_s}{a_3}\right)$; $a_{89} = \frac{\tau_s}{a_3}$; and $b_{d_{83}} = -\frac{\tau_s}{a_3}$.

5.1.1 LQR Design

With the objective to obtain a classical state-space realization of the linearized discrete-time system (5.4), the delays are transformed into states. In this direction, the proposed change of variables is shown in Figure 5.1, where $x_1(k) = \delta x_{dn_1}(k)$; $x_2(k) = \delta q_1(k-2)$; $x_3(k) = \delta q_1(k-1)$; $x_4(k) = \delta x_{dn_2}(k)$; $x_5(k) = \delta q_2(k-3)$; $x_6(k) = \delta q_2(k-2)$; $x_7(k) = \delta q_2(k-1)$; $x_8(k) = \delta x_{dn_3}(k)$; $x_9(k) = \delta q_3(k-2)$; $x_{10}(k) = \delta q_3(k-1)$; and z^{-1} is the representation of a discrete time delay. With this change of variables, the discrete linear system can be described as

$$\begin{aligned}
x_1(k+1) &= a_{11}x_1(k) + a_{12}x_2(k) + b_{12}\delta q_2(k) + b_{d_{11}}\delta q_{out_1}(k) \\
x_2(k+1) &= x_3(k) \\
x_3(k+1) &= \delta q_1(k) \\
x_4(k+1) &= a_{44}x_4(k) + a_{45}x_5(k) + b_{43}\delta q_3(k) + b_{d_{42}}\delta q_{out_2}(k) \\
x_5(k+1) &= x_6(k) \\
x_6(k+1) &= x_7(k) \\
x_7(k+1) &= \delta q_2(k) \\
x_8(k+1) &= a_{88}x_8(k) + a_{89}x_9(k) + b_{d_{83}}\delta q_{out_3}(k) \\
x_9(k+1) &= x_{10}(k) \\
x_{10}(k+1) &= \delta q_3(k).
\end{aligned} \tag{5.5}$$

Therefore, the discrete-time linear system can be synthesized using a classical state-space realization of the form $x(k+1) = Ax(k) + B\delta q(k) + B_d\delta q_{out}(k)$; and $y(k) = Cx(k)$, where $x(k) \in \mathbb{R}^{10}$ is the state vector; $\delta q(k) \in \mathbb{R}^3$ the input vector; $\delta q_{out}(k) \in \mathbb{R}^3$ the disturbance vector; $A \in \mathbb{R}^{10\times10}$ the state matrix; $B \in \mathbb{R}^{10\times3}$ the input matrix; $B_d \in \mathbb{R}^{10\times3}$ the disturbances matrix; and $C \in \mathbb{R}^{3\times10}$ the output matrix such that $y(k) = [x_1(k)\ x_4(k)\ x_8(k)]^\top$.

Figure 5.2 shows the proposed structure of a centralized LQR control for OCIS. Note that as it is shown in the change of variables, z^- indicates the states that can be obtained from time delays of the flow variations, and the integral part is included with the objective

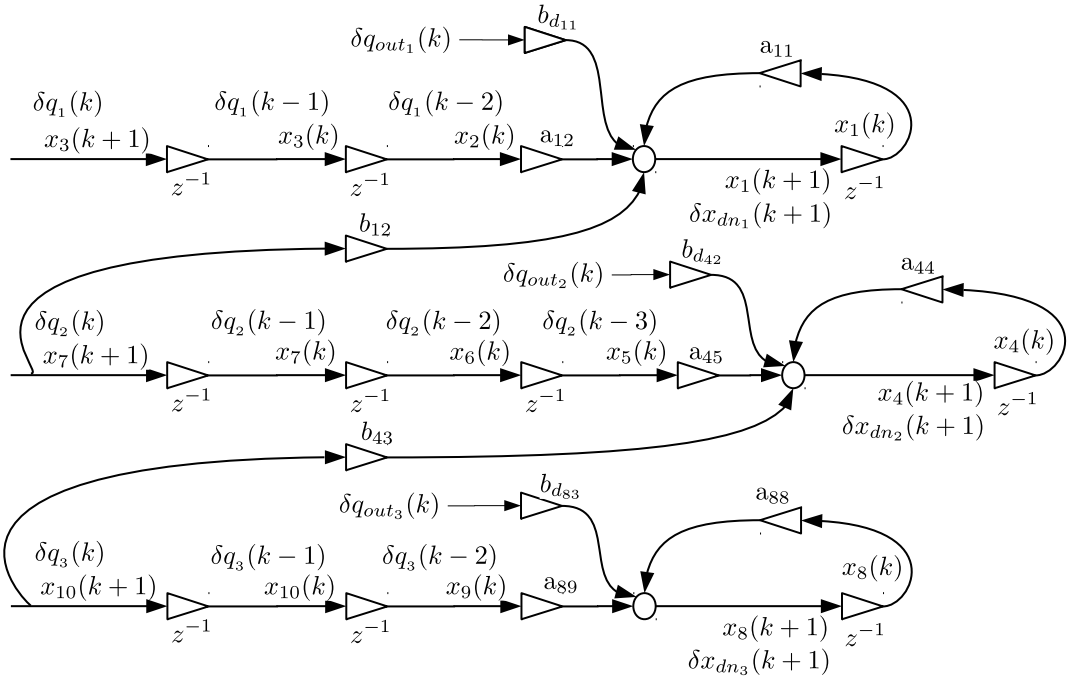

Fig. 5.1. Graphical description of the delays transformation into states, where $a_{i,j}$ is a constant at the i, j position of the state matrix, $b_{i,j}$ is a constant at the i, j position of the input matrix, and $b_{d_{i,j}}$ is a constant at the i, j position of the disturbances matrix.

of having null steady-state error. Therefore, the controller is designed using an augmented system of the form $x_A(k+1) = A_A x_A(k) + B_A \delta q(k)$; and $y_A(k) = C_A x_A(k)$, where $x_A(k) \in \mathbb{R}^{13}$ is the augmented state vector; $A_A \in \mathbb{R}^{13\times 13}$ the augmented state matrix; $B_A \in \mathbb{R}^{13\times 3}$ the augmented input matrix; and $C_A \in \mathbb{R}^{3\times 13}$ the augmented output matrix. In specific,

$$A_A = \begin{bmatrix} \mathbf{I} & C \\ \mathbf{0} & A \end{bmatrix},\ B_A = \begin{bmatrix} \mathbf{0} \\ B \end{bmatrix},\ C_A = \begin{bmatrix} \mathbf{0} & C \end{bmatrix},$$

where $\mathbf{I}$ and $\mathbf{0}$ are identity and zero matrices with suitable dimensions, respectively.

In Figure 5.2, it is observed that the control law is given by $q(k) = \bar{q} + \delta q$. This control law does not include information about the outlet flows, hence the controlled system has an FB configuration. Moreover, $K \in \mathbb{R}^{3\times 13}$ is the control matrix. In order to obtain K, in the LQR controllers, the optimization problem to be solved is to maintain the state vector close to the origin without an excessive expenditure of control effort (Kirk, 2004). Then, the objective function to be minimized is given by

$$J = \sum_{k=0}^{\infty} \left({x_A}^{\top}(k) \mathcal{Q} x_A + \delta q^{\top}(k) \mathcal{R} \delta q(k) \right), \tag{5.6}$$

where $\mathcal{Q}$, $\mathcal{R}$ are diagonal weighting matrices that are used as tuning parameters that penalize the state and control variables. This test has been developed with diagonal values of 100 and 1 for $\mathcal{Q}$ and $\mathcal{R}$, respectively. The optimal regulation law is a linear

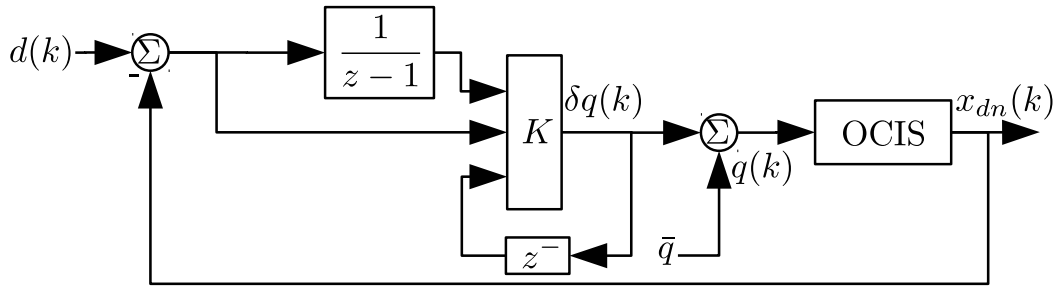

Fig. 5.2. Proposed structure of an LQR for OCIS.

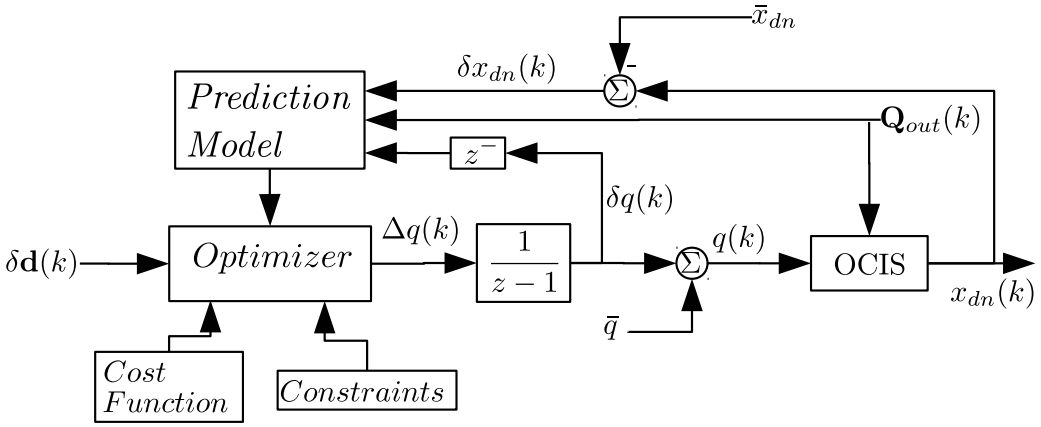

Fig. 5.3. Proposed structure of an MPC for an OCIS.

combination of the system states of the form $\delta q(k) = -Kx_A(k)$, and the matrix K is obtained through the solution of the Riccati Equation (Kirk, 2004).

5.1.2 MPC Design

Figure 5.3 shows the proposed structure of the MPC, where the integral action is an essential part of this control strategy, and is added at the input of the system. Therefore, an augmented description of the discrete-time linear system (5.5) is given by

$$
\begin{aligned}
x_1(k+1) &= a_{11}x_1(k) + a_{12}x_2(k) + b_{12}\delta q_2(k) + b_{d_{11}}\delta q_{out_1}(k)\\
x_2(k+1) &= x_3(k)\\
x_3(k+1) &= x_{11}(k)\\
x_4(k+1) &= a_{44}x_4(k) + a_{45}x_5(k) + b_{43}\delta q_3(k) + b_{d_{42}}\delta q_{out_2}(k)\\
x_5(k+1) &= x_6(k)\\
x_6(k+1) &= x_7(k)\\
x_7(k+1) &= x_{12}(k)\\
x_8(k+1) &= a_{88}x_8(k) + a_{89}x_9(k) + b_{d_{83}}\delta q_{out_3}(k)\\
x_9(k+1) &= x_{10}(k)\\
x_{10}(k+1) &= x_{13}(k)\\
x_{11}(k+1) &= x_{11}(k) + \Delta q_1(k)\\
x_{12}(k+1) &= x_{12}(k) + \Delta q_2(k)\\
x_{13}(k+1) &= x_{13}(k) + \Delta q_3(k),
\end{aligned}
\tag{5.7}
$$

then, it is obtained a classical state-space realization of the form $x_M(k+1) = A_M x_M(k) + B_M\Delta q(k) + B_{dM}\delta q_{out}(k)$, where $x_M(k) \in \mathbb{R}^{13}$ is the state vector; $A_M \in \mathbb{R}^{13\times 13}$ the augmented state matrix; $B_M \in \mathbb{R}^{13\times 3}$ the input matrix; $B_{dM} \in \mathbb{R}^{13\times 3}$ the input disturbances matrix; and $\Delta q(k) \in \mathbb{R}^3$, the input vector. As shown in Figure 5.3, the MPC has information about the outlet flows, hence the centralized controller has $FB + FF$ configuration. The prediction and control horizons chosen are $H_p = H_c = 5$. In that way, Maciejowski (2002) points out that the model for control design, assuming that all states are measurable, has the form

$$\mathbf{y(k+1)} = \mathbf{\Psi}x(k \mid k) + \mathbf{\Upsilon}\Delta\mathbf{q(k)} + \mathbf{\Omega q_{out}}(\mathbf{k}), \tag{5.8}$$

where $\Delta\mathbf{q}(\mathbf{k}) = [\Delta q(k \mid k)\, \Delta q(k+1 \mid k)\, \ldots\, \Delta q(k+5 \mid k)]^\top$, $\mathbf{q_{out}}(\mathbf{k}) = [q_{out}(k)\, q_{out}(k+1)\, \ldots\, q_{out}(k+5)]^\top$, $\mathbf{\Psi} \in \mathbb{R}^{15\times 13}$, $\mathbf{\Upsilon} \in \mathbb{R}^{15\times 15}$, and $\mathbf{\Omega} \in \mathbb{R}^{15\times 15}$.

The optimization problem to be solved consists of finding the signal control $\Delta q(k)$ that minimizes the deviation of the estimated controlled variable from the upcoming reference values and minimize the change in the control-action variable (Le-Duy-Lay et al., 2017). In this sense, the objective function for the MPC-based closed-loop scheme is given by

$$\mathbf{V(k)} = \|\delta\mathbf{r(k)} - \Psi\mathbf{x(k)} - \Upsilon\Delta\mathbf{q(k)} - \Omega\mathbf{q_{out}}(\mathbf{k})\|^2{}_{\mathcal{Q}} + \|\Delta\mathbf{q(k)}\|^2{}_{\mathcal{R}}, \tag{5.9}$$

where $\delta\mathbf{r}(\mathbf{k}) = [\delta r(1)\, \delta r(2)\, \ldots,\, \delta r(5)]^\top$ is the reference vector, and $\mathcal{Q}$, $\mathcal{R}$ are diagonal weighting matrices. This test has been developed with diagonal values of 10 and 1 for $\mathcal{Q}$ and $\mathcal{R}$, respectively. Assuming that there is a dynamic behavior in the master-slave flow control, in this problem constraints in maximum flow variations are imposed. The restrictions are expressed in the form $-0.01 \leq \Delta\mathbf{q(k)} \leq 0.01$, which means that in one unit of time the flow can only change by $0,01\text{m}^3/\text{s}$. Finally, the optimization problem is formulated as a quadratic programming problem (Maciejowski, 2002), which is solved with the interior-point-convex algorithm (MATLAB, 2019).

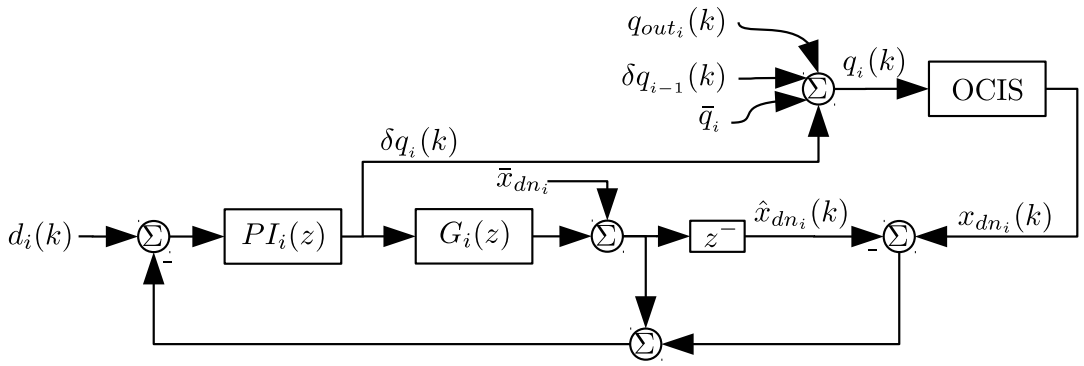

Fig. 5.4. Proposed structure of a PI control + Smith predictor for OCIS.

5.1.3 PI + Smith Predictor Design

Figure 5.4 shows the structure of a PI + Smith predictor control for a channel i, where a distributed control architecture is proposed. Each $PI_i(z)$ controller is designed from the transfer function that describes the dynamic behavior of the channel, where the linearized system has output $\delta x_{dn_i}(k)$, input $\delta q_i(k - \lfloor \frac{\tau_i}{\tau_s} \rceil)$, and the inputs $\delta q_{i-1}(k)$ and q_{out_i} are assumed to be disturbances. The operator $\lfloor . \rceil$ indicates the nearest integer, and the discrete-time delay associated to a transfer function can be denoted by $z^{-\lfloor \frac{\tau_i}{\tau_s} \rceil}$. However, in order to maintain the uniformity of the presented control strategies, z^- is used to indicate the time delay associated with a transfer function. Therefore, the transfer function that describes the channel i is given by

$$\frac{\delta x_{dn_i}(z)}{\delta q_i(z)} = G_i(z)z^-.$$

Here, $G_i(z) = \frac{\tau_s}{a_i z + \tau_s - 1}$ is used for designing the $PI_i(z)$ controller, obtaining a proportional gain $kp_i = 1$ and an integral gain $ki_i = \frac{\tau_s}{2A_i}$. Moreover, $G_i(z)z^-$ is used to build the predictor with output $\hat{x}_{dn_i}(k)$ and input $\delta q_i(k)$. In this control system, the objective is to minimize the tracking and prediction error by using the variation of $q_i(k)$, which classically includes the PI controller output ($\delta q_i(k)$), and the operation point ($\bar{q}_i$). In this design, it is proposed to compensate the amount of flow required by the neighbor channel $\delta q_{i-1}(k)$ and outlet flows $q_{out_i}(k)$, obtaining a distributed and $FB+FF$ architecture with a control law given by

$$q_i(k) = \bar{q}_i + \delta q_i(k) + \delta q_{i-1}(k) + q_{out_i}(k). \tag{5.10}$$

5.1.4 Simulation and Results

The tracking behavior of the three approaches, evaluated on the nonlinear system, is shown in Figure 5.5, where all of them show adequate performance. Additionally, it is seen that the PI + Smith predictor shows high decoupling behavior for reference changes

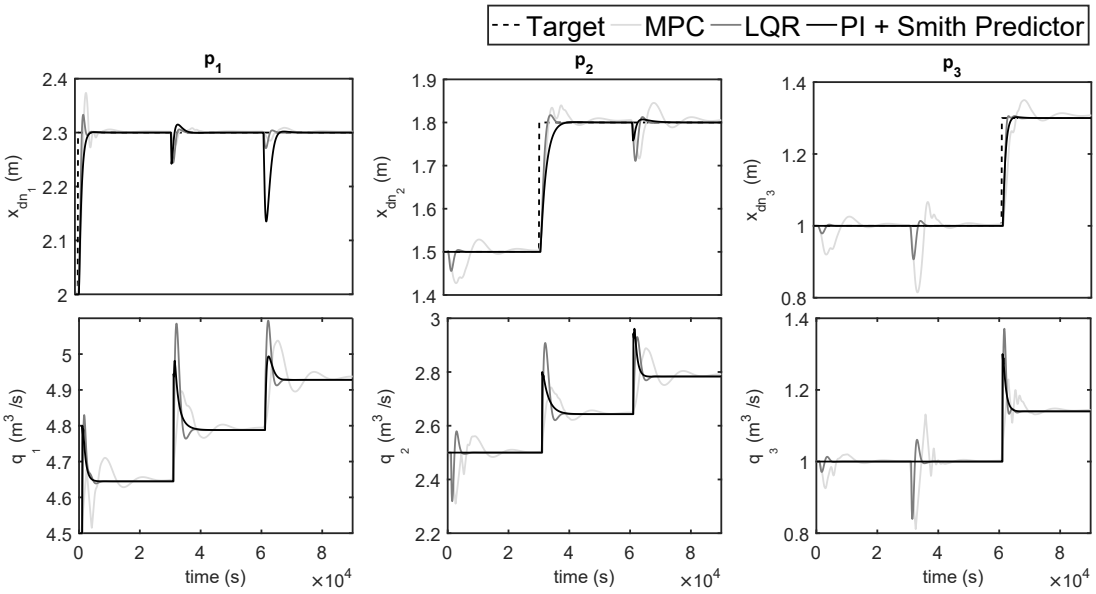

Fig. 5.5. Tracking behavior of the system controlled with MPC, LQR and PI + Smith predictor. The black dashed lines represent the targets for y_{dn}.

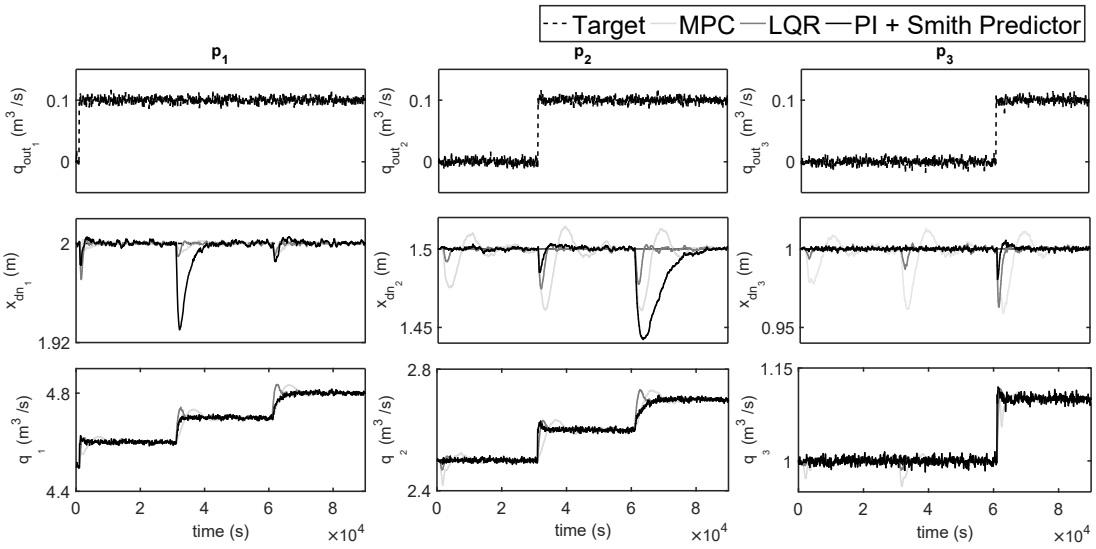

Fig. 5.6. Disturbances-rejection behavior of the system controlled with MPC, LQR and PI + Smith predictor.

at upstream channels but low decoupling behavior for reference changes at downstream channels. This is due to the fact that the control law in (5.10) maintains a mass balance by the addition of changes at the upstream flow $q_{i-1}(k)$. The decoupling behavior of the LQR and MPC controllers is uniform for references and outlet flows changes at both upstream and downstream channels. Also, in Figure 5.5, it is observed that the control signals of the LQR and PI controllers are more aggressive than the control signal computed by the MPC controller. One advantage of the MPC is the possibility of including constraints in the control signal, therefore, the MPC shows the less aggressive control signal, obeying

Table 5.1. Normalized key performance indicators that summarize the disturbances-rejection behavior of the system controlled with MPC, LQR, and PI + Smith predictor.

	p_1			p_2			p_3		
	MPC	LQR	PI	MPC	LQR	PI	MPC	LQR	PI
MAE	0.20	0.37	0.82	0.67	0.39	0.99	1.00	0.95	0.52
IAE	0.10	0.11	0.34	0.74	0.18	0.64	1.00	0.25	0.14
StE	0.05	0.01	0.05	0.69	0.10	1.00	0.89	0.02	0.02
IAQ	0.07	0.37	0.93	0.15	0.23	1.00	0.16	0.27	0.96

the flow variation constraint. Moreover, in Figure 5.5 it is possible to see the control prediction effect, where the control signal starts before the change in the reference signal. The disturbances-rejection behavior of the system controlled with MPC, LQR, and PI + Smith predictor is shown in Figure 5.6, and summarized in Table 5.1. As shown in Figure 5.6, the disturbances q_{out_i} have permanent and normally distributed components. As it has been previously highlighted, the control law (5.10) of the PI + Smith predictor produce high decoupling behavior for permanent disturbances at upstream channels but a low decoupling behavior for permanent disturbances at downstream channels. Moreover, it must be highlighted that in the PI + Smith predictor case, the third channel presents the lowest integral absolute error, but this result is reached by inducing high inflow channel variations. However, this behavior could generate risks for the canal infrastructure. In most of the cases, the LQR presents the best StE indicators, showing that this could be a suitable option to reject normally distributed disturbances. On the other hand, the MPC presents the IAQ better indicators, showing the advantages in the inclusion of constraints in order to obtain less aggressive control actions.

Moreover, according to the results, the three control strategies have shown appropriate behavior and can be implemented following systematic procedures. Furthermore, it must be highlighted that the LQR and MPC strategies also can be performed using distributed and $FF+FB$ configurations. On the other hand, the use of the ID model as a design model shows that this strategy is successful in designing conventional control strategies with multiple control configurations. However, due to the over simplicity of the ID modeling strategy, in order to assert the suitability of control strategies designed from simplified models, the development of control strategies comparisons on real systems is necessary.

5.2 Control of Interacting Channels

OCIS with undershoot gates have interactions between channels, and according to the United States Department of Agriculture (U. S. Department of the Interior, 2001) undershoot gates are the most common hydraulic regulation structures in open-channels. This can be seen in the irrigation districts in Tolima-Colombia, where only undershoot gates are used to regulate flows and levels along the channels. However, in OCIS, most of the research has dealt with the problem of modeling and control of OCIS without channel interaction (e.g., Cantoni et al. 2007; Weyer 2008; Rabbani et al. 2009b; Aguilar et al. 2009; van Overloop et al. 2010b; Nasir and Muhammad 2011; Herrera et al. 2013; Sadowska

et al. 2015a). Recently, the research around modeling and control of interactive OCIS has earned significant relevance and some research such as (Le-Duy-Lay et al., 2017; Aydin et al., 2017; Horváth et al., 2015b; Breckpot et al., 2013) has been developed in the field. However, these works avoid the nonlinear interaction by linearization such as the work developed by Le-Duy-Lay et al. (2017), where the desired behavior is restricted around the equilibrium point, or by the strong assumption that there is a perfect flow control for each discharge structure (e.g., Aydin et al. 2017; Horváth et al. 2015b; Breckpot et al. 2013). On the other hand, there are nonlinear control techniques that have shown suitable behavior controlling interactive nonlinear systems with delays but had not been used in OCIS. In a specific way, the nonlinear control technique known as backstepping has shown a successful performance over nonlinear systems with delays (Hua et al., 2009), where the control technique is applied to a two-stage chemical reactor with delayed recycle streams. The work developed by Mazenc and Bliman (2006) shows a control technique where backstepping is used to stabilize nonlinear systems with large delays. Finally, Choi and Yoo (2016) shows the implementation of backstepping for nonlinear large-scale systems with delayed interactions. In this section the control-oriented modeling strategy that assumes a constant potential energy difference along the channels is used in the design of a nonlinear control strategy useful to overcome nonlinearities, delays, and interactions in the OCIS. The control strategy is tested over a proposed system with two channels, showing proper performance in the presence of parameter variation.

5.2.1 Nonlinear Control Strategy

In the following, the control-oriented modeling strategy that assumes a constant potential energy difference along the channels is considered, where each channel can be described with the following differential equation:

$$\begin{aligned} a_i \dot{x}_{up_i} = {} & w_{_i} u_{_i} \sqrt{2g} c_{_i} \sqrt{l_{h_{i-1}} x_{up_{i-1}}(t-\tau_{_{i-1}}) - x_{up_i}} \\ & - w_{_{i+1}} u_{_{i+1}} \sqrt{2g} c_{_i} \sqrt{l_{h_i} x_{up_i}(t-\tau_{_i}) - x_{up_{i+1}}} + q_{out_i}, \end{aligned} \tag{5.11}$$

where levels and flows are proposed to be controlled by action of the downstream regulation structures $u_{_{i+1}}$. Note that if the proposed model is used for M channels, a highly interactive model of M differential equations with M inputs and M outputs will be obtained and could be described by

$$\dot{x}_{up} = f(x_{up}, x_{up}(t-\tau), u), \tag{5.12}$$

with $x_{up} \in \mathbb{R}^M$, and $u \in \mathbb{R}^M$.

In this strategy, the control objective is to maintain a constant depth at the upstream end of the channel. Therefore, with the aim to ensure zero stationary error for the controlled system, the open loop system is augmented with an integral action. Then, for the model that describes a channel in (5.11), with regularization error $e_{_i} = x_{\mathrm{ref_i}} - x_{up_i}$,

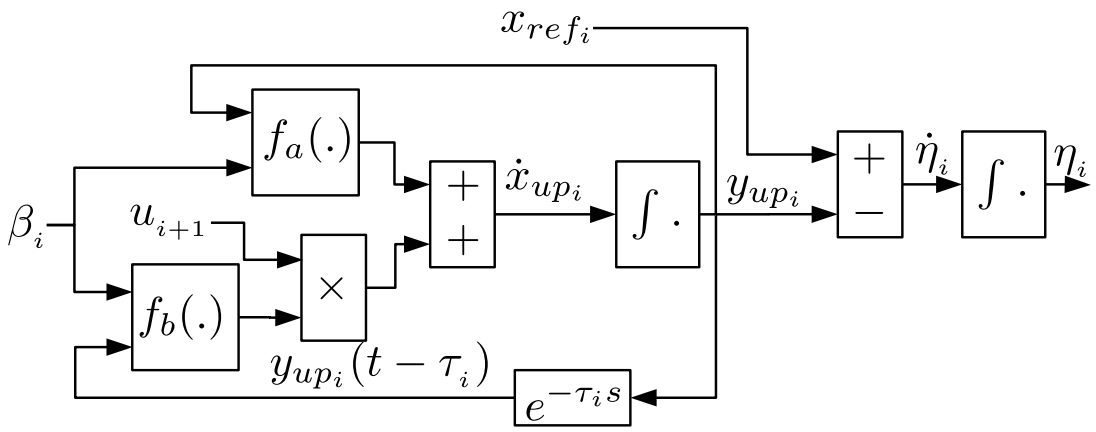

Fig. 5.7. Augmented system in cascade configuration.

where x_{ref_i} is the desired depth for the channel i, the system is augmented with $\dot{\eta}_i = e_i$. Hence, the resultant system is given by

$$\dot{\eta}_i = x_{\text{ref}_\text{i}} - x_{up_i}, \tag{5.13a}$$
$$\dot{x}_{up_i} = f_a(x_{up_i}, \boldsymbol{\beta_i}) + f_b(x_{up_i}(t-\tau_i), \boldsymbol{\beta_i}) u_{i+1}, \tag{5.13b}$$

where $[\eta_i, x_{up_i}]^T \in \mathbb{R}^2$, $\eta_i \in \mathbb{R}$, and $x_{up_i} \in \mathbb{R}$ are the state variables, $u_{i+1} \in \mathbb{R}$ is the control signal, $f_a : D \to \mathbb{R}$, $f_b : D \to \mathbb{R}$, for that the operator $\sqrt{.}$ is changed by $sgn(.)\sqrt{|.|}$, and $\boldsymbol{\beta_i}$ is a vector with external variables that can be measured and used for control purpose, $\boldsymbol{\beta_i} = (x_{up_{i-1}}, x_{up_{i-1}}(t-\tau_{i-1}), x_{up_{i+1}}, u_i)$. As shown in Figure 5.7, the augmented system could be seen as a cascade system, where the objective is to find a control strategy u_{i+1} that ensures the stability of the origin ($\eta_i = 0$, $x_{up_i} = 0$), for all $x_{\text{ref}_\text{i}} = 0$. The control technique could be seen as a step-by-step method, where:

1. A change of variable $x_{up_i} = \phi_i(\eta_i)$, $\phi(0) = 0$ is proposed. Then, in (5.13a), $\phi_i(\eta_i)$ is assumed as a control variable with the objective that $\phi_i(\eta_i)$ ensures the global asymptotic stability so that $\dot{\mathbf{V}}_{1_i} < -W_{1_i}(\eta)$, where $W_{1_i}(\eta)$ is positive definite and $\mathbf{V}_{1_i}(\eta)$ is a known Lyapunov function. The control variable is

$$\phi_i(\eta_i) = x_{\text{ref}_\text{i}} - \lambda_{a_i}\eta_i,$$

   where $(\lambda_{a_i} \in \mathbb{R} : \lambda_{a_i} < 0)$ is used as a tuning constant. Then, according to the control law, now (5.13a) is given by $\dot{\eta}_i = \lambda_{a_i}\eta_i$, and with $\mathbf{V}_{1_i}(\eta_i) = \frac{1}{2}{\eta_i}^2$, $\dot{\mathbf{V}}_{1_i} = \lambda_{a_i}{\eta_i}^2$. Hence, the origin of (5.13a) is globally exponentially stable.

2. According to the last assumption, a new variable emerges in the system. This variable is the error between the control signal $\phi_i(\eta_i)$ and the variable x_{up_i}; this error is denoted by $z_i = x_{up_i} - \phi_i(\eta_i)$, then the dynamical behavior of the error is given by $\dot{z}_i = f_a(x_{up_i}, \boldsymbol{\beta_i}) + f_b(x_{up_i}(t-\tau_{i+1}), \boldsymbol{\beta_i}) u_{i+1} - \frac{d}{dt}[x_{\text{ref}_\text{i}} - x_{up_i}]$, then

$$\begin{aligned}\dot{z}_i =& \frac{q_i}{a_i} + \lambda_{a_i} x_{\text{ref}_\text{i}} - \lambda_{a_i} x_{up_i} \\ &- \frac{w_i u_i(t)\sqrt{2g} c_i \sqrt{l_{h_i} x_{up_i}(t-\tau_{i+1}) - x_{up_{i+1}}}}{a_i} \\ &+ \frac{w_i u_i(t)\sqrt{2g} c_i \sqrt{l_{h_{i-1}} x_{up_{i-1}}(t-\tau_{i-1}) - x_{up_i}}}{a_i},\end{aligned} \tag{5.14}$$

where a feedback law for u_{i+1} is now chosen with the objective to ensure the global asymptotic stability of (5.14). In this case, $\dot{\mathbf{V}}_i(\eta_i, x_{up_i}) < -W_i(\eta_i, x_{up_i})$, where $W_i(\eta_i, x_{up_i})$ is positive definite and $\mathbf{V}_i(\eta_i, x_{up_i}) = V_{i,1}(\eta_i) + \frac{1}{2} {z_i}^2$. Hence, the desired system $\dot{z}_i = \lambda_b z$ is proposed, where $\lambda_{b_i} \in \mathbb{R} : \lambda_{b_i} < 0$, is used as a tuning constant and the control law for u_{i+1} is given by

$$\begin{aligned}u_{i+1} =& \frac{1}{w_i \sqrt{2g} c_i \sqrt{l_{h_i} x_{up_i}(t-\tau_{i+1}) - x_{up_{i+1}}}} (q_i \\ &+ w_i u_i \sqrt{2g} c_i \sqrt{l_{h_{i-1}} x_{up_{i-1}}(t-\tau_{i-1}) - x_{up_i}} \\ &+ \lambda_{a_i} x_{\text{ref}_\text{i}} a_i - \lambda_{a_i} x_{up_i} a_i \\ &- \lambda_{b_i} x_{up_i} a_i - \lambda_{b_i} \lambda_{a_i} \eta_i a_i + \lambda_{b_i} x_{\text{ref}_\text{i}} a_i).\end{aligned}$$

Then, $\dot{\mathbf{V}}_i(\eta_i, x_{up_i}) = \lambda_{a_i} {\eta_i}^2 + \lambda_{b_i} {z_i}^2$. Hence,the origin ($\eta = 0$, $z = 0$) is asymptotically stable and due to the fact that $\phi(0) = 0$, the origin ($\eta = 0$, $y = 0$) is also asymptotically stable.

3. The dynamical behavior of the controlled system is given by

$$\begin{aligned}\dot{\eta}_i &= x_{\text{ref}_\text{i}} - x_{up_i} \\ \dot{x}_{up_i} &= \lambda_{a_i} \lambda_{b_i} \eta_i + (\lambda_{a_i} + \lambda_{b_i}) x_{up_i} - (\lambda_{a_i} + \lambda_{b_i}) x_{\text{ref}_\text{i}},\end{aligned}$$

which is an uncoupled second order system with characteristic polynomial given by $P_i(s) = s^2 + s(-\lambda_{a_i} - \lambda_{b_i}) + \lambda_{a_i} \lambda_{b_i}$.

5.2.2 Simulation and Results

In order to validate the control technique performance, an OCIS with two channels is proposed. The model is simulated in the SWMM software (Lewis, 2017). In this software, the model is codified by a graphic description of the system as presented in Figure 5.8, and the most relevant parameters of the simulation are listed in Table 5.2.

Parameters Adjustment and Model Validation

Figure 5.9 shows the dynamic behavior of the depth at the upstream and downstream end of the channels simulated in SWMM. This test is developed with null initial conditions and with an intake of $0.6\text{m}^3/\text{s}$. The parameters for the proposed model are obtained from

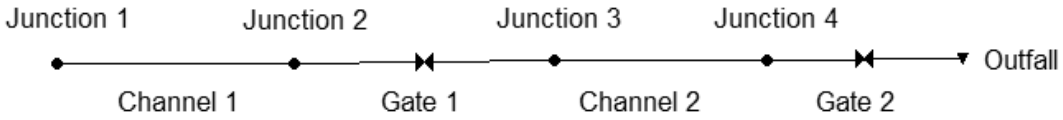

Fig. 5.8. Simulation diagram of an OCIS with two channels in the SWMM software.

Table 5.2. Most relevant parameters of the two channels system

Junction 1,2	Inflow	$0.6\text{m}^3/\text{s}$, 0
Channel 1,2	Shape	Rectangular
	Width	1m
	Lenght	1000m
	Roughness	0.005
Gate 1,2	Category	Orifice
	Type	Side
	Shape	Rectangular
	Width	1m
	Discharge Coeff.	0.9
	Height	0.35m, 0.1m

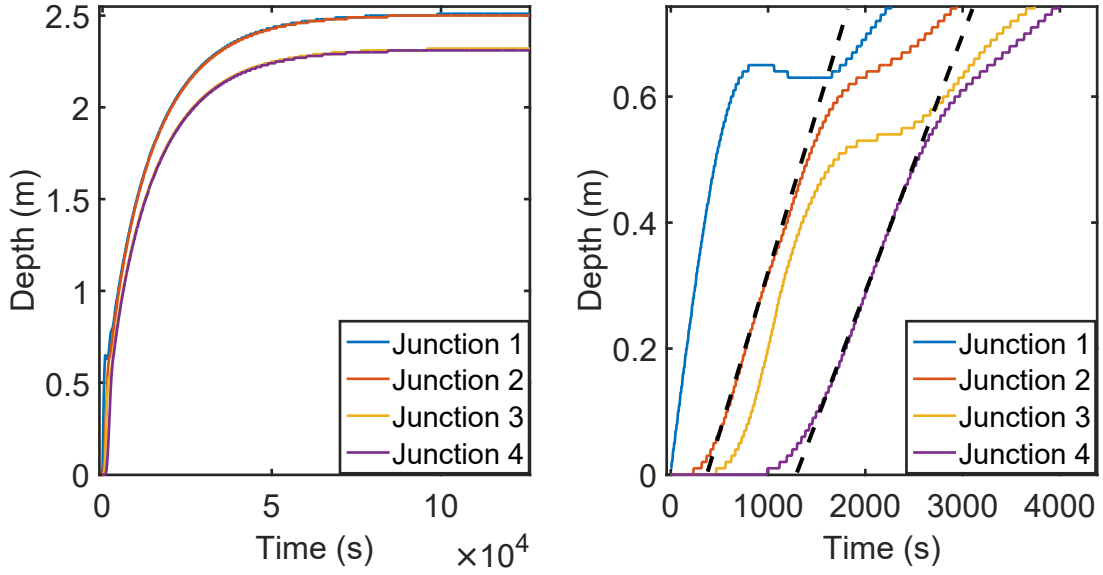

Fig. 5.9. Dynamic depth behavior in SWMM.

the experimental results shown in Figure 5.9, where l_{h_1} and l_{h_2} are obtained from the stationary system behavior, with equilibrium points in $\bar{x}_{up_1} = 2.58\text{m}$, $l_{h_1}\bar{x}_{up_1} = 2.56\text{m}$, $\bar{x}_{up_2} = 2.35\text{m}$, and $l_{h_2}\bar{x}_{up_2} = 2.31\text{m}$. To obtain τ_1 y τ_2, the dynamical behavior is analyzed as shown in Figure 5.9, where the first intersection corresponds to the value of $\tau_1 \approx 320\text{s}$, and the second is used to obtain the value of $\tau_2 \approx 1205\text{s} - \tau_1$. Then, the values assigned to the proposed model are collected in Table 5.3.

Table 5.3. Values of the parameters assigned to the proposed model

Parameter	Value
M	2
a_1,a_2	1000m^2,1000m^2
l_{h_1},l_{h_2}	0.99,0.98
q_1,q_2	0.6 m^3/s,0 m^3/s
u_1,u_2	0.35m,0.1m
w	1m
c_i	0.9

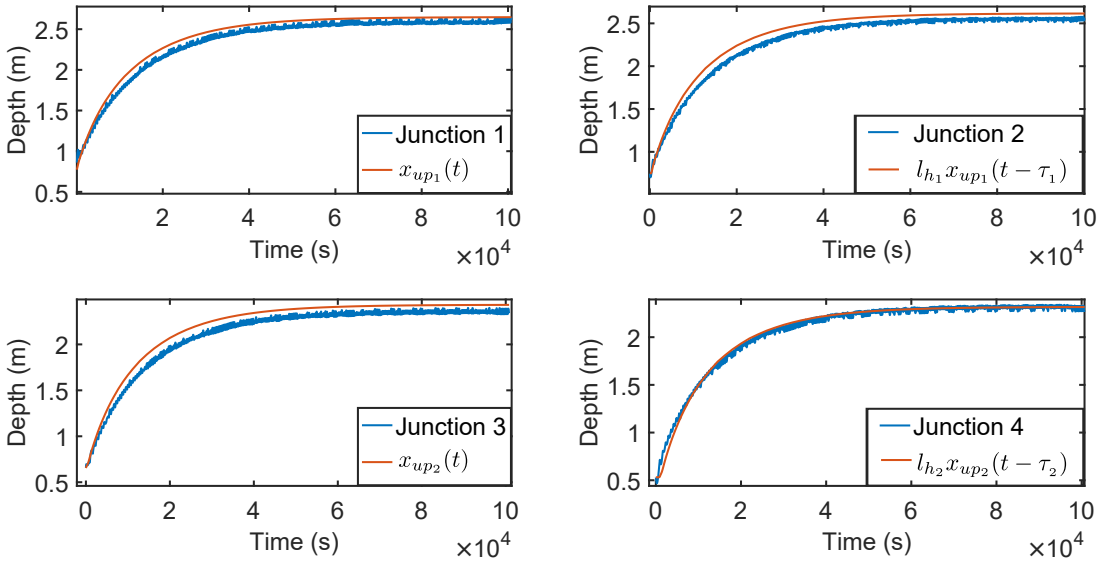

Fig. 5.10. SWMM vs. proposed model for a step of 0.6m^3/s in the intake flow.

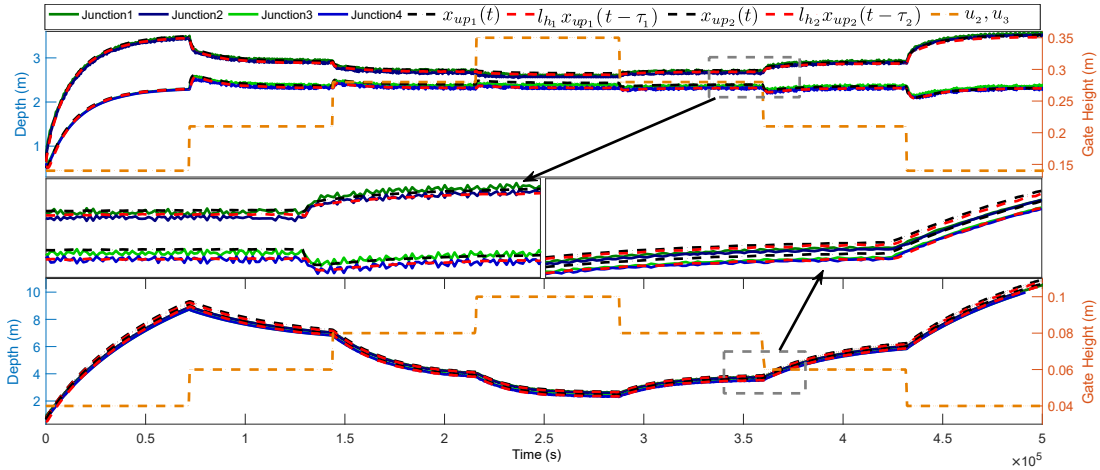

Fig. 5.11. Model simulated in SWMM vs. proposed model for changes in gates 1 and 2.

Figure 5.10 shows the comparison between the model simulated in SWMM and the proposed model for a step of 0.6m^3/s at the intake flow. In this figure, it is observed that

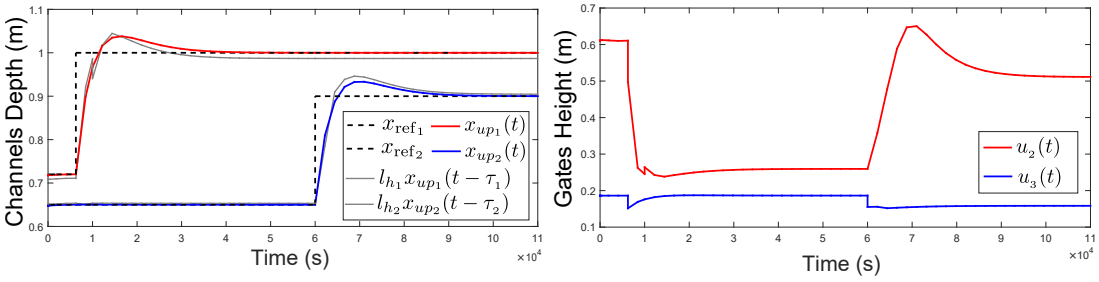

Fig. 5.12. Level tracking test.

the proposed model presents similar behavior to the model simulated in the specialized software SWMM. On the other hand, Figure 5.11 shows a comparison between both systems. In this case, a step variation is made in the height of the first gate (u_1) and the height of the second gate (u_2). According to the results of the comparison (Figures 5.10,5.11), the proposed model have similar dynamical and statical behavior than the model simulated in the specialized software. Additionally, the procedure presented to obtain the parameters of the proposed model is also suitable to obtain the parameters of any real system.

Performance of the closed-loop scheme

The backstepping control strategy is implemented in the proposed system. As a result, a linear system with eigenvalues in λ_{a_1}, λ_{b_1}, λ_{a_2}, and λ_{b_2} is obtained. The control system is tuned with $\lambda = -0.0002$ with the purpose of ensuring a constant time close to the open-loop system in Figure 5.9. In the test, some changes in the references are performed; Figure 5.12 shows the tracking performance for each channel depth, and each control signal. This figure reveals that the controlled system presents the expected behavior with zero-stationary error, time response equal to 1/0.0002, and smooth control signal. Moreover, the presented overshoot corresponds to the time solution of the closed-loop system, for $\lambda_{a_1}, \lambda_{b_1}, \lambda_{a_2}, \lambda_{b_2} = \lambda$, which is described by a diagonal matrix of identical transfer functions given by $\frac{y_{up,i}(s)}{y_{\text{ref,i}}(s)} = \frac{\frac{2s}{-\lambda}+1}{(\frac{s}{-\lambda}+1)^2}$.

Finally, the robustness of the controlled system is tested with an increment of 10% in the parameters (area, gate width, outtake flow, and delay). Figure. 5.13 shows the closed-loop system behavior in the presence of these disturbances, where the controlled system maintains stability and desired dynamical behavior. This shows the robustness of the control technique, which implies that changes in areas and delays due to diverse events like sedimentation, cause small disturbances in the performance of the controlled system. On the other hand, flow changes due to gate width variations, and intake or outtake flow, cause a significant effort in the control signal. However, the controlled system overcomes the problem and return to an equilibrium state.

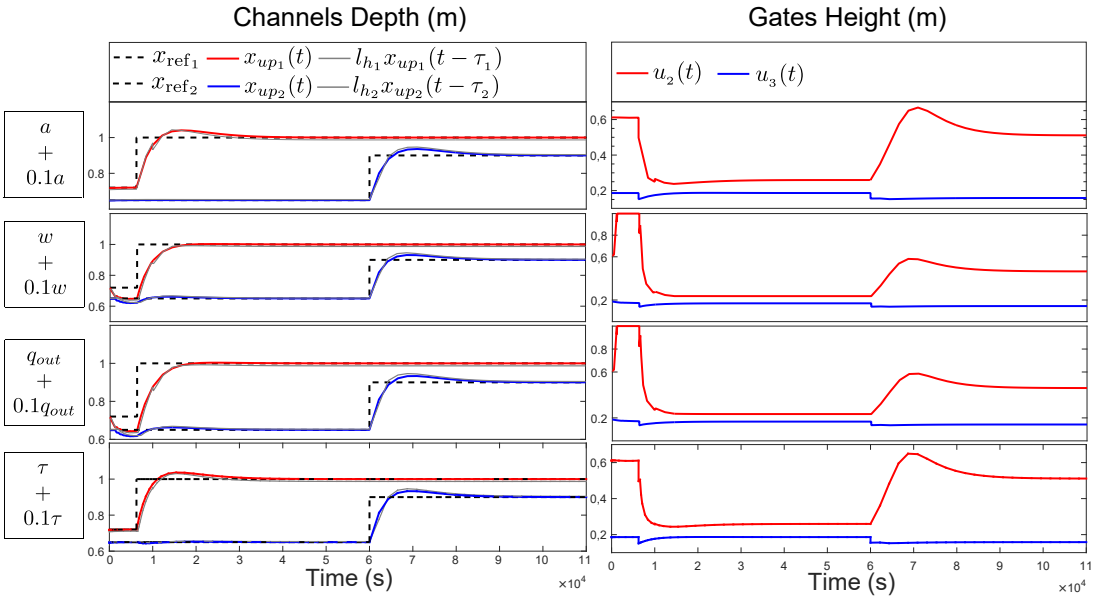

Fig. 5.13. Level tracking test with model variations and disturbances.

5.3 An Efficient Control Approach for OCIS

Water scarcity can be seen as one of the most relevant worldwide challenges. Currently, multiple efforts are focused on either overcoming or mitigating the water shortage, which is a problem that increases with the imminent global population growth (Niswonger et al., 2017; Uniyal and Dietrich, 2021). Moreover, the agriculture can be seen as the main responsible for water scarcity; it is well known that most of the water consumed for the humanity is used in irrigation process (Zhu et al., 2019; Uniyal and Dietrich, 2021). Furthermore, additionally to the world population increase and the increasing demand for water (Loch et al., 2020), there are multiple factors that might contribute to the future water scarcity, e.g., i) climate change; ii) growing food demands; iii) biophysical, ecological, and political limits for croplands expansions; iv) water pollution; and v) new intensive production techniques in agriculture that use irrigated agriculture because this is more productive than rain-fed agriculture (Zhu et al., 2019). One of the main solutions to deal with the current/future water scarcity problem is to increase the efficiency of the crops' production process (Zhu et al., 2019; Uniyal and Dietrich, 2021), where the challenge is to increase crop yield using less or almost the same amount of water. Such a goal can be reached by minimizing water losses along the production process. In this direction, it is important to realize that most of the water used for agricultural purposes is transported through networks of open-channel irrigation systems (OCIS), and in these systems, more than half of water is lost by leaks, seepage, and evaporation (Swamee et al., 2002).

In OCIS, losses due to leaks and seepage are usually reduced with structural maintenance and design. For example, Swamee et al. (2002) propose an optimal structural design of minimum water loss sections for triangular, rectangular, and trapezoidal canals. On the other hand, as it has been highlighted by Conde et al. (2021b), to the best of

the authors' knowledge, the reduction of losses due to leaks and seepage has not been studied from a control point of view. Specifically, most of the reported works on control of OCIS have been developed around the upstream and downstream control objectives of maintaining a constant depth at either upstream or downstream end of the channels (e.g., Segovia et al. (2019); Ke et al. (2020); Shahverdi et al. (2020); Zeng et al. (2020); Arauz et al. (2020)), and by position adjustment of the outlet structures, the required discharge is regulated to each user (Cantoni et al., 2007). Moreover, leaks and seepage have a direct hydraulic relation with the water level at the point where each leak or seepage occurs. Therefore, the objective of maintaining a constant depth, also ensures permanent losses in the OCIS. In order to overcome this problem, a new control strategy that accomplishes the users' demands minimizing the water levels along the channels is proposed.

The proposed strategy takes advantage from the on-request operational mode of the OCIS. In such an operational mode, the users must request in advance to the central administration the amount of hydraulic resource that will be consumed. Then, the programmed demands and an accurate model of the system are employed in the development of a nonlinear model predictive control (NLMPC) strategy, which has the objective of delivering an appropriate amount of water to the users, maintaining the channels levels as low as possible, and into an operation range where the overflows and, ecological or infrastructural damage are avoided.

Therefore, it is presented a proposal to change the conventional control objective of maintaining constant levels that ensure constant losses, for a new control strategy where the channel levels and flows can variate to satisfy the users demands, minimizing levels, and preventing overflows, and ecological or infrastructural damage. In this direction, three challenges are addressed:

- To choose a modeling strategy that accurately describes the levels and flow dynamics of the OCIS over different operation conditions.
- To design a receding cost function that delivers the appropriate amount of water to the users, minimizing levels, and satisfying hydraulic constraints.
- To establish the conditions that avoid the overflows and ecological, or infrastructural damage.

As a result, the main contribution of this chapter is the development of a new OCIS control strategy capable of delivering an appropriate amount of water to the users, reducing losses due to seepage and leaks, preventing overflows, and either ecological or infrastructural damage.

5.3.1 Problem Statement

In OCIS, the conventional upstream and downstream automatic control approaches maintain a fix level at the upstream or downstream end of the channels. The use of these automatic control strategies reduces losses due to inopportune responses, or errors in manual operations. However, these strategies maintain a constant level, which also maintains constant losses due to leaks and seepage. Note that leaks and seepage are modeled as

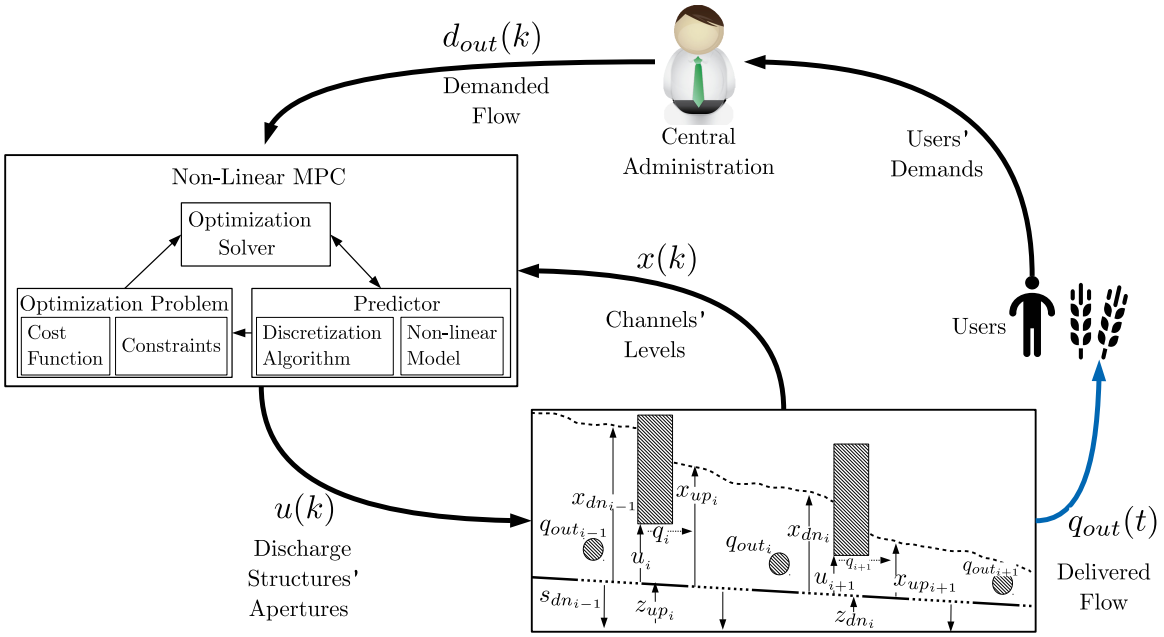

Fig. 5.14. Schematic of the control strategy and its implementation into the operation of the OCIS.

functions of the levels where these losses occur (Harr, 1991; Swamee et al., 2002; Bedjaoui et al., 2009). In specific, in this thesis, losses at the upstream end of the channels are modeled as

$$s_{up_i}(t) = \kappa_{up_i}\sqrt{x_{up_i}(t)}, \tag{5.15}$$

and losses at the downstream end of the channels are modeled as

$$s_{dn_i}(t) = \kappa_{dn_i}\sqrt{x_{dn_i}(t)}, \tag{5.16}$$

where i is used to identify the i^{th} channel; $x_{up_i}(t)$ and $x_{dn_i}(t)$ are depths at the upstream and downstream end of the channels; and κ_{up_i} and κ_{dn_i} are parameters associated to the physical aspects that produce the leaks or seepage, such as the dimensions and forms of an orifice that produce a leak. In this order of ideas, in OCIS, leaks and seepage can be minimized by minimizing the levels of the channels. However, in order to guarantee the system operativity, this minimization must be performed with the accomplishment of the users' demands and the hydraulic constraints that the OCIS presents.

5.3.2 Proposed Approach

The objective of the proposed control approach is to supply the scheduled amount of water whilst, minimizing losses due to leaks and seepage. In this direction, a control strategy that operates in on-request mode is proposed. Figure 5.14 shows the schematic

of the control strategy and its implementation for the operation of the OCIS, where it is observed that the users demands are evaluated by the central administration of the system, who is in charge of scheduling the demands (d_{out_i}) into the control strategy. Such a strategy is based on the nonlinear model predictive control (NLMPC) approach, where a dynamic optimization problem is solved to find either an optimal or sub-optimal control action that accomplishes with the user's demands while the OCIS levels are minimized. In the NLMPC strategy, the idea is to recursively use a model of the system to predict and find the control actions that optimize the future system's behavior (Grüne and Pannek, 2011), while satisfying some physical and operational constraints.

In order to predict the future behavior of the OCIS, a dynamic behavioral evolution of the OCIS must be obtained. In NLMPC, the dynamic behavioral evolution is achieved by discretization and numerical solution of the discretized model along the time. Therefore, the prediction accuracy depends on the accuracy of both the modeling approach, and the discretization method. In this direction, the fundamental models that describe the OCIS are the Saint-Venant Equations (SVE), but the direct use of these equations for control systems design is impractical (Rabbani et al., 2010). Therefore, in the literature, multiple types of linear control-oriented models that describe the OCIS dynamics have been reported (Conde et al., 2021b). The problem is that most of the reported control-oriented models are suitable when the control objective is to maintain the upstream or downstream levels close to an operation region. However, in this control approach, the proposed control strategy finds the optimal flows and levels that accomplish the users' demands at the same time that water levels along the channels are minimized. This implies that the controlled OCIS can operate along multiple operation regions (levels). Therefore, the modeling approach presented in (Conde et al., 2020), which has shown that is capable to describe the OCIS along a wide operation region, is used[1]. In the modeling approach, each channel is described as two storage units and by performing mass and energy balances for each one of the units, the dynamics of the i^{th} channel can be described by two nonlinear differential equations as follows:

$$\begin{aligned} a_{up_i}\dot{x}_{up_i}(t) &= q_i(t) - q_{tr_i}(t) - s_{up_i}(t) \\ a_{dn_i}\dot{x}_{dn_i}(t) &= q_{tr_i}(t) - q_{out_i}(t) - q_{i+1}(t) - s_{dn_i}(t), \end{aligned} \tag{5.17}$$

where the flow transition between the upstream and downstream storage units is obtained from energy channel balances (Conde et al., 2020). The flow transition is described by

$$q_{tr_i}(t) = k_{tr_i}x_{up_i}(t)\sqrt{x_{up_i}(t) - x_{dn_i}(t) + z_{up_i} - z_{dn_i}}. \tag{5.18}$$

In this section, the hydraulic structures that regulate the flows $q_i(t)$ and $q_{out_i}(t)$ are considered to be gates structures, where the flows can be described by

$$q_i(t) = c_i w_i u_i(t)\sqrt{2g}\sqrt{x_{dn_{i-1}}(t) - x_{up_i}(t)}, \tag{5.19}$$

and

$$q_{out_i}(t) = c_{out_i} w_{out_i} u_{out_i}(t)\sqrt{2g}\sqrt{x_{dn_i}(t)}, \tag{5.20}$$

[1]The model variables have been defined in Chapter 3.

respectively.

Moreover, to take into account the volume of demanded and delivered water to the users, the proposed model (5.17) is augmented by the inclusion of cumulative variables that indicate the volume of delivered and demanded water until a certain instant of time. Therefore, the augmented model is described by

$$\begin{aligned} a_{up_i}\dot{x}_{up_i}(t) &= q_i(t) - q_{tr_i}(t) - s_{up_i}(t) \\ a_{dn_i}\dot{x}_{dn_i}(t) &= q_{tr_i}(t) - q_{out_i}(t) - q_{i+1}(t) - s_{dn_i}(t) \\ \dot{\phi}_{out_i}(t) &= q_{out_i}(t) \\ \dot{\theta}_{out_i}(t) &= d_{out_i}(t), \end{aligned} \tag{5.21}$$

where d_{out_i} is the demanded flow profile of the i^{th} user, q_{out_i} is the flow of delivered water, θ_{out_i} is the volume of demanded water, and ϕ_{out_i} is the volume of delivered water.

As shown by Sánchez et al. (2017), in NLMPC, the discretization of nonlinear systems can be addressed by using different numeric strategies, such as:

- Direct multiple shooting.
- Direct collocation.
- Successive linearizations.

Another alternative could be the use of an Euler discretization method. However, this method is discarded here since it is not as accurate as the others mentioned before. In the proposed strategy, the model (5.21) is discretized by using a direct multiple shooting method. This method is highly intuitive since the system discretization is developed by the implementation of a 4^{th} order Runge-Kutta (RK4) method, which is one of the most used and accurate numerical methods to solve ordinary differential equations (ODEs) (Rawlings et al., 2017).

The augmented model (5.21) is written as a synthesized model, i.e.,

$$\dot{\boldsymbol{\gamma}}(t) = f(\boldsymbol{\gamma}(t), \boldsymbol{u}(t), \boldsymbol{d}(t)), \tag{5.22}$$

where $f(\boldsymbol{\gamma}(t), \boldsymbol{u}(t), \boldsymbol{d}(t)) \to \mathbb{R}^{4M}$,

$$\begin{aligned} \boldsymbol{\gamma}(t) &= [x_{up_1}\ x_{dn_1}\ \phi_{out_1}\ ...\ \ \theta_{out_M}]^\top,\ \boldsymbol{\gamma} \in \mathbb{R}^{4M} \\ \boldsymbol{d}(t) &= [d_{out_1}\ d_{out_2}\ ...\ d_{out_M}]^\top,\ \boldsymbol{d} \in \mathbb{R}^{M} \\ \boldsymbol{u}(t) &= [u_1\ u_{out_1}\ u_2\ u_{out_2}\ ...\ u_{out_M}]^\top,\ \boldsymbol{u} \in \mathbb{R}^{2M}. \end{aligned}$$

In this strategy, the vector of regulation structures positions $\boldsymbol{u}(t)$ is considered the vector of control action variables.

The discretization of (5.22) by using the RK4 method leads to

$$\boldsymbol{\gamma}(k+1) = \boldsymbol{\gamma}(k) + \frac{\tau_s}{6}\left(\boldsymbol{\lambda}_1(k) + 2\boldsymbol{\lambda}_2(k) + 2\boldsymbol{\lambda}_3(k) + \boldsymbol{\lambda}_4(k)\right), \tag{5.23}$$

where

$$\begin{aligned}
\boldsymbol{\lambda}_1(k) &= f\left(\boldsymbol{\gamma}(k), \boldsymbol{u}(k), \boldsymbol{d}(k)\right), \\
\boldsymbol{\lambda}_2(k) &= f\left(\boldsymbol{\gamma}(k) + \frac{\tau_s}{2}\boldsymbol{\lambda}_1(k), \boldsymbol{u}(k), \boldsymbol{d}(k)\right) \\
\boldsymbol{\lambda}_3(k) &= f\left(\boldsymbol{\gamma}(k) + \frac{\tau_s}{2}\boldsymbol{\lambda}_2(k), \boldsymbol{u}(k), \boldsymbol{d}(k)\right) \\
\boldsymbol{\lambda}_4(k) &= f\left(\boldsymbol{\gamma}(k) + \tau_s\boldsymbol{\lambda}_3(k), \boldsymbol{u}(k), \boldsymbol{d}(k)\right),
\end{aligned}$$

being τ_s the sampling time, and k an instant of time.

In the NLMPC strategy, the discretized model is used to predict the behavior of the OCIS along a certain window ahead in time. Then, the OCIS evolution along a prediction horizon N can be approximated by

$$\begin{aligned}
\boldsymbol{\gamma}(k+1 \mid k) &= \boldsymbol{\gamma}(k \mid k) + \frac{\tau_s}{6}(\boldsymbol{\lambda}_1(k \mid k) + 2\boldsymbol{\lambda}_2(k \mid k) + 2\boldsymbol{\lambda}_3(k \mid k) + \boldsymbol{\lambda}_4(k \mid k)) \\
\boldsymbol{\gamma}(k+2 \mid k) &= \boldsymbol{\gamma}(k+1 \mid k) + \frac{\tau_s}{6}(\boldsymbol{\lambda}_1(k+1 \mid k) + 2\boldsymbol{\lambda}_2(k+1 \mid k) \ + 2\boldsymbol{\lambda}_3(k+1 \mid k) \\
&\quad + \boldsymbol{\lambda}_4(k+1 \mid k)) \\
&\ \ \vdots \\
\boldsymbol{\gamma}(k+N \mid k) &= \boldsymbol{\gamma}(k+N-1 \mid k) + \frac{\tau_s}{6}(\boldsymbol{\lambda}_1(k+N-1 \mid k) \\
&\quad + 2\boldsymbol{\lambda}_2(k+N-1 \mid k) + 2\boldsymbol{\lambda}_3(k+N-1 \mid k) \ + \boldsymbol{\lambda}_4(k+N-1 \mid k)).
\end{aligned} \tag{5.24}$$

As shown in Figure 5.14, the behavioral evolution of the system is used to state the optimization problem, where the objective is to find an either optimal or sub-optimal control sequence

$$\begin{aligned}
\mathbf{u}^*(k) = [&u_{_1}(k \mid k)\ u_{out_1}(k \mid k)\ u_{_2}(k \mid k)\ u_{out_2}(k \mid k)\ ...\ u_{out_M}(k \mid k)\ u_{_1}(k+1 \mid k) \\
&u_{out_1}(k+1 \mid k)\ u_{_2}(k+1 \mid k)\ u_{out_2}(k+1 \mid k)\ ...\ u_{out_M}(k+1 \mid k)\ ... \\
&u_{_1}(k+N-1 \mid k)\ u_{out_1}(k+N-1 \mid k)\ u_{_2}(k+N-1 \mid k) \\
&u_{out_2}(k+N-1 \mid k)\ ...\ u_{out_M}(k+N-1 \mid k)]^\top,
\end{aligned} \tag{5.25}$$

which delivers the proper amount of water to the users, minimizing losses due to leaks and seepage at the same time that the hydraulic operational conditions of the OCIS are accomplished. Henceforth, next a detailed description of the proposed objectives and constraints that must be included in the optimization problem are presented.

Objective function

The objective function $J(k)$ is composed of the sum of four terms, which correspond to: i) the amount of leaks and seepage; ii) the delivery flow error; iii) the control effort; and iv) the delivery volume error.

In this direction, as shown in (5.15) and (5.16), leaks and seepage are functions of the channels' levels. Henceforth, over a prediction horizon, the minimization of leaks and

seepage is reached by the minimization of the upstream and downstream levels. Therefore, the first term of the objective function is given by,

$$J_1(k) = \sum_{j=1}^{N} \|\boldsymbol{x}(k+j \mid k)\|^2_{\mathbf{R_x}},$$

where $\boldsymbol{x}(k+j \mid k) = [x_{up_1}(k+j \mid k)\ x_{dn_1}(k+j \mid k)\ x_{up_2}(k+j \mid k)\ ...\ x_{dn_M}(k+j \mid k)]^\top$, $\boldsymbol{x}(k+j \mid k) \in \mathbb{R}^{2M}$, and $\mathbf{R_x} \in \mathbb{R}^{2M \times 2M}$ is a diagonal matrix used to prioritize the respective upstream and downstream levels over the prediction horizon.

Intending to minimize the difference between demanded and delivered flows, the second term of the objective function is given by

$$J_2(k) = \sum_{j=0}^{N-1} \|\boldsymbol{d_{out}}(k+j \mid k) - \boldsymbol{q_{out}}(k+j \mid k)\|^2_{\mathbf{R_d}}, \tag{5.26}$$

where $\boldsymbol{d_{out}}(k+j \mid k) = [d_{out_1}(k+j \mid k)\ d_{out_2}(k+j \mid k)\ ...\ d_{out_M}(k+j \mid k)]^\top$, $\boldsymbol{d_{out}}(k+j \mid k) \in \mathbb{R}^M$, $\boldsymbol{q_{out}}(k+j \mid k) = [q_{out_1}(k+j \mid k)\ q_{out_2}(k+j \mid k)\ ...\ q_{out_M}(k+j \mid k)]^\top$, $\boldsymbol{q_{out}}(k+j \mid k) \in \mathbb{R}^M$, and $\mathbf{R_d} \in \mathbb{R}^{M \times M}$ is a diagonal matrix used to prioritize $J_2(k)$ over the prediction horizon.

Furthermore, strong control actions can induce excessive waves in controlled OCIS (Weyer, 2006). Therefore, with the aim to reduce these negative effects, the third term of the objective function is related to the control effort minimization given by

$$J_3(k) = \sum_{j=0}^{N-1} \|\boldsymbol{u}(k+j \mid k)\|^2_{\mathbf{R_u}},$$

where $\boldsymbol{u}(k+j \mid k) = [u_1(k+j \mid k)\ u_{out_1}(k+j \mid k)\ ...\ u_M(k+j \mid k)\ u_{out_M}(k+j \mid k)]^\top$, $\boldsymbol{u}(k+j \mid k) \in \mathbb{R}^{2M}$, and $\mathbf{R_u} \in \mathbb{R}^{2M \times 2M}$ is a diagonal matrix used to prioritize $J_3(k)$ over the prediction horizon.

As mentioned above, in on-request mode, the user must request in advance the amount of hydraulic resource that will be used. However, in agricultural systems an exact flow accomplishment of the demanded profile is not necessary. This is due to:

- some users store the delivered water in reservoirs;
- in crops the dynamics of the humidification and absorption processes are characterized to be slow.

Therefore, in this control approach, it could be considered that an exact accomplishment of the demanded profile is not the principal control objective. However, the delivery flow error minimization is contemplated by (5.26). Under these circumstances, if there is not an exact accomplishment of the demanded profile, the volume of demanded water, which, in most cases is used to establish the users' payment, must be accomplished to satisfy the users' requirements. In this direction, the fourth term of the objective function is

established to reduce the volume error between demanded and delivered water. Note that, at the k^{th} instant, the error between demanded and delivered water volume of the i^{th} user can be obtained from

$$\boldsymbol{e_v}(k \mid 0) = \boldsymbol{\theta_{out}}(k \mid 0) - \boldsymbol{\phi_{out}}(k \mid 0).$$

Similarly, over a prediction window, the predicted volume error can be obtained from

$$\boldsymbol{e_v}(k+N \mid k) = \tau_s \sum_{j=1}^{N} \boldsymbol{d_{out}}(k+j \mid k) - \tau_s \sum_{j=1}^{N} \boldsymbol{q_{out}}(k+j \mid k).$$

As a result, the fourth term of the cost function is given by

$$J_4(k) = \|\boldsymbol{e_v}(k \mid 0) + \boldsymbol{e_v}(k+N \mid k)\|^2_{\mathbf{R_v}},$$

where $\boldsymbol{e_v}(k \mid k) = [e_{v_1}(k \mid k)\ e_{v_2}(k \mid k)\ ...\ e_{v_M}(k \mid k)]^\top$, $\boldsymbol{e_v}(k \mid k) \in \mathbb{R}^M$, $\boldsymbol{\theta_{out}}(k \mid k) = [\theta_{out_1}(k \mid k)\ \theta_{out_2}(k \mid k)\ ...\ \theta_{out_M}(k \mid k)]^\top$, $\boldsymbol{\theta_{out}}(k \mid k) \in \mathbb{R}^M$, $\boldsymbol{\phi_{out}}(k \mid k) = [\phi_{out_1}(k \mid k)\ \phi_{out_2}(k \mid k)\ ...\ \phi_{out_M}(k \mid k)]^\top$, $\boldsymbol{\phi_{out}}(k \mid k) \in \mathbb{R}^M$, $d_{out}(k \mid k) = [d_{out_1}(k \mid k)\ d_{out_2}(k \mid k)\ ...\ d_{out_M}(k \mid k)]^\top$, $d_{out}(k \mid k) \in \mathbb{R}^M$, $q_{out}(k \mid k) = [q_{out_1}(k \mid k)\ q_{out_2}(k \mid k)\ ...\ q_{out_M}(k \mid k)]^\top$, $q_{out}(k \mid k) \in \mathbb{R}^M$, and $\mathbf{R_v} \in \mathbb{R}^{M \times M}$ is a diagonal matrix used to prioritize J_4 over the prediction horizon.

Constraints

The optimization problem is formulated into a search space of the decision variables. Such a search space is defined by constraints, such as manufacturing limits of the regulation structures, hydraulic conditions of the regulation structures, level limits, and limits in the delivery flow error, which are discussed next.

The regulation structures can operate into manufacturing limits, which are established as

$$0 \leq u_i(k+j \mid k) \quad \leq u_i^{max} \quad \forall j \in [0, N-1], \tag{5.27a}$$
$$0 \leq u_{out_i}(k+j \mid k) \leq u_{out_i}^{max} \quad \forall j \in [0, N-1], \tag{5.27b}$$

where u_i^{max} and $u_{out_i}^{max}$ are the maximum positions of the discharge and delivery regulation structures, respectively. Moreover, in the regulation structures, the mathematical descriptions of the flows are valid under specific hydraulic conditions, for example the mathematical descriptions of submerged gates and weirs are valid if the regulation structures are submerged. In addition, assuming that in operating conditions of the OCIS, the level $x_{dn_{i-1}}(k)$ is always greater than $x_{up_i}(k)$, and that the outflow point is at the downstream end of the channels, then the constraints that guarantee the submerged operation of the regulation structures are given by

$$0 \leq u_i(k+j \mid k) \quad \leq x_{up_i}(k+j \mid k) \quad \forall j \in [0, N-1], \tag{5.28a}$$
$$0 \leq u_{out_i}(k+j \mid k) \leq x_{dn_i}(k+j \mid k) \quad \forall j \in [0, N-1]. \tag{5.28b}$$

Similarly, in the operation of the OCIS, maximum levels that avoid overflows, and minimum levels that avoid ecological, or infrastructure damage must be established. Therefore, constraints for the upstream and downstream levels of the channels are included as

$$x_{up_i}^{min} \leq x_{up_i}(k+j \mid k) \leq x_{up_i}^{max} \quad \forall j \in [1, N], \tag{5.29a}$$
$$x_{dn_i}^{min} \leq x_{dn_i}(k+j \mid k) \leq x_{dn_i}^{max} \quad \forall j \in [1, N]. \tag{5.29b}$$

Finally, despite the accomplishment of an exact flow demanded profile is not the main objective of the proposed control strategy, in this approach, limits in the delivery flow error are included to accomplish with specific users requirements. These limits are included by using the following constraint:

$$e_{d_i}^{min}(k+j \mid k) \leq d_{out_i}(k+j \mid k) - q_{out_i}(k+j \mid k) \leq e_{d_i}^{max}(k+j \mid k) \quad \forall j \in [0, N-1], \tag{5.30}$$

where $e_{d_i}^{min}(k \mid k)$ and $e_{d_i}^{max}(k \mid k)$ are the established minimum and maximum errors between demanded and delivered flow, respectively.

Optimization problem

In summary, the open-loop, discrete-time, finite-horizon optimization problem that should be solved is written as follows:

$$\begin{aligned}
\min_{\mathbf{u}(k)} \quad & J(k) = \sum_{i=1}^{4} J_i(k) \\
\text{s.t.} \quad & (5.23), \\
& 0 \leq u_{_i}(k+j \mid k) \leq u_{_i}^{max} && \forall j \in [0, N-1], \\
& 0 \leq u_{out_i}(k+j \mid k) \leq u_{out_i}^{max} && \forall j \in [0, N-1], \\
& 0 \leq u_{_i}(k+j \mid k) \leq x_{up_i}(k+j \mid k) && \forall j \in [0, N-1], \\
& 0 \leq u_{out_i}(k+j \mid k) \leq x_{dn_i}(k+j \mid k) && \forall j \in [0, N-1], \\
& x_{up_i}^{min} \leq x_{up_i}(k+j \mid k) \leq x_{up_i}^{max} && \forall j \in [1, N], \\
& x_{dn_i}^{min} \leq x_{dn_i}(k+j \mid k) \leq x_{dn_i}^{max} && \forall j \in [1, N], \\
& e_{d_i}^{min} \leq d_{out_i}(k+j \mid k) - q_{out_i}(k+j \mid k) \leq e_{d_i}^{max} && \forall j \in [0, N-1].
\end{aligned} \tag{5.31}$$

Assuming the feasibility of (5.31), its solution yields the optimal (or suboptimal) sequence $\mathbf{u}^*(k)$ as in (5.25), from which and considering the receding horizon philosophy behind the NLMPC strategy sets

$$\begin{aligned}
\boldsymbol{u}_{\text{MPC}}(k) &= \boldsymbol{u}^*(k) \\
&= [u_{_1}(k)\ u_{out_1}(k)\ u_{_2}(k)\ u_{out_2}(k) \dots u_{out_M}(k)]^\top,
\end{aligned} \tag{5.32}$$

and disregards the computed inputs from $k = 1$ to $k = N - 1$, repeating the process for the next time instant $k + 1$ taking into consideration the feedback information coming from the system (either measured or estimated states) as initial conditions. Notice that

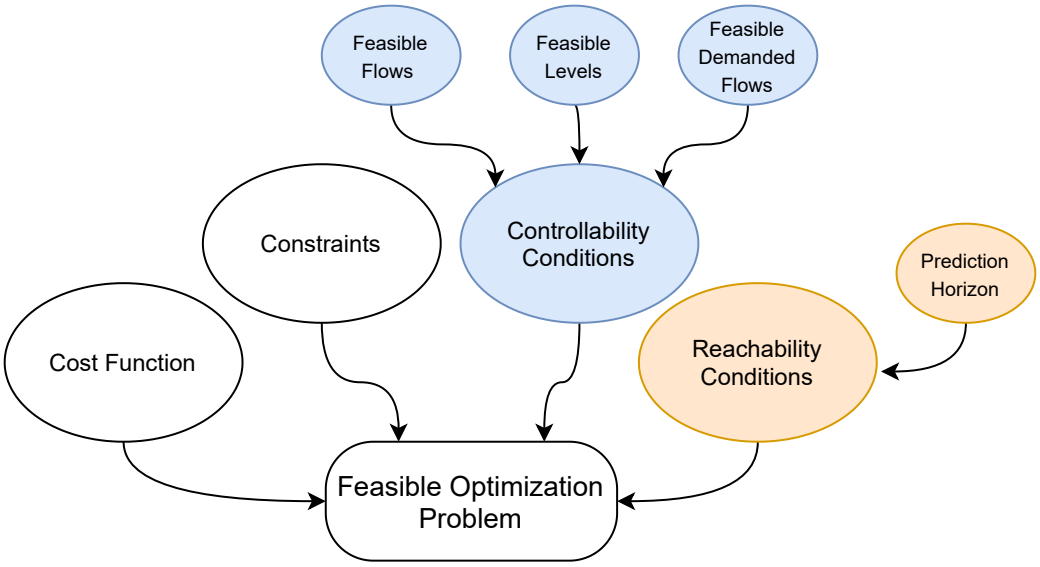

Fig. 5.15. Schematic of the feasible optimization problem, where the optimization problem (5.31) is enhanced with controllability and reachability conditions that guarantee its feasibility.

(5.32) corresponds with the well-known *MPC law*, being it the sequence of actions to be applied to the system at each time instant (Ocampo-Martinez, 2010).

Now, with the purpose of establish operational conditions of the proposed control approach, the stability conditions that guarantee the proper operation of the controlled system are presented next.

5.3.3 Operational Conditions of the Proposed Control Approach

Once the optimization problem has been proposed, it is necessary to establish its feasibility, which is closely related to the hydraulic characteristics, physical behavior, topology, and management of the OCIS. Therefore, toward to obtain a feasible solution of the optimization problem, the physical conditions that must be accomplished are also included as controllability and reachability conditions. As it is shown in Figure 5.15, the controllability conditions are related to obtain solutions that:

- ensure real values of the flows;
- provide levels that can be reached
- guarantee the accomplishment of imposed demands.

On the other hand, the reachability conditions are related to the time interval that the system expends reaching the operational conditions, which must be used in the establishment of the prediction horizon.

Note that, in NLMPC the feasibility of the optimization problem is related to the stability of the controlled system, where a stable operation of the controlled OCIS guarantee

that the channel levels will always belong to the range where the overflows are avoided, also preventing from ecological and/or infrastructural damage. In the OCIS, levels might be modified by changes in the hydraulic structures positions $\boldsymbol{u}(k)$ and external actions or disturbances, such as leaks, seepage and rains. Such external actions could be strong enough that the controlled system stability cannot be reached by the control actions $\boldsymbol{u}^*(k)$ in (5.32), and this is a problem that must be solved during the system design. In contrast, under ideal operation conditions (i.e., small disturbances, and an accurate system modeling) a control sequence $\mathbf{u}^*(k)$ that accomplishes with the imposed constraints (5.27) - (5.30) guarantees the controlled system stability. Therefore, if $\mathbf{u}^*(k)$ is a feasible solution of (5.31), even sub-optimal solutions of $\mathbf{u}^*(k)$ guarantee the controlled system stability. A generalization of this finding has been previously reported by Scokaert et al. (1999), and its adapted description is presented in Theorem 1.

Theorem 1. *Let $\mathbb{U} \subset \mathbb{R}^{2M}$ be the feasible set of control actions in a way of gate positions as established in (5.27), (5.28), and (5.30), $\mathbb{X} \subset \mathbb{R}^{2M}$ the feasible set of levels established by (5.28), (5.29), and (5.30), $\mathbb{F} \subset \mathbb{R}^{2M}$ the set of levels for which there exists a control sequence that satisfies $\mathbf{u}(k) \in \mathbb{U}$, $x(k) \in \mathbb{X}$, and $x(k+N \mid k) \in \mathbb{W}$, where $\mathbb{W} \subset \mathbb{R}^{2M}$ is a subset of $\mathbb{F}$. Then a sub-optimal NLMPC law is asymptotically stabilizing with a region of attraction $\mathbb{W}$.*

The corresponding proof of Theorem 1 has been addressed by Scokaert et al. (1999). Therefore, assuming that under feasible conditions the proposed problem has feasible solutions, the stability of the controlled OCIS can be guaranteed by establishing the corresponding controllability and reachability conditions.

Controllability Conditions

According to Yuan et al. (2011), the controllability has been defined from several points of view. In this thesis, adopting the concept given by Kalman (1960), the state controllability of the OCIS is given by using Definition 1.

Definition 1 (Controllability)**.** *The levels $x(k+N \mid k)$ of the OCIS are controllable if there are feasible control sequences $\mathbf{u}(k)$, i.e., a feasible sequence of gate positions, such that the levels $x(k \mid k)$ can be driven to $x(k+N \mid k)$ during a finite time interval.*

As a result, the controllability of the OCIS can be established by analyzing the simplified model (5.17), which shows that each channel is an affine system, and for each channel, the upstream and downstream levels receive a direct influence of $u_i(t)$ and $u_{out_i}(t)$, respectively. However, in OCIS there are multiple hydraulic conditions that must be included to establish the system controllability.

In this order of ideas, a set of controllability conditions is proposed, which is developed under Assumption 4.

Assumption 4 ($x^{max} \in \mathbb{F}$)**.** *It is assumed that the maximum levels x^{max} are established such that a feasible control sequence $\boldsymbol{u}^*(k) \in \mathbb{U}$ exists, then that $x(k \mid k)$ can be driven to $x(k+N \mid k) = x^{max}$ even in the maximum water demand operation.*

Remark 1. *Into the optimization problem, levels $x_{up_i}^{max}$ and $x_{dn_i}^{max}$ have been defined as the maximum upstream and downstream levels that avoid overflows. Therefore, the upstream and downstream maximum levels can be obtained from the physical dimensions of the OCIS. However, to guarantee the stability of the controlled system, even the controllability of x_{up_i} and x_{dn_i} to reach $x_{up_i}^{max}$ and $x_{dn_i}^{max}$ must be guaranteed. Note that OCIS under maximum water demand presents the lowest levels. Therefore, to establish controllable values of $x_{up_i}^{max}$ and $x_{dn_i}^{max}$, a steady-state analysis of the OCIS in the highest water demand case, where $u_{out_i} = x_{dn_i}^{max}$ is recommended.*

Once the maximum upstream and downstream levels are assumed to be controllable, by analyzing the hydraulic descriptions of the flow transition (5.18), the channel inflow (5.19), and the user's outflow (5.20), which must exist and be real, and by including the operative levels conditions of the systems, a set of controllable conditions can be established as

$$x_{dn_{i-1}}(k+j \mid k) - x_{up_i}(k+j \mid k) > 0 \qquad \forall j \in [1, N], \tag{5.33a}$$
$$x_{up_i}(k+j \mid k) > 0 \qquad \forall j \in [1, N], \tag{5.33b}$$
$$x_{up_i}(k+j \mid k) - x_{dn_i}(k+j \mid k) + z_{up_i} - z_{dn_i} \geq 0 \qquad \forall j \in [1, N], \tag{5.33c}$$
$$x_{dn_i}(k+j \mid k) > 0 \qquad \forall j \in [1, N], \tag{5.33d}$$
$$x_{up_i}(k+j \mid k) \leq x_{up_i}^{max} \quad \forall j \in [1, N], \tag{5.33e}$$
$$x_{dn_i}(k+j \mid k) \leq x_{dn_i}^{max} \quad \forall j \in [1, N], \tag{5.33f}$$

where (5.33a)-(5.33d) ensure real values of the flows q_i, q_{tr_i}, and q_{out_i}. On the other hand, (5.33e) and (5.33f) guarantee that, under Assumption 4, the levels $x_{up_i}(k)$ and $x_{dn_i}(k)$ can be reached by a feasible control sequence $\mathbf{u}^*(k)$ in (5.25).

As a result, aiming to guarantee the system controllability, also the initial conditions and the minimum levels must be included into the set of controllable conditions, that is

$$x_{dn_{i-1}}(0) - x_{up_i}(0) > 0 \tag{5.34a}$$
$$x_{up_i}(0) > 0 \tag{5.34b}$$
$$x_{up_i}(0) - x_{dn_i}(0) + z_{up_i} - z_{dn_i} \geq 0 \tag{5.34c}$$
$$x_{dn_i}(0) > 0 \tag{5.34d}$$
$$x_{up_i}(0) \leq x_{up_i}^{max} \tag{5.34e}$$
$$x_{dn_i}(0) \leq x_{dn_i}^{max}, \tag{5.34f}$$

and

$$x_{dn_{i-1}}^{min} - x_{up_i}^{min} > 0 \tag{5.35a}$$
$$x_{up_i}^{min} > 0 \tag{5.35b}$$
$$x_{up_i}^{min} - x_{dn_i}^{min} + z_{up_i} - z_{dn_i} \geq 0 \tag{5.35c}$$
$$x_{dn_i}^{min} > 0 \tag{5.35d}$$
$$x_{up_i}^{min} \leq x_{up_i}^{max} \tag{5.35e}$$
$$x_{dn_i}^{min} \leq x_{dn_i}^{max}. \tag{5.35f}$$

Moreover, note that in order to accomplish with the maximum error limits in the delivery flow (5.30), the demanded flow must not exceed the maximum capacity of the i^{th} outflow regulation structure, establishing that

$$d_{out_i}(k+j \mid k) \leq q_{out_i}^{max} - e_{d_i}^{max} \quad \forall j \in [0, N-1], \tag{5.36}$$

with

$$q_{out_i}^{max} = c_{out_i} w_{outi} u_{out_i}^{max} \sqrt{2g x_{dn_i}^{max}}. \tag{5.37}$$

The controllability conditions can be used in the establishment and schedule of the users' demands. However, note that the proposed controllability conditions, which have been established by analysis in steady state, are highly conservative. Therefore, these controllability conditions are sufficient but not necessary.

Reachability Conditions

In the reachability case, as opposed to the controllability, the feasibility is analyzed during a finite interval. Schürmann et al. (2018) have defined reachability as stated next.

Definition 2 (Reachability)**.** *A feasible solution of* $\mathbf{u}(k)$ *exists if* $x(k+N \mid k)$ *is feasible, and* N *is large enough such that* $x(k \mid k)$ *can be driven to* $x(k+N \mid k)$ *during the time interval associated to* N*.*

A clear example of infeasibility in terms of reachability is an immediate outflow demand with a downstream level insufficient to accomplish such a demand. This kind of sudden requirements are outside the controllable conditions set (5.30). Note that, intending to accomplish this requirement, the time that the system takes to reach a requested level must be considered. Therefore, if the initial conditions of the OCIS are into the controllable conditions set, the demands must be scheduled taking into account the OCIS dynamics, in order to guarantee reachability. For example, the reachability conditions could be obtained from the time that the OCIS takes to satisfy the most time-expensive requests, by analyzing the time intervals that each channel spends to reach the maximum operation capacity. This reachability condition is established in the next lemma.

Lemma 2. *Under controllable conditions (5.33)-(5.37), let* N_i *be the elapsed time to drive the downstream level of the* i^{th} *channel from initial conditions* $x(k \mid k) = x^{min}$ *to the maximum level of the* i^{th} *channel* $x_{dn_i}(k+N_i \mid k) = x_{dn_i}^{max}$*, where* $N_i < N_{i+1} < N_M$*. Then, if the prediction horizon is established such as* $N \geq N_M$ *and all the demands* d_{out_i} *are scheduled after the longest elapsed time* N_M*, the constraint associated to the limits in the delivery flow errors (5.30) can be accomplished.*

Proof. The maximum demanded flows can be accomplished by driving the OCIS to $x_{dn_i}^{max}$ (5.37). Under controllable conditions (5.33)-(5.37), there exists a feasible control sequence $\mathbf{u}(k)$ such that the OCIS can be driven to $x_{dn_i}^{max}$ during a finite time (see Assumption 4). Then, by analytical or experimental procedures, this time can be found. Under the fact that to drive the farthest channel to maximum levels takes more time than to drive

the other channels to maximum levels (i.e., $N_{_M} > N_{_i}$), any channel can be driven to $x_{dn_i}^{max}$ during the associated time $N_{_M}$. Therefore, there exists a feasible control sequence $\mathbf{u}(k)$, which during an associated time $N_{_M}$ can accomplish even the maximum demanded flow. □

Similar to the controllability conditions, the reachability condition presented in Lemma 2 is sufficient but not necessary, and to schedule the demands after the longest elapsed time $N_{_M}$ is highly conservative. Then, the development of a demand schedule strategy that guarantees the system stability appears as an interesting future direction that is out of the scope of this thesis.

Reformulated Optimization Problem

In summary, the open-loop, discrete-time, finite-horizon optimization problem that includes both reachability and controllability conditions, and guarantees the closed-loop system stability is now written as follows:

$$\begin{aligned} \min_{\mathbf{u}(k)} \quad & J(k) = \sum_{i=1}^{4} J_i(k) \\ \text{s.t.} \quad & \text{The accurate OCIS discretized model in (5.23),} \\ & \text{The physical/operational constraints in (5.27)-(5.30),} \\ & \text{The controllability conditions in (5.33)-(5.37),} \\ & \text{The reachability condition } N = N_{_M}. \end{aligned} \tag{5.38}$$

Now, the optimization problem in (5.38) should be used to find the control actions in (5.32) to be applied to the OCIS and then closing the proposed NLMPC-based controlled loop.

5.3.4 Simulation Test

The proposed NLMPC strategy is tested by using the two first channels of a benchmark based on the Corning canal in California. This benchmark has been presented by Clemmens et al. (1998) and the ASCE Task Committee on Canal Automation Algorithms as a standardized testbed on OCIS with well-studied and realistic properties. The channel characteristics are shown in Table 5.4.

As shown in Figure 5.16, the testbed has been implemented in the storm water management model (SWMM), and used as a reference model to tune and validate the approximated model variables. Then, the validated model has been used in the design and testing of the control strategy.

As a matter of fact, the principal parameter that must be obtained is the sampling time τ_s, which is acquired from experimental analyses over the model. Following the recommendations proposed by Litrico and Fromion (2009), the obtained sampling time is $\tau_s = 1000$s, which corresponds to a value ten times smaller than the rising time of x_{dn_1}.

As shown by Conde et al. (2020) in the modeling and validation of the Corning canal, the approximated model areas a_{up_i}, and a_{dn_i} have been obtained by using data fitting,

Table 5.4. Physical characteristics of the case study.

Source	*Level*	*0.7* m			
	Length	7000 m		*Length*	3000 m
	w_1	7 m		w_2	7 m
	c_1	0.65		c_2	0.65
	z_{up_1}	4 m		z_{up_2}	3.3 m
Channel 1	z_{dn_1}	3.3 m	**Channel 2**	z_{dn_2}	2.8 m
	κ_{up_1}	0.2 m^6/s		κ_{up_2}	0.2 m^6/s
	κ_{dn_1}	0.2 m^6/s		κ_{dn_2}	0.2 m^6/s
	w_{out_1}	1 m		w_{out_2}	1 m
	c_{out_1}	0.65		c_{out_2}	0.65

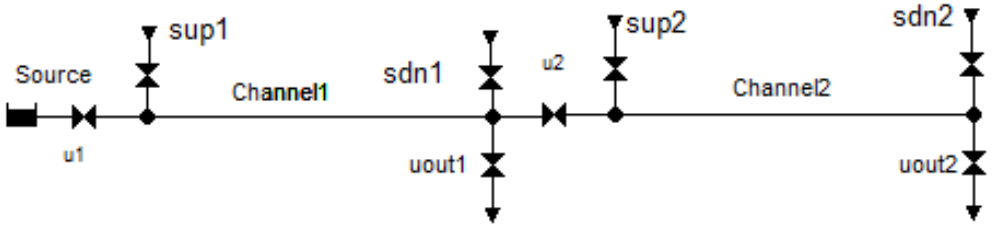

Fig. 5.16. Case study implementation in EPA-SWMM.

where data from the reference model are used. Hence, the obtained areas are: $a_{up_1} = 21864\text{m}^2$, $a_{dn_1} = 27136\text{m}^2$, $a_{up_2} = 12086\text{m}^2$, and $a_{dn_2} = 8914\text{m}^2$.

Similarly, the transition constants (k_{tr_i}) are obtained analyzing the system (5.17) in steady-state operation using flow and level data from the model. The obtained transition constants are $k_{tr_1} = 6$, and $k_{tr_2} = 9$.

Moreover, in order to implement the control strategy, the multiple parameters that guarantee stability and the desired performance of the controlled system are established, where the maximum upstream and downstream levels are obtained from steady-state analysis of the system (5.17) under the maximum water demand case. In this analysis, it has been assumed that the physical limits of the regulation structures are higher or equal to the maximum levels under the maximum water demand case. Therefore, toward accomplish with the hydraulic conditions of the regulation structures (5.28), the highest water demand can be supplied by the maximum outflow, which is given with $u_{out_i}^{max} = x_{dn_i}^{max}$, and this maximum outflow can be accomplished with a maximum channel inflow, which is given by $u_i^{max} = x_{up_i}^{max}$. As a result, by performing the respective substitutions in (5.17), which is analyzed in the steady-state regime, the obtained upstream and downstream maximum level values are given by $x_{up_1}^{max} = 0.59\text{m}$, $x_{dn_1}^{max} = 0.57\text{m}$, $x_{up_2}^{max} = 0.53\text{m}$, and $x_{dn_2}^{max} = 0.79\text{m}$. Note that the obtained maximum levels are consistent with the hydraulic conditions presented in (5.33) ensuring that the corresponding flows q_i, q_{tr_i}, and q_{out_i} are real values.

Furthermore, as in a well dimensioned systems, the maximum physical limits of the regulation structures have been chosen equal than the associated upstream or downstream

maximum levels. In that form, $u_1^{max} = 0.59$m, $u_{out_1}^{max} = 0.57$m, $u_2^{max} = 0.53$m, and $u_{out_2}^{max} = 0.79$m.

Additionally, in order to guarantee the accomplishment of the conditions presented in (5.33), (5.34), and (5.35), the minimum levels have been chosen as 1% of the maximum levels, and the initial conditions have been chosen as 10% of the maximum levels.

With the purpose of find a prediction horizon N, and the minimum time to schedule the respective demands, a simulation with $u_1 = u_1^{max}$, $u_{out_1} = u_{out_1}^{max}$, $u_2 = u_2^{max}$, and $u_{out_2} = u_{out_2}^{max}$ is performed, obtaining that $x_{dn_1}^{max}$ is reached in 5×10^4s, and $x_{dn_2}^{max}$ is reached in 6×10^4s. Therefore, the prediction horizon is chosen as $N = 60$, and the time restrictions to schedule the respective demands are established as $N_1 = 50$, and $N_2 = 60$. Furthermore, to establish magnitudes for the upstream and downstream demands, the maximum outflow capacity and the limits in the delivery flow are presented. From (5.37), the maximum outflow demands are given by $q_{out_1}^{max} = 1.24\text{m}^3/\text{s}$, and $q_{out_2}^{max} = 2.02\text{m}^3/\text{s}$. On the other hand, the limits in the delivery flow error are parameters that the users impose. In this case, a limit of ten percent of the demanded flow is established.

Even though the penalization parameters can be used as tuning parameters that improve the performance of the controlled system, for sake of simplicity, in the proposed test, the parameters have been set as normalization parameters that balance the multiple terms of the total cost function. Specifically, the penalization parameters have been set as: $R_{up_i} = (1/x_{up_i}^{max})^2$, $R_{dn_i} = (1/x_{dn_i}^{max})^2$, $R_{d_i} = (1/d_{out_i}^{max})^2$, $R_{u_i} = (1/u_i^{max})^2$, $R_{v_i} = (1/\theta_{out_i}(N))^2$, where $d_{out_i}^{max}$ is the maximum demand of the i^{th} channel, and $\theta_{out_i}(N)$ is the demanded volume of the i^{th} user. However, as a future direction, more tests and sensitive analyses around the influence of the penalization parameters can be performed.

Finally, the optimization problem is solved by using CasADi, which is an open-source tool designed to deal with optimization problems. This tool includes multiple solvers for optimal control problems. In this test, the IPOPT (interior-point optimizer) solver is used, which solves large-scale nonlinear programming problems by using a nonlinear interior point method (Andersson et al., 2019).

5.3.5 Simulation Results and Discussion

In the simulation results, the performance of the controlled system is analyzed in two scenarios:

- Supplying demands that are into the reachable set.
- Supplying demands that are not into the reachable set.

Finally, losses due to leaks and seepage are contrasted with the amount of leaks and seepage that could be obtained by using a conventional control strategy that maintains a fixed level at the downstream end of each channel.

Demands Inside the Reachable Set

Figures 5.17(a) and 5.17(b) show the performance of the controlled system in presence of reachable demands, where it is observed that the demands are successfully accomplished

according to the users' constraints. Moreover, it is observed that there is not a perfect tracking of the demanded outflow, and in most of the cases the upstream and downstream outflows follow the lower outflow allowed, and the delivered volume difference is compensated by delivering flow at instants where the demand has not been scheduled.

The downstream levels behaviors of the two channels are presented in Figures 5.17(c) and 5.17(d). Moreover, in these figures, the respective behavior of the outflow discharge structures is included. From these figures, it is highlighted that the downstream levels and the outflow regulation structures accomplish with the maximum avoided levels and apertures, satisfying the imposed constraint (5.27). Moreover, it is observed that the regulation structures apertures are always lower than the downstream levels, satisfying the hydraulic constraint given in (5.28). Also, it is observed how the downstream levels are maintained as low as can, and before of the scheduled demands, the levels start to increase to accomplish the respective demands.

Figures 5.17(e) and 5.17(f) show the upstream levels and inflow regulation structures positions of the controlled system. These figures also corroborate the accomplishment of the constraints, note that: the upstream levels and regulation structures always are lower than the maximum allowed; the positions of the regulation structures are always lower than the upstream levels; and iii) the upstream level is always bigger than the minimum allowed.

The total demanded and delivered volumes are described in Figure 5.18, where a difference between demanded and delivered volumes lower than 3% is observed. In a real operation of the system, this difference could be compensated with the users' payment for the service. Moreover, if this difference is considered excessive, the respective penalization parameter can be adjusted to modify the undesired behavior.

Figure 5.19, shows the quantitative relationship between losses using the proposed NLMPC strategy and using a conventional control strategy that maintains a constant level at the downstream end of the channel. The corresponding losses of using a conventional control strategy have been obtained by the assumption of maximum constant levels in the leaks and seepage descriptions given by Equations (5.15) and (5.16). The result evidences that, with the proposed strategy, 50% of the losses could be reduced. In the same direction, an efficiency performance indicator p_e is evaluated, where, for OCIS, the efficiency is the ratio of volume of delivered water to volume of water extracted from the source (Mareels et al., 2005). With the aim of compare the efficiency between the proposed strategy and a conventional control strategy that maintains a constant level at the downstream end of the channel, the efficiency performance indicator is established as

$$p_e = \frac{\tau_s \sum_{k=0}^{k_f} \sum_{i=1}^{M} q_{out_i}(k)}{\tau_s \sum_{k=0}^{k_f} \sum_{i=1}^{M} q_{out_i}(k) + s_{up_i} + s_{dn_i}}, \tag{5.39}$$

where k_f is the length of data associated to the simulation time. In the comparison, it is obtained that by using a conventional control strategy, the efficiency of the controlled system is close to 18%. In contrast, by using the proposed control strategy in this thesis, the efficiency of the controlled system is close to 31%, corroborating the advantages in the use of the proposed control strategy.

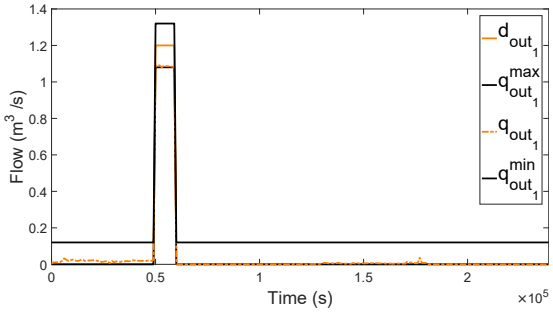

(a) Demanded and delivered outflow behavior at the first channel, where the accomplishment of the demands and constraints is observed.

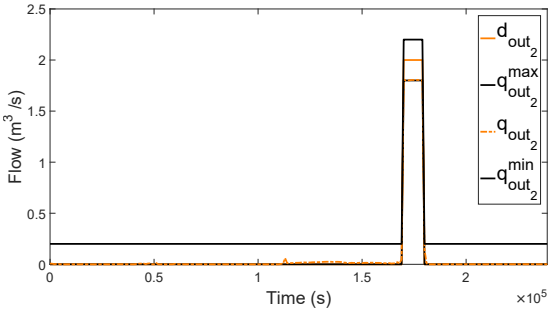

(b) Demanded and delivered outflow behavior at the second channel, where the accomplishment of the demands and constraints are observed.

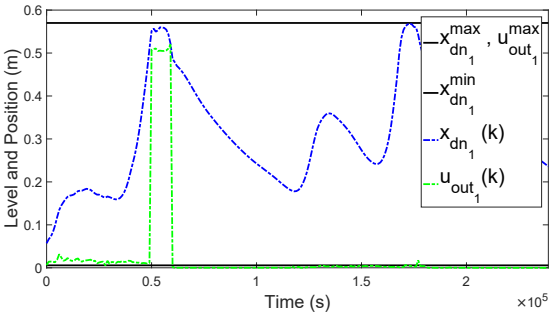

(c) Downstream levels and outflow regulation structures behavior of the first channel, where it is observed that the downstream levels and the outflow regulation structures apertures accomplish with the maximum and minimum avoided levels and apertures.

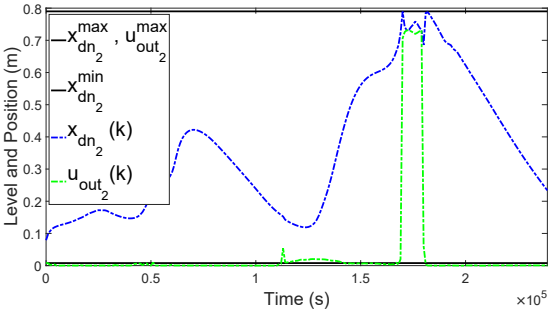

(d) Downstream levels and outflow regulation structures behavior of the second channel, where it is observed that the downstream levels and the outflow regulation structures apertures accomplish with the maximum and minimum avoided levels and apertures.

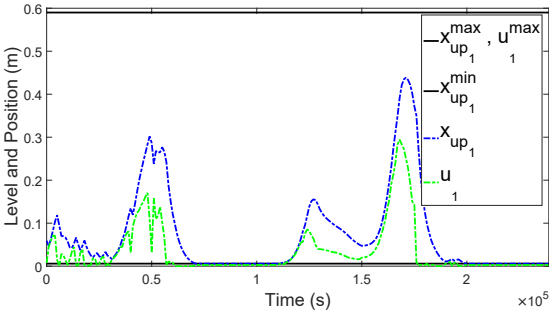

(e) Upstream levels and inflow regulation structures behavior of the first channel, where the accomplishment of the constraints is observed.

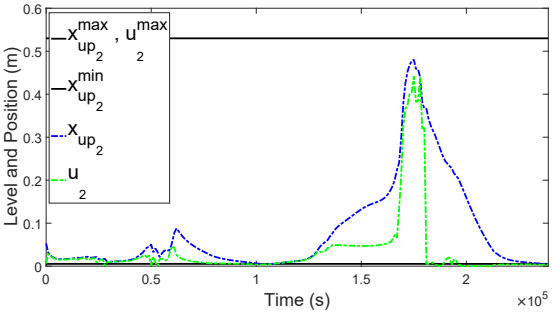

(f) Upstream levels and inflow regulation structures behavior of the second channel, where the accomplishment of the constraints is observed.

Fig. 5.17. Controlled system performance for demands that are into the reachable set.

A key aspect in the implementability of the control strategy is the time that the solver spends finding a feasible solution. Figure 5.20, shows the elapsed time that the solver

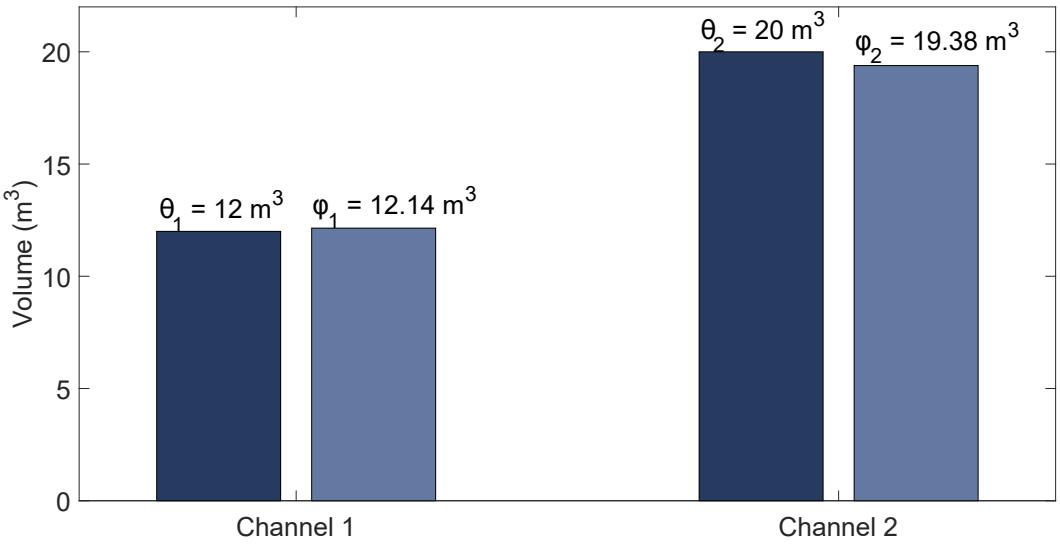

Fig. 5.18. Demanded and delivered total volume of the first and second channels, where a difference lower than 3% is observed.

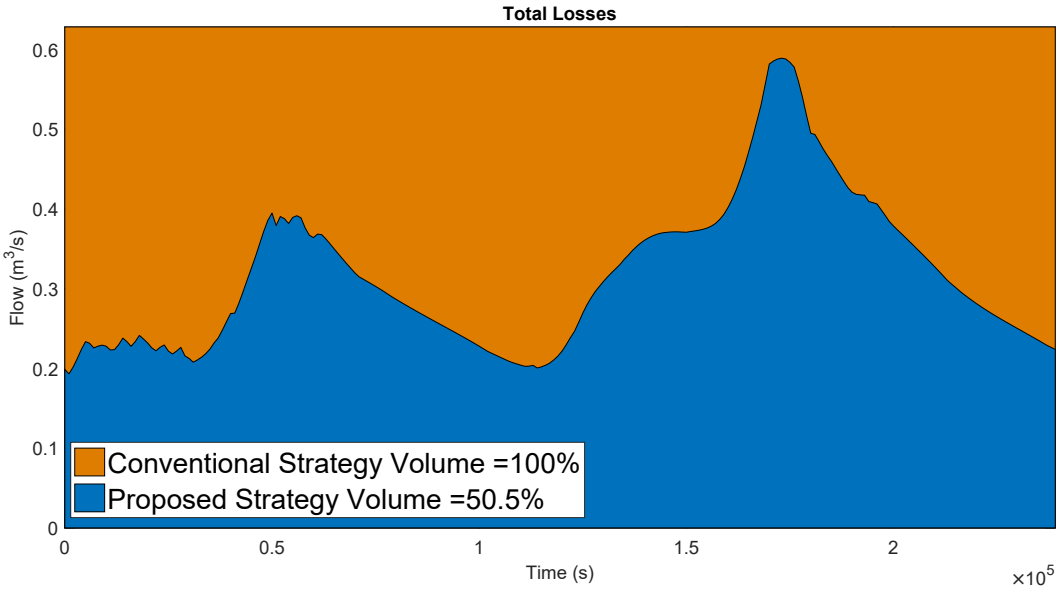

Fig. 5.19. Comparison between losses using the proposed strategy and using a conventional control strategy that maintains a constant level at the downstream end of the channel, where it is highlighted that by using the proposed strategy, 50% of the losses could be reduced.

spends to find an appropriate solution. There, it is important to mention that this test has been performed on a computer with an Intel i7 processor running at 2.7 MHz using 16 GB of RAM. In this figure, it is highlighted that the mean elapsed time is 2.56s and that the maximum elapsed time is close to 7s. Therefore, due to the OCIS are slow systems, where for control purpose long sampling-times are used, the use of NLMPC strategies is totally possible.

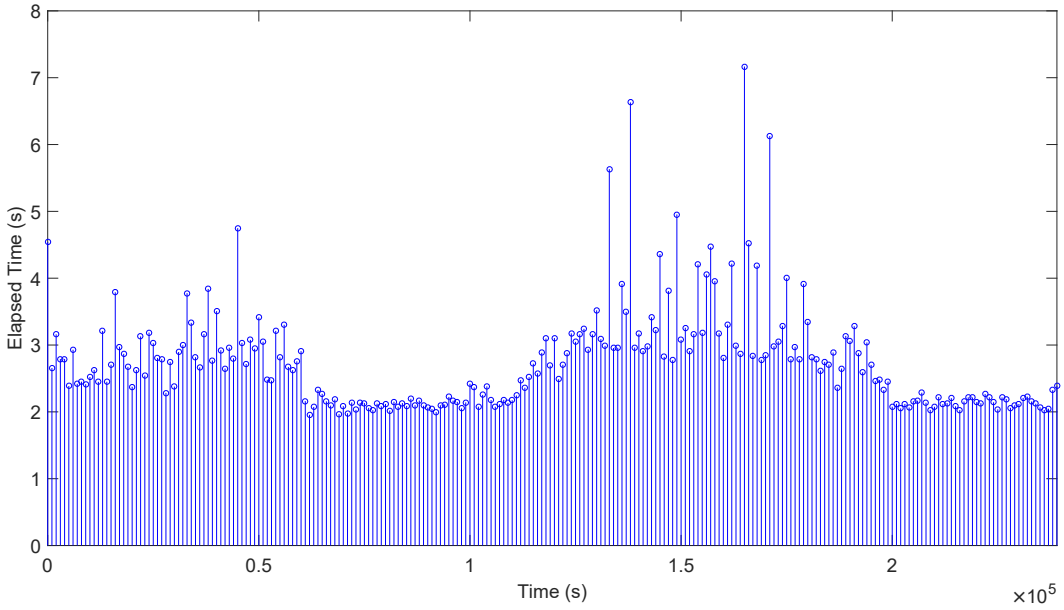

Fig. 5.20. Elapsed time to solve each optimization problem, note that the average elapsed time is 2.56s and that the maximum elapsed time is close to 7s.

Demands Outside the Reachable Set

Figures 5.21(a) and 5.21(b) show the performance of the controlled system in presence of an unreachable demand over the second channel. In this case, d_{out_2} is an instantaneous demand bigger than $q_{out_2}^{max}$. Figure 5.21(a) shows that despite the unreachable demand d_{out_2}, the outflow constraints of the first channel are accomplished. Conversely, in the second channel (Figure 5.21(b)) the demand is not accomplished. However, it is observed that q_{out_2} recovers the desired behavior.

Similarly, Figure 5.21(d) shows that the downstream level of the second channel presents problems in the accomplishment of the constraints. Meanwhile, the problems reported in the first channel (Figure 5.21(c)) are imperceptible.

Figures 5.21(e) and 5.21(f) show that the demand affects the upstream constraints of both channels. In the first channel, in order to accomplish this sudden demand, the inflow regulation structure aperture exceeds the channel level. However, when this suddenly demand is finished, both channels recover the desired behavior.

Respecting to the total demanded and delivered volume (Figure 5.22), the unreachable demand presents a high difference between the demanded and delivered water. On the other hand, the demands in the first channel are well accomplished.

Finally, it is important to realize that when the sudden demand is finished, the controlled system recovers the desired behavior without the affectation of posterior events. This is also an important finding because it confirms that the proposed stability conditions are sufficient but not necessary. However, a depth analyses of this phenomenon is proposed for future directions. Moreover, the real system implementation, the exploration of different objective functions, and constraints alternatives are also proposed as future directions.

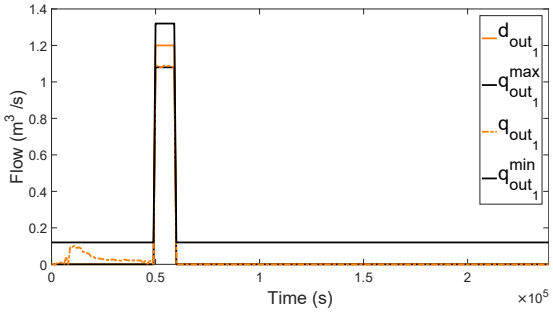

(a) Demanded and delivered outflow behavior at the first channel, where the reachable demand, and the imposed constraints are accomplished.

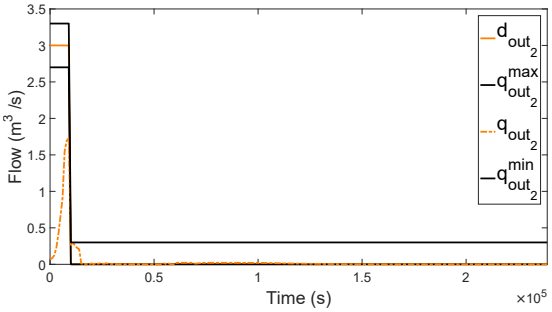

(b) Outflow behavior at the second channel, where the reachable demand cannot be accomplished. However, the flow q_{out_2} recovers the desired behavior.

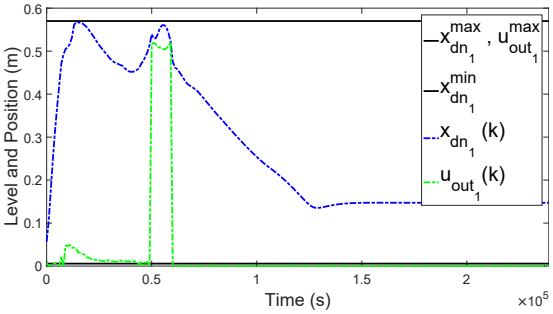

(c) Downstream levels and outflow regulation structures behavior of the first channel, where it is observed the accomplishment of the constraints.

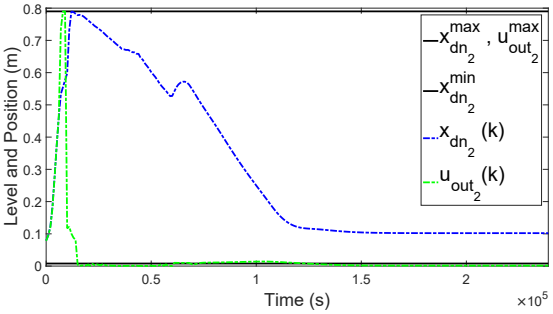

(d) Downstream levels and outflow regulation structures behavior of the second channel, where there are problems in the accomplishment of the imposed constraints.

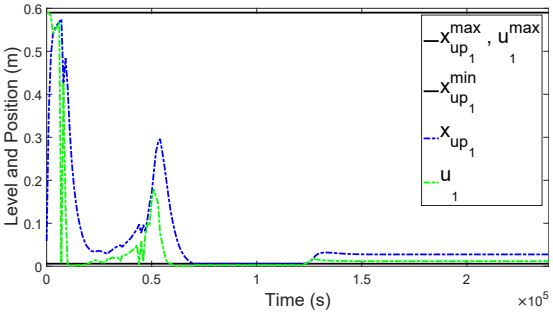

(e) Upstream level and inflow regulation structure behavior of the first channel, where it is observed that the sudden demand also affects the accomplishment of the constraints. However, when the sudden demand is finished, this channel recovers the desired behavior.

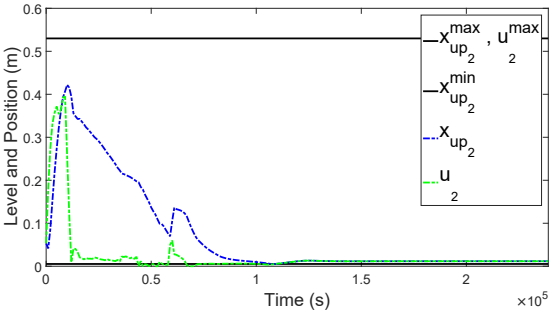

(f) Upstream level and inflow regulation structure behavior of the second channel, where it is observed that the sudden demand affects the accomplishment of the constraints. However, when the sudden demand is finished, this channel recovers the desired behavior.

Fig. 5.21. Controlled system performance for demands that are not into the reachable set.

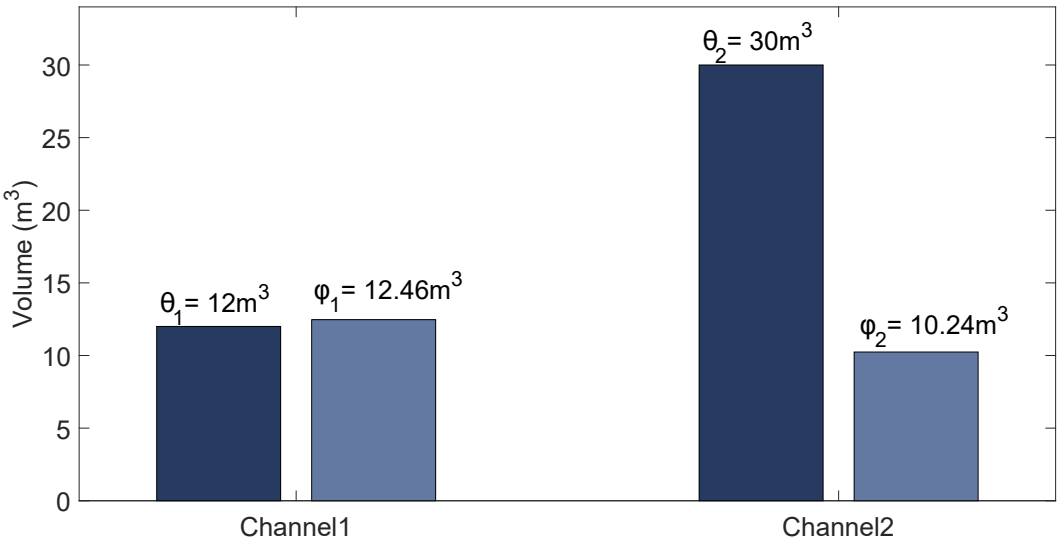

Fig. 5.22. Demanded and delivered total volume of the first and second channels, where it is observed that unreachable demands also affects the demanded total volume of the second channel.

5.4 Summary

This chapter addresses the problem of control in OCIS. In Section 5.1, an illustrative example is used to explain conventional modeling and control approaches that are used in OCIS. In Section 5.2, a nonlinear control technique for interacting OCIS has been presented, showing that with the proposed strategy it is possible to guarantee in a broad operation region null steady-state error, to adjust the speed response, and to overcome the problems of non-linearities, the interaction between channels, and internal delays. Finally, in Section 5.3, an efficient control strategy for OCIS is proposed. The strategy is developed with the objective of supplying an appropriate amount of water to the users minimizing losses due to seepage and leaks. In the design process, sufficient controllability and reachability conditions that guarantee the controlled system stability have been presented. The results show that by using this strategy an appropriate amount of water to the users can be supplied and that the waste of water could be reduced by up to 50%.

Chapter 6

Concluding Remarks

6.1 Contributions

In this thesis, the design and evaluation of modeling, control, and estimation strategies for OCIS that contribute to the mitigation of losses due to leaks and seepage, are addressed. Thus, as the *first contribution* of this thesis, a detailed classification of the reported control-oriented models for OCIS has been presented in Chapter 2. Based on this classification, it is identified the need for control-oriented models useful to describe interacting OCIS, and that include information about nonlinear hydraulic flow relations and potential energy difference along the channels. Therefore, as the *second contribution*, a nonlinear control-oriented modeling approach that assumes delays and a CPED along the channels has been proposed and validated in Chapter 3. The validation results show that this control-oriented modeling approach offers an accurate description of the system in a broad operation region. However, it is observed that the potential energy difference cannot be constant, depends on the upstream and downstream levels of each channel. Hence, as a *third contribution*, in Chapter 3, a nonlinear control-oriented modeling approach designed from approximated M&PEB has been proposed and validated. This modeling approach does not contemplate delays, instead, contemplates the division of the channel into two storage units connected by a flow transition, where the areas of the storage units can be adjusted by experimental data, subject to the addition of the model areas must be equal to the total area of the real system. This requirement ensures that the global mass balance of the model must be equal to the global mass balance of the real system. Moreover, in this modeling strategy, the flow transition is obtained by using an approximated potential energy balance and simplifications over a hydraulic description of the head loss due to friction, obtaining a description of the flow transition that can be adjusted by experimental data and is a function of the channels levels. The validation results show the accuracy of the proposed control-oriented modeling strategy. Some qualities of the proposed strategy designed from approximated M&PEB are:

- An exact overall mass balance for each channel can be guaranteed.
- The dynamic behavior of the real system can be adjusted by adjusting the upstream and downstream areas with real data.

- The upstream and downstream channel levels can be used in the nonlinear hydraulic description of inflows and outflows of interacting channels.
- The flow transition obeys a potential energy balance and can be adjusted with real data.
- The modeling strategy offers an accurate channel description in a broad operation region.

It is important to realize that in Chapter 4, it is shown that this modeling strategy is not useful to describe systems with small or inexistent head loss due to friction (e.g., a short and wide channel). And this is logical because the dynamic behavior of these type of systems is close to the dynamic behavior of a water storage unit.

Based on the proposed modeling strategy, in Chapter 4 the problem of DIMEUF in OCIS has been addressed, as a result, the *fourth contribution* of this thesis is the design of two strategies for detection isolation and magnitude estimation of unknown flows, which take into account the effects of flow conduction. These strategies have been designed exploiting the advantages that the MHE approach shows in dealing with constrained nonlinear systems. However, in the design of the strategies, the problem of obtaining suboptimal estimations of the unknown flow has been shown, and this problem has been overcome by using detection and isolation mechanisms that enhance the MHE strategy. The estimation approaches have been designed from deterministic and stochastic points of view, showing that including information about noise and expected level values increase the estimation performance. The estimation strategies have been validated by using two well-known benchmarks, which have been implemented in SWMM, showing that although the strategies have been designed by using a simplified modeling approach, they are capable of accurately estimate the channel behavior and unknown flows in broad operation regions.

In this thesis, the problem of control in OCIS has been addressed first, by the revision, analysis, and implementation of the conventional control strategies that are reported in the literature. At this point, it is identified that the most common control objective is to maintain a constant depth at the upstream or downstream end of the OCIS. Moreover, it is identified that most of the control-oriented models and conventional control strategies are useful for noninteracting OCIS. Therefore, a nonlinear control strategy designed from the control-oriented modeling strategy that assumes delays and CPED along the channels has been proposed. At this point, a nonlinear model-based control strategy for interacting OCIS, which ensures the system stability despite nonlinearities, internal delays, and channel interactions has been obtained. In this case, the nonlinear model-based control strategy has as control objective to maintain a constant depth at the upstream end of the channels, reaching the desired results. However, it is found that a constant depth at the upstream or downstream end of the channels maintains constant losses due to leaks and seepage.

Therefore, as a *fifth contribution*, an NLMPC strategy with the objective of supplying an appropriate amount of water to the users minimizing losses due to seepage and leaks has been proposed. This control strategy takes advantage of information about profiles

of user's requirements, and the control-oriented modeling approach designed from approximated M&PEB, which has shown accurate performance in a broad operation region. The main idea is to maintain the upstream and downstream levels as low as possible. However, in order to accomplish the users' demands, the respective level must reach an operation condition. As a result, the evolution of the control-oriented model is used in the development of an online optimization problem over a finite time horizon, where the objective is supplying an appropriate amount of water to the users minimizing losses due to seepage and leaks, at the same time that hydraulic constraints are accomplished. In this control strategy, the operative conditions that ensure the system stability are deduced, and the simulation results have shown that these operative conditions ensure a desired performance of the controlled OCIS. Moreover, the simulation results show that in OCIS this control strategy could minimize 50% of losses due to leaks and seepage.

6.2 Answering the Research Questions

The conclusions are synthesized by answering the key research questions presented in Chapter 1 as follows:

(Q1) *What is the current context of modeling, estimation, and control in OCIS, and what are the main research gaps in this context that contribute to the OCIS efficiency increase?*

In Chapter 2 it has been shown that despite the abundance of research around the control in OCIS, and the environmental relevance of these systems, most of the OCIS operate manually. Therefore, modeling, estimation, and control in OCIS is an open problem where all the contributions are relevant. Moreover, as it has been shown in Chapter 2, in modeling, the reported simplified and approximated models present limitations in the dynamic descriptions of interacting channels and the descriptions of the potential energy difference along the channels. In this thesis, these limitations have been overcome by the proposing of two control-oriented modeling approaches described in Chapter 3. The opportune DIMEUF in OCIS appears as a valuable tool to increase the efficiency of the OCIS. In estimation, most of the strategies for DIMEUF have been designed from control-oriented models that do not contemplate potential energy balances along the channels, and this can induce drift in the results. In Chapter 3 a DIMEUF strategy designed from a control-oriented that contemplates mas and energy balances along the channels has been proposed. In control, in most of the reported works, the main objective is to maintain a constant depth at the downstream or upstream end of the channels. This objective ensures constant leaks and seepage. Therefore, in Chapter 5 an NLMPC approach with the objective of supplying an appropriate amount of water to the users minimizing losses due to seepage and leaks has been proposed.

(Q2) *What are the decision features to select or design a suitable control-oriented modeling strategy for OCIS?*

Chapter 2 evidences that due to the SVE complexity, the direct use of these equations for control systems design is impractical. Therefore, in the literature, there are reported the use of simplified and approximated control-oriented modeling approaches, but as it is shown in Chapter 2, the need for new control-oriented modeling approaches has been identified, and the requirements for these models are described next:

- The control-oriented model must be useful to describe most of the dynamic behavior of the real system, even adverse conditions, disturbances, noise, parameter variations, etc.
- The model must let the development of tests of the designed controllers in presence of external disturbances and realistic scenarios.
- The control-oriented model must be able to describe the nonlinear dynamic behavior of interacting open-channels with gates in submerged-flow, where the flow depends on the upstream and downstream depths of the regulation structures.
- The modeling strategy must include information about potential energy balances along the channels.

In this direction, in Chapter 3 two control-oriented modeling approaches have been proposed and validated, showing that by using approximated M&PEB accurate descriptions of the OCIS can be reached. Moreover, in Chapters 4, and 5 it has been shown that this control-oriented modeling strategy is useful in the description and controlled system validations in presence of adverse conditions, disturbances, noise, and parameter variations. Also, in these chapters, it has been shown that in this modeling strategy, the nonlinear descriptions of different kinds of regulation structures can be included and that the dynamic and static effects of the potential energy balances along the channels can be included in this control-oriented modeling strategy.

(Q3) *How to design implementable approaches for recursive DIMEUF such as leaks and seepage in OCIS?*

In instrumented OCIS the most commonly measured variables are the upstream and downstream levels at the end of the channels. Therefore, the design of strategies for DIMEUF must be developed from these measured variables and models developed from previous system information. Therefore, the development of strategies for DIMEUF must deal with measurement uncertainties (i.e, measurement noise), and model uncertainties (discrepancies between real system and model). In DIMEUF, the measurement uncertainties treatment is a key aspect, note that in OCIS high inflow or outflow variations produce small level variations of the system, and the unknown flows can easily be masked into measurement noise. Note that, in estimation, the noise treatment can be addressed in the instrumentation process and/or by including noise information into the estimation strategy. In Chapter 4, the noise

treatment is developed first by the inclusion of filtering strategies, taking advantage of the slow dynamics that characterize the OCIS, and second by designing an stochastic DIMEUF strategy that contemplates the effects of measurement noise. On the other hand, the model uncertainties can be minimized by using an accurate model of the real system. At this point, the use of the SVE appears as the first option, but the complexity of the SVE leads to complex estimation strategies with hard online implementation. Conversely, the reported simplified and approximated models do not include information about potential energy along the channels and most of them do not include the nonlinear descriptions that characterize the hydraulic behavior of the OCIS. Therefore, in order to minimize the model uncertainties, in Chapter 4 the problem of design a DIMEUF strategy from the proposed modeling approach that assumes approximated M&PEB and has shown an accurate description of the OCIS in a broad operation region has been addressed. The results showed that the proposed DIMEUF strategy can accurately estimate the channel behavior and unknown flows in a long operation region, overcoming measurement and model uncertainties.

(Q4) *How can the optimization-based control techniques contribute to improving the OCIS efficiency?*

As it has been presented in Chapter 2 in OCIS the most common control strategy is to maintain a constant depth at the upstream or downstream end of the channel, and by action in the outlet hydraulic structure, the flow is regulated at each user. Therefore, in most of the control strategies, the key performance indicators account for the error between the desired and controlled systems level, and most of the reported literature offers control alternatives to improve this kind of performance indicator. However, in a real system, the upstream or downstream level can present considerable deviations with respect to the desired level, and these deviations must be compensated with the hydraulic outlet structure. Therefore, in real OCIS a rigorous level tracking could be not the main objective. Instead, the levels of the OCIS must be into operation regions that avoid overflows and ensure the water user's availability. This operation principle for OCIS can be seen as a starting point in the design of optimization-based control techniques oriented to improve the OCIS efficiency. From this point, In Chapter 5 the development of an optimization-based control approach has been proposed, where an accurate model of the system and knowledge about future user's demands is used in the formulation of a finite-horizon optimization problem. Then the optimization problem is solved to find optimal or sub-optimal control actions that accomplish the user's demands at the same time that leaks and seepage are minimized, and physical limits, as well as hydraulic conditions, are included as constraints. The simulation results show that with this control strategy losses due to leaks and seepage can be halved at the same time that the user's demands are accomplished. In conclusion, in OCIS the use of optimization-based control techniques appears as a promising control alternative to reduce losses as long as the traditional control objective of maintaining a constant upstream or downstream level evolves to efficiency maximization objectives.

6.3 Directions for Future Research

Chapter 1 identifies some problems that in this dissertation have been addressed by developing new control-oriented modeling approaches, new strategies for DIMEUF, and a new high-efficiency control approach. However, other identified research gaps remain opens and are summarized next:

- Control of OCIS integrated with crop dynamics.
- Water robbery detection in OCIS.
- Inclusion of human agents in the sensing and actuation of optimization-based control strategies.
- Inclusion of climate forecast into optimization-based control strategies.
- Integration of water quality objectives into the control problem.
- Integration of sustainable objectives such as groundwater protection.

On the other hand, the developed research also points out new open problems for future directions, which are outline below:

- The control-oriented modeling approach developed from approximated M&PEB assumes the division of each channel into two storage unities, where the storage unities areas are obtained by using data fitting. The accuracy and usefulness of this control-oriented modeling strategy could be improved by assuming more than two storage units for each channel description, but the challenge of identify more than two areas from the upstream and downstream end level measurements appears as an open problem.
- The proposed estimation strategies are useful for DIMEUF at the upstream and downstream ends of the channels. However, in long channels, a precise DIMEUF at an specific point along the channels could be helpful to take opportune actions regarding loss mitigation. Therefore, the design of new DIMEUF strategies for precise localization of unknown flows appears as an important future direction.
- The NLMPC strategy proposed in Chapter 5 is a centralized control strategy that had reached desired results. However, as it has been shown in Chapter 2, decentralized or distributed control approaches offer the possibility of keeping the system controlled (with a possible performance degradation) even if part of the information is lost. In addition, non-centralized architectures allow partial implementations in channels according to budget and relevance. Therefore, the development of distributed and decentralized control strategies focused on increase system efficiency appears as the next step in matters of efficient control approaches.

- Chapter 5 addresses stability conditions for OCIS under an efficient control approach, where the stability is deduced from highly conservative controllability and reachability conditions. However, the simulation results have shown that the controlled system can be stable even under unreachable demands. This phenomenon can be used in the improvement of the implemented control strategies and deserves to be analyzed for future applications.

- In this dissertation, the simulation results of the proposed modeling, estimation, and control strategies, have been obtained by using models validated against specialized software. However, the real implementation could present challenges not contemplated. Therefore, the real implementation of the estimation and control strategies is identified as an important future direction.

- Most of the approximated and simplified modeling strategies proposed by different authors are parametrized from the hydraulic characteristics of the OCIS, and these modeling strategies parametrized from experimental data might improve its performance. Therefore, the use of experimental data into a rigorous analysis intending to identify the best simplified or approximated modeling structure for OCIS appears as an interesting future work.

Bibliography

Aguilar, J.V., Langarita, P., Linares, L., Rodellar, J., 2009. Automatic control of flows and levels in an irrigation canal. IEEE Transactions on Industry Applications 45, 2198–2208.

Akhenak, A., Duviella, E., Bako, L., Lecoeuche, S., 2013. Online fault diagnosis using recursive subspace identification: Application to a dam-gallery open channel system. Control Engineering Practice 21, 797–806.

Alessandri, A., Baglietto, M., Battistelli, G., 2006. Design of state estimators for uncertain linear systems using quadratic boundedness. Automatica 42, 497–502.

Alessandri, A., Baglietto, M., Battistelli, G., 2008. Moving-horizon state estimation for nonlinear discrete-time systems: New stability results and approximation schemes. Automatica 44, 1753–1765.

Amin, S., Litrico, X., Sastry, S., Bayen, A., 2013a. Cyber security of water SCADA systems-part I: Analysis and experimentation of stealthy deception attacks. IEEE Transactions on Control Systems Technology 21, 1963–1970.

Amin, S., Litrico, X., Sastry, S., Bayen, A., 2013b. Cyber security of water SCADA systems-part II: Attack detection using enhanced hydrodynamic models. IEEE Transactions on Control Systems Technology 21, 1679–1693.

Andersson, J.A.E., Gillis, J., Horn, G., Rawlings, J.B., Diehl, M., 2019. CasADi: a software framework for nonlinear optimization and optimal control. Mathematical Programming Computation 11, 1–36.

Arauz, T., Maestre, J.M., Tian, X., Guan, G., 2020. Design of PI controllers for irrigation canals based on linear matrix inequalities. Water (Switzerland) 12.

Aydin, B., van Overloop, P., Rutten, M., Tian, X., 2017. Offset-free model predictive control of an open water channel based on moving horizon estimation. Journal of Irrigation and Drainage Engineering 143.

Aydın, B., Hagedooren, H., Rutten, M., Delsman, J., Oude Essink, G., van de Giesen, N., Abraham, E., 2019. A greedy algorithm for optimal sensor placement to estimate salinity in polder networks. Water 11, 1101.

Baillieul, J., Samad, T., 2015. Encyclopedia of systems and control. Springer International Publishing, London.

Balogun, O., Hubbard, M., Devries, J., 1988. Automatic control of canal flow using linear quadratic regulator theory. Journal of Hydraulic Engineering 114.

Bedjaoui, N., Litrico, X., Koenig, D., Malaterre, P.O., 2006. H_∞ observer for time-delay systems application to FDI for irrigation canals, in: Proceedings of the IEEE Conference on Decision and Control, pp. 532–537.

Bedjaoui, N., Litrico, X., Koenig, D., Ribot-Bruno, J., Malaterre, P.O., 2008. Static and dynamic data reconciliation for an irrigation canal. Journal of Irrigation and Drainage Engineering 134, 778–787.

Bedjaoui, N., Weyer, E., 2011. Algorithms for leak detection, estimation, isolation and localization in open water channels. Control Engineering Practice 19, 564–573.

Bedjaoui, N., Weyer, E., Bastin, G., 2009. Methods for the localization of a leak in open water channels. Networks and Heterogeneous Media 4, 189–210.

Begovich, O., Ruiz, V., Besançon, G., Aldana, C., Georges, D., 2007. Predictive control with constraints of a multi-pool irrigation canal prototype. Latin American Applied Research 37, 177–185.

Besançon, G., Dulhoste, J.F., Georges, D., 2008. Nonlinear observer-based feedback for open-channel level control. Journal of Hydraulic Engineering 134, 1267–1274.

Bhatia, R., 2015. Positive Definite Matrices. Princeton University Press.

Blesa, J., Puig, V., Bolea, Y., 2010. Fault detection using interval LPV models in an open-flow canal. Control Engineering Practice 18, 460–470.

Bolea, Y., Puig, V., Blesa, J., 2014a. Gain-scheduled smith predictor PID-based LPV controller for open-flow canal control. IEEE Transactions on Control Systems Technology 22, 468–477.

Bolea, Y., Puig, V., Blesa, J., 2014b. Linear parameter varying modeling and identification for real-time control of open-flow irrigation canals. Environmental Modelling and Software 53, 87–97.

Bolea, Y., Puig, V., Grau, A., 2014c. Discussion on Muskingum versus integrator-delay models for control objectives. Journal of Applied Mathematics 2014.

Bonet, E., Gómez, M., Yubero, M., Fernández-Francos, J., 2017. GoRoSoBo: An overall control diagram to improve the efficiency of water transport systems in real time. Journal of Hydroinformatics 19, 364–384.

Breckpot, M., Agudelo, O., Moor, B., De Moor, B., 2013. Flood control with model predictive control for river systems with water reservoirs. Journal of Irrigation and Drainage Engineering 139, 532–541.

Burt, C., Mills, R., Khalsa, R., Ruiz C, V., 1998. Improved proportional-integral (PI) logic for canal automation. Journal of Irrigation and Drainage Engineering 124, 53–57.

Cantoni, M., Weyer, E., Li, Y., Ooi, S., Mareels, I., Ryan, M., 2007. Control of large-scale irrigation networks. Proceedings of the IEEE 95, 75–91.

Canute, V., 1971. Water thievery in a rice irrigation system in Taiwan. Annals of the Association of American Geographers 61, 156–179.

Cembrano, G., Quevedo, J., Puig, V., Pérez, R., Figueras, J., Verdejo, J., Escaler, I., Ramón, G., Barnet, G., Rodríguez, P., Casas, M., 2011. PLIO: A generic tool for real-time operational predictive optimal control of water networks. Water Science and Technology 64, 448–459.

Cen, L., Wu, Z., Chen, X., Zou, Y., Zhang, S., 2017. On modeling and constrained model predictive control of open irrigation canals. Journal of Control Science and Engineering 2017.

Cescon, M., Weyer, E., 2017. Modeling and identification of irrigation channel dynamics affected by wind, in: Proceedings of the 20th IFAC World Congress, Elsevier B.V., Department of Electrical and Electronic Engineering, The University of Melbourne, Parkville, VIC 3010, Australia. pp. 5386–5391.

Chaudhry, M., 2008. Open-channel flow. Second ed., Springer Science+Business Media, Columbia.

Choi, Y., Yoo, S., 2016. Minimal-approximation-based decentralized backstepping control of interconnected time-delay systems. IEEE Transactions on Cybernetics 46, 3401–3413.

Choy, S., Weyer, E., 2006. Reconfiguration schemes to mitigate faults in automated irrigation channels: Experimental results. Control Engineering Practice 16, 1184–1194.

Clemmens, A., ASCE, M., Tian, X., van Overloop, P.J., Litrico, X., 2017. Integrator delay zero model for design of upstream water-level controllers. Journal of Irrigation and Drainage Engineering 143.

Clemmens, A., Kacerek, T., Grawitz, B., Schuurmans, W., 1998. Test cases for canal control algorithms. Journal of Irrigation and Drainage Engineering 124, 23–30.

Conde, G., Quijano, N., Ocampo-Martinez, C., 2020. Control-oriented modeling approach for open channel irrigation systems, in: Proceedings of the IFAC 21s World Congress, Berlin, Germany. pp. 16630–16635.

Conde, G., Quijano, N., Ocampo-Martinez, C., 2021a. An unknown input moving horizon estimator for open channel irrigation systems, in: Proceedings of the European Control Conference (To appear).

Conde, G., Quijano, N., Ocampo-Martinez, C., 2021b. Modeling and control in open-channel irrigation systems: A review. Annual Reviews in Control 51, 153–171.

Corriga, G., Sanna, S., Usai, G., 1980. Frequency response and dynamic behaviour of canal networks with self-levelling gates. Applied Mathematical Modelling 4, 125–129.

Dalmas, V., Robert, G., Besançon, G., Georges, D., 2017. Simplified non-uniform models for various flow configurations in open channels. IFAC-PapersOnLine 50, 12320–12325.

Darnault, C.J.G., 2008. Overexploitation and contamination of shared groundwater resources: management, (Bio)technological, and political approaches to avoid conflicts. NATO Science for Peace and Security Series C: Environmental Security, Springer Netherlands.

Darouach, M., Zasadzinski, M., 1997. Unbiased minimum variance estimation for systems with unknown exogenous inputs. Automatica 33, 717–719.

Darrigol, O., 2006. Worlds of flow: A history of hydrodynamics from the Bernoullis to Prandtl. volume 59. Oxford University Press.

Diamantis, M., Papageorgiou, M., Kosmatopoulos, E., Chamilothoris, G., 2011. Identification and adaptive control for open channel water flow systems. Computer-Aided Civil and Infrastructure Engineering 26, 464–480.

Ding, Y., Wang, L., Li, Y., Li, D., 2018. Model predictive control and its application in agriculture: A review. Computers and Electronics in Agriculture 151, 104–117.

Domingues, J., Valério, D., Sá Da Costa, J., 2011. Rule-based fractional control of an irrigation canal. Journal of Computational and Nonlinear Dynamics 6.

Dos Santos, V., Prieur, C., 2008. Boundary control of open channels with numerical and experimental validations. IEEE Transactions on Control Systems Technology 16, 1252–1264.

Dulhoste, J.F., Georges, D., Besançon, G., 2004. Nonlinear control of open-channel water flow based on collocation control model. Journal of Hydraulic Engineering 130, 254–266.

Durdu, O., 2004. Regulation of irrigation canals using a two-stage linear quadratic reliable control. Turkish Journal of Agriculture and Forestry 28, 111–120.

Durdu, O., 2006. Control of transient flow in irrigation canals using Lyapunov fuzzy filter-based gaussian regulator. International Journal for Numerical Methods in Fluids 50, 491–509.

Durdu, O., 2010. Fuzzy logic adaptive Kalman filtering in the control of irrigation canals. International Journal for Numerical Methods in Fluids 64, 187–208.

Duviella, E., Rajaoarisoa, L., Blesa, J., Chuquet, K., 2013. Fault Detection and Isolation of inland navigation channel: Application to the Cuinchy-Fontinettes reach, in: Proceedings of the 52nd IEEE Conference on Decision and Control, pp. 4877–4882.

Dysarz, T., 2018. Application of python scripting techniques for control and automation of HEC-RAS simulations. Water (Switzerland) 10.

Eurén, K., Weyer, E., 2005. System identification of open water channels with undershot and overshot gates, in: Proceedings of the 16th Triennial World Congress, Prague, Czech Republic. pp. 0–5.

Farhadi, A., Khodabandehlou, A., 2016. Distributed model predictive control with hierarchical architecture for communication: application in automated irrigation channels. International Journal of Control 89, 1725–1741.

Fele, F., Maestre, J.M., Hashemy, S.M., Mu, D., Camacho, E.F., 2014. Coalitional model predictive control of an irrigation canal. Journal of Process Control 24, 314–325.

Feliu-Batlle, V., Pérez, R., Rodríguez, L., 2007. Fractional robust control of main irrigation canals with variable dynamic parameters. Control Engineering Practice 15, 673–686.

Feliu-Batlle, V., Rivas-Perez, R., Castillo-Garcia, F., 2009a. Fractional order controller robust to time delay variations for water distribution in an irrigation main canal pool. Computers and Electronics in Agriculture 69, 185–197.

Feliu-Batlle, V., Rivas-Perez, R., Castillo-Garcia, F., Sanchez-Rodriguez, L., Linarez-Saez, A., 2011. Robust fractional order controller for irrigation main canal pools with time-varying dynamical parameters. Computers and Electronics in Agriculture 76, 205–217.

Feliu-Batlle, V., Rivas-Perez, R., Sanchez-Rodriguez, L., Ruiz-Torija, M., 2009b. Robust fractional-order PI controller implemented on a laboratory hydraulic canal. Journal of Hydraulic Engineering 135, 271–282.

Feng, X., Wang, K., 2011. Stability analysis on automatic control methods of open canal. Wuhan University Journal of Natural Sciences 16, 325–331.

Ficchì, A., Raso, L., Dorchies, D., Pianosi, F., Malaterre, P.O., van Overloop, P.J., Jay-Allemand, M., 2016. Optimal operation of the multireservoir system in the Seine river basin using deterministic and ensemble forecasts. Journal of Water Resources Planning and Management 142, 5015005.

Figueiredo, J., Botto, M., Rijo, M., 2013. SCADA system with predictive controller applied to irrigation canals. Control Engineering Practice 21, 870–886.

Fovet, O., Litrico, X., Belaud, G., Genthon, O., 2013. Adaptive control of algae detachment in regulated canal networks. Journal of Hydroinformatics 15, 321–334.

Franze, G., Famularo, D., 2018. Robust fault detection for constrained uncertain linear systems: A moving horizon estimation approach, in: Proceedings of the IEEE Conference on Decision and Control, pp. 5574–5579.

Garcia, A., Hubbard, M., De Vries, J., 1992. Open channel transient flow control by discrete time LQR methods. Automatica 28, 255–264.

Gomez, M., Rodellar, J., Mantecon, J., 2002. Predictive control method for decentralized operation of irrigation canals. Applied Mathematical Modelling 26, 1039–1056.

Goudiaby, M., Sene, A., Kreiss, G., 2013. A delayed feedback control for network of open canals. International Journal of Dynamics and Control 1, 316–329.

Grüne, L., Pannek, J., 2011. Nonlinear Model Predictive Control. Springer London, London. p. 355.

Harr, M.E., 1991. Groundwater and Seepage. Dover Civil and Mechanical Engineering Series, Dover.

Hashemy Shahdany, S.M., Firoozfar, A., Maestre, J.M., Mallakpour, I., Taghvaeian, S., Karimi, P., 2018. Operational performance improvements in irrigation canals to overcome groundwater overexploitation. Agricultural Water Management 204, 234–246.

Hashemy Shahdany, S.M., Taghvaeian, S., Maestre, J.M., Firoozfar, A.R., 2019. Developing a centralized automatic control system to increase flexibility of water delivery within predictable and unpredictable irrigation water demands. Computers and Electronics in Agriculture 163.

Hassani, Y., Hashemy Shahdany, S.M., Maestre, J.M., Zahraie, B., Ghorbani, M., Hennebery, S.R., Kulshreshtha, S.N., 2019. An economic-operational framework for optimum agricultural water distribution in irrigation districts without water marketing. Agricultural Water Management 221, 348–361.

Hayami, S., 1951. On the propagation of flood waves. Bulletins - Disaster Prevention Research Institute, Kyoto University , 1–16.

Hernández, J., Merkley, G., 2010a. Canal structure automation rules using an accuracy-based learning classifier system, a genetic algorithm, and a hydraulic simulation model. I: Design. Journal of Irrigation and Drainage Engineering 137, 1–11.

Hernández, J., Merkley, G., 2010b. Canal structure automation rules using an accuracy-based learning classifier system, a genetic algorithm, and a hydraulic simulation model. II: Results. Journal of Irrigation and Drainage Engineering 137, 12–16.

Herrera, J., Ibeas, A., De La Sen, M., 2013. Identification and control of integrative MIMO systems using pattern search algorithms: An application to irrigation channels. Engineering Applications of Artificial Intelligence 26, 334–346.

Horváth, K., Blesa, J., Duviella, E., Rajaoarisoa, L., Puig, V., Chuquet, K., 2014a. Sensor fault diagnosis of inland navigation system using physical model and pattern recognition approach. Proceedings of the 19th IFAC World Congress 47, 5309–5314.

Horváth, K., Galvis, E., Rodellar, J., Valentín, M., 2014b. Experimental comparison of canal models for control purposes using simulation and laboratory experiments. Journal of Hydroinformatics 16, 1390–1408.

Horváth, K., Galvis, E., Valentín, M., Benedé, J., 2015a. Is it better to use gate opening as control variable than discharge to control irrigation canals? Journal of Irrigation and Drainage Engineering 141.

Horváth, K., Galvis, E., Valentín, M., Rodellar, J., Gómez, M., Rodellar, J., 2015b. New offset-free method for model predictive control of open channels. Control Engineering Practice 41, 13–25.

Hua, C., Liu, P., Guan, X., 2009. Backstepping control for nonlinear systems with time delays and applications to chemical reactor systems. IEEE Transactions on Industrial Electronics 56, 3723–3732.

Janon, A., Nodet, M., Prieur, C., Prieur, C., 2016. Global sensitivity analysis for the boundary control of an open channel. Mathematics of Control, Signals, and Systems 28, 1–27.

Kalman, R.E., 1960. On the general theory of control systems. IFAC Proceedings Volumes 1, 491–502.

Ke, Z., Guanghua, G., Xin, T., María, M.J., Zhonghao, M., 2020. Evaluating optimization objectives in linear quadratic control applied to open canal automation. Journal of Water Resources Planning and Management 146, 1–12.

Ke, Z., Guanghua, G., Zhonghao, M., Wenjun, L., Changcheng, X., Su, H., 2018. Linear quadratic optimal controller design for constant downstream water-level PI feedback control of open-canal systems, in: Proceedings of the International Symposium on Water System Operations, EDP Sciences, State Key Laboratory of Water Resources and Hydropower Engineering Science, Wuhan University, Wuhan, 430072, China.

Kirk, D., 2004. Optimal control theory: an Introduction. 2nd ed., Dover Publications, New York.

Koenig, D., Bedjaoui, N., Litrico, X., 2005. Unknown input observers design for time-delay systems application to an open-channel, in: Proceedings of the 44th IEEE Conference on Decision and Control, pp. 5794–5799.

Lacasta, A., Morales-Hernández, M., Brufau, P., García-Navarro, P., 2018. Application of an adjoint-based optimization procedure for the optimal control of internal boundary conditions in the shallow water equations. Journal of Hydraulic Research 56, 111–123.

Lamnabhi-Lagarrigue, F., Annaswamy, A., Engell, S., Isaksson, A., Khargonekar, P., Murray, R.M., Nijmeijer, H., Samad, T., Tilbury, D., Van den Hof, P., 2017. Systems & control for the future of humanity, research agenda: Current and future roles, impact and grand challenges. Annual Reviews in Control 43, 1–64.

Le-Duy-Lay, N., Prodan, I., Lefevre, L., Genon-Cattlot, D., 2017. Distributed model predictive control of irrigation systems using cooperative controllers, in: IFAC PapersOnLine, pp. 6748–6753.

Lemos, J., Machado, F., Nogueira, N., Rato, L., Rijo, M., 2009. Adaptive and non-adaptive model predictive control of an irrigation channel. Networks and Heterogeneous Media 4, 303–324.

Lemos, J., Sampaio, I., 2015. Distributed LQG control for multiobjective control of water canals, in: Ocampo-Martinez, C., Negenborn, R.R. (Eds.), Transport of water versus transport over water. Springer International Publishing, Cham. chapter Distribute, pp. 59–73.

Leon, A.S., Goodell, C., 2016. Controlling HEC-RAS using MATLAB. Environmental Modelling and Software 84, 339–348.

Lewis, A., 2017. Storm water management model reference manual volume II hydraulics. U.S. Environmental Protection Agency, Cincinnati.

Li, Y., Cantoni, M., Weyer, E., 2005. On water-level error propagation in controlled irrigation channels. Proceedings of the 44th IEEE Conference on Decision and Control, and the European Control Conference, CDC-ECC '05 2005, 2101–2106.

Liao, W., Guan, G., Tian, X., 2019. Exploring explicit delay time for volume compensation in feedforward control of canal systems. Water 11, 1–12.

Litrico, X., Fromion, V., 2003. Advanced control politics and optimal performance for an irrigation canal, in: Proceedings of the European Control Conference 2003, pp. 820–825.

Litrico, X., Fromion, V., 2004a. Analytical approximation of open-channel flow for controller design. Applied Mathematical Modelling 28, 677–695.

Litrico, X., Fromion, V., 2004b. Frequency modeling of open-channel flow. Journal of Hydraulic Engineering 130, 806–815.

Litrico, X., Fromion, V., 2004c. Simplified modeling of irrigation canals for controller design. Journal of Irrigation and Drainage Engineering Volume 130, Pages 373–383.

Litrico, X., Fromion, V., 2006a. Hinf control of an irrigation canal pool with a mixed control politics. IEEE Transactions on Control Systems Technology 14, 99–111.

Litrico, X., Fromion, V., 2006b. Tuning of robust distant downstream PI controllers for an irrigation canal pool. I: Theory. Journal of Irrigation and Drainage Engineering 132, 359–368.

Litrico, X., Fromion, V., 2009. Modeling and control of hydrosystems. Springer, London.

Litrico, X., Fromion, V., Baume, J.P., Rijo, M., 2003. Modelling and PI control of an irrigation canal, in: Proceedings of the European Control Conference 2003, pp. 850–855.

Litrico, X., Georges, D., 1999. Robust continuous time and discrete time flow control of a dam river system. (II) Controller design. Applied Mathematical Modelling 23, 829–846.

Litrico, X., Malaterre, P.O., Baume, J.P., Vion, P.I., Ribot-Bruno, J., 2007. Automatic tuning of PI controllers for an irrigation canal pool. Journal of Irrigation and Drainage Engineering 133, 27–37.

Liu, F., Feyen, J., Berlamont, J., 1995. Downstream control of multireach canal systems. Journal of Irrigation and Drainage Engineering 121, 179–190.

Liu, F., Feyen, J., Malaterre, P.O., Baume, J.P., Kosuth, P., 1998. Development and evaluation of canal automation algorithm CLIS. Journal of Irrigation and Drainage Engineering 124, 40–46.

Ljung, L., 2010. Perspectives on system identification. Annual Reviews in Control 34, 1–12.

Loch, A., Adamson, D., Dumbrell, N.P., 2020. The fifth stage in water management: policy lessons for water governance. Water Resources Research 56, 1–17.

Lozano, D., Arranja, C., Rijo, M., Mateos, L., 2010. Simulation of automatic control of an irrigation canal. Agricultural Water Management 97, 91–100.

Maciejowski, J., 2002. Predictive control: With constraints. Pearson Education, California.

Maestre, J.M., van Overloop, P.J., Hashemy, M., Sadowska, A., Camacho, E.F., 2014. Human in the loop model predictive control: an irrigation canal case study, in: Proceedings of the 53rd IEEE Conference on Decision and Control, pp. 4881–4886.

Maestre, J.M., Raso, L., van Overloop, P.J., De Schutter, B., 2012. Distributed tree-based model predictive control on a drainage water system. Journal of Hydroinformatics 15, 335–347.

Malaterre, P.O., 1995. Regulation of irrigation canals - Characterisation and classification. Irrigation and Drainage Systems 9, 297–327.

Malaterre, P.O., 1998. PILOTE: Linear quadratic optimal controller for irrigation canals. Journal of Irrigation and Drainage Engineering 124, 187–194.

Malaterre, P.O., 2008. Control of irrigation canals: Why and how?, in: Proceedings of the International Workshop on Numerical Modelling of Hydrodynamics for Water Resources, pp. 271–292.

Malaterre, P.O., Baume, J.P., 1998. Modeling and regulation of irrigation canals: existing applications and ongoing researches, in: Anon (Ed.), Proceedings of the 1998 IEEE International Conference on Systems, Man, and Cybernetics, IEEE, Cemagref, Montpellier, France. pp. 3850–3855.

Malaterre, P.O., Khammash, M., 2003. L1 controller design for a high-order 5-pool irrigation canal system. Journal of Dynamic Systems, Measurement and Control 125, 639–645.

Malaterre, P.O., Rogers, D., Schuurmans, J., 1998. Classification of canal control algorithms. Journal of Irrigation and Drainage Engineering 124, 3–10.

Mareels, I., Weyer, E., Ooi, S., Cantoni, M., Li, Y., Nair, G., 2005. Systems engineering for irrigation systems: Successes and challenges. Annual Reviews in Control 29, 191–204.

MATLAB, 2019. version (R2019). The MathWorks Inc.

Mazenc, F., Bliman, P.A., 2006. Backstepping design for time-delay nonlinear systems. IEEE Transactions on Automatic Control 51, 149–154.

McCarthy, G., 1939. The unit hydrograph and flood routing. U.S. Engineer Office, Providence, R.I.

Mohan Reddy, J., 1995. Kalman filtering in the control of irrigation canals. Applied Mathematical Modelling 19, 201–209.

Mohan Reddy, J., Dia, A., Oussou, A., 1992. Design of control algorithm for operation of irrigation canals. Journal of Irrigation and Drainage Engineering 118, 852–867.

Mohan Reddy, J., Jacquot, R., 1999. Stochastic optimal and suboptimal control of irrigation canals. Journal of Water Resources Planning and Management 125, 369–378.

Montero, R.A., Schwanenberg, D., Hatz, M., Brinkmann, M., 2013. Simplified hydraulic modelling in model predictive control of flood mitigation measures along rivers. Journal of Applied Water Engineering and Research 1, 17–27.

Munir, S., Schultz, B., Suryadi, F., Bharati, L., 2012. Evaluation of hydraulic performance of downstream-controlled Maira-PHLC irrigation canals under crop-based irrigation operations. Irrigation and Drainage 61, 20–30.

Nasir, H., Cantoni, M., Weyer, E., 2018. An efficient implementation of stochastic MPC for open channel water-level planning, in: Proceedings of the 2017 IEEE 56th Annual Conference on Decision and Control, pp. 511–516.

Nasir, H.A., Cantoni, M., Li, Y., Weyer, E., 2021. Stochastic model predictive control based reference planning for automated open-water channels. IEEE Transactions on Control Systems Technology 29, 607–619.

Nasir, H.A., Muhammad, A., 2011. Control of very-large scale irrigation networks: A CPS approach in a developing-world setting, in: in IFAC Proceedings Volumes, pp. 10739–10745.

Negenborn, R., van Overloop, P., Keviczky, T., De Schutter, B., 2009. Distributed model predictive control of irrigation canals. Networks and Heterogeneous Media 4, 359–380.

Niswonger, R.G., Morway, E.D., Triana, E., Huntington, J.L., 2017. Managed aquifer recharge through off-season irrigation in agricultural regions. Water Resources Research 53, 6970–6992.

Ocampo-Martinez, C., 2010. Model Predictive Control of Wastewater Systems. Springer-Verlag London, New York.

OECD, 2018. Managing water sustainably is key to the future of food and agriculture.

Ooi, S., Weyer, E., 2005. Detection of sluggish control loops in irrigation channels, in: Proceedings of the 16th IFAC World Congress, pp. 19–24.

Ooi, S., Weyer, E., 2008a. Control design for an irrigation channel from physical data. Control Engineering Practice 16, 1132–1150.

Ooi, S., Weyer, E., 2008b. Detection of oscillatory control loops in irrigation channels. IFAC Proceedings Volumes (IFAC-PapersOnline) 17, 5500–5505.

Ooi, S., Weyer, E., 2011. Detection of oscillations in control loops in irrigation channels. Control Engineering Practice 19, 311–319.

Ouarit, H., Lefevre, L., Georges, D., Begovich, O., 2003. A way to deal with non-linear boundary conditions in open-channel optimal control problems, in: Proceedings of the 42nd IEEE International Conference on Decision and Control (IEEE Cat. No.03CH37475), pp. 336–341 Vol.1.

van Overloop, P., Horvath, K., Ekin, B., 2014. Model predictive control based on an integrator resonance model applied to an open water channel. Control Engineering Practice 27, 54–60.

van Overloop, P.J., Clemmens, A., Strand, R., Wagemaker, R., Bautista, E., 2010a. Real-time implementation of model predictive control on Maricopa-Stanfield irrigation and drainage District's WM canal. Journal of Irrigation and Drainage Engineering 136, 747–756.

van Overloop, P.J., Clemmens, A.J., Strand, R.J., Wagemaker, R.M.J., Bautista, E., 2010b. Real-time implementation of model predictive control on maricopa-stanfield irrigation and drainage district's WM canal. Journal of Irrigation and Drainage Engineering 136, 747–756.

van Overloop, P.J., Maestre, J.M., Sadowska, A.D., Camacho, E.F., Schutter, B.D., 2015. Human-in-the-loop model predictive control of an irrigation canal [applications of control]. IEEE Control Systems Magazine 35, 19–29.

van Overloop, P.J., Miltenburg, I.., Bombois, X., Clemmens, A., Strand, R., van de Giesen, N., Hut, R., 2010c. Identification of resonance waves in open water channels. Control Engineering Practice 18, 863–872.

van Overloop, P.J., Miltenburg, I., Clemmens, A., Strand, R., 2008a. Identification of pool characteristics of irrigation canals, in: Proceedings of the World Environmental and Water Resources Congress 2008.

van Overloop, P.J., Schuurmans, J., Brouwer, R., Burt, C., 2005. Multiple-model optimization of proportional integral controllers on canals. Journal of Irrigation and Drainage Engineering 131, 190–196.

van Overloop, P.J., Weijs, S., Dijkstra, S., 2008b. Multiple model predictive control on a drainage canal system. Control Engineering Practice 16, 531–540.

Pages, J., Compas, J., Sau, J., 1998. MIMO predictive control with constraints by using an embedded knowledge based model, in: Anon (Ed.), Proceedings of the IEEE International Conference on Systems, Man, and Cybernetics, IEEE, Lyon, France. pp. 3902–3907.

Papageorgiou, M., 1983. Automatic control strategies for combined sewer systems. Journal of Environmental Engineering (United States) 109, 1385–1402.

Papageorgiou, M., Messmer, A., 1985. Continuous-time and discrete-time design of water flow and water level regulators. Automatica 21, 649–661.

Pham, T.V., Georges, D., Besançon, G., 2010. Infinite-dimensional receding horizon optimal control for an open-channel system. IFAC Proceedings Volumes (IFAC-PapersOnline) , 391–396doi:10.3182/20100901-3-IT-2016.00216.

Pocher, O.L., Duviella, E., Bako, L., Chuquet, K., 2012. Sensor fault detection of a real undershot/overshot gate based on physical and nonlinear black-box models. Proceedings of the I8th IFAC Symposium on Fault Detection, Supervision and Safety of Technical Processes 45, 1083–1088.

Puig, V., Ocampo-Martinez, C., Negenborn, R., 2015. Transport of water versus transport over water: Model predictive control for combined water supply and navigability / sustainability in river systems, in: Ocampo-Martinez, C., Negenborn, R.R. (Eds.), Transport of Water versus Transport over Water. Springer International Publishing, pp. 13–32.

Qiao, Q.S., Yang, K.L., 2010. Modeling unsteady open-channel flow for controller design. Journal of Irrigation and Drainage Engineering 136, 383–391.

Rabbani, T., Di Meglio, F., Litrico, X., Bayen, A., 2010. Feed-forward control of open channel flow using differential flatness. IEEE Transactions on Control Systems Technology 18, 213–221.

Rabbani, T., Munier, S., Dorchies, D., Malaterre, P.O., Bayen, A., Litrico, X., 2009a. Flatness-based control of open-channel Flow in an irrigation canal using SCADA. IEEE Control Systems 29, 22–30.

Rabbani, T., Munier, S., Dorchies, D., Malaterre, P.O., Bayen, A., Litrico, X., 2009b. Flatness-Based Control of Open-Channel flow in an Irrigation Canal Using SCADA. IEEE Control Systems Magazine 29, 22–30.

Raso, L., van de Giesen, N., Stive, P., Schwanenberg, D., van Overloop, P.J., 2013. Tree structure generation from ensemble forecasts for real time control. Hydrological Processes 27, 75–82.

Raso, L., Schwanenberg, D., van de Giesen, N.C., van Overloop, P.J., 2014. Short-term optimal operation of water systems using ensemble forecasts. Advances in Water Resources 71, 200–208.

Rato, L., Salgueiro, P., Lemos, J., Rijo, M., 2007. Adaptive predictive controller applied to an open water canal, in: Proceedings of the Fourth International Conference on Informatics in Control, Automation and Robotics, Signal Processing, Systems Modeling and Control, CITI-UE, Universidade de Évora, R. Romão Ramalho 59, 7000-671 Évora, Portugal. pp. 357–360.

Rawlings, J.B., Mayne, D.Q., Diehl, M., 2017. Model Predictive Control: Theory, Computation, and Design. Nob Hill Publishing.

Reddy, M., 1990a. Evaluation of optimal constant-volume control for irrigation canals. Applied Mathematical Modelling 14, 450–458.

Reddy, M., 1990b. Local optimal control of irrigation canals. Journal of Irrigation and Drainage Engineering 116, 616–631.

Reddy, M., 1996. Design of global control algorithm for irrigation canals. Journal of Hydraulic Engineering 122, 503–511.

Rijo, M., Arranja, C., 2010. Supervision and water depth automatic control of an irrigation canal. Journal of Irrigation and Drainage Engineering 136, 3–10.

Rivas Perez, R., Feliu Batlle, V., Sanchez Rodriguez, L., 2007. Robust system identification of an irrigation main canal. Advances in Water Resources 30, 1785–1796.

Roffel, B., Betlem, B., 2007. Process dynamics and control: Modeling for control and prediction. Wiley.

Romera, J., Ocampo-Martinez, C., Puig, V., Quevedo, J., 2013. Flooding Management using Hybrid Model Predictive Control: Application to the Spanish Ebro River. Journal of Hydroinformatics 15, 366.

Sadowska, A., De Schutter, B., van Overloop, P.J., 2015a. Delivery-oriented hierarchical predictive control of an irrigation canal: Event-driven versus time-driven approaches. IEEE Transactions on Control Systems Technology 23, 1701–1716.

Sadowska, A., van Overloop, P.J., Maestre, J.M., Schutter, B.D., 2015b. Human-in-the-loop control of an irrigation canal using time instant optimization model predictive control, in: Proceedings of the 2015 European Control Conference (ECC), pp. 3274–3279.

Sánchez, G., Murillo, M., Genzelis, L., Deniz, N., Giovanini, L., 2017. MPC for nonlinear systems: A comparative review of discretization methods, in: 2017 XVII Workshop on Information Processing and Control (RPIC), pp. 1–6.

Schürmann, B., Kochdumper, N., Althoff, M., 2018. Reachset model predictive control for disturbed nonlinear systems, in: 2018 IEEE Conference on Decision and Control (CDC), pp. 3463–3470.

Schuurmans, J., 1997. Control of water levels in open-channels. Ph.D. thesis. Delft University of Technology.

Scokaert, P.O.M., Mayne, D.Q., Rawlings, J.B., 1999. Suboptimal model predictive control (feasibility implies stability). IEEE Transactions on Automatic Control 44, 648–654.

Segovia, P., Blesa, J., Duviella, E., Rajaoarisoa, L., Nejjari, F., Puig, V., 2018a. Sliding window assessment for sensor fault model-based diagnosis in inland waterways. Proceedings of the 1st IFAC Workshop on Integrated Assessment Modelling for Environmental Systems IAMES 2018 51, 31–36.

Segovia, P., Blesa, J., Horváth, K., Rajaoarisoa, L., Nejjari, F., Puig, V., Duviella, E., 2018b. Modeling and fault diagnosis of flat inland navigation canals. Proceedings of the Institution of Mechanical Engineers. Part I: Journal of Systems and Control Engineering 232, 761–771.

Segovia, P., Rajaoarisoa, L., Nejjari, F., Duviella, E., Puig, V., 2019. Model predictive control and moving horizon estimation for water level regulation in inland waterways. Journal of Process Control 76, 1–14.

Segovia, P., Rajaoarisoa, L., Nejjari, F., Puig, V., Duviella, E., 2017. Decentralized control of inland navigation networks with distributaries: application to navigation canals in the north of France, in: Proceedings of the 2015 American Control Conference (ACC), Seatle.

Segovia, P., Rajaoarisoa, L., Nejjari, F., Puig, V., Duviella, E., 2018c. Modeling of interconnected flat open-channel flow: application to inland navigation canals, in: Water, S. (Ed.), Advances in Hydroinformatics, Springer, Singapore. pp. 87–95.

Sepulveda, C., 2007. Instrumentation , model identification and control of an experimental irrigation canal. Doctoral thesis. Universitat Politécnica de Catalunya.

Shahverdi, K., Maestre, J.M., Alamiyan-Harandi, F., Tian, X., 2020. Generalizing fuzzy SARSA learning for real-time operation of irrigation canals. Water 12, 2407.

Shahverdi, K., Monem, M.J., 2015. Application of reinforcement learning algorithm for automation of canal structures. Irrigation and Drainage 64, 77–84.

Shahverdi, K., Monem, M.J., Nili, M., 2016. Fuzzy sarsa learning of operational instructions to schedule water distribution and delivery. Irrigation and Drainage 65, 276–284.

Shang, Y., Liu, R., Li, T., Zhang, C., Wang, G., 2011. Transient flow control for an artificial open channel based on finite difference method. Science China Technological Sciences 54, 781–792.

Shibu, M.E., Leffelaar, P.A., van Keulen, H., Aggarwal, P.K., 2010. LINTUL3, a simulation model for nitrogen-limited situations: Application to rice. European Journal of Agronomy 32, 255–271.

Soler, J., Gómez, M., Rodellar, J., 2013a. GoRoSo: Feedforward control algorithm for irrigation canals based on sequential quadratic programming. Journal of Irrigation and Drainage Engineering 139, 41–54.

Soler, J., Gómez, M., Rodellar, J., Gamazo, P., 2013b. Application of the GoRoSo feedforward algorithm to compute the gate trajectories for a quick canal closing in the case of an emergency. Journal of Irrigation and Drainage Engineering 139, 1028–1036.

Swamee, P., Mishra, G., Chahar, B., 2002. Design of minimum water-loss canal sections. Journal of Hydraulic Research 40, 215–220.

Tavares, I., Borges, J., Mendes, M., Botto, M., 2013. Assessment of data-driven modeling strategies for water delivery canals. Neural Computing and Applications 23, 625–633.

Tian, X., Guo, Y., Negenborn, R., Wei, L., Lin, N., Maestre, J., 2019. Multi-scenario model predictive control based on genetic algorithms for level regulation of open water systems under ensemble forecasts. Water Resources Management 33, 3025–3040.

U. S. Department of the Interior, 2001. Water measurement manual. U.S. Government Printing Office, Washington, DC.

United Nations Department of Economic and Social Affairs Population Division, 2021. World population prospects.

Uniyal, B., Dietrich, J., 2021. Simulation of irrigation demand and control in catchments – A review of methods and case studies. Water Resources Research 57, e2020WR029263.

Van Thang, P., Chopard, B., Lefevre, L., Ondo, A.D., Mendes, E., 2017. Study of the 1D lattice Boltzmann shallow water equation and its coupling to build a canal network. archives-ouvertes.fr .

Verhaegen, M., Verdult, V., 2007. Filtering and System Identification: A Least Squares Approach. Cambridge University Press.

Wagenpfeil, J., Arnold, E., Linke, H., Sawodny, O., 2013. Modelling and optimized water management of artificial inland waterway systems. Journal of Hydroinformatics 15, 348–365.

Wahlin, B., 2004. Performance of model predictive control on ASCE test canal 1. Journal of Irrigation and Drainage Engineering 130, 227–238.

Wahlin, B., Zimbelman, D., 2014. Canal automation for irrigation systems. volume 67. American Society of Civil Engineers (ASCE), WEST Consultants, Tempe, AZ, United States.

Weyer, E., 2001. System identification of an open water channel. Control Engineering Practice 9, 1289–1299.

Weyer, E., 2002. Decentralised PI control of an open water channel, in: Proceedings of the 5th Triennial World Congress, pp. 95–100.

Weyer, E., 2006. Multivariable LQ control of an irrigation channel: Experimental results and robustness analysis. Proceedings of the 45th IEEE Conference on Decision and Control , 6642–6647.

Weyer, E., 2008. Control of irrigation channels. IEEE Transactions on Control Systems Technology 16, 664–675.

Weyer, E., Bastin, G., 2008. Leak detection in open water channels, in: Proceedings of the 17th World Congress, IFAC, Seoul. pp. 7913–7918.

de Wit, A., Boogaard, H., Fumagalli, D., Janssen, S., Knapen, R., van Kraalingen, D., Supit, I., van der Wijngaart, R., van Diepen, K., 2019. 25 years of the WOFOST cropping systems model. Agricultural Systems 168, 154–167.

Xu, M., 2013. Real-time control of combined water quantity & quality in open channels. Ph.D. thesis. Delft University of Technology.

Xu, M., Negenborn, R., van Overloop, P., van de Giesen, N., 2012. De Saint-Venant equations-based model assessment in model predictive control of open channel flow. Advances in Water Resources 49, 37–45.

Yuan, Z., Chen, B., Zhao, J., 2011. An overview on controllability analysis of chemical processes. AIChE Journal 57, 1185–1201.

Zafra-Cabeza, A., Maestre, J.M., Ridao, M.A., Camacho, E.F., Sánchez, L., 2011. A hierarchical distributed model predictive control approach to irrigation canals: A risk mitigation perspective. Journal of Process Control 21, 787–799.

Zeng, N., Cen, L., Xie, Y., Zhang, S., 2020. Nonlinear optimal control of cascaded irrigation canals with conservation law PDEs. Control Engineering Practice 100.

Zhang, P., Weyer, E., 2005. Performance monitoring of control loops in irrigation channels using reference models, in: Proceedings of the IFAC 16th Trienial World Congress, pp. 359–364.

Zhang, Y., Wu, J., Xu, B., 2018. Human health risk assessment of groundwater nitrogen pollution in Jinghui canal irrigation area of the loess region, northwest China. Environmental Earth Sciences 77, 273.

Zheng, Z., Wang, Z., Zhao, J., Zheng, H., 2019. Constrained model predictive control algorithm for cascaded irrigation canals. Journal of Irrigation and Drainage Engineering 145.

Zhu, T., Ringler, C., Rosegrant, M.W., 2019. Viewing agricultural water management through a systems analysis lens. Water Resources Research 55, 1778–1791.

Zou, L., Wang, Z., Hu, J., Han, Q.L., 2020. Moving horizon estimation meets multi-sensor information fusion: Development, opportunities and challenges. Information Fusion 60, 1–10.

Nomenclature

$\alpha_i \in \mathbb{R}$	Parameter used to avoid the change of the unlikely unknown flow
$\boldsymbol{\beta_i}$	Vector of measured variables
$\beta_i \in \mathbb{R}$	Parameter used to avoid the change of the unlikely unknown flow
$\hat{\bar{\boldsymbol{y}}}_i \in \mathbb{R}^{2N_h}$	Vector of estimated expected values of the output
$\hat{\boldsymbol{\theta}}_i(k-1) \in \mathbb{R}^{3N_h}$	Sequence of unknown parameters estimated in a previous iteration
$\hat{\boldsymbol{\theta}}_i(k) \in \mathbb{R}^{3N_h}$	Vector of unknown parameters to be estimated
$\hat{\boldsymbol{y}}_i \in \mathbb{R}^{2N_h}$	Vector of estimated outputs
$\boldsymbol{\Omega}_i(k) \in \mathbb{R}^{3N_h \times 3N_h}$	Estimation matrix of hydraulic relations
$\boldsymbol{\Phi}_i \in \mathbb{R}^{2N_h \times 2}$	State estimation matrix
$\boldsymbol{\Sigma}_{\Delta_i}(k) \in \mathbb{R}^{2N_h \times 2N_h}$	Process detection covariance
$\boldsymbol{\Sigma}_i(k) \in \mathbb{R}^{2N_h \times 2N_h}$	Process covariance
$\boldsymbol{\xi}_i(k) \in \mathbb{R}^{3N_h}$	Vector of known inputs
$\boldsymbol{T}_i \in \mathbb{R}^{3N_h \times 3}$	Block of identity matrices
$\boldsymbol{B}_i \in \mathbb{R}^{2N_h \times 3N_h}$	Unknown flows estimation matrix
$\boldsymbol{B}_{f_i} \in \mathbb{R}^{2N_h \times 3N_h}$	Known inputs estimation matrix
$\boldsymbol{J}_i \in \mathbb{R}$	Detection cost function
$\boldsymbol{n}_{\Delta_i}(k+1) \in \mathbb{R}^{2N_h}$	Process measurement noise vector
$\boldsymbol{n}_i(k+1) \in \mathbb{R}^{2N_h}$	Measurement noise vector
$\boldsymbol{u}(k) \in \mathbb{R}^{2MN}$	Optimal or sub-optimal control sequence
$\boldsymbol{V}_i \in \mathbb{R}$	Estimation cost function
$\boldsymbol{V}_{s_i} \in \mathbb{R}$	Stochastic estimation cost function
$\boldsymbol{w}_{\Delta_i}(k) \in \mathbb{R}^{2N_h}$	Process detection noise vector
$\boldsymbol{w}_i(k) \in \mathbb{R}^{2N_h}$	Process noise vector
$\boldsymbol{y}_i \in \mathbb{R}$	Vector of measured levels
$\Delta\boldsymbol{\xi}_i(k) \in \mathbb{R}^{3N_h}$	Vector of the known inputs variation
$\Delta\hat{y}_i(k+1) \in \mathbb{R}^2$	Vector of estimated variation of the outputs
$\Delta\xi_i(k) \in \mathbb{R}^3$	Vector of variations of known inputs
$\Delta\hat{\boldsymbol{\psi}}_i(k-1) \in \mathbb{R}^{3N_h}$	Sequence of variations of the unknown flows estimated in a previous iteration
$\Delta\hat{\boldsymbol{\psi}}_i(k) \in \mathbb{R}^{3N_h}$	Vector of the estimated variations of the

		unknown flows
$\Delta\hat{\boldsymbol{y}}_i \in \mathbb{R}^{2N_h}$		Vector of the estimated variations of the outputs
$\Delta\boldsymbol{y}_i \in \mathbb{R}^{2N_h}$		Vector of the measured variations of the outputs
$\Delta\hat{\psi}_i(k) \in \mathbb{R}^3$		Vector of estimated variations of the inputs
$\Delta\hat{x}_i(k) \in \mathbb{R}^2$		Vector of estimated variation of the states
$\Delta\hat{x}_i(N_{hp} \mid N_{hp}) \in \mathbb{R}^2$		Initial estimated variations of the states
η_i	(ms)	Error integral
$\hat{\bar{k}}_{dn_i}(k) \in \mathbb{R}$		Expected value of the estimated downstream unknown flow parameter
$\hat{\bar{k}}_{tr_i}(k) \in \mathbb{R}$		Expected value of the estimated transition parameter
$\hat{\bar{k}}_{up_i}(k) \in \mathbb{R}$		Expected value of the estimated upstream unknown flow parameter
$\hat{\psi}_i(k) \in \mathbb{R}^3)$		Vector of estimated unknown flows
$\hat{\theta}_i(k) \in \mathbb{R}^3$		Vector of unknown parameters to be estimated
$\hat{x}_{dn_i}(k) \in \mathbb{R}$	(m)	Estimated downstream level
$\hat{x}_{up_i}(k) \in \mathbb{R}$	(m)	Estimated upstream level
$\hat{k}_{dn_i}(k) \in \mathbb{R}$		Estimated downstream unknown flow parameter
$\hat{k}_{tr_i}(k) \in \mathbb{R}$		Estimated transition parameter
$\hat{k}_{up_i}(k) \in \mathbb{R}$		Estimated upstream unknown flow parameter
$\hat{q}_{tr_i}(k) \in \mathbb{R}$	(m^3/s)	Estimated flow transition
$\hat{s}_{dn_i}(k) \in \mathbb{R}$		Estimated downstream unknown flow parameter
$\hat{s}_{up_i}(k) \in \mathbb{R}$		Estimated upstream unknown flow parameter
$\hat{x}_i(k) \in \mathbb{R}^2$		Vector of estimated states
$\hat{x}_i(N_{hp} \mid N_{hp}) \in \mathbb{R}^2$		Initial estimated states over the estimation window
$\hat{y}_i(k+1) \in \mathbb{R}^2$		Vector of estimated outputs
$\kappa_{dn_i}(t) \in \mathbb{R}$	($m^{2.5}/s$)	Downstream unknown flow parameter
$\kappa_{up_i}(t) \in \mathbb{R}$	($m^{2.5}/s$)	Upstream unknown flow parameter
$\Lambda_{\Delta_i} \in \mathbb{R}^2$		Threshold value
$\lambda_i \in \mathbb{R}$		Tuning constant
$\mathbf{d} \in \mathbb{Z}$		Number of disturbances
$\mathbf{n} \in \mathbb{Z}$		Number of states
$\mathbf{u} \in \mathbb{Z}$		Number of inputs
$\mathbf{y} \in \mathbb{Z}$		Number of outputs
$\bar{\mathbf{x}}_{\mathbf{dn_i}} \in \mathbb{R}$	(m)	Mean of $\mathbf{x}_{\mathbf{dn_i}}$
$\boldsymbol{\Omega} \in \mathbb{R}^{H_p\mathbf{d}\times H_p\mathbf{d}}$		Matrix used in MPC formulation
$\boldsymbol{\Psi} \in \mathbb{R}^{H_p\mathbf{y}\times n}$		Matrix used in MPC formulation
$\boldsymbol{\Upsilon} \in \mathbb{R}^{H_p\mathbf{u}\times H_p\mathbf{u}}$		Matrix used in MPC formulation
$\mathbf{V}_i$		Lyapunov function
$\mathbf{x}_{\mathrm{ref_i}} \in \mathbb{R}^{N_f}$		Desired level vector
$\mathbf{x}_{\mathbf{dn_i}} \in \mathbb{R}^{N_f}$		Vector of N_f level measurements
$\mathcal{D}_{1_i} \in \mathbb{R}^{2N_h\times 2N_h}$		Detection weighting matrix
$\mathcal{D}_{2_i} \in \mathbb{R}^{3N_h\times 3N_h}$		Detection weighting matrix

$\mathcal{Q} \in \mathbb{R}^{\mathbf{n}\times\mathbf{n}}$		Diagonal weighting matrix
$\mathcal{R} \in \mathbb{R}^{\mathbf{u}\times\mathbf{u}}$		Diagonal weighting matrix
$\mathcal{R}_{1_i} \in \mathbb{R}^{2N_h\times 2N_h}$		Estimation weighting matrix
$\mathcal{R}_{2_i} \in \mathbb{R}^{3N_h\times 3N_h}$		Estimation weighting matrix
$\mathcal{R}_{kdn_i} \in \mathbb{R}$		Estimation weighting parameter related to downstream unknown flows
$\mathcal{R}_{ktr_i} \in \mathbb{R}$		Estimation weighting parameter related to the flow transition
$\mathcal{R}_{kup_i} \in \mathbb{R}$		Estimation weighting parameter related to upstream unknown flows
$\nabla^2 \in \mathbb{R}^2$		Hessian operator
$\nu_{\Delta i}(k) \in \mathbb{R}^2$		Measurement detection noise
$\nu_{_i}(k) \in \mathbb{R}^2$		Remaining measurement noise
$\nu_{dn_i}(k) \in \mathbb{R}$		Downstream remaining measurement noise
$\nu_{up_i}(k) \in \mathbb{R}$		Upstream remaining measurement noise
$\omega_{\Delta i}(k) \in \mathbb{R}^2$		Process detection noise
$\Omega_{_i}(k) \in \mathbb{R}^{3\times 3}$		Matrix of hydraulic relations
$\omega_{_i}(k) \in \mathbb{R}^2$		Process estimation noise
$\omega_{dn_i}(k) \in \mathbb{R}$		Normally distributed downstream process noise
$\omega_{up_i}(k) \in \mathbb{R}$		Normally distributed upstream process noise
$\phi_{x_i} \in \mathbb{R}^{n\times 2}$		Matrix of n measured levels variations
$\sigma_{\nu dn_i} \in \mathbb{R}$		Standard deviation of the downstream measurement noise
$\sigma_{\nu up_i} \in \mathbb{R}$		Standard deviation of the upstream measurement noise
$\sigma_{\omega dn_i} \in \mathbb{R}$		Standard deviation of the downstream process noise
$\sigma_{\omega up_i} \in \mathbb{R}$		Standard deviation of the upstream process noise
$\tau_{_i} \in \mathbb{R}$	(s)	Time delay
$\tau_s \in \mathbb{R}$	(s)	Sampling time
$\theta_{a_i} \in \mathbb{R}^2$		Vector of upstream and downstream areas
$\gamma \in \mathbb{R}^{4M}$		Augmented state vector
$\hat{\bar{\theta}}_{_i}(k) \in \mathbb{R}^3$		Vector of the unknown parameters expected values
$\xi_{_i}(k) \in \mathbb{R}^3$		Vector of known inputs
$e_{_i}(k+1) \in \mathbb{R}^{2N_h}$		Estimation error
$P_{_i}(k+1) \in \mathbb{R}^{2\times 2}$		Process covariance
$P_{\Delta_i}(k+1) \in \mathbb{R}^{2\times 2}$		Process detection covariance
$d \in \mathbb{R}^M$		Disturbances vector
$G_{_i} \in \mathbb{R}^{2\times 2}$		State matrix
$H_{_i} \in \mathbb{R}^{2\times 3}$		Unknown flows matrix
$H_{f_i} \in \mathbb{R}^{2\times 3}$		Known inputs matrix
$u \in \mathbb{R}^{2M}$		Inputs vector

$A \in \mathbb{R}^{\mathbf{n}\times\mathbf{n}}$		State matrix
$a_{_i} \in \mathbb{R}$	(m^2)	Channel area
$a_{dn_i} \in \mathbb{R}$	(m^2)	Area of the downstream part of the channel
$a_{m_i} \in \mathbb{R}$	(m^2)	Area of an m_i part of the channel
$a_{up_i} \in \mathbb{R}$	(m^2)	Area of the upstream part of the channel
$B \in \mathbb{R}^{\mathbf{n}\times\mathbf{u}}$		Input matrix
$B_d \in \mathbb{R}^{\mathbf{n}\times\mathbf{d}}$		Disturbances matrix
$B_d \in \mathbb{R}^{\mathbf{y}\times\mathbf{n}}$		Output matrix
$c_{_i} \in \mathbb{R}$		Discharge coefficient
$c_{out_i} \in \mathbb{R}$		Discharge coefficient of the outlet
d_{out}		Vector of users demands
e_d		Error between demanded and delivered flow
e_v		Volume error between demanded and delivered water
f_i		Friction factor
$g \in \mathbb{R}$	(m/s^2)	Gravity constant
$h_{l_i} \in \mathbb{R}$	(m)	Head loss due to friction
H_c		Control horizon MPC
H_p		Prediction horizon MPC
$i \in \mathbb{Z}$		Stage number (e.g., $i = 1$ denotes the first channel)
$J(k)$		Cost function component
$K \in \mathbb{R}^{\mathbf{u}\times\mathbf{n}}$		Control matrix
$k_{tr_i}(t) \in \mathbb{R} \in \mathbb{R}$	(m^2/s)	Transition parameter
$l_{_i}$	(m)	Channel length
$l_{h_i} \in \mathbb{R}$		Constant associated with a difference of potential along the channel
$M \in \mathbb{Z}$		Amount of channels
N		Prediction horizon NMPC
$N_{hp} \in \mathbb{Z}$		Initial position of the estimation window
$N_h \in \mathbb{Z}$		Estimation window length
$p_{_i}$		i^{th} channel
$q_{_i} \in \mathbb{R}$	(m^3/s)	p_i inflow
$q_{out_i} \in \mathbb{R}$	(m^3/s)	Outflow to the users
$q_{m_i} \in \mathbb{R}$	(m^3/s)	Flow at m_i position
$q_{tr_i}(t) \in \mathbb{R}$	(m^3/s)	Flow transition
$R \in \mathbb{R}^{2\times2}$		Process variance
R		Penalization matrix
$R_\Delta \in \mathbb{R}^{2\times2}$		Process detection variance
$r_{m_i} \in \mathbb{R}$	(m)	Hydraulic radius at an m_i position
$S \in \mathbb{R}^{2\times2}$		Measurement variance
$S_\Delta \in \mathbb{R}^{2\times2}$		Process detection covariance
$s_{m_i} \in \mathbb{R}$	(m^3/s)	Leak or seepage at an m_i position
$u_{_i} \in \mathbb{R}$	(m)	Regulation structure position

$v_{dn_i} \in \mathbb{R}$		Downstream mean flow velocity
$v_{up_i} \in \mathbb{R}$		Upstream mean flow velocity
W_i		Positive defined function
$w_{m_i} \in \mathbb{R}$	(m)	width at an m_i position
$x \in \mathbb{R}^{2M}$		Vector of upstream and downstream levels
$x_{\mathrm{ref_i}}$	(m)	desired depth for the i^{th} channel
$x_{dn_i} \in \mathbb{R}$	(m)	Downstream depth
$x_{dn} \in \mathbb{R}^M$		Vector of downstream levels
$x_{m_i} \in \mathbb{R}$	(m)	Depth at an m_i position
$x_{up_i} \in \mathbb{R}$	(m)	Upstream depth
$x_{up} \in \mathbb{R}^M$		Vector of upstream levels
$y_{q_i} \in \mathbb{R}^n$		Vector of inflows and outflows
$z_{dn_i} \in \mathbb{R}$	(m)	Downstream elevation
$z_{s_i} \in \mathbb{R}$		Channel's slope
$z_{up_i} \in \mathbb{R}$	(m)	Upstream elevation